Inhibition of Protein Arginine Methyltransferase-5 and Enhancer of Zeste Homolog-2 by Phytocompounds

A thesis submitted to the University of Hyderabad, for the award of

in
Plant Sciences

by

Nalla Kirankumar (Reg. No. 17LPPH18)



Department of Plant Sciences
School of Life Sciences
University of Hyderabad
(P.O.) Central University, Gachibowli,
Hyderabad – 500046 Telangana
India

July 2024



University of Hyderabad (A central University established in 1974 by Act of Parliament)

School of Life Sciences Department of Plant Sciences Hyderabad-500046



CERTIFICATE

This is to certify that the thesis entitled "<u>Inhibition of Protein Arginine Methyltransferase-5 and Enhancer of Zeste Homolog-2 by Phytocompounds</u>" submitted by <u>Mr. Nalla Kirankumar</u> bearing Registration Number <u>17LPPH18</u> in partial fulfilment of the requirements for award of Doctor of Philosophy in the Plant Sciences is a bonafide work carried out by him under my supervision and guidance.

This thesis is free from plagiarism and has not been submitted previously in part or in full to this or any other University or Institution for award of any degree or diploma.

Further, the student has the following publication(s) before submission of the thesis/monograph for adjudication and has produced evidence for the same in the form of acceptance letter or the reprint in the relevant area of his research:

- i) Nalla, K., Chatterjee, B., Poyya, J., Swain, A., Ghosh, K., Pan, A., & Kanade, S. R. (2024). Epigallocatechin-3-gallate inhibit the protein arginine methyltransferase 5 and Enhancer of Zeste homolog 2 in breast cancer both in vitro and in vivo. bioRxiv, 2024-02. https://doi.org/10.1101/2024.02.18.580855 (Under review in Archives of Biochemistry & Biophysics (ABB) Elsevier).
- ii) Nalla, K., Chatterjee, B., Poyya, J., Swain, A., Ghosh, K., Pan, A., ... & Kanade, S. R. (2024). Ellagic acid: a potential inhibitor of enhancer of zeste homolog-2 and protein arginine methyltransferase-5. *bioRxiv*, 2024-05. doi: https://doi.org/10.1101/2024.05.22.595443 (Under review in FEBS letters)
- iii) Baka, D., Kishore, R., Sunkara, S., Varadhi, G., Kashanna, J., Tripuramallu, B. K., Nalla, K., & Kanade, S. R. (2024). Design, Synthesis, and Cytotoxicity of 1H-1,2,3-Triazole Tethered-Benzophenone Based Derivatives as Potent Candidate Anti-Breast Cancer Agents. In ChemistrySelect (Vol. 9, Issue 17). Wiley. https://doi.org/10.1002/slct.202401005
- iv) Rao, K. S., Nalla, K., Ramachandraiah, C., Chandrasekhar, K. B., Kanade, S. R., & Saha, S. (2023). Design and Synthesis of New Triazole-Benzimidazole Derivatives as Potential PRMT5 Inhibitors. *ChemistrySelect*, 8(11), e202204474. https://doi.org/10.1002/slct.202204474

and has made presentations in the following conferences:

- Oral presentation in Current trends and future prospectus of plant biology (CTFPPB) organized by Department of Plant Sciences, School of Life Sciences, university of Hyderabad, held during 23rd -25th February 2023
- Oral presentation in 15th International Symposium on Recent Trends in Cancer Prevention and Interception - Bench to Bedside organized by School of Life Sciences, Jawaharlal Nehru University, New Delhi, India, February 22-23, 2022.

- 3. Oral presentation in -Virtual Conference on Proteomics in Agriculture and Healthcare- School of Life Sciences, University of Hyderabad held during March 13-14, 2021.
- 4. Presented a Poster at EMBL Conference: Chromatin and epigenetics EMBL Advanced Training Centre, Heidelberg-Germany Held during 15 - 18 May 2023.
- 5. Presented a poster at "3rd International Conference on Applications of Natural compounds, Nanomaterials, Oncolytic in Cancer Biology and Biotechnology (ICANNOCB-22)" organized by School of Life Sciences and Association of Cancer Education and Research (ACER), B.S. Abdur Rahman Crescent Institute of Science & Technology, Chennai, India in association with Purdue University, USA on 27th-28th October, 2022.
- 6. Presented a poster in Horizons in Molecular Biology", which took place online September 13th 16th 2021.
- 7. Presented a poster in National Conference on Frontiers in Plant Biology, organized by Department of Plant Sciences, School of Life science, University of Hyderabad-February 2020.

Further, the student has passed the following courses towards fulfilment of coursework requirements for the award of Ph.D.

COURSE	TITLE OF THE COURSE	CREDIT	RESULT
NO	THE OF THE COURSE	s	s
S801	RESEARCH METHODOLOGY/ ANALYTICAL TECHNIQUES	4	PASS
S802	RESEARCH ETHICS, BIOSAFETY, DATA	1	PASS
3602	ANALYSIS	4	rass
S803	RESEARCH PROPOSAL AND SCIENTIFIC WRITING	4	PASS

18.07.2024

Dr. SANTOSH R. KANADE

Professor Dept. of Plant Sciences School of Life Sciences University of Hyderabad

Hyderabad-500 046. T.S. India

HEAD

Dept. of Plant Sciences School of Life Sciences University of Hyderabad Hyderabad-500 046, INDIA

Dean of the School

जीव विज्ञान संकाय / School of Life Sciences हैदराबाद विश्वविद्यालय / University of Hyderabad हैदराबाद / Hyderabad-500 046.





University of Hyderabad (A central University established in 1974 by Act of Parliament)

School of Life Sciences Department of Plant Sciences Hyderabad-500046

DECLARATION

I Nalla Kirankumar hereby declare that this thesis entitled "Inhibition of Protein Arginine Methyltransferase-5 and Enhancer of Zeste Homolog-2 by Phytocompounds" submitted by me under the supervision of Prof. Santosh R Kanade is a bonafide research work. I also declare that it has not been submitted previously in part or in full to this University or any other University or Institution for the award of any degree or diploma.

Nalla Kirankumar

Regd. No. 17LPPH18

Prof. Santosh R Kanade (Research Supervisor)

Dr. SANTOSH R. KANADE

Professor

Dept. of Plant Sciences
School of Life Sciences
University of Hyderabad
Hyderabad-500 046, T.S. India.

Acknowledgements

The completion of this thesis would not have been possible without the help and support of many important people in my life. I would like to thank each one of them for their contributions and encouragement. In particular:

First and foremost, I would like to thank my mentor, **Prof. Santosh R. Kanade**, Department of Plant Sciences, School of Life Sciences, University of Hyderabad, Hyderabad, for welcoming me into his laboratory, accepting me as a PhD student, providing invaluable guidance, constant encouragement, and critical reviews. He is always accessible for help and advice throughout my research inquiries. I could not have imagined having a better advisor and mentor for my Ph.D. His attention, moral support and timely suggestions were useful in the preparation of my thesis. It has been a great privilege to have embarked on my journey into the world of science under his supervision. I am always grateful to my supervisor for everything. I cannot forget his persistent support during the hard times in research. I am thankful to him for teaching research and helping me compete in a challenging environment. I am indeed most privileged to have such an esteemed and influential person as my guide at the dawn of my research career.

I am equally grateful to my Doctoral Committee members, **Prof. S Rajagopal & Dr. J. Madhu Prakash**, Dept. of Plant Sciences, for their timely advice and immense support.

I extend my heartfelt gratitude to our esteemed collaborators, Prof. Bramanandam Manavathi, for generously providing animal house facilities, the invaluable gift of cell lines (MCF7, MDA-MB-231, and HEK293), and expert guidance throughout our in-vivo experiments. I am equally indebted to the contributions of Dr. Archana Pan, Ms. Aishwarya Swain, from the Department of Bioinformatics, Pondicherry University, and Prof. Chandra Sekhar Joshee (Mangalore University) and his student Dr. Jagadeesha Poyya, Assistant professor at SDM Research Institute for Biomedical Sciences-Dharwad, whose assistance proved instrumental in conducting our molecular docking and molecular dynamic simulations studies. Additionally, I am grateful to Prof. A. Bindu Madhav Reddy for graciously providing the DU145 and PC3 cell lines, which were vital to our research endeavours. Special thanks are due to **Dr. Mahesh Jerald**, the animal facility in-charge at CCMB, for his invaluable assistance with our IHC studies, which significantly contributed to the depth of our research findings. I am highly grateful to Mrs. Monica Kannan (Proteomics Facility, School of Life Sciences, UoH) and Dr. K Praveen (Cytiva) for helping in the analysis of SPR data. I also thank Dr. Radheshyam Maurya, Ms. Madhulika, and Mr. B. Manikanta for their help in doing FACS analysis. My heartfelt gratitude to Prof. S Rajagopal (Present Head), Prof. G Padmaja, and Prof. Ch Venkata Ramana (Former Heads), Department of Plant Sciences, School of Life Sciences, University of Hyderabad, for always providing common facilities accessibility without hindering the work. My sincere thanks to Prof. Anand K Kondapi (Dean) and Prof. N Siva Kumar, Prof. S Dayananda, Prof. K.V.A Ramaiah, and Prof. P. Reddana (former Deans) for providing all the research facilities in school and making them available to us.

I thank all the faculty members of the Dept. of Plant Sciences and School of Life Sciences for inspiring me and helping me directly or indirectly during my research period. I thank all the office staff of the Dept. of Plant Sciences and School of Life Sciences, finance, and fellowship section for their timely help during my research period.

I thank my fellow lab mates—Ms. Risha Ravi, Mr. Manish Yadav, Ms. Sakshi Dubey, Ms. Archana, Mr. Subin Boban, Dr. Jyoti Chaitanya, Dr. Dhanya—for their encouragement and cooperation during my research work. And I am thankful to Dr. Krishna Ghosh and Dr. Biji Chatterjee, former students of Prof. SRK, for their support in the current studies. I am grateful to Master's project students Prakashi, Swetha, Kavitha, Anisha, Tejaswini, Paulomi, and Hena Ghosh for the opportunity to guide and learn alongside them, which has enhanced and upgraded my skills. I thank and express my gratitude to my Master's dissertation Supervisor Dr. Gopinath Kodetham for his guidance and motivation to continue in the field of research. I thank CSIR, SERB, and IoE-UoH for funding our lab. I specially thank UoH-Non-Net fellowship (6 months) and Department of Science and Technology, Govt. of India (DST/INSPIRE/03/2017/000035 & IVR No-201700011820) for DST-INSPIRE for providing the fellowship, and IoE-UOH for travel grant to attend EMBL conference in Germany. I specially thank Dr. D. Shanmukha Kumar, Post Doc at Heidelberg University, for his help during my visit to EMBL-Heidelberg Germany.

I am deeply grateful to Dr. Punjala Vinay Kumar (Surgical gastroenterologist-Apollo hospital-Hyderabad), Mr. Puli Sekhar garu (Rean cloud-USA), and Mr. Nanda Kumar garu from **Asha-Jyoti Foundation** for their invaluable support during my master's studies by providing a laptop and 4th-semester fee. Similarly, I extend my sincere thanks to **Mr. Gopal Rao Master** and the Rajahmundry Walkers and Laughing Club members for their generous financial assistance during my master's studies in Sri Venkateswara University-Tirupati. Their support and encouragement helped me to become a researcher today.

I must acknowledge the indispensable guidance and aid provided by my school teacher, our family friend, and well-wisher, **Mr. Kanchumarthi Jagannadha Rao** (chess master), as well as English **Professor Y. Panduranga Rao.** Their mentorship played an integral role in shaping my academic journey, and I am truly indebted to them for their unwavering support.

I would like to thank my Newton Baba proposed mentor, Dr. Matthew Brook from Edinburgh; Namaste+ Plus Germany student exchange program proposed mentors, Dr. Carmelo Ferrari, and Prof. Argyris Papantonis from Göttingen University; and finally, Prof. Richard Eckert from the University of Maryland (Fulbright proposed guide). Although I was not selected, I gained enormous experience and exposure to proposal writing and received substantial training under their guidance. I am equally thankful to all. In the end, my stay in HCU would not have been better without my friends and seniors Dr. Mallikarjuna T, Sanjay, Bharat, Netrika, Sruchytha, Yasaswi, Sri Ram, Govind, Prodosh Da, Anu Bhagat, Priyam Bada, Satyabrata, Aditya, Dr. Veeranna, Swati Verma, Akshay, Calvin, Dr. Saratchandra, Mohan, Aswini, Phebe Florence, Dr Santi Swarupini, Dr Syam Babu, Prasad Anna Dr. Surabhi, Dr. Chukhu, Ravi Polireddy, T Rithwik, MD Atheeq, Harish Anna, Ratal anna and especially all my PhD batchmates (2017 batch), I thank them for making this journey pleasant for me.

and I Specially thank all my bachelor's and master's lecturers who supported and inspired me continue my studies especially, Venkat Prasanna, Ch Chaitanya, Prakash, Eswar, Ramakrishna, Lalu prasad, Ravi Chandra, Shahul, Naik, Suresh sir, Ravi, Sunil and all other officer group members . And I thank all my master's and bachelor's friends for their support and encouragement to do Ph.D. Thanks to all my teachers right from school days to Master's, who inspired and motivated me. Thankful to HCU-EU friends & family for their constant support and prayers throughout my stay at HCU. Bro Nehemiah's family, Dr. Johnson Anna's family, Bro. Ashish Joseph, Bro Herbert Jose's family, Bro Solomon's family, Bro. Kishore Dasari's family and all other HCU-EGF graduates and all HCU-EU family members and Special thanks to UESI OPED team for their constant prayer support.

I would like to dedicate this thesis to Bishop B. Jaya Sankar Garu, I am indebted to him for my entire life, and I convey my thanks and acknowledge the constant support and encouragement from the founder and director of CEM campus, the late Bishop B. Jaya Sankar Garu, and Mrs. B. Jaya Lakshmi Garu, who have helped me with my studies since high school and continue to do so.

I would like to thank my friends and seniors, who are like family members to me, Dr. Jagadeesh Gandla and Dr. Raga Deepthi. Dr. Jagadeesh, who is also my career mentor hired me and provided financial support during difficult times when I was not receiving any fellowship. Their constant support, strength, and advice have been invaluable during the challenging times of my PhD submission. Additionally, I extend my gratitude to Dr. Jayakumar, my master's teacher, friend, and senior, who has been a big support like a brother. All three of these individuals care about me a lot.I am forever beholden to my family: my father, mother, sister (Dr. Nagendra Prasad, Rajya Lakshmi, & Suma) and all my cousins for their huge support, unwavering love, and encouragement. Their affection and sacrifices were always a source of inspiration to achieve my goals. Finally, I am thankful to the **Almighty God** for everything.

						K	ï	i	r	a	n	L	-	11	n		.	r	ī	J	•	П	6	
						n	·	ш	1	и	п	IK	ч	ш	ш	12	4	ľ	- 1	N	и	ш	12	1

Dedicated to **Bishop B. Jaya Sankar Garu**, for his endless affection, support, and encouragement in pursuing my dreams of higher education

"I can do all things through Christ who strengthens me" Philippians 4:13



LIST OF ABBREVIATIONS

Г	LIST OF ADDREVIATIONS
%	Percentage
℃	Degree Celsius
μL	Microliter
μM	Micromolar
ADMA	Asymmetric dimethylarginine
AVO	Acidic vesicular organelles
AO	Acridine orange
BSA	Bovine serum albumin
CpG	Cytosine-Guanine dinucleotide with phosphate bond
CGI	CpG island
cm	Centimetre
DNA	Deoxyribonucleic acid
DMSO	Dimethyl sulfoxide
DMEM	Dulbecco's Modified Eagle's Medium
DNMT	DNA 5m-cytosine methyltransferase
EB	Ethidium bromide
EA	Ellagic acid
EDC	N-ethyl-N'- dimethylaminopropyl carbodiimide
EGCG	Epigallocatechin-3-gallate
EZH2	Enhancer of Zeste homolog 2
ELISA	Enzyme linked immunosorbent assay
FC	Flow cell
FBS	Fetal bovine serum
g	Acceleration due to gravity
HAT/KAT	Histone acetyltransferase/Lysine acetyltransferase
HDAC/ KDAC	Histone deacetylase/Lysine deacetylase
H3K27	H3 residue on lys27
H3K27me3	Trimethylated lysine 27 on histone H3
H4R3	H4 residue on Arg3
H4R3me2s	Symmetrically dimethylated arginine 4 on histone H4
HMTs	Histone methyltransferases
HTVS	High-throughput virtual screening
IHC	Immunohistochemistry
hr	hour
HDM	Histone demethylases
kDa	Kilodalton
KMT	Lysine methyltransferase
MEP50	Methylosome protein 50
	v 1
MMA	Monomethylarginine
min	Minute
mL	Millilitre
NHS	N-hydroxysuccinimide
nm	Nanometre
PRMT5	Protein arginine methyltransferase 5
PRMTs	Protein arginine methyltransferases
PRC2	Polycomb Repressive Complex 2
PBS	Phosphate buffer saline
PAGE	Polyacrylamide gel electrophoresis
PcG	Polycomb group
PMSF	Phenylmethanesulfonylfluoride
RNA	Ribonucleic acid
rpm	Revolutions per minute
RU	Response unit
SAM	S-adenosyl methionine
SDMA	Symmetric dimethylarginine
SPR	Surface plasmon resonance
SDS	Sodium dodecyl Sulphate
TET	Ten eleven translocases
Tris	Tris (hydroxymethyl) amino methane
V/V	Volume by volume
W/V	Weight by volume
WHO	World health organization

Table of Contents

S. No	Section	Page no
a	List of abbreviations	ix
b	List of figures	xiv-xvi
С	List of tables	xvi
	CHAPTER-1	
1.0	Introduction	2
1.1	The Versatility of Epigenetic mechanisms	3
1.1.1	DNA methylation	5
1.1.2	Histone modifications	5
1.1.3	Non-coding RNA mediated signaling pathways	6
1.1.3.1	MicroRNAs: Biogenesis and function	6
1.1.4	Protein methyltransferases	7
1.1.4.1	Arginine methylation and lysine methylation	7
1.1.4.2	Arginine methylation	7
1.1.4.3	lysine methylation	8
1.1.5	Poly comb repressive complexes	9
1.1.5.1	PRC2 Composition and Function	10
1.1.5.2	PRC1 Composition and Function	10
1.1.5.3	Biological roles of PRCs	10
1.1.5.4	Dysregulation of PRCS and Disease	11
1.2	Epigenetics and cancer	12
1.3	Overview of breast cancer (India & aboard)	12
1.3.1	Cancer Statistics	12
1.3.2	Cancer in India and around the world	13
1.3.3	Breast Cancer	14
1.3.4	Dysregulation of epigenetic regulators lead to cancer	15
1.3.4	Cancer databases	15
1.4.1		16
1.4.1	The Cancer Genome Atlas (TCGA)	17
1.4.3	cBioportal for cancer genomics Versatile role of PRMT5 and EZH2	17
1.4.5	Epigenetic targets: A frontier in cancer therapy	21
1.5.1	Epigenetic targets. A frontier in cancer therapy Epidrugs and Natural phytocompounds as cancer therapeutics	22
1.5.2		23
1.5.3	DNA methyltransferase inhibitors Histone deacetylase inhibitors	24
1.5.4	Non-coding RNA regulators	24
1.5.5	Natural phytocompounds in cancer treatment	
1.5.6	Phytocompounds as Epidrugs Antiproliferative Compounds as Epigenetic Moduletors	26
1.5.7	Antiproliferative Compounds as Epigenetic Modulators	
1.5.8	Clinical potential and challenges	35
1.6	Objectives of the study	35
1.7	References CHAPTER-2	36
2.1		49
	Introduction Motorials & Mothada	
2.2	Materials & Methods	50
2.2.1	Databases and Chemicals	50
2.2.1.1	Databases	50
2.2.1.2	Chemicals	50
2.2.2	Literature and database search for medicinal plants and Indian spices	51
2.2.3	Chemical library preparation and ADMET analysis	51
2.2.4	Chemical preparation of modulators	51

2.2.5	Cell culture and maintenance	52
2.2.6	Cell proliferation assay using MTT	52
2.2.6.1	Trypan blue dye exclusion assay	53
2.2.7	Impact of phytocompounds on epigenetic regulators through	53
	Real time quantitative polymerase chain reaction (qPCR) assay	
2.2.8	cBioPortal dataset search for PRMT5 & EZH2 Pathogenesis in	55
	cancer	
2.2.9	Kaplan Meier survival plot analysis of PRMT5 & EZH2 in breast	55
	cancer patient datasets	
2.2.10	Statistical analysis	56
2.3	Results	56
2.3.1	The ligand library signifies chemically, diverse natural phytochemicals	56
2.3.2	Impact of anti-proliferative molecules on cancer cell lines at	58
2.3.2	different concentrations	
2.3.2.1	MTT assay	58
2.3.2.2	Trypan blue dye exclusion assay	63
2.3.3	Anti-proliferative molecules targeted the expression of	64
2.0.0	epigenetic regulators	
2.3.4	Comprehensive Analysis of Cancer Types: Insights from	73
	CBioPortal Dataset on Amplification, Mutation, Deep Deletion,	, -
	and Multiple Alterations	
2.3.4.1	PRMT5 gene alterations	73
2.3.4.2	EZH2 gene alterations	74
2.3.5	Amplification Analysis Unveils High-Frequency Presence:	75
	PRMT5 and EZH2 Exhibit Over 90% Amplification Frequency	
	in Breast Cancer	
2.3.6	Survival Analysis Unveils Negative Correlation Between	77
	PRMT5 & EZH2 Expression and Patient Survival in Breast	
	Cancer: Oncoprint Data Validation	
2.3.7	Discussion	79
2.3.8	References	85
	CHAPTER-3	
3.1	Introduction	89
3.2	Materials and methods	90
3.2.1	Preparation of the protein structure	90
3.2.2	virtual screening	91
3.2.2.1	Molecular docking	91
3.2.2.2	Molecular dynamic simulations	92
3.2.3	Surface plasmon resonance analysis for protein-ligand	92
	interaction & pharmacokinetics analysis for phytocompounds	
3.2.4	Cell culture and treatment with EGCG, EA and combination	93
3.2.5	Cytotoxicity assays	93
3.2.5.1	MTT (3-(4,5-Dimethylthiazol-2-yl)-2,5-Diphenyltetrazolium	94
	Bromide) assay	
3.2.5.2	Trypan blue dye exclusion assay and Colony formation assay	94
3.2.5.3	Ao-Etbr double staining assay	94
3.2.6	Western blotting	95
3.2.7	Histones acid extraction from HEK293 cells	95
3.2.7.1	In-vitro methylation and ELISA	96
3.2.8	Apoptosis and Cell cycle analysis through flow cytometry	96
3.2.9	Acidic vesicular organelles (AVOs) formation assay	97
3.2.10	Colony formation assay	97

3.3	Results	98
3.3.1	Virtual docking revealed top 14 interacting molecules to PRMT5	98
	and EZH2	
3.3.2	Interaction of EGCG with PRMT5:MEP50 & EZH2 (Molecular	101
	docking)	
3.3.2.1	Molecular Dynamic Simulation Studies Interaction of EGCG	103
	with PRMT5 and EZH2	
3.3.2.2	Surface Plasmon Resonance studies for EGCG with	104
	PRMT5:MEP50 and EZH2	
3.3.3	Impact of EGCG on growth of multiple cancer cell lines	106
3.3.3.1	Effect of EGCG on Apoptosis & Cell cycle	108
3.3.3.2	EGCG induced autophagy in MDA-MB-231 cells	109
3.4	Interaction of EA with PRMT5 and EZH2	110
3.4.1	Molecular Dynamics Simulation Results for EA with PRMT5	112
3.4.1	and EZH2	112
3.4.2	Binding study of EA with PRMT5:MEP50 and EZH2 by	113
	Surface Plasmon Resonance	
3.4.3	Inhibition of EA on growth of multiple cancer cell lines	114
3.4.4	Impact of EA on Apoptosis and Cell cycle	117
3.4.5	EA mediate the autophagy in cells	118
3.4.3		119
3.5.1	Impact of Combination (EGCG+EA)	119
	Impact of Combo on human malignant cell lines	
3.5.2	Surface Plasmon Resonance Analysis of combination with EZH2 and PRMT5:MEP50	120
3.5.3	Effect of combination on H3K27me3 and H4R3me2s Methylation Marks	122
3.5.4	Effect of combination on Cellular Proliferation Dynamics	122
3.5.5	Induction of Apoptosis by combination in Breast Cancer Cells	124
3.5.6	Combination Induces Autophagy in Breast Cancer Cells	124
3.6	Discussion	125
3.7	References	130
4.1	CHAPTER-4	105
4.1	Introduction	135
4.2	Materials and methods	135
4.2.1	Tumor Xenografts Preparation of Lysate from Tumor Samples	136 136
4.2.3	Immunohistochemical Assays	136
4.2.4	Study Design	137
4.2.5	Body Weight Measurement and Random Grouping Before	137
	Tumor Induction	
4.2.6	Cell Lines Derived Xenograft Model Development	137
4.2.7	Tumor Size Measurement by Digital Vernier Caliper	138
4.2.8	Mice Body Mass Measurement	138
4.2.9	Drug Administration Schedule & Drug Preparation for Oral Dosage	138
4.2.10	Tumor Growth Inhibition (TGI) Studies	138
4.2.11	Western Blotting	140
4.2.12	Immunohistochemistry Tests	140
4.2.13	H & E Staining	140
4.3	Results	141
· · · · · · · · · · · · · · · · · · ·		·

4.3.1	Impact of EGCG on tumor xenograft mouse model	141
4.3.2	Impact of EA on tumor xenograft mouse model	142
4.3.3	Impact of Combo on tumor xenografts mouse model	145
4.4	Discussion	146
4.5	References	148
	CHAPTER-5	
5	Summary and conclusion	152
	ANNEXURE	
Ι	Publications	155-161
II	Conferences & Seminars	162
III	Certificates (Awards & Recognitions)	164
Iv	Appendix	174
V	Plagiarism report	191

LIST OF FIGURES

Fig No	List of Figures	Page No
1	Pictorial Representation of Epigenetic Mechanisms in the Nucleus and Cytoplasm	3
1.1	Concept of Epigenetic Readers, Writers, and Erasers	4
1.2	Arginine Methylation by Protein Arginine Methyltransferases (PRMTs)	8
1.3	Lysine Methylation with Respect to Enhancer of Zeste Homolog 2 (EZH2) and Polycomb Repressive Complexes (PRCs)	9
1.4	GLOBOCAN 2020 Cancer Data Analysis	13
1.5	In-depth analysis of cancer mortality from GLOBOCAN 2020 data	14
1.6	The Versatile Role of PRMT5 and EZH2 in Cancer	21
1.7	Epigenetic Therapeutic Molecules	26
2.3.1	Chemical Library Preparation Module Workflow.	57
2.3.2	Diverse Chemical Landscape of natural molecules in ligand library preparation	57
2.3.3	Impact of Curcumin (Cur) on the proliferation of human malignant cell lines	59
2.3.4	Impact of Brazilin (Brz) on the proliferation of human malignant cell lines	59
2.3.5	Impact of Resveratrol (Rvr) on the proliferation of human malignant cell lines	60
2.3.6	Impact of Piperine (Ppr) on the proliferation of human malignant cell lines	60
2.3.7	Impact of Quercetin (Qct), on the proliferation of human malignant cell lines	61
2.3.8	Impact of Epigallocatechin-3-gallate (EGCG), on the proliferation of hu malignant cell lines	61
2.3.9	Impact of Ellagic-acid (EA), on the proliferation of human malignant cell lines	62
2.3.10	Trypan blue exclusion assay performed to determine the cell viability of compounds	64
2.3.11	Impact of anti-proliferative molecules on the expression of DNA methyltransferases.	65
2.3.12	Impact of anti-proliferative molecules on the expression of protein arginine methyltransferases	67
2.3.13	Impact of anti-proliferative molecules on the expression of the lysine acetyltransferases.	68
2.3.14	Impact of anti-proliferative molecules on the expression of the histone deacetylases.	69
2.3.15	Impact of anti-proliferative molecules on the expression of the polycomb repressive complex 1 core members	70
2.3.16.	Impact of anti-proliferative molecules on the expression of the polycomb repressive complex 2 core members	71
2.3.17	Illustration of alteration frequencies of PRMT5 across different cancer types	74
2.3.18	Illustration of alteration frequencies of EZH2 across different cancer types	75
2.3.19	Amplification Data and Oncoprint Analysis of PRMT5 and EZH2 Genes in Various Cancer Types	76
2.3.20	Survival Plot (Kaplan-Meier Plot) for PRMT5 in Breast Cancer Patients	78
2.3.21	Survival Plot (Kaplan-Meier Plot) for EZH2 in Breast Cancer Patients	79
3.2.1	Workflow for Molecular Docking	91
3.2.2	Structures of Compounds Used for Molecular Docking	92
3.3.1	Schematic Flowchart of In-Silico Screening Results	101
3.3.2.1	Chemical structure of Epigallocatechin-3-gallate	102
3.3.2.2	Interaction Profile of EGCG with Human PRMT5 and EZH2 Complexes	102

3.3.2.3	Root Mean Square Deviation (RMSD) and Root Mean Square Fluctuation	104
	(RMSF) Analysis of EGCG with PRMT5:MEP50 Complex and Enhancer of	
3.3.2.4	Zeste Homolog 2 (EZH2). Surface Plasmon Resonance (SPR) sensorgram depicting the immobilization	105
3.3.2.4	of PRMT5 and EZH2 on a CM5 sensor chip are shown in panels	103
3.3.2.5	Surface plasmon resonance (SPR) studies were conducted to analyze the	105
3.3.2.3	interaction of EGCG with PRMT5-MEP50 and EZH2 complexes on a CM5	103
	sensor chip.	
3.3.2.6	Impact of EGCG on human malignant cell lines	106
3.3.2.7	Impact of EGCG on methylation marks	107
3.3.2.8	Impact of EGCG on cell proliferation	107
3.3.2.9	EGCG Induces Apoptosis and Autophagy in Breast Cancer Cells	109
3.3.2.9	Chemical structure of EA (Mol wt. 302.19 g/mol, chemical formula: C14H6O8	111
3.4.1		111
	Interaction profiles of EA with the human EZH2 and PRMT5: MEP50	113
3.4.2	Molecular dynamics simulations were conducted to assess the stability of EA with PRMT5 and EZH2	113
3.4.3	Surface Plasmon Resonance Analysis of EA with EZH2 and PRMT5:MEP50	114
3.4.4	Impact of EA on Human Cancer Cell Lines	115
3.4.5	Effect of EA on H3K27me3 and H4R3me2s Methylation Marks.	116
3.4.6	Effect of EA on Cellular Proliferation Dynamics	117
3.4.7	Induction of Apoptosis by EA in Breast Cancer Cells	118
3.4.8	EA Induces Autophagy in Breast Cancer Cells	119
3.5	Impact of Combo on Human Cancer Cell Lines: Various human cancer cell lines	120
3.5.1	Surface Plasmon resonance Studies for Combo with PRMT5:MEP50 and EZH2	121
3.5.2	Effect of Combo on H3K27me3 and H4R3me2s Methylation Marks.	122
3.5.3	Effect of Combo on Cellular Proliferation Dynamics	123
3.5.4	Induction of Apoptosis by combo in Breast Cancer Cells	124
3.5.5	Combo Induces Autophagy in Breast Cancer Cells	125
4.3.1	In-vivo Xenograft Studies with oral EGCG Dosage	141
4.3.2	Immunohistochemistry Studies for EGCG treated mice group	142
4.3.2	In-Vivo Xenograft Model Studies with oral EA Dosage	143
4.4.1	Immunohistochemistry (IHC) Studies for EA treated mice group	144
4.4.1	In-Vivo Xenograft Model Studies with oral Combo Dosage	145
4.5.1	Immunohistochemistry (IHC) Studies for Combo treated mice group	145
4.5.1	minumonistochemistry (HTC) studies for Combo deated mice group	140

LIST OF TABLES

Table	List of Tables	Page
No		No
1.1	Epigenetic Dysregulation and its Association with Various Cancer Types	16
1.2	Role of PRMT5 and EZH2 in various cancers and their mechanism of action	18
1.3	Role of PRMT5 in Cancer and Chronological Order of PRMT5 Inhibitors and	18
	Clinical Trials up to June 2024	
1.4	Role of EZH2 in Cancer and Chronological Order of EZH2 Inhibitors and	20
	Clinical Trials till date.	
1.5	Comprehensive table summarizing the status of epigenetic drugs, including	23
	those targeting DNMTs, HDACs, IDHs, HMTs, PRMTs.	
1.6	PRMT5 Targeted Drugs in Clinical Trials: Phases, Companies, and Indication	24
1.7	EZH2 Targeted Drugs in Clinical Trials: Phases, Companies, and Indication	25
1.8	Molecular Targets of Anti-Proliferative Agents: Epigenetic Regulators and	30
	Their Role in Cancer Therapy	
2.1	Details of the primers used for RT-PCR studies	54
2.2	Impact of anti-proliferative molecules on the malignant cell proliferation	63
2.3	Impact of the anti-proliferative molecules on epigenetic regulator expression.	72
3.1	Top interacting molecules & known substrates to human PRMT5: MEP50	100
	complex	
3.2		100
	Top interacting molecules & known substrates to human EZH2 complex	
3.3	The common interaction profiles of the EGCG with human PRMT5: MEP50	103
	and EZH2	
3.4	The common interaction profiles of EA with human EZH2 and	112
	PRMT5:MEP50	
4.1	Grouping of Mice	137
4.2	Drug dosage schedule for 21 Days	139

APPENDIX-1

Fig	List of Figures	Page
No		No
1.1	Interaction Profile of Brazilin with Human PRMT5 and EZH2 Complexes	174
1.2	Interaction Profile of Resveratrol with Human PRMT5 and EZH2 Complexes	175
1.3	Interaction Profile of Sfp with Human PRMT5 and EZH2 Complexes	176
1.4	Interaction Profile of Apdn with Human PRMT5 and EZH2 Complexes	177
1.5	Interaction Profile of Cpcn with Human PRMT5 and EZH2 Complexes	178
1.6	Interaction Profile of Qct with Human PRMT5 and EZH2 Complexes	179
1.7	Interaction Profile of Ect with Human PRMT5 and EZH2 Complexes	180
1.8	Interaction Profile of Egl with Human PRMT5 and EZH2 Complexes	181
1.9	Interaction Profile of Gba with Human PRMT5 and EZH2 Complexes	182
1.10	Interaction Profile of vorinostat with Human PRMT5 and EZH2 Complexes	183
1.11	Interaction Profile of Ppr with Human PRMT5 and EZH2 Complexes	184
1.12	Interaction Profile of Atl with Human PRMT5 and EZH2 Complexes	185
3.1	Full blot images for ECCG interaction with PRMT5:MEP50 & EZH2	186
3.2	Full blot images for EA interaction with PRMT5:MEP50 & EZH2	187
3.3	Full blot images for COMBO interaction with PRMT5:MEP50 & EZH2	188
4.1	EGCG animal studies western blot (4.3.1section)	189
4.2	EA animal studies western blots (4.4 section)	189
4.3	EA animal studies western blots (4.5 section)	190

CHAPTER# 1 BACKGROUND

1.0 Introduction

Cancer remains a leading cause of death globally, presenting formidable challenges to healthcare systems around the world. Each year, millions of new cancer cases are identified, and the burden is expected to grow significantly in the coming decades ^[1,2]. According to the latest WHO reports, cancer is a major contributor to global mortality, accounting for about one-sixth of all deaths and affecting nearly every household ^[1]. In 2022, approximately 20 million new cancer cases were reported, resulting in 9.7 million deaths worldwide. Projections indicate that by 2050, the cancer burden will increase by around 77%, further straining health systems, individuals, and communities ^[2]. In 2023, nearly 2 million people in the United States alone were diagnosed with cancer, with breast cancer being most common among women and prostate cancer among men ^[3].

Prostate and breast cancer can be influenced by factors such as physical inactivity, obesity, age, family history, and the use of oral contraceptives. The development of these cancers involves both genetic and epigenetic alterations, primarily through epigenetic mechanisms including DNA methylation and histone modifications like methylation, acetylation, phosphorylation, sumoylation, and ubiquitination.^[5]. Among various factors which inducing cancer development and progression, the major hallmark feature will be the epigenetic dysregulation.^[3]. Multicellular organisms consist of specialized cells formed by specific genes being switched on or off to establish cellular identity. In the 1940s, Conrad H. Waddington introduced "epigenetic" factors, proposing the "epigenetic landscape" to describe how cellular differentiation is regulated epigenetically [7-8]. Advances in the twenty-first century have expanded our understanding of epigenetic regulatory mechanisms in gene expression. Defective epigenetic factors can cause dysregulated gene expression, leading to various diseases, including cancer [9-12]. Researchers now target these dysregulated regulators, resulting in clinically approved 'epigenetic drugs' or 'epidrugs,' with many under clinical trials [10]. Researchers are increasingly focusing on 'epigenetic drugs' or 'epidrugs' to treat cancer, targeting dysregulated epigenetic factors, these epidrugs, some of them already clinically approved and others in trials, offer promising new avenues for cancer therapy [14-18]. The following sections discuss the key features of different epigenetic modifications and their relevance to cancer, and finally, the potential of understanding the anti-proliferative mechanisms of naturally occurring chemical molecules for various medicinal applications is

reviewed and documented. A literature survey was conducted to explore the possibilities and challenges of modulating epigenetic mechanisms generally deregulated in cancer.

1.1 The Versatility of Epigenetic mechanisms

The adaptability and versatility of epigenetic mechanisms stem from a myriad of processes operating within cells, including DNA methylation process, post-translational modifications (PTMs) of histones, and miRNA (microRNA) mediated signaling (**Figure-1**) ^[19].

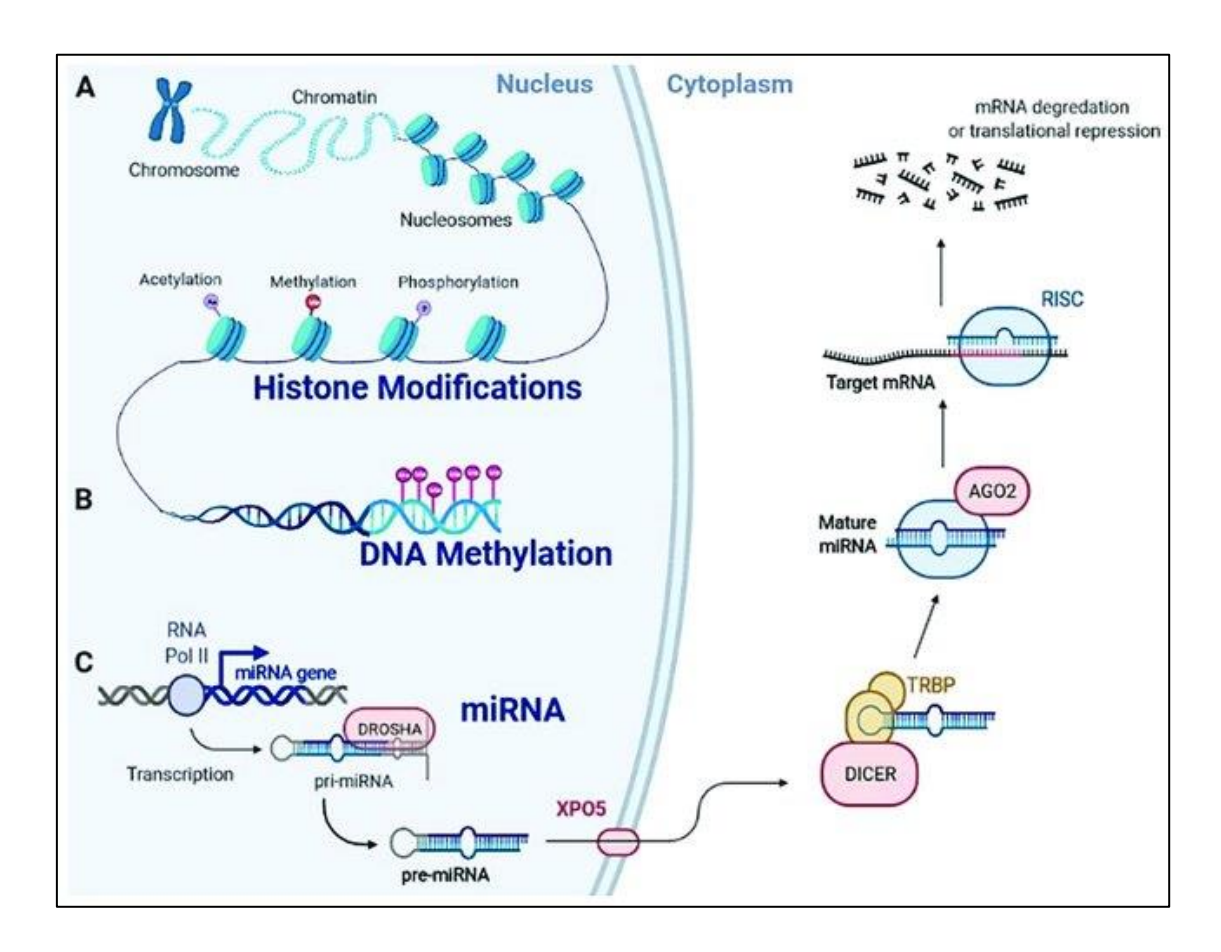


Figure 1: Pictorial Representation of Epigenetic Mechanisms in the Nucleus and Cytoplasm-This figure depicts the major epigenetic mechanisms occurring within the nucleus and cytoplasm of a cell. Key processes include: DNA Methylation: The addition of methyl groups to DNA, primarily at cytosine bases within CpG islands, typically leading to gene silencing. Histone Modification: Various chemical modifications of histone proteins, such as acetylation, methylation, phosphorylation, and ubiquitination, which influence chromatin structure and gene expression. These modifications can either activate or repress transcription depending on the specific modification and its location. Non-coding RNA Regulation: The involvement of microRNAs (miRNAs) and long non-coding RNAs (lncRNAs) in post-transcriptional regulation of gene expression. These RNAs can bind to messenger RNAs (mRNAs) or chromatin to modulate gene expression and protein synthesis. These mechanisms work together to dynamically regulate gene expression and maintain cellular function, and their dysregulation can contribute to the development and progression of cancer. (Image adapted from Rotondo et al, 2021.)

These intricate processes orchestrate a diverse array of chemical modifications within the nucleosome, crucial for maintaining the integrity and functionality of genetic material.

Enzymes play pivotal roles in catalysing the 'addition' of chemical groups, such as methyl, acetyl, ribosyl, ubiquityl, and sumoyl groups, alongside phosphates.

Conversely, another set of enzymes facilitates the removal of these chemical modifications, allowing for dynamic changes in epigenetic marks. Beyond enzymatic processes, proteins adept at 'reading' these chemical signatures transmit altered epigenetic information to various biological machinery, ultimately culminating in epigenetic-based cellular responses ^[17]. This intricate interplay involves a complex network of writers, readers, and erasers, encompassing a multitude of epigenetic regulators (**Figure-1.1**). Subsequent sections delve into these regulators, offering comprehensive insights into their mechanisms of action and biological functions.

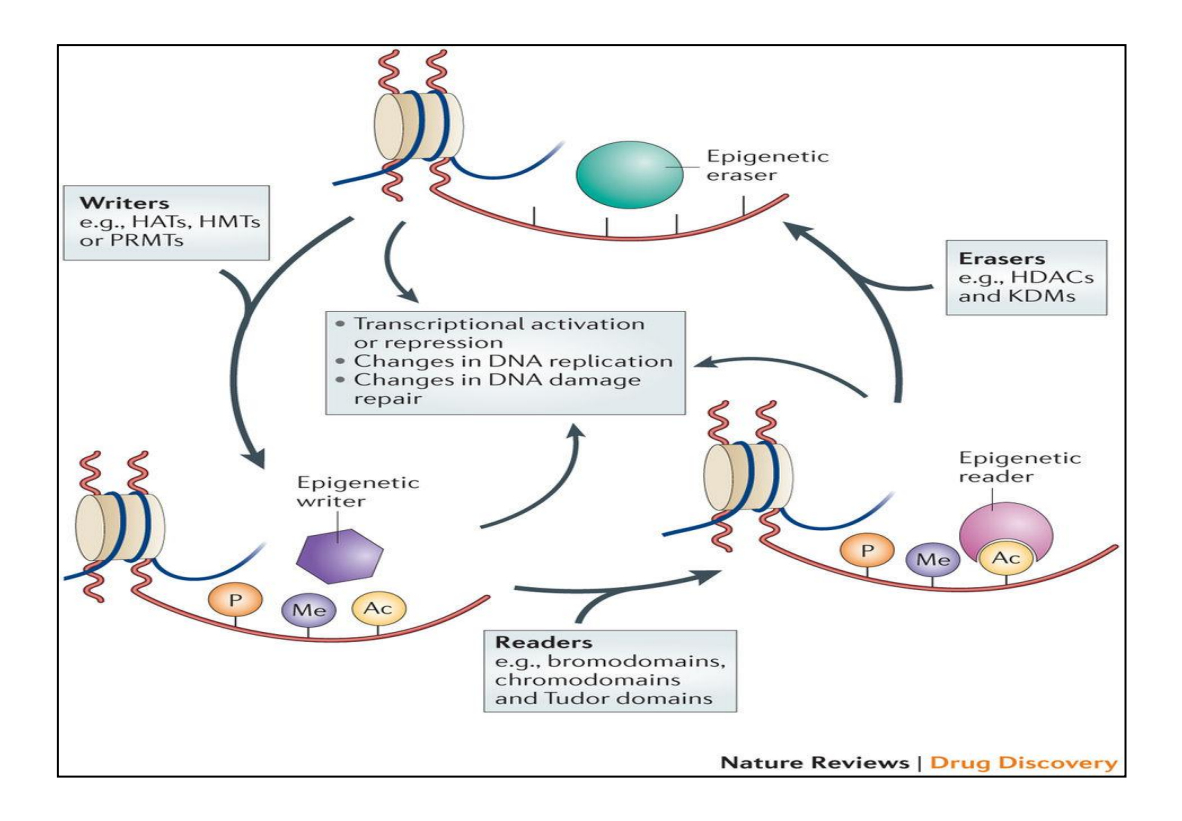


Figure 1.1: Concept of Epigenetic Readers, Writers, and Erasers: Illustration of roles of epigenetic readers, writers, and erasers in the regulation of gene expression: Writers: Enzymes that add chemical modifications to DNA and histones. Examples include DNA methyltransferases (DNMTs), which add methyl groups to DNA, and histone acetyltransferases (HATs), which acetylate histones to promote transcriptional activation. Erasers: Enzymes that remove chemical modifications from DNA and histones. Key examples are histone deacetylases (HDACs), which remove acetyl groups from histones leading to chromatin condensation and gene repression, and ten-eleven translocation (TET) enzymes, which are involved in DNA demethylation. Readers: Proteins that recognize and bind to specific epigenetic modifications, interpreting the epigenetic code to modulate chromatin structure and gene expression. Examples include bromodomain-containing proteins that recognize acetylated histones and methyl-CpG-binding domain proteins that bind to methylated DNA. Together, these components establish, maintain, and interpret epigenetic marks, thereby regulating gene expression patterns essential for cellular identity and function. Dysregulation of these processes is often implicated in cancer and other diseases (Image adapted from Falkenberg, et al.,2014.)

1.1.1 DNA methylation

DNA methylation is a crucial and familiar epigenetic mechanism that modifies gene expression and ensures genome integrity in eukaryotic cells. This process involves adding a methyl group to the DNA molecule, specifically targeting cytosine bases within CpG dinucleotides. DNA methylation's primary function is to regulate gene activity and it is crucial for differentiation, normal development, and cellular activity. DNA methylation is carried out by DNA methyltransferase enzymes, primarily DNMT1, DNMT3A, and DNMT3B. DNMT1 is responsible for maintaining existing methylation patterns during DNA replication, while DNMT3A and DNMT3B are crucial for establishing new methylation marks. [21-24]. These enzymes add methyl groups to cytosines, predominantly in CpG islands located near gene promoters. This methylation generally suppresses gene expression by recruiting proteins transcription factor and preventing transcription factor binding that compact chromatin structure [24-27]. In addition to its role in gene regulation, which also involves in crucial biological functions like genomic imprinting and X-chromosome inactivation. However, abnormal methylation patterns are linked to various diseases, especially cancer, where excessive methylation of tumor suppressor genes can inhibit their expression and contribute to malignancy. Hence, DNA methylation process is a main focused area of study for understanding gene regulation and developing epigenetic therapies [27-28].

1.1.2 Histone modifications

Post translational histone modifications are pivotal for regulating gene expression and chromatin structure. These alterations, which go beyond DNA methylation, encompass a broad spectrum of post-translational changes to histone protein's amino acid side chains. These modifications occur in a highly orchestrated manner, influencing how DNA is packaged and accessed by various cellular machinery. Among the most extensively studied histone modifications, methylation of arginine and lysine residues and lysine acetylation are well studied. These modifications act as dynamic switches, fine-tuning gene expression patterns and ultimately impacting biological processes such as development, differentiation, and response to environmental stimuli. [29].

One particularly noteworthy aspect of histone modification is its intersection PRCs, which determines the epigenetic landscape. PRCs are essential regulators of chromatin structure and function, exerting control over gene expression programs through their ability to modify

histones. By catalysing specific histone modifications, PRCs plays a contribution role in transcriptional repression establishment and maintenance, in so doing influencing cellular identity and fate. Understanding the intricate interplay between histone modifications and PRCs provides valuable insights into the mechanisms governing epigenetic regulation and underscores their implication in moulding biological functions and disease states ^[30-31].

1.1.3 Non-coding RNA mediated signaling pathways

ncRNAs (non-coding RNAs) are varied group of RNA molecules that are not translated into proteins but are essential for regulating gene expression and cellular activities. Among these, microRNAs (miRNAs) are small, typically 20-24 nucleotides long, and are main players in post-transcriptional regulation of the genes. Their role in epigenetic mechanisms has garnered significant attention due to their capacity to regulate the expression of various genes and influence numerous cellular processes. [32].

1.1.3.1 MicroRNAs: Biogenesis and Function

The formation of microRNAs (miRNAs) occurs through several stages. Initially, RNA polymerase II transcribes primary miRNAs (pri-miRNAs). These pri-miRNAs are subsequently processed in the nucleus by the Drosha-DGCR8 complex into precursor miRNAs (pre-miRNAs). These pre-miRNAs are approximately 70 nucleotides in length and have a characteristic hairpin structure. These pre-miRNAs are transported by Exportin-5 to cytoplasm. In the cytoplasm, the enzyme Dicer further processes them into mature miRNA duplexes. One strand of the duplex, identified as the guide strand, is merged into the RISC (RNA-induced silencing complex), while on the other strand, called the passenger strand, is usually degraded. Once integrated into the RISC complex, miRNAs guide the complex to complementary sequences on target messenger RNAs (mRNAs), resulting in mRNA degradation or translational repression. This effectively reduces the target gene expression. Through this mechanism, miRNAs fine-tune the expression of numerous genes involved in several cellular pathways, plays key role in regulation of epigenetic mechanism by influencing chromatin structure, DNA methylation, and histone modification pathways. They target DNA methyltransferases to regulate DNA methylation, modulate histone modifications by targeting enzymes like EZH2, and interact with polycomb repressive complexes. Dysregulation of miRNAs is implicated in diseases, particularly cancer, making them promising therapeutic targets [34].

1.1.4 Protein methyltransferases (PMTs)

Protein methyltransferases (PMTs) are enzymes responsible for transferring methyl groups from S-adenosylmethionine (SAM) to specific amino acid residues found on target proteins. primarily lysine and arginine [35]. This post-translational modification mediates a key functional role in protein regulation, stability, and interaction with other molecules, impacting various processes. Arginine methyltransferases (PRMTs) methyltransferases (KMTs) are the two main classes of these enzymes. KMTs, such as the SET domain-containing family, modify histone proteins by adding methyl groups to lysine residues, influencing chromatin structure and gene expression. For example, SETD1 and SETD2 are involved in the methylation of histone H3 at lysine 36 (H3K36), and lysine 4 (H3K4) respectively, marks connected with active transcription [36-37]. PRMTs methylate arginine residues and are classified into type I, II, and III, based on the kind of methylation reaction they mediate. PRMT1, type I PRMTs generate ADMA (asymmetric dimethylarginine), whereas type II PRMTs, such as PRMT5, generate SDMA (symmetric dimethylarginine) (Figure-1.2). These modifications can regulate gene expression, RNA processing, and signal transduction [38-39]. Dysregulation of protein methyltransferases is connected to several diseases, including cancer. Thus, they are targets for therapeutic intervention, with inhibitors being developed to modulate their activity and restore normal cellular functions [40].

1.14.1 Arginine methylation and lysine methylation

1.1.4.2 Arginine Methylation

Arginine methylation plays a crucial role as post-translational modification that regulates numerous cellular processes. Executed by protein PRMT's, this modification entails adding a methyl group to arginine residues within proteins. Its impact spans gene expression, RNA processing, signal transduction, and protein-protein interactions. PRMTs can either activate or repress target proteins' functions through arginine methylation, as exemplified by its role in histone proteins' methylation for chromatin remodeling and gene transcription regulation. Furthermore, arginine methylation influences RNA-binding proteins' activity, thereby affecting RNA metabolism and processing [41-42]. Dysregulation of this process is concerned in various diseases, such as neurodegenerative disorders and cancer. Understanding arginine

methylation's mechanisms and consequences provides insights into both normal physiology and disease pathology, offering potential therapeutic avenues ^[43].

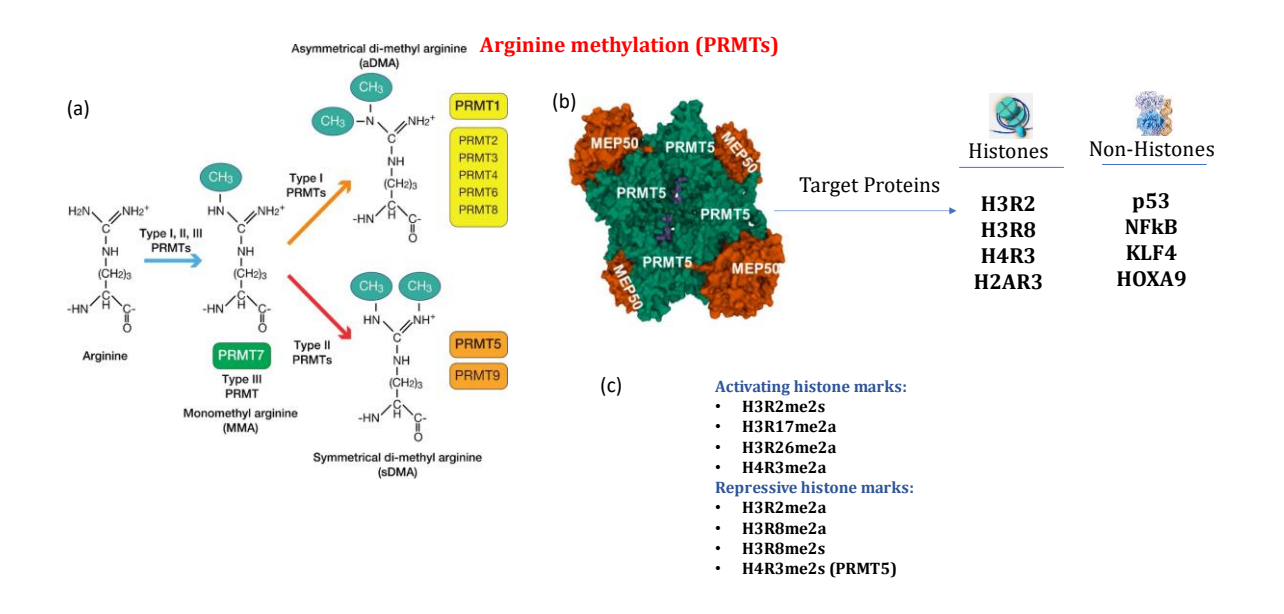


Figure 1.2: Arginine Methylation by Protein Arginine Methyltransferases (PRMTs): (a) **Arginine Methylation Reaction:** This panel illustrates the methylation reaction catalyzed by PRMTs, using S-adenosylmethionine (SAM) as the methyl donor. PRMTs transfer methyl groups to the guanidino nitrogen atoms of arginine residues on target proteins. The types of PRMTs include: Type I PRMTs: Catalyze the formation of asymmetric dimethylarginine (aDMA). Type II PRMTs: Catalyze the formation of symmetric dimethylarginine (sDMA). Type III PRMTs: Catalyze the formation of monomethylarginine (MMA). (b) Crystal Structure of PRMT5-MEP50 Complex: This panel shows the crystal structure of the PRMT5-MEP50 complex interacting with both histone and non-histone substrates. PRMT5, a type II PRMT, works with its cofactor MEP50 to facilitate the symmetric dimethylation of arginine residues, highlighting the structural basis for substrate recognition and catalysis. (c) Active and Repressive Marks: This panel depicts the role of arginine methylation marks in gene regulation. Active marks (such as H3R17me2a, catalyzed by type I PRMTs) are associated with transcriptional activation, while repressive marks (such as H4R3me2s, catalyzed by PRMT5) are linked to transcriptional repression. These modifications influence chromatin dynamics and gene expression by recruiting specific reader proteins that interpret these epigenetic marks.

1.1.4.3 Lysine Methylation

Lysine methylation is another crucial post-translational modification vital for cellular regulation. Catalyzed by lysine methyltransferases, this modification entails adding a methyl group to lysine residues within proteins (**Figure-1.3**). Its roles encompass gene expression, DNA repair, and protein-protein interactions. Lysine methylation of histone proteins works by either activating or repressing gene transcription, conditional on the lysine residue involved chromatin environment conditions. [44-45]. Moreover, lysine methylation regulates non-histone proteins, impacting signaling pathways and metabolic processes.

Lysine methylation (EZH2)

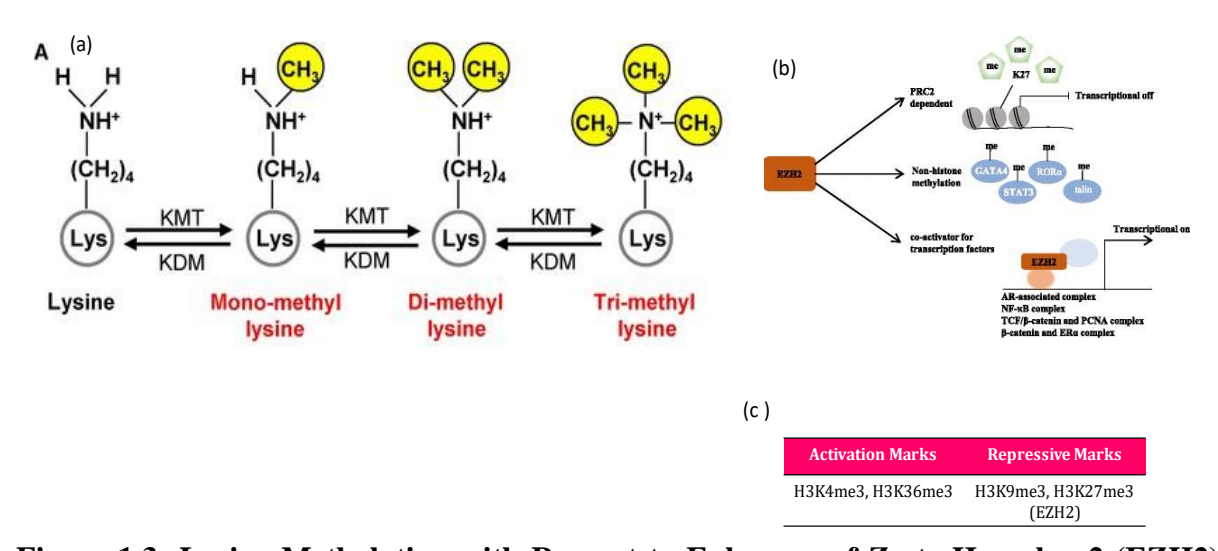


Figure 1.3: Lysine Methylation with Respect to Enhancer of Zeste Homolog 2 (EZH2) and Polycomb Repressive Complexes (PRCs): (a) Lysine Methylation: This panel illustrates the lysine methylation reaction, a key epigenetic modification catalyzed by histone lysine methyltransferases (HKMTs). Lysine residues on histone tails are mono-, di-, or trimethylated, leading to alterations in chromatin structure and gene expression regulation. (b) **EZH2 with Polycomb Repressive Complex (PRC) and Other Domains:** This panel depicts EZH2, a histone lysine methyltransferase component of the Polycomb Repressive Complex 2 (PRC2). EZH2 catalyzes the methylation of histone H3 lysine 27 (H3K27me3), leading to transcriptional repression. The figure also shows other domains of EZH2, such as the SET domain responsible for methyltransferase activity and the WD40 domain involved in protein-protein interactions within the PRC2 complex. (c) **Repressive and Active Marks:** This panel highlights the role of lysine methylation marks in gene regulation. Repressive marks, such as H3K27me3 catalyzed by EZH2, are associated with transcriptional repression, while active marks, such as H3K4me3, are linked to transcriptional activation. These modifications contribute to the establishment of chromatin states that regulate gene expression patterns and cellular identity (image adopted and modified accordingly Morales2016, Kim 2021, & Gan 2018).

Dysregulation of this process is implicated in diseases like cancer and metabolic syndromes, emphasizing its role in cellular balance. Understanding lysine methylation's mechanisms and consequences provides insights into both normal physiology and disease progression, offering potential therapeutic targets ^[45-46].

1.1.5 Poly comb repressive complexes

Epigenetic regulation plays a crucial role in controlling gene expression by reorganizing local chromatin structures. Among the factors regulating chromatin, Polycomb group (PcG) proteins are key players in epigenetic control and chromatin organization. The initial PcG gene, Polycomb (PC), was discovered in *Drosophila melanogaster* in 1947 by Dr. Pamela Lewis, who noticed that Pc mutant larvae exhibited altered segmentation phenotypes ^[194]. Later genetic screens identified more genes with similar phenotypes, defining the group of Polycomb (PcG) genes. Research, including yeast two-hybrid assays and biochemical studies, has

demonstrated that PcG proteins assemble into two main protein complexes: PRC1 (Polycomb Repressive Complex) and PRC2 (Polycomb Repressive Complex 2) [195,196].

PRCs are critical regulatory mechanisms in eukaryotic cells, essential for gene silencing and directing developmental processes. These complexes consist of Polycomb group proteins and are primarily categorized into PRC1 and PRC2, each with distinct roles in modulating gene expression.

1.1.5.1 PRC2 Composition and Function

PRC2 consists of core subunits such as EZH2 (Enhancer of Zeste Homolog2), EED (Embryonic Ectoderm Development), and SUZ12 (Suppressor of Zeste 12). PRC2 is responsible for trimethylating H3K27me3 (histone H3 at lysine 27) [47-48], a repressive histone modification essential for gene silencing. This modification signals chromatin compaction and transcriptional repression, regulating genes that must be inactive during specific developmental stages or cell types [197-198].

1.1.5.2 PRC1 Composition and Function

PRC1, which includes core components such as Chromobox (CBX) proteins, Ring finger proteins (RING1A/B), and Polyhomeotic (PHC) proteins, recognizes the H3K27me3 mark established by PRC2. PRC1 is then recruited to these sites, where it monoubiquitinates H2AK119ub (histone H2A at lysine 119). These modification leads to further chromatin compaction and stable gene repression. The interplay between PRC1 and PRC2 ensures precise control over gene expression patterns, which is crucial for processes like cellular differentiation, stem cell maintenance, and embryonic development [48-50].

1.1.5.3 Biological Roles of PRCs

PRCs are indispensable for regulating gene expression throughout development and maintaining cellular identity. During developmental processes, PRCs facilitate the transition from pluripotent stem cells to differentiated cell types by dynamically modulating gene expression. They create a repressive chromatin environment at specific genomic loci, crucial for the activation and repression of genes needed for determining cell fate. In stem cells, PRCs help maintain pluripotency by silencing lineage-specific genes, thus preserving the

undifferentiated state. When differentiation signals are received, PRC-mediated repression is lifted at these genes, allowing for their expression and the emergence of specialized cell identities.

Beyond their roles in development, PRCs play significant roles in maintaining cellular homeostasis and responding to environmental changes. These proteins are involved in numerous cellular processes, including DNA repair, stress responses and cell cycle regulation. By modulating genes responsive to stress, PRCs enable cells to adapt to changing conditions and maintain proper physiological functions. For instance, in DNA repair, PRCs can silence genes that promote apoptosis, allowing for cell survival and recovery. PRCs regulates cyclins expressions and cell cycle-associated proteins in cell cycle, thereby ensuring controlled cell proliferation and preventing uncontrolled cell growth, which can lead to cancer.

1.1.5.4 Dysregulation of PRCs and Disease

Aberrations in Polycomb complex function are implicated in various pathologies, underscoring their significance in normal cellular physiology and disease etiology. Dysregulation of PRCs can lead to improper activation or gene silencing leading to diseases mainly such as cancer, neurodevelopmental disorders, and other age-related conditions. For example, overexpression of EZH2, a component of PRC2, has been notified in several cancers, which includes breast and prostate cancer, where it leads to the tumor suppressor genes silencing and promotes uncontrolled cell proliferation. Similarly, mutations in components of PRC1 and PRC2 have been connected to developmental disorders for example Kabuki syndrome and Wiedemann-Steiner syndrome, which are characterized by intellectual disability, growth delays, and distinct facial features [199-200].

In cancer, the dysregulation of PRCs often contribute to the tumor suppressor genes silencing and oncogenes activation, contributing to tumor development and progression. In neurodevelopmental disorders, mutations in PRC components can lead to aberrant neuronal differentiation and function, resulting in cognitive impairments and other neurological symptoms. In age-related diseases, changes in PRC function can affect the regulation of genes implicated in cellular senescence and aging, potentially contributing to the decline in tissue function and the onset of age-related pathologies. In summary, PRCs are essential for regulating gene expression, maintaining cellular identity, and ensuring proper development and physiological function. The dysregulation of PRCs can contribute to a several of diseases,

emphasizing the importance of comprehending their mechanisms and roles in both health and disease ^[199-201].

1.2 Epigenetics and Cancer

Epigenetics, is the branch of science, refers to the study of heritable changes in gene expression without any alterations in the DNA sequence, is increasingly recognized as a critical factor in cancer development. Dysregulation of DNA methylation, histone modifications, and chromatin remodeling, contributes to abnormal gene expression patterns observed in various cancers ^[51]. Key regulators of these processes, such as DNMTs, HDACs, and HATs, and ATP-dependent chromatin remodelers, play crucial roles in maintaining genomic stability, controlling cellular differentiation, and regulating pathways involved in tumor suppression and oncogenesis. Dysregulation of these epigenetic regulators can lead to oncogenes activation or tumor suppressor genes silencing and promotes cancer initiation, progression, and metastasis. Moreover, epigenetic alterations contribute to the heterogeneity of cancer cells and their [52] adaptation to changing microenvironments, complicating treatment strategies Understanding the intricate interplay between epigenetic dysregulation and cancer biology offers opportunities for the progress of novel epigenetic therapies and precision medicine methods tailored to target specific epigenetic vulnerabilities in individual cancers, potentially improving patient outcomes [52-53].

1.3 Overview of breast cancer (India & abroad):

1.3.1 Cancer Statistics:

Cancer continues to be a significant global health burden, with millions of new cases diagnosed annually. According to recent data, cancer affects people of all ages and backgrounds, with incidence rates varying across regions and populations ^[58]. In many countries, cancer incidence rates are rising due to factors such as population growth, aging populations, changes in lifestyle habits, and environmental exposures. This trend emphasizes the urgent need for comprehensive cancer prevention and control strategies aimed at mitigating the impact of this disease on individuals and communities worldwide. Among the myriad types of cancer, certain forms are consistently reported at higher rates across different populations. These include lung cancer, which is strongly connected with tobacco smoking and consumption, and breast cancer, which affects both genders but is more common in women. Other frequently observed cancers include prostate cancer in males and colorectal cancer in both females and males. These cancers often

receive heightened attention due to their significant impact on morbidity, mortality, and healthcare resources ^[3,59].

1.3.2 Cancer in India and around the world:

In India, the projected number of cancer new cases for the year 2022 was 1,461,427, with a raw data of 100.4 per 100,000 individuals. Frighteningly, it is reported that one in nine people in India may develop cancer during their lifetime. Lung cancer emerged as the predominant cancer amongst males, although breast cancer ranked highest among females (**Figure 1.4**).

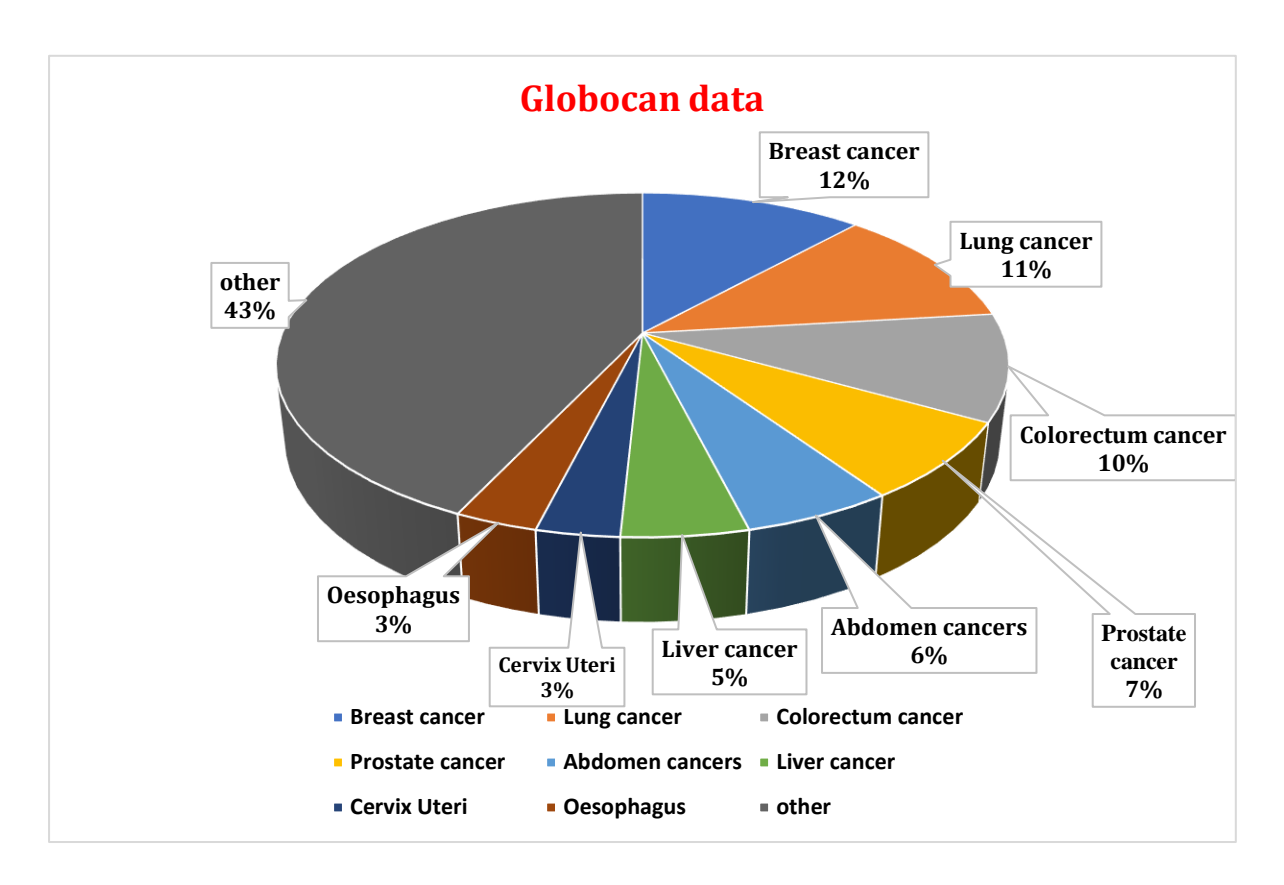


Figure 1.4: GLOBOCAN 2020 Cancer Data Analysis: Comprehensive analysis of global cancer data from globocan 2020: total number of cancer cases in 2020 across both sexes and all age groups- illustrating the total number of cancer cases and deaths globally across all ages and both sexes. Among the various cancer types, breast cancer emerged as the most diagnosed, surpassing lung cancer, with an estimated 2.3 million new cases, representing nearly 12% of all new cancer cases in 2020. Additionally, the total number of cancer-related deaths in 2020 is depicted, with breast cancer accounting for 7% (684,996 deaths) of the total fatalities across both sexes and all age groups.

Among children aged 0-14 years, lymphoid leukemia was the most prevalent cancer type. Projections indicate a worrisome increase of 12.8% in cancer cases by 2025 compared to 2020 ^[58]. These findings highlight the critical importance of implementing comprehensive cancer prevention and control strategies, focusing on early detection, risk reduction, and effective management to combat this growing health challenge in India.

According to the latest GLOBOCAN data, in 2023 (https://gco.iarc.fr/en) the estimations revealed that occurrence of 19.3 million cancer cases and approximately 10 million global cancer deaths. The most prevalent cancers included lung, breast, prostate, colorectal, and stomach cancers. Breast cancer was the maximum frequently diagnosed, (Figure-1.5) lung cancer remained the top cause of cancers with 2.3 million new cancer cases, and leading cause for cancer death. responsible for 1.8 million fatalities. These statistics underscore the critical need and action plan for enhanced early detection for cancer prevention, and effective treatment strategies worldwide to address the growing burden of this disease [59].

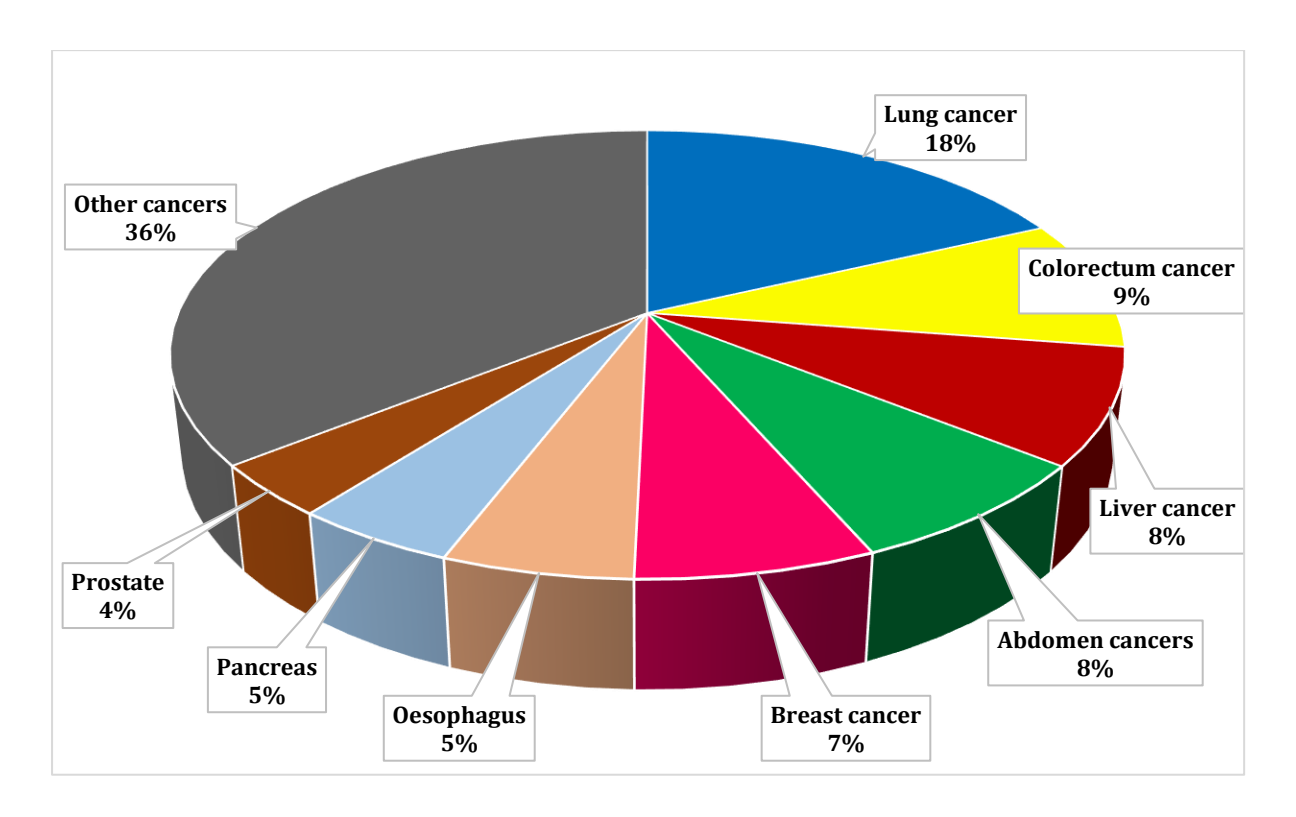


Figure-1.5: **In-depth analysis of cancer mortality from GLOBOCAN 2020 data:** Detailing the total number of deaths across various cancer types, both sexes, and all age groups. Leading cancers such as lung, colorectal, and liver cancer are highlighted, along with their respective mortality figures. Additionally, the percentage of deaths attributable to each cancer type is calculated, providing a comprehensive overview of global cancer burden.

1.3.3 Breast Cancer: most highly reported cancer among all

Breast cancer stands out as one of the most highly reported cancers globally, affecting millions of women each year. The prevalence of breast cancer is particularly notable in countries like India and abroad. Several factors contribute to the high incidence of breast cancer in these regions. Firstly, lifestyle changes, including delayed childbearing, reduced breastfeeding, and increased alcohol consumption, have been linked to an elevated risk of breast cancer ^[6]. Additionally, genetic predisposition, family history, and hormonal factors play significant roles

in breast cancer development ^[3]. Furthermore, limited access to screening, early detection, and healthcare services in certain regions exacerbates the problem. In India, cultural and societal factors may also influence breast cancer reporting and diagnosis, including stigma associated with the disease, lack of awareness, and misconceptions about breast health. In conclusion, breast cancer's high incidence in India and abroad is multifactorial, arising from a complex interaction of genetic, environmental, lifestyle, and healthcare access issues ^[60]. Addressing these challenges requires a comprehensive approach, including awareness campaigns, educational trips, equitable access to screening and treatment services and improved healthcare infrastructure, by addressing these underlying issues, these factors can work towards reducing the burden of cancer incidences especially breast cancer and which eventually improves outcomes for affected individuals globally ^[61].

1.3.4 Dysregulation of Epigenetic regulators lead to cancer

Dysregulation of epigenetic regulators is a pivotal driver in cancer development, where alterations in gene expression patterns and chromatin structure contribute to oncogenesis. Aberrant activity of enzymes like DNMTs, HMTs and HDACs disrupts the normal epigenetic landscape, promoting tumor initiation and progression (**Table-1.1**). This dysregulation can eventually lead to oncogenes activation or tumor suppressor genes silencing, fuelling uninhibited cell growth, metastasis, and therapeutic resistance. Understanding and targeting these epigenetic abnormalities offer promising avenues for cancer diagnosis, prognosis, and therapy development, heralding a new era in precision oncology ^[64].

1.4 Cancer databases:

Cancer databases are vital tools in oncology, compiling genetic, clinical, and molecular data to advance research. Developed through large-data scale projects such as the International Cancer Genome Consortium (ICGC), and well-known The Cancer Genome Atlas (TCGA) and these databases gather and store information from genomic sequencing, medical imaging, clinical trials, and patient records. Platforms like cBioPortal provide user-friendly access to this data, facilitating analysis and visualization. Multidisciplinary teams, including bioinformaticians and oncologists, ensure data accuracy through continuous updates and validation. These databases foster global collaboration, significantly contributing to cancer research and the development of new treatments.

Table-1.1 Epigenetic Dysregulation and its Association with Various Cancer Types

Epigenetic	Alteration	Reference
Regulator		
EZH2	Histone methyltransferase activity leading to H3K27 methylation and gene silencing	[65,68]
PRMT5	Protein arginine methyltransferase activity affecting histones and non-histone proteins	[67,68]
DNMT3B	DNA methyltransferase activity leading to DNA methylation and gene silencing	[69]
HDACs	Histone deacetylase activity leading to histone deacetylation and gene repression	[70]
TET2	Loss-of-function mutations leading to altered DNA methylation and gene expression	[71]
MLL	Rearrangements and fusion proteins leading to histone H3K4 methylation and gene activation	[69, 72]
IDH1/2	Gain-of-function mutations leading to the production of 2-hydroxyglutarate and altered DNA/histone methylation	[73]
LSD1	Histone demethylase activity leading to H3K4 demethylation and gene regulation	[74]

Cancer databases like TCGA ^[52](https://www.cancer.gov/ccg/research/genome-sequencing/tcga) and cBioPortal ^[53-54] (https://www.cbioportal.org/) offer comprehensive molecular characterization of cancer, aiding researchers in understanding genetic alterations and clinical outcomes across various cancer types. Researchers can easily access and retrieve data from these platforms, integrating information from diverse cancer projects and atlases to facilitate in-depth analyses and accelerate discoveries in cancer research. Freely available cancer databases provide valuable resources for researchers to access and analyse the database of genomic, transcriptomic, and clinical datasets for various cancer types.

1.4.1 The Cancer Genome Atlas (TCGA)

TCGA is an all-inclusive and comprehensive resource that provides molecular characterization of various cancer types, including genomic, transcriptomic, and epigenomic data. It contains data from thousands of cancer patients and is a cornerstone of cancer research.

1.4.2 cBioPortal for Cancer Genomics

cBioPortal is an open-access cancer database platform that enables visualization and analysis of large-scale database and curative cancer genomics databases, together with data from TCGA and other studies. It allows researchers to explore genetic alterations, gene expression, and clinical outcomes across different cancer types. cBioPortal offers user-friendly interfaces for querying and visualizing genomic data, making it accessible to researchers with varying levels of bioinformatics expertise. It integrates diverse types of data, including copy number alterations, somatic mutations, and mRNA expression, facilitating comprehensive analyses of cancer genomes. Additionally, cBioPortal provides tools for exploring relationships between genetic alterations and clinical outcomes, aiding in the identification of potential therapeutic targets and biomarkers. TCGA datasets, available through cBioPortal and other platforms, have revolutionized cancer research by providing a wealth of molecular data from a large cohort of patients. These datasets enable researchers to conduct integrative analyses, uncovering novel insights into the molecular mechanisms driving cancer progression and finding possible therapeutic opportunities. By leveraging freely available resources like cBioPortal and TCGA datasets, researchers can accelerate discoveries in cancer biology and facilitate the development of personalized cancer therapies.

1.4.3 Versatile role of PRMT5 and EZH2

PRMT5 and EZH2 are frequently overexpressed in cancer, playing crucial roles in regulating gene expression through methylation mechanisms. PRMT5 catalyzes the methylation of arginine residues on both histones and other proteins, while EZH2 mediates the methylation process on lysine 27 of histone H3. Table 1.2 summarises the role of PRMT5 and EZH2 in various cancers and their mechanism of action clearly.

The detailed literature and web-based search information related to the role of PRMT5 and EZH2 in cancer, along with an up-to-date chronological list of inhibitors and clinical trial compounds for PRMT5 and EZH2 are tabulated in Table-1.3 & 1.4

Table 1.2 Role of PRMT5 and EZH2 in various cancers and their mechanism of action

Target	Role in Cancer	Mechanism	Associated Cancer Types	References
PRMT5	Promotes tumor growth and survival	Methylates arginine residues on histones and other proteins, regulating gene expression	Glioblastoma, lymphoma, lung cancer, breast cancer, prostate cancer, leukemia, melanoma, bladder cancer, ovarian cancer	[156-160]
PRMT5	Modulates splicing of mRNA	Alters the splicing of pre-mRNA, affecting protein production and cell cycle regulation	Prostate cancer, leukemia, breast cancer, lung cancer, melanoma	[68, 159,160]
PRMT5	Induces epigenetic silencing	Represses tumor suppressor genes through methylation of histone H4R3	Melanoma, bladder cancer, lung cancer, ovarian cancer	[160-162]
EZH2	Enhances cancer cell proliferation	Methylates lysine 27 on histone H3 (H3K27me3), leading to gene silencing	Prostate cancer, breast cancer, lymphoma, lung cancer, ovarian cancer, glioblastoma, leukemia, bladder cancer	[163-165]
EZH2	Facilitates metastasis	Regulates epithelial-to- mesenchymal transition (EMT), promoting invasion and metastasis	Prostate cancer, ovarian cancer, breast cancer, melanoma, lung cancer	[166-167]
EZH2	Inhibits differentiation	Maintains stemness and inhibits differentiation of cancer stem cells	Leukemia, glioblastoma, breast cancer, prostate cancer, lung cancer	[163, 167,168]

Table-1.3- Role of PRMT5 in cancer and chronological order of PRMT5 Inhibitors and clinical trials up to June 2024

Discovery of PRMT5 role in Cancer							
S. No	Event happened	Year	Reference				
1	Initial characterization of PRMT5 and its catalytic activity on symmetric dimethylarginine residues was published	1998-2001	[202]				
2	PRMT5 was identified as a regulator of histone methylation, implicating it in transcriptional repression of tumor suppressor genes	2004	[203]				
3	PRMT5 was implicated in the regulation of cell proliferation and differentiation, hinting at its potential involvement in oncogenesis	2010	[204]				
4	Studies demonstrated that PRMT5 is overexpressed in several cancers, including lymphoma and leukemia, suggesting its role in cancer development	2013	[205]				
5	Further research confirmed that PRMT5 promotes tumorigenesis through epigenetic silencing of tumor suppressor genes	2014	[206]				
Discovery of PRMT5 Inhibitors and Clinical Trials							
6	Discovery of the first small-molecule inhibitors targeting PRMT5. These inhibitors showed promise in preclinical models of cancer (Cell Stress).	2015	[207]				

The role of PRMT5 in solid tumors, including lung cancer, was established PRMT5 inhibitors were further optimized for better and specificity. Preclinical studies demonstrated that PRMT5 inhibits synergize with other cancer therapies, including cher and immunotherapy. Clinical interest in PRMT5 inhibitors increased, with pharmaceutical companies initiating drug developrograms. Initial preclinical studies indicated that PRMT5 could overcome resistance to existing cancer treatms. Early-phase clinical trials (Phase I) for PRMT5 began, focusing on safety, tolerability, and preficacy in patients with advanced cancers. GSK and were notable companies initiating these trials. Ongoing Phase I clinical trials showed encouraging anti-tumor activity in patients with hematologic materials and solid tumors. GSK's GSK3326595 and Epizym 2302 were prominent PRMT5 inhibitors in these trials. Phase II clinical trials were initiated to further ever efficacy and safety of PRMT5 inhibitors in a larger patients. Companies like GSK and Epizyme led these Combination studies with other targeted therapies and combination studies wi	er efficacy 2016 ation could motherapy ith several velopment 2017 inhibitors ents 2018 inhibitors reliminary d Epizyme g signs of 2019	[208]
Preclinical studies demonstrated that PRMT5 inhibit synergize with other cancer therapies, including cher and immunotherapy. 8 Clinical interest in PRMT5 inhibitors increased, with pharmaceutical companies initiating drug developrograms. Initial preclinical studies indicated that PRMT5 could overcome resistance to existing cancer treatmed began, focusing on safety, tolerability, and prefficacy in patients with advanced cancers. GSK and were notable companies initiating these trials. 10 Ongoing Phase I clinical trials showed encouraging anti-tumor activity in patients with hematologic materials and solid tumors. GSK's GSK3326595 and Epizymed 2302 were prominent PRMT5 inhibitors in these trials. 11 Phase II clinical trials were initiated to further ever efficacy and safety of PRMT5 inhibitors in a larger patients. Companies like GSK and Epizyme led these	ition could motherapy ith several velopment inhibitors ents inhibitors reliminary d Epizyme g signs of 2019	[209]
synergize with other cancer therapies, including cher and immunotherapy. Clinical interest in PRMT5 inhibitors increased, with pharmaceutical companies initiating drug devaprograms. Initial preclinical studies indicated that PRMT5 could overcome resistance to existing cancer treatms. Early-phase clinical trials (Phase I) for PRMT5 began, focusing on safety, tolerability, and preficacy in patients with advanced cancers. GSK and were notable companies initiating these trials. Ongoing Phase I clinical trials showed encouraging anti-tumor activity in patients with hematologic math and solid tumors. GSK's GSK3326595 and Epizym 2302 were prominent PRMT5 inhibitors in these trials. Phase II clinical trials were initiated to further ever efficacy and safety of PRMT5 inhibitors in a larger patients. Companies like GSK and Epizyme led these	ith several velopment 2017 inhibitors ents inhibitors reliminary d Epizyme g signs of 2019	[210]
pharmaceutical companies initiating drug deverograms. Initial preclinical studies indicated that PRMT5 could overcome resistance to existing cancer treatmed. Early-phase clinical trials (Phase I) for PRMT5 began, focusing on safety, tolerability, and prefficacy in patients with advanced cancers. GSK and were notable companies initiating these trials. Ongoing Phase I clinical trials showed encouraging anti-tumor activity in patients with hematologic mand solid tumors. GSK's GSK3326595 and Epizym 2302 were prominent PRMT5 inhibitors in these trials. Phase II clinical trials were initiated to further ever efficacy and safety of PRMT5 inhibitors in a larger patients. Companies like GSK and Epizyme led these	inhibitors ents inhibitors reliminary d Epizyme g signs of 2019	[210]
 could overcome resistance to existing cancer treatm Early-phase clinical trials (Phase I) for PRMT5 began, focusing on safety, tolerability, and prefficacy in patients with advanced cancers. GSK and were notable companies initiating these trials. Ongoing Phase I clinical trials showed encouraging anti-tumor activity in patients with hematologic mand solid tumors. GSK's GSK3326595 and Epizym 2302 were prominent PRMT5 inhibitors in these trials. Phase II clinical trials were initiated to further ever efficacy and safety of PRMT5 inhibitors in a larger patients. Companies like GSK and Epizyme led these 	ents inhibitors 2018 reliminary d Epizyme g signs of 2019	
 Early-phase clinical trials (Phase I) for PRMT5 began, focusing on safety, tolerability, and prefficacy in patients with advanced cancers. GSK and were notable companies initiating these trials. Ongoing Phase I clinical trials showed encouraging anti-tumor activity in patients with hematologic mand solid tumors. GSK's GSK3326595 and Epizym 2302 were prominent PRMT5 inhibitors in these trials. Phase II clinical trials were initiated to further ever efficacy and safety of PRMT5 inhibitors in a larger patients. Companies like GSK and Epizyme led these 	inhibitors reliminary d Epizyme g signs of 2019	
anti-tumor activity in patients with hematologic ma and solid tumors. GSK's GSK3326595 and Epizym 2302 were prominent PRMT5 inhibitors in these tria Phase II clinical trials were initiated to further ev efficacy and safety of PRMT5 inhibitors in a larger patients. Companies like GSK and Epizyme led these		F005 0107
efficacy and safety of PRMT5 inhibitors in a larger patients. Companies like GSK and Epizyme led thes	als.	[207-210]
checkpoint inhibitors were launched.	cohort of se efforts.	[207-210]
Results from Phase I/II trials were published, dem significant clinical benefit in certain patient po particularly those with PRMT5-dependent tumors. Prelude Therapeutics joined the efforts with its inhibitor, PRT543, entering clinical trials.	opulations,	[211]
Expanded Phase II trials included a broader range of and biomarker studies were initiated to identify patalikely to benefit from PRMT5 inhibition. GSK, Epis Prelude Therapeutics were key players. Novel PRMT5 inhibitors with improved pharms properties entered clinical trials.	ients most zyme, and	[212]
Ongoing trials continued to show promising results, PRMT5 inhibitors advancing to Phase III trials. Resulted the mechanisms of resistance to PRMT5 inhibit potential combination strategies intensified. GSK3326595 and Prelude's PRT543 were among the candidates.	search into bitors and . GSK's	[207-212]
The first Phase III trial results were anticipated, pleading to the first regulatory approvals of PRMT5 for specific cancer indications. Continued exploit PRMT5 inhibitors in combination with other including immunotherapy and targeted agents. GSK, and Prelude Therapeutics remained at the forefrond developments.	inhibitors pration of therapies, Epizyme,	[207,212]

Table-1.4- Role of EZH2 in cancer and chronological order of EZH2 inhibitors and clinical trials till date.

	overy of EZH2 role in Cancer		
S.	Event happened	Year	Reference
No	Event nappened	1 cai	Reference
1	The significance of EZH2 in cancer was first realized when Varambally and colleagues linked EZH2 upregulation to prostate cancer prognosis, indicating its association with advanced stages and poor prognosis	2002	[213]
2	Studies identified EZH2 overexpression in various solid malignancies, including breast, lung, liver, colorectal, and pancreatic cancers, establishing its role in cancer progression and poor prognosis	2003-04	[214]
3	EZH2 was shown to promote epithelial-mesenchymal transition (EMT), invasion, and metastasis in multiple cancers, including melanoma, pancreatic cancer, and breast cancer	2007-10	[215]
4	Research demonstrated that EZH2 overexpression could lead to drug resistance in cancer treatment, notably in prostate cancer, by interacting with androgen receptor signaling	2011	[216]
5	The first <i>in vivo</i> studies showed that EZH2 knockdown could significantly reduce metastasis in mouse models of melanoma and lung cancer	2013	[217]
6	EZH2 was found to play a dual role in cancer, acting as both an oncogene and a tumor suppressor depending on the cellular context. This was particularly noted in myeloid malignancies and some solid tumors	2015-17	[218-219]
7	Detailed mechanistic studies uncovered the involvement of EZH2 in various signaling pathways, such as PI3K/Akt, Wnt/β-catenin, and p53, highlighting its central role in cancer cell survival, proliferation, and metastasis	2020	[220]
Yea	r-wise discovery of EZH2 inhibitors and clinical trials		
6	Discovery of the first EZH2-specific inhibitor, EPZ-6438 (Tazemetostat), by Epizyme. Preclinical studies demonstrated its potential in reducing tumor growth in EZH2-mutant cancers	2012	[221]
7	Tazemetostat entered Phase I clinical trials for patients with relapsed or refractory B-cell non-Hodgkin lymphomas and advanced solid tumors	2014	[222]
8	GSK126, another EZH2 inhibitor developed by GlaxoSmithKline, showed promising results in preclinical studies and entered early-phase clinical trials for various cancers	2017	[223]
9	CPI-1205, an EZH2 inhibitor by Constellation Pharmaceuticals, began Phase I/II clinical trials, focusing on patients with metastatic castration-resistant prostate cancer (mCRPC)	2018	[224]
10	Tazemetostat received accelerated approval from the FDA for the treatment of epithelioid sarcoma, marking the first EZH2 inhibitor to reach the market	2019	[225]
11	Novartis initiated Phase I clinical trials for MAK683, targeting hematologic malignancies and solid tumors with EZH2 dysregulation	2021	[226]
12	Additional clinical trials were launched for Tazemetostat, exploring its efficacy in combination therapies for various cancers, including ovarian and endometrial cancers	2022	[227]
13	Ongoing trials for newer EZH2 inhibitors, such as PF-06821497 by Pfizer, are exploring their potential in treating different types of lymphoma and solid tumors	2023	[228]

Both enzymes influence chromatin structure as well as show influence on transcription, impacting gene expression levels and contributing to oncogenic methods such as uncontrolled cell proliferation, metastasis, and resistance to apoptosis. Their dysregulation makes them attractive targets for cancer therapy development. (**Figure-1.6**) and table-1.2 summarizes the roles and mechanisms of PRMT5 and EZH2 in various cancers, based on data from cBioPortal and other sources.

Inhibition of PRMT5 and EZH2 activity has shown promise in preclinical studies and clinical trials, with several small molecule inhibitors under investigation. Targeting these enzymes offers a multifaceted approach to cancer treatment, potentially disrupting key pathways driving tumor growth and development. As research progresses in deciphering the complexities of epigenetic regulation in cancer, PRMT5 and EZH2 remain focal points for drug discovery efforts focused on enhancing patient outcomes and broadening treatment options in oncology.

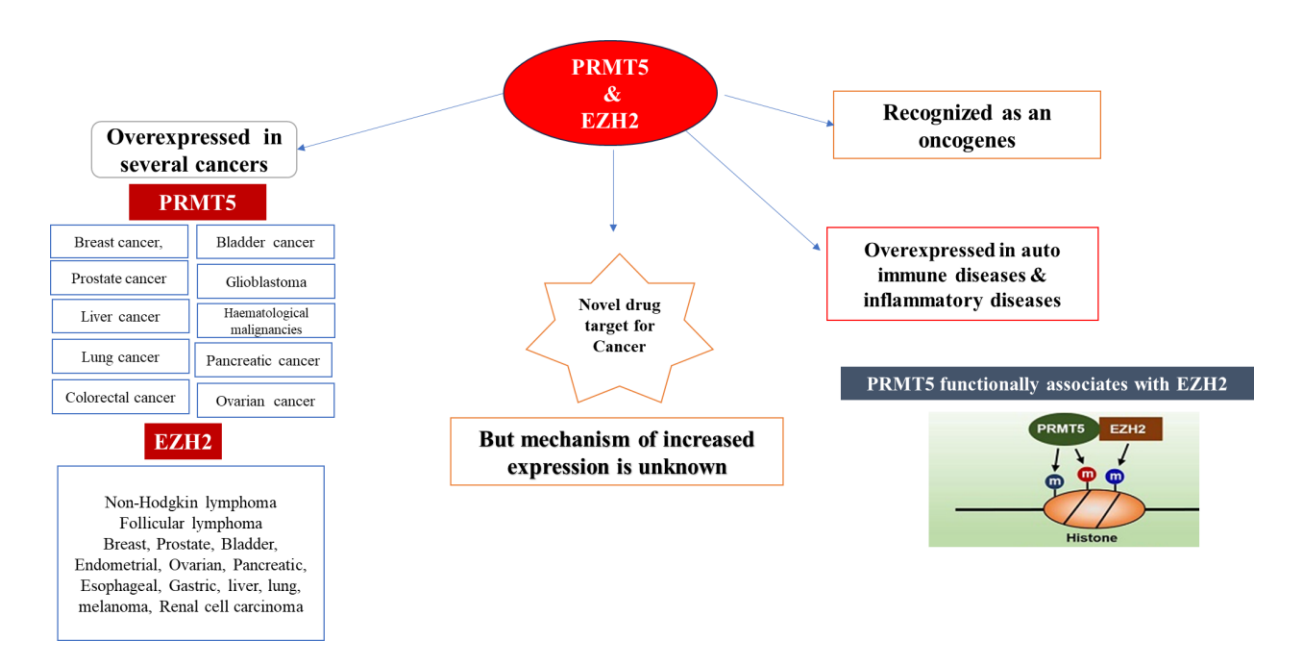


Figure-1.6: The Versatile Role of PRMT5 and EZH2 in Cancer PRMT5 and EZH2 play multifaceted roles in cancer, with their overexpression being strongly associated with various cancer types. Both enzymes have emerged as prominent drug targets due to their pivotal involvement in epigenetic regulation and cancer pathogenesis. PRMT5 catalyzes arginine methylation, while EZH2 mediates lysine methylation, impacting gene expression and chromatin dynamics. Their dysregulation contributes to oncogenic processes, making them attractive targets for therapeutic intervention in cancer treatment strategies.

1.5 Epigenetic Targets: A Frontier in Cancer Therapy

Epigenetic regulators serve as promising targets for anti-cancer therapeutics by orchestrating gene expression and chromatin dynamics. Modulating enzymes like DNMTs, HDACs and HMTs aims to rectify aberrant epigenetic patterns, curtailing tumor advancement. This targeted

approach offers potential for heightened efficacy and diminished toxicity compared to conventional chemotherapy. DNMT and HDAC inhibitors, among emerging epigenetic drugs, show substantial clinical promise, undergoing extensive preclinical and clinical scrutiny. Novel epigenetic-based therapies signify a frontier in oncology, paving the way for precision medicine and ameliorated patient outcomes ^[75]. In tandem, Protein Arginine Methyltransferases (PRMTs) and Polycomb Repressive Complexes (PRCs) emerge as pivotal anti-cancer targets. Collaborating with DNMTs and HDACs, these enzymes regulate gene expression and chromatin dynamics crucial for tumor modulation. Targeting PRMTs and PRCs tailors' cancer treatment, striving to normalize epigenetic signatures and impede tumor progression. The advent of PRMT and PRC inhibitors heralds promising prospects for personalized cancer therapy, augmenting the oncological arsenal with precision medicine. This dynamic frontier in oncology promises innovative therapeutic strategies, fostering enhanced precision and efficacy in combating cancer ^[76].

1.5.1 Epidrugs and natural phytocompounds as cancer therapeutics

Epidrugs, or epigenetic drugs, specifically target the reversible and dynamic modifications of the epigenome, which show a vital role in cancer development and progression. These drugs focus on DNA methylation, post-translational histone modification, and non-coding RNA mediated signaling pathway regulation.

Epigenetic therapeutic drugs offer innovative approaches to cancer treatment by targeting the reversible modifications of the epigenome. These drugs include FDA-approved inhibitors of DNMTs and HDACs, which are critical for regulating gene expression. DNMT inhibitors, for example azacitidine and decitabine, work by demethylating DNA, thereby reactivating silenced tumor suppressor genes. HDAC inhibitors, like Vorinostat and romidepsin, enhance histone acetylation, leading to a more open chromatin structure and the reactivation of repressed genes. Additionally, there are several inhibitory molecules targeting other epigenetic regulators, such as PRMT5 and EZH2, currently undergoing clinical trials. These inhibitors show promise in altering gene expression to combat tumor progression. Furthermore, natural phytocompounds are being explored for their potential as epigenetic modulators, offering a diverse and promising avenue for future drug development. This multifaceted approach to targeting epigenetic mechanisms underscores the potential of epigenetic drugs to advance precision medicine and improve cancer treatment outcomes.

1.5.2 DNA Methyltransferase inhibitors

This process includes the attachment of a methyl group to the DNA molecule, regularly leads to gene silencing. Epidrugs like DNA methyltransferase inhibitors (DNMTis) can reverse this methylation, reactivating tumor suppressor genes. Examples of DNMTis include azacitidine and decitabine, which have demonstrated efficacy in treating hematological malignancies such as myelodysplastic syndromes and acute myeloid leukemia.

Table 1.5 Comprehensive table summarizing the status of epigenetic drugs, including those targeting DNMTs, HDACs, IDHs, HMTs, PRMTs.

Drug Class	Drug	Target	Indication	Status	References
2149 01488	Name				
DNMT Inhibitors	Azacitidine (Vidaza)	DNMT	Myelodysplastic Syndromes (MDS)	Approved	[169]
	Decitabine (Dacogen)	DNMT	Myelodysplastic Syndromes, Acute Myeloid Leukemia (AML)	Approved	[170-171]
	Hydralazine	DNMT	Various (Exploratory)	Investigational	[172]
HDAC Inhibitors	Vorinostat (Zolinza)	HDAC	Cutaneous T-cell Lymphoma	Approved	[173-175]
	Romidepsin (Istodax)	HDAC	Peripheral and Cutaneous T-cell Lymphoma	Approved	[176]
	Belinostat (Beleodaq)	HDAC	Peripheral T-cell Lymphoma	Approved	[177]
	Panobinostat (Farydak)	HDAC	Multiple Myeloma	Withdrawn (2019)	[178]
	Chidamide (Epidaza)	HDAC	Peripheral T-cell Lymphoma (China)	Approved (China)	[179]
IDH Inhibitors	Enasidenib (Idhifa)	IDH2	Acute Myeloid Leukemia (AML)	Approved	[180]
	Ivosidenib (Tibsovo)	IDH1	Acute Myeloid Leukemia (AML)	Approved	[181]
HMT Inhibitors	Tazemetosta t (Tazverik)	EZH2	Epithelioid Sarcoma, Follicular Lymphoma	Approved	[182]
	Pinometostat (EPZ-5676)	DOT1L	Leukemia	Investigational	[183-184]
PRMT Inhibitors	GSK332659 5	PRMT5	Various Cancers	Investigational	[185-186]
	EPZ015666 (GSK33687 15)	PRMT5	Various Cancers	Investigational	[187]
Sirtuin Inhibitors	SRT1720	SIRT1	Metabolic Diseases	Investigational	[188]
	Selisistat (EX-527)	SIRT1	Huntington's Disease	Investigational	[189]
Bromodomai n Inhibitors	OTX015 (MK-8628)	BRD2/3/ 4	Hematologic Malignancies	Investigational	[190]
	CPI-0610	BRD4	Various Cancers	Investigational	[191]
Histone Demethylase Inhibitors	GSK-J4	JMJD3/ UTX	Inflammatory Diseases, Cancer	Investigational	[192]
	IOX1	KDMs	Various Cancers	Investigational	[193]

1.5.3 Histone deacetylase inhibitors

Histones are proteins around which DNA winds, and their modification can significantly impact gene expression. Histone deacetylase inhibitors (HDACis) are a prominent type of epidrugs that target this mechanism.

By inhibiting histone deacetylases, these drugs can increase acetylation levels, leading to a more relaxed chromatin structure and reactivation of suppressed genes. Notable HDACis include Vorinostat (SAHA) and romidepsin, which have been effective in treating certain solid tumors and hematological cancers, such as cutaneous T-cell lymphoma. Epidrugs represent a promising approach in oncology by modulating gene expression through epigenetic pathways. By reactivating tumor suppressor genes and altering the expression of oncogenes, these drugs offer significant therapeutic potential for various cancers, leading to advancements in precision medicine and improved patient outcomes. Comprehensive the status of epigenetic drugs, including those targeting DNMTs, HDACs, IDHs, HMTs, PRMTs are tabulated in table 1.5 & 1.6

1.5.4 Non-coding RNA Regulators

Non-coding RNAs, together with microRNAs (miRNAs) and long non-coding RNAs (lncRNAs), are involved in regulating gene expression at the post-transcriptional level. Although this area is still under exploration, targeting non-coding RNA pathways holds potential for developing new epidrugs.

Table 1.6: PRMT5 targeted drugs in clinical trials: phases, companies, and indication

Drug Name	Phases	Company	Indications
GSK3326595	Phase 1	GlaxoSmithKline	Hematologic Neoplasms, Lymphoma, and Multiple Myeloma
JNJ-64619178	Phase 1/2	Janssen	Hematologic Neoplasms, Lymphoma, and Solid Tumors
PRT543	Phase 1/2	Prelude	Solid Tumors
CC-90009	Phase 1	Celgene	Solid Tumors, Lymphoma, and Multiple Myeloma
PF-06939999	Phase 1/2	Pfizer	Solid Tumors, Lymphoma, and Multiple Myeloma

Despite significant advancements in the development of clinical trial compounds targeting PRMT5 and EZH2, none of these compounds have yet been approved for market release. These

epigenetic regulators have shown promise in preclinical and early clinical studies, demonstrating potential efficacy in treating various cancers by modulating gene expression. However, the rigorous process of clinical validation, including ensuring safety, efficacy, and therapeutic benefit over existing treatments, has so far precluded any of these compounds from receiving final approval from regulatory authorities.

Table 1.7: EZH2 targeted drugs in clinical trials: phases, companies, and indication

Drug Name	Phases	Company	Indications		
GSK3326595	Phase 1	GlaxoSmithKline	Hematologic Neoplasms, Lymphoma, and		
			Multiple Myeloma		
JNJ-64619178	Phase 1/2	Janssen	Hematologic Neoplasms, Lymphoma, and Solid		
			Tumors		
PRT543	Phase 1/2	Prelude	Solid Tumors		
CC-90009	Phase 1	Celgene	Solid Tumors, Lymphoma, and Multiple		
			Myeloma		
PF-06939999	Phase 1/2	Pfizer	Solid Tumors, Lymphoma, and Multiple		
			Myeloma		

Tables 1.6 and 1.7 provide comprehensive summaries of clinical trials investigating targeted drugs aimed at PRMT5 and EZH2, respectively. These tables outline the development phases, pharmaceutical companies involved, and specific cancer indications being studied for each drug. They serve as valuable resources for understanding the current landscape of therapeutic interventions targeting these epigenetic regulators and their potential implications for cancer treatment strategies. Therefore, we are focusing on targeting PRMT5 and EZH2 using phytocompounds, which offer a novel and potentially effective approach to overcome the current limitations and advance these promising therapies toward clinical use. Below is the list of compounds which are under various clinical phases for PRMT5 and EZH2.

1.5.5 Natural Phytocompounds in Cancer Treatment

Natural phytocompounds are bioactive chemicals derived from plants that exhibit potential anticancer properties. These compounds offer a complementary approach to conventional cancer therapies by targeting various molecular pathways involved in cancer progression. Phytocompounds such as curcumin, resveratrol, and EGCG have shown promising impact on both preclinical and clinical trials. Their mechanisms of action include antioxidant activity,

inhibition of cell proliferation, apoptosis induction, and along with suppression of metastasis. Phytocompounds are being explored for their synergistic effects when combined with traditional chemotherapy and radiotherapy (**Figure 1.7**).

1.5.6 Phytocompounds as Epidrugs

Some natural phytocompounds act as epidrugs, modulating the epigenetic landscape of cancer cells. These compounds can influence key epigenetic mechanisms like DNA methylation, histone modification, and non-coding RNA mediated expression, leads to changes or alterations in gene expression that inhibit cancer cell growth and promote apoptosis. Examples of phytocompounds with epigenetic effects include:

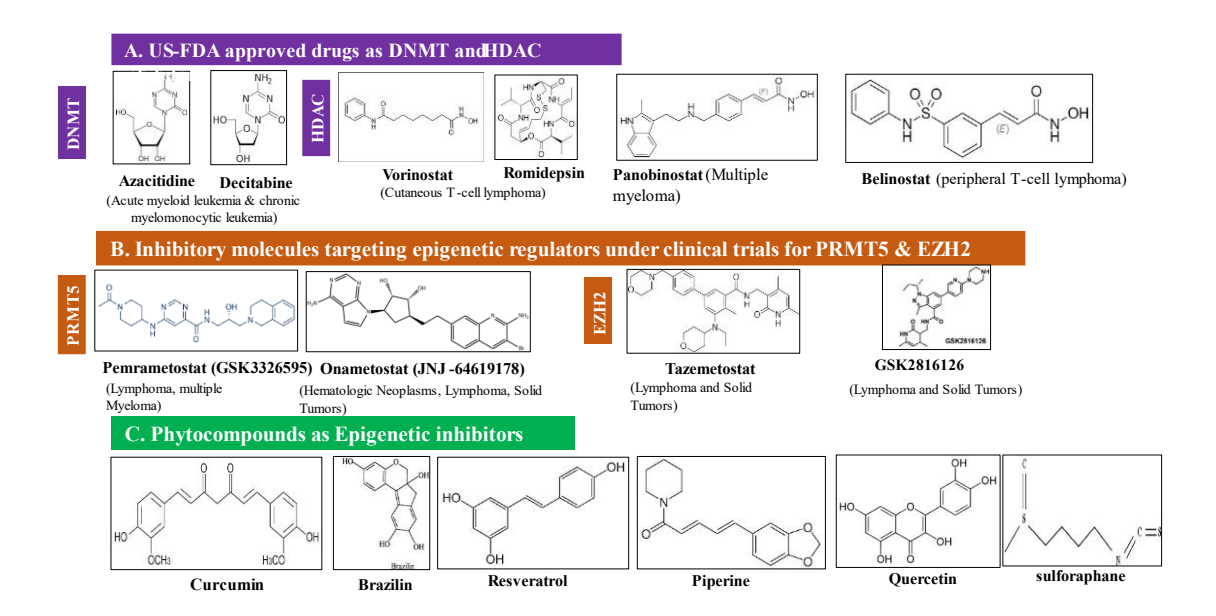


Figure-1.7: Epigenetic Therapeutic Molecules:(A) US FDA-approved drugs targeting DNA methyltransferases (DNMT) and histone deacetylases (HDAC). (B) Inhibitory molecules targeting epigenetic regulators PRMT5 and EZH2 currently under clinical trials. (C) Phytocompounds acting as epigenetic modulators. (Chemical structures sourced from PubChem).

The necessity for developing natural compounds as epidrugs stems from the urgent need to find safer and more effective treatments for various diseases, particularly cancer. Epigenetic alterations have a vital role in gene regulation, and dysregulation is often linked to disease progression. Synthetic epigenetic drugs have shown promise but also come with significant challenges, including potential toxicity and resistance. Natural compounds, derived from plants and other sources, offers a rich reservoir for bioactive molecules with inherent biological compatibility and fewer side effects. By harnessing these natural compounds as epidrugs, researchers aim to develop innovative therapies that can modulate epigenetic targets with

improved safety profiles and therapeutic efficacy, eventually leads to best and better patient outcomes and advancing the field of precision medicine. (**Table 1.8**) presents the molecular targets of anti-proliferative agents, focusing on epigenetic regulators and their crucial roles in cancer therapy. These targets include key enzymes like PRMT5 and EZH2, whose inhibition is being explored to disrupt cancer progression and improve treatment outcomes.

1.5.7 Antiproliferative Compounds as Epigenetic Modulators:

Accumulating reports of bioactive molecules with anti-proliferative properties in various experimental and clinical studies have augmented the field of anti-cancer drug discovery [72-77]. These molecules, often isolated from natural sources like medicinal plants or derived synthetically from them, exhibit promising potential in targeting various hallmarks of cancer. They facilitate the restoration of tumor suppressors and the inactivation of oncogenes, ultimately leading to increased cancer cell death [78,79]. As discussed in the preceding section, numerous epigenetic modifications significantly contribute to neoplastic development alongside genetic mutations. Cancer emerges as a disease rooted in deregulated epigenetic mechanisms upon a backdrop of genetic susceptibility. This reversible behavior of epigenetic changes has spurred the process and development of therapeutic strategies aimed at undoing dysregulated epigenetic alterations for cancer treatment. A concise survey of literature reveals that many anti-proliferative natural molecules target epigenetic regulators of DNA/histone methylation and histone acetylation (see Table 1.6). Among these molecules, commonly known phytochemicals such as curcumin, EGCG, genistein, resveratrol, sulforaphane, phenethyl isothiocyanate, etc., target DNMTs, HDACs, and HATs in cancer cells, inducing growth arrest and apoptosis. So far, several nature-derived molecules have either been approved as epigenetic drugs (epidrugs) or are undergoing testing for efficacy in multiple clinical or preclinical studies [69,70,79]. When used in combination with chemotherapeutics or immune-therapeutics, epidrugs show higher potential for cancer treatment, although numerous pharmacokinetic and mechanical challenges remain, necessitating further investigations into the mechanism of action. To address such challenges effectively, there is an ongoing need to discover novel epidrugs for therapeutic targeting of various epigenetic enzymes or proteins (writers, erasers, and readers) as well as non-coding RNAs. As illustrated in Table 1.6, natural molecules modulate several epigenetic regulators alongside the target genes responsible for their antiproliferative characteristics. In the following discussion, a few commonly studied natural molecules are explored in terms of their molecular targeting and modulation of epigenetic regulators.

Anacardic acid (2-hydroxy-6-pentadecylbenzoic acid) is well-known phenolic lipid compound abundantly found in the shell of cashew nuts. It emerges as a therapeutic agent for various pathophysiological disorders, including cancer, oxidative damage, inflammation, and obesity. Anacardic acid acts as a nonspecific inhibitor of histone acetyltransferase enzymes (p300/CBP and PCAF) [80,81].

Brazilin is an organic heterotetracyclic compound and a natural red dye obtained from the wood of the Caesalpinia sappan plant, and it exhibits diverse pharmacological activities, including anticancer effects, as well as roles as a histological dye, antioxidant, and anti-inflammatory agent ^[84-87].

Capsaicin is a significant chemical ingredient which has pungent ingredient in Capsicum fruits, induces apoptosis in various human cancer cells, making it a potential candidate for cancer therapy [89-93].

Curcumin is a vibrant yellow-pigmented bioactive polyphenolic compound obtained from the rhizome of *Curcuma longa*, commonly known as turmeric. This compound shows various biological processes such as anti-cancer, anti-inflammatory, anti-lipidemic and anti-oxidative, properties. Recent research highlights its involvement in epigenetic regulation, including the reversal of DNA methylation, modification of histones, and targeting of various miRNAs. ^[99-103]

Ellagic acid is usually can be found in many fruits (cranberries, strawberries, raspberries, and pomegranates) and in few vegetables. It is under investigation as a potential and strong drug for of Follicular Lymphoma treatment (phase II), brain injury protection of growth-restricted (intrauterine) babies (phase I/II), and improvement of cardiovascular function in obese adults (phase II). Its therapeutic action mostly involves antioxidant and anti-proliferative effects as it inhibits several enzymes, such as inositol-trisphosphate 3-kinase, inositol-polyphosphate multikinase, DNA topoisomerase, tyrosinase, arylamine N-acetyltransferase, glycogen phosphorylase, glutathione transferase, DNA-directed DNA polymerase and nucleoside-diphosphate kinase [108-111].

(-) **Epigallocatechin-3-gallate** well known as EGCG, is a bioactive polyphenol compound abundantly found in green tea, extensively studied for its potent anti-cancer properties. EGCG (Epigallocatechin gallate) demonstrates its anti-cancer effects through diverse mechanisms, notably by inhibiting epigenetic-modifying enzymes like DNMTs (DNA methyltransferases) and HATs (histone acetyltransferases) [98,105-108].

Eugenol is naturally available phenolic compound can obtain from various plants like cinnamon, clove, and bay leaves. It is known for its various biological activities ranging from anti-inflammatory, antipyretic, antioxidant, neuroprotective antifungal, and analgesic properties, though the precise mechanisms remain unclear [112-114].

Gambogic acid is a xanthonoid derived from the resin of the *Garcinia hanburyi* tree that can modulate various cellular targets involved in apoptosis induction, cell cycle arrest, and cancer therapy [118-120].

Piperine is an alkaloid commonly present in both long pepper (*Piper longum*) and black pepper (*Piper nigrum*) that can modulate various cellular targets involved in antioxidant defense, anti-inflammatory responses, and bioavailability enhancement of other compounds [136-137].

Resveratrol is well known for its phytoalexin ingredient which can be found in many fruits but rich in red grape skin and berries. It is a non-flavonoid polyphenol with significant antioxidant, anti-inflammatory, and anticancer properties in many cancers through modulation of epigenetic mechanisms such as DNMT and HDAC inhibition. Several reports revealed the anticancer activity of resveratrol has been widely studied for its impact on various tumors at different stages, including cancer initiation and progression, through multiple mechanisms. Its therapeutic efficacy against breast cancer patients is well-documented [95, 144-145].

Sulforaphane (SFN) is an isothiocyanate compound found in mainly cruciferous vegetables that can modulate various cellular targets involved in cell proliferation, apoptosis induction, and cancer protection ^[146-148].

Table-1.8: Molecular targets of anti-proliferative agents: epigenetic regulators and their role in cancer therapy

Molecule	Source	Antiproliferative	Reference	Epigenetictarget	Referenc
Anacardicacid	Anacardium	activity against Human breast	s [80]	mechanism inhibits histone	es [81]
	occidentale	cancer cells		acetyltransferases (HATs), leading to reduced histone acetylation and subsequent suppression of gene expression involved in cancer cell proliferation.	
Betulin	Betula alba; Betula pendula	Several human cancer cell lines; human tumor primary cultures	[82]	induces apoptosis and inhibits cancer cell proliferation by modulating epigenetic mechanisms, including the inhibition of histone deacetylases (HDACs)	[83]
Brazilin	Haematoxylu m brasiletto; Caesalpinia sappan	Human cancer cell lines;	[84,85]	modulates epigenetic mechanisms by inhibiting histone deacetylases (HDACs), protein arginine methyltransferases (PRMTs), and DNA methyltransferases (DNMTs), leading to altered histone acetylation, methylation, and DNA methylation, respectively, resulting in suppression of oncogene expression and inhibition of cancer cell proliferation.	[87,88]
Brazilein	Caesalpinia sappan	Human cancer cell lines	[88,89]	modulates epigenetic mechanisms by inhibiting histone deacetylases (HDACs), leading to altered histone acetylation and suppression of oncogene expression, contributing to its antiproliferative effects in cancer cells.	[90]
Capsaicin	Capsicum annuum	Several human cancer cell lines	[89-92]	acts as an epigenetic regulator by modulating histone acetylation and DNA methylation, thereby influencing gene expression linked to inflammation, cancer, and metabolic disorders.	[93]
Cambinol	Synthetic	Burkitt lymphoma cell lines	[94]	epigenetic regulator by inhibiting SIRT1 and SIRT2 deacetylases, leading to increased acetylation of histones and	[94]

				non-histone proteins, which affects gene expression and has potential anticancer properties.	
Chaetocin	Chaetomium minutum	Myeloma cell lines	[95]	acts as an epigenetic regulator by inhibiting the histone methyltransferase SUV39H1, leading to reduced H3K9 methylation and affecting gene expression related to cancer and other diseases.	[96]
Cinnamic acid	Cinnamomu m verum	Human melanoma cell line	[97]	serves as an epigenetic regulator by modulating histone acetylation and inhibiting histone deacetylases (HDACs), thereby influencing gene expression involved in inflammation, cancer, and metabolic disorders.	[98]
Curcumin	Curcuma longa	Human breast tumoreell lines; Human gallbladder adenocarcinoma cells	[99,100]	DNMTs;HATs; HDACs; miRNAs;EZH2	[101- 103]
Diallyl sulfide, Diallyl disulfide, Diallyl trisulfide	Allium sativum	Human cancer cell lines	[104]	act as epigenetic regulators by modulating histone acetylation and DNA methylation, thereby affecting gene expression linked to cancer, inflammation, and cardiovascular health.	[104]
EGCG	Camellia sinensis	Human hepatocellular carcinoma cells; Human pancreatic cancer cells	[105,107]	functions as an epigenetic regulator by inhibiting DNA methyltransferases (DNMTs), histone deacetylases (HDACs), protein arginine methyltransferases (PRMTs), and the enhancer of zeste homolog (EZH), thereby altering gene expression involved in cancer, neurodegenerative diseases, and metabolic disorders.	[98, 107]
Ellagic acid	Punica granatum; Fistulina epatica	Colorectal, Breast, Lung, Prostate, bladder and hepatocellular cancer cells	[108]	acts as an epigenetic regulator by inhibiting DNA methyltransferases (DNMTs) and histone deacetylases (HDACs), protein arginine methyltransferases (PRMTs), and the enhancer of zeste homolog (EZH), as	[109- 111]

				well as modulating histone acetylation, thereby affecting gene expression related to cancer, inflammation, and metabolic disorders.	
Eugenol	Syzygium aromaticum	Human breast cancer cell lines; Several human- cancer cells	[112,113]	functions as an epigenetic regulator by modulating histone acetylation and inhibiting histone deacetylases (HDACs), thereby influencing gene expression associated with cancer, inflammation, and neuroprotection.	[114]
Erucin	Eruca sativa	Human prostate cancer cells; breast cancer cells	[115-117]	acts as an epigenetic regulator by modulating histone deacetylation and DNA methylation, thereby influencing gene expression linked to cancer prevention, inflammation, and detoxification processes.	[117]
Gambogicacid	Garcinia hanburyi	Human hepatocellular carcinoma cells	[118]	functions as an epigenetic regulator by inhibiting histone deacetylases (HDACs) and modulating histone acetylation, thereby affecting gene expression related to cancer, apoptosis, and cell cycle regulation and miRNA	[119- 120]
Garcinol	Garcinia indica	Human colon cancer cells; human gallbladder carcinoma cell lines	[121,122]	acts as an epigenetic regulator by inhibiting histone acetyltransferases (HATs) and modulating histone acetylation, thereby influencing gene expression linked to cancer, inflammation, and neurodegenerative diseases.	[123]
Genistein	Glycine max	Hepatocellular carcinoma cell line	[124]	modulates histone acetylation and DNA methylation, influencing gene expression tied to cancer, cardiovascular health, and hormone-related disorders.	[104]
Gingerol	Zingiber officinale	Several human cancer cell lines	[125]	acts as an epigenetic regulator by modulating histone acetylation, affecting gene expression associated with inflammation, gastrointestinal health, and cancer prevention.	[126]

Hydroxycitrate	Garcinia gummi-gutta	Neuroblastoma cell line	[127]	functions as an epigenetic regulator by inhibiting histone acetyltransferases (HATs), impacting gene expression linked to metabolism and weight management.	[128]
Kaempferitrin	Justicia spicigera	HeLa cells	[129]	serves as an epigenetic regulator by modulating histone modifications, influencing gene expression involved in antioxidant activity, inflammation, and cancer prevention.	[130]
Kazinol Q	Broussonetia kazinoki	Human breast cancer cells	[131]	acts as an epigenetic regulator by modulating histone acetylation, affecting gene expression related to cancer, inflammation, and neuroprotection.	[131]
Lycopene	Solanum lycopersicum	Human breast cancer cell lines	[132]	influences epigenetic mechanisms through modulating DNA methylation and histone modifications, impacting gene expression associated with cancer prevention and cardiovascular health.	[132]
Phenethyl isothiocyanate	Cruciferous vegetables	Human ovarian cancer cells; human laryngeal carcinoma cells	[133,134]	functions as an epigenetic regulator by inhibiting histone deacetylases (HDACs), influencing gene expression involved in cancer prevention, inflammation, and detoxification.	[135]
Piperine	Piper nigrum	HeLa cells	[136]	acts as an epigenetic regulator by modulating histone modifications, affecting gene expression linked to metabolism, inflammation, and cancer prevention.	[137]
ProtosappaninB	Caesalpinia sappan	Human bladder cancer cell line	[138]	modulates histone acetylation and DNA methylation, influencing gene expression tied to inflammation, cardiovascular health, and cancer.	[139]
Psammaplin A	Marine sponge	Human endometrial cancer cells	[140]	serves as an epigenetic regulator by inhibiting histone deacetylases (HDACs) and DNA methyltransferases (DNMTs), impacting gene	[141]

				expression involved in cancer, inflammation, and neurodegenerative diseases.	
Quercetin	Many organisms	Human hepatocellular carcinoma cells	[142]	acts as an epigenetic regulator by modulating histone acetylation and DNA methylation, influencing gene expression linked to inflammation, cardiovascular health, and cancer prevention.	[98,143]
Resveratrol	Grapes and Berries	Human breast cancer cell line; human hepatoma cells	[144,145]	functions as an epigenetic regulator by modulating histone acetylation and DNA methylation, impacting gene expression involved in aging, cancer prevention, and cardiovascular health.	[95]
Sulforaphane	Cruciferous vegetables	Human ovarian cancer cell line	[146]	acts as an epigenetic regulator by modulating histone modifications, affecting gene expression related to inflammation, detoxification, and cancer prevention.	[147,148]
Trichostatin A	Streptomyces hygroscopicu s	Human leukemic cells	[149]	inhibits histone deacetylases (HDACs), influencing gene expression involved in cancer, neurodegenerative diseases, and epigenetic research.	[150]
Ursolic acid	Apple, pears, prunes	Human cervical carcinoma cell lines	[151]	serves as an epigenetic regulator by modulating histone modifications, impacting gene expression linked to inflammation, muscle growth, and cancer prevention.	[151]
Valproic acid	Synthetic	Human prostate cancer cells	[152]	inhibits histone deacetylases (HDACs), influencing gene expression involved in epilepsy, bipolar disorder, and cancer.	[152]

1.5.8 Clinical Potential and Challenges

While epidrugs and natural phytocompounds offer promising avenues for cancer therapy, several challenges remain. The bioavailability and stability of phytocompounds can be limiting factors, necessitating the development of advanced delivery systems. Additionally, the specificity and potential side effects of epidrugs require careful consideration in clinical applications. Ongoing research aims to optimize the therapeutic efficacy and safety profiles of

these agents, with the goal of integrating them into standard cancer treatment regimens. Combining epidrugs and phytocompounds with existing therapies holds potential for more effective and personalized cancer care.

1.6 Objectives of the study:

The scope of this work encompasses the identification and evaluation of phytochemicals with antiproliferative properties, focusing on their effects on gene expression of epigenetic regulators. The study aims to screen and identify plant-derived compounds that inhibit cancer cell growth and modulate epigenetic gene expression. Furthermore, the research will validate the inhibition of key epigenetic regulators, PRMT5 and EZH2, by these phytochemicals using *in vitro* methods. Finally, the tumor inhibitory potential of the identified phytocompounds will be investigated through mouse xenograft models, providing comprehensive insights into their therapeutic efficacy and mechanisms of action. To achieve these the following objectives were designed and planned:

- I. To screen and identify the phytochemicals with antiproliferative properties and its effects on gene expression of epigenetic regulators.
- II. To validate inhibition of PRMT5 and EZH2 by phytocompounds using *in vitro* methods.
- III. To investigate the tumor inhibitory potential of phytocompounds using mouse xenografts.

1.7 References:

- **1.** <u>Cancer fact sheet.</u> World Health Organization; 2022. (https://www.who.int/news-room/fact-sheets/detail/cancer)
- 2. Cancer Tomorrow tool. International Agency for Research on Cancer. (https://gco.iarc.fr/tomorrow/en)
- **3.** Hoxha, I., Sadiku, F., Hoxha, L., Nasim, M., et al., (2024). Breast Cancer and Lifestyle Factors: Umbrella Review. *Hematology/oncology clinics of North America*, 38(1), 137–170. https://doi.org/10.1016/j.hoc.2023.07.005
- **4.** Feng, Y., Spezia, M., Huang, S., Yuan, C., Zeng, Z., et al., (2018). Breast cancer development and progression: Risk factors, cancer stem cells, signaling pathways, genomics, and molecular pathogenesis. *Genes & Diseases*, 5(2), 77-106. https://doi.org/10.1016/j.gendis.2018.05.001
- 5. Thakur, C., Qiu, Y., Fu, Y., Bi, Z., Zhang, W., Ji, H., & Chen, F. (2022). Epigenetics and environment in breast cancer: New paradigms for anti-cancer therapies. *Frontiers in Oncology*, 12. https://doi.org/10.3389/fonc.2022.971288
- **6.** Arnold, M., Morgan, E., Rumgay, H., Mafra, A., Singh, D., Laversanne, M., Vignat, J., et al., (2022). Current and future burden of breast cancer: Global statistics for 2020 and 2040. *Breast (Edinburgh, Scotland)*, 66, 15–23. https://doi.org/10.1016/j.breast.2022.08.010
- 7. Dupont, C., Armant, D. R., & Brenner, C. A. (2009). Epigenetics: definition, mechanisms and clinical perspective. *Seminars in reproductive medicine*, 27(5), 351–357. https://doi.org/10.1055/s-0029-1237423
- **8.** Ladewig, J., Koch, P., & Brüstle, O. (2013). Leveling Waddington: the emergence of direct programming and the loss of cell fate hierarchies. *Nature reviews. Molecular cell biology*, *14*(4), 225–236. https://doi.org/10.1038/nrm3543
- **9.** Jiang, Y. H., Bressler, J., & Beaudet, A. L. (2004). Epigenetics and human disease. *Annual review of genomics and human genetics*, *5*, 479–510. https://doi.org/10.1146/annurev.genom.5.061903.180014
- **10.** Zoghbi, H. Y., & Beaudet, A. L. (2016). Epigenetics and Human Disease. *Cold Spring Harbor perspectives in biology*, 8(2), a019497. https://doi.org/10.1101/cshperspect.a019497
- **11.** Moosavi, A., & Motevalizadeh Ardekani, A. (2016). Role of Epigenetics in Biology and Human Diseases. *Iranian biomedical journal*, 20(5), 246–258. https://doi.org/10.22045/ibj.2016.01
- **12.** Cavalli, G., & Heard, E. (2019). Advances in epigenetics link genetics to the environment and disease. *Nature*, *571*(7766), 489–499. https://doi.org/10.1038/s41586-019-1411-0
- **13.** Miranda Furtado, C. L., Dos Santos Luciano, M. C., Silva Santos, R. D., Furtado, G. P., Moraes, M. O., & Pessoa, C. (2019). Epidrugs: targeting epigenetic marks in cancer treatment. *Epigenetics*, *14*(12), 1164–1176. https://doi.org/10.1080/15592294.2019.1640546
- **14.** Costa, P. M. D. S., Sales, S. L. A., Pinheiro, D. P., Pontes, et al., (2023). Epigenetic reprogramming in cancer: From diagnosis to treatment. *Frontiers in cell and developmental biology*, *11*, 1116805. https://doi.org/10.3389/fcell.2023.1116805
- **15.** Morel, D., Jeffery, D., Aspeslagh, S., Almouzni, G., & Postel-Vinay, S. (2020). Combining epigenetic drugs with other therapies for solid tumours past lessons and future promise. *Nature reviews. Clinical oncology*, *17*(2), 91–107. https://doi.org/10.1038/s41571-019-0267-4
- **16.** Flavahan, W. A., Gaskell, E., & Bernstein, B. E. (2017). Epigenetic plasticity and the hallmarks of cancer. *Science (New York, N.Y.)*, 357(6348), eaal2380. https://doi.org/10.1126/science.aal2380
- **17.** Esteller M. (2017). Epigenetic drugs: More than meets the eye. *Epigenetics*, *12*(5), 307. https://doi.org/10.1080/15592294.2017.1322881
- **18.** Hananya, N., Koren, S., & Muir, T. W. (2024). Interrogating epigenetic mechanisms with chemically customized chromatin. *Nature reviews. Genetics*, 25(4), 255–271. https://doi.org/10.1038/s41576-023-00664-z
- **19.** Navarro Quiroz, E., Chavez-Estrada, V., Macias-Ochoa, K., Ayala-Navarro, M. F., Flores-Aguilar, A. S., et al., (2019). Epigenetic Mechanisms and Posttranslational Modifications in Systemic Lupus Erythematosus. *International journal of molecular sciences*, 20(22), 5679. https://doi.org/10.3390/ijms20225679
- **20.** Al Aboud NM, Tupper C, Jialal I. Genetics, Epigenetic Mechanism. [Updated 2023 Aug 14]. In: StatPearls [Internet]. Treasure Island (FL): StatPearls Publishing; 2024 Jan-. Available from: https://www.ncbi.nlm.nih.gov/books/NBK532999/
- 21. K Lim, D. H., & Maher, E. R. (2009). DNA methylation: A form of epigenetic control of gene expression. *The Obstetrician & Gynaecologist*, 12(1), 37-42. https://doi.org/10.1576/toag.12.1.037.27556

- **22.** Jones P. A. (2012). Functions of DNA methylation: islands, start sites, gene bodies and beyond. *Nature reviews. Genetics*, *13*(7), 484–492. https://doi.org/10.1038/nrg3230
- **23.** Edwards, J. R., Yarychkivska, O., Boulard, M., & Bestor, T. H. (2017). DNA methylation and DNA methyltransferases. *Epigenetics & chromatin*, *10*, 23. https://doi.org/10.1186/s13072-017-0130-8
- **24.** Dor, Y., & Cedar, H. (2018). Principles of DNA methylation and their implications for biology and medicine. *Lancet (London, England)*, 392(10149), 777–786. https://doi.org/10.1016/S0140-6736(18)31268-6
- **25.** Mattei, A. L., Bailly, N., & Meissner, A. (2022). DNA methylation: A historical perspective. *Trends in Genetics*, *38*(7), 676-707. https://doi.org/10.1016/j.tig.2022.03.010
- **26.** Du, Q., Luu, P. L., Stirzaker, C., & Clark, S. J. (2015). Methyl-CpG-binding domain proteins: readers of the epigenome. *Epigenomics*, 7(6), 1051–1073. https://doi.org/10.2217/epi.15.39
- 27. Nishiyama, A., & Nakanishi, M. (2021). Navigating the DNA methylation landscape of cancer. *Trends in Genetics*, 37(11), 1012-1027. https://doi.org/10.1016/j.tig.2021.05.002
- **28.** Jin, B., Li, Y., & Robertson, K. D. (2011). DNA methylation: superior or subordinate in the epigenetic hierarchy?. *Genes & cancer*, 2(6), 607–617. https://doi.org/10.1177/1947601910393957
- **29.** Burton, A., Bannister, A. J., & Schneider, R. (2022). Histone post-translational modifications Cause and consequence of genome function. *Nature Reviews Genetics*, 23(9), 563-580. https://doi.org/10.1038/s41576-022-00468-7
- **30.** Baile, F., Gómez-Zambrano, Á., & Calonje, M. (2021). Roles of Polycomb complexes in regulating gene expression and chromatin structure in plants. *Plant communications*, *3*(1), 100267. https://doi.org/10.1016/j.xplc.2021.100267
- **31.** Khan, A. A., Lee, A. J., & Roh, T. Y. (2015). Polycomb group protein-mediated histone modifications during cell differentiation. *Epigenomics*, 7(1), 75–84. https://doi.org/10.2217/epi.14.61
- **32.** Dey, P., Buragohain, T., Das, M., & Banerjee, S. (2023). Exploring the role of non-coding RNA mediated regulation of signaling pathways in endometrial cancer. *Advances in Cancer Biology Metastasis*, 9, 100111. https://doi.org/10.1016/j.adcanc.2023.100111
- 33. Shang, R., Lee, S., Senavirathne, G., & Lai, E. C. (2023). MicroRNAs in action: Biogenesis, function and regulation. *Nature Reviews Genetics*, 24(12), 816-833. https://doi.org/10.1038/s41576-023-00611-y
- **34.** Annese, T., Tamma, R., De Giorgis, M., & Ribatti, D. (2020). microRNAs Biogenesis, Functions and Role in Tumor Angiogenesis. In Frontiers in Oncology (Vol. 10). Frontiers Media SA. https://doi.org/10.3389/fonc.2020.581007
- **35.** Copeland, R. A., Solomon, M. E., & Richon, V. M. (2009). Protein methyltransferases as a target class for drug discovery. *Nature Reviews Drug Discovery*, 8(9), 724-732. https://doi.org/10.1038/nrd2974
- **36.** Boriack-Sjodin, P. A., & Swinger, K. K. (2016). Protein Methyltransferases: A Distinct, Diverse, and Dynamic Family of Enzymes. *Biochemistry*, 55(11), 1557–1569. https://doi.org/10.1021/acs.biochem.5b01129
- **37.** Copeland R. A. (2018). Protein methyltransferase inhibitors as precision cancer therapeutics: a decade of discovery. *Philosophical transactions of the Royal Society of London. Series B, Biological sciences*, 373(1748), 20170080. https://doi.org/10.1098/rstb.2017.0080
- **38.** Hwang, J. W., Cho, Y., Bae, G., Kim, S., & Kim, Y. K. (2021). Protein arginine methyltransferases: Promising targets for cancer therapy. *Experimental & Molecular Medicine*, *53*(5), 788-808. https://doi.org/10.1038/s12276-021-00613-y
- **39.** Haghandish, N., & Côté, J. (2015). The Role of Histone Mark Writers in Chromatin Signaling: Protein Arginine Methyltransferases. *Chromatin Signaling and Diseases*, 55-74. https://doi.org/10.1016/B978-0-12-802389-1.00003-4
- **40.** Shailesh, H., Zakaria, Z. Z., Baiocchi, R., & Sif, S. (2018). Protein arginine methyltransferase 5 (PRMT5) dysregulation in cancer. *Oncotarget*, *9*(94), 36705–36718. https://doi.org/10.18632/oncotarget.26404
- **41.** Wu, Q., Schapira, M., & Arrowsmith, C. H. (2021). Protein arginine methylation: From enigmatic functions to therapeutic targeting. *Nature Reviews Drug Discovery*, 20(7), 509-530. https://doi.org/10.1038/s41573-021-00159-8
- **42.** Wang, Y., & Bedford, M. T. (2023). Effectors and effects of arginine methylation. *Biochemical Society Transactions*, *51*(2), 725-734. https://doi.org/10.1042/BST20221147
- **43.** Li, X., Song, Y., Mu, W., Hou, X., Bate, B., & Ji, S. Dysregulation of Arginine Methylation in Tumorigenesis. *Frontiers in Molecular Biosciences*, 11, 1420365. https://doi.org/10.3389/fmolb.2024.1420365

- **44.** Al Temimi, A. H. K., Martin, M., Meng, Q., Lenstra, D. C., Qian, P., Guo, H., Weinhold, E., & Mecinović, J. (2020). Lysine Ethylation by Histone Lysine Methyltransferases. *Chembiochem : a European journal of chemical biology*, *21*(3), 392–400. https://doi.org/10.1002/cbic.201900359
- **45.** Han, D., Huang, M., Wang, T., Li, Z., Chen, Y., Liu, C., Lei, Z., & Chu, X. (2019). Lysine methylation of transcription factors in cancer. *Cell Death & Disease*, 10(4), 1-11. https://doi.org/10.1038/s41419-019-1524-2
- **46.** Aziz, N., Hong, Y. H., Kim, H. G., Kim, J. H., & Cho, J. Y. (2023). Tumor-suppressive functions of protein lysine methyltransferases. *Experimental & Molecular Medicine*, *55*(12), 2475-2497. https://doi.org/10.1038/s12276-023-01117-7
- **47.** Piunti, A., & Shilatifard, A. (2021). The roles of Polycomb repressive complexes in mammalian development and cancer. *Nature Reviews Molecular Cell Biology*, 22(5), 326-345. https://doi.org/10.1038/s41580-021-00341-1
- **48.** Blackledge, N. P., & Klose, R. J. (2021). The molecular principles of gene regulation by Polycomb repressive complexes. *Nature reviews. Molecular cell biology*, 22(12), 815–833. https://doi.org/10.1038/s41580-021-00398-y
- **49.** Dong, J., Xu, L., Qi, R., Yuan, Q., & Zhao, W. (2022). Critical Roles of Polycomb Repressive Complexes in Transcription and Cancer. *International Journal of Molecular Sciences*, 23(17). https://doi.org/10.3390/ijms23179574
- **50.** Shi, T. H., Sugishita, H., & Gotoh, Y. (2024). Crosstalk within and beyond the Polycomb repressive system. In Journal of Cell Biology (Vol. 223, Issue 5). Rockefeller University Press. https://doi.org/10.1083/jcb.202311021
- **51.** Sharma, S., Kelly, T. K., & Jones, P. A. (2010). Epigenetics in cancer. *Carcinogenesis*, *31*(1), 27–36. https://doi.org/10.1093/carcin/bgp220
- **52.** Yu, X., Zhao, H., Wang, R., Chen, Y., Ouyang, X., Li, W., Sun, Y., & Peng, A. (2024). Cancer epigenetics: From laboratory studies and clinical trials to precision medicine. *Cell Death Discovery*, 10(1), 1-12. https://doi.org/10.1038/s41420-024-01803-z
- **53.** Baylin, S. B., & Jones, P. A. (2016). Epigenetic Determinants of Cancer. *Cold Spring Harbor perspectives in biology*, 8(9), a019505. https://doi.org/10.1101/cshperspect.a019505
- **54.** Roberti, A., Valdes, A. F., Torrecillas, R., Fraga, M. F., & Fernandez, A. F. (2019). Epigenetics in cancer therapy and nanomedicine. *Clinical Epigenetics*, 11. https://doi.org/10.1186/s13148-019-0675-4
- **55.** Cancer Genome Atlas Research Network, Weinstein, J. N., Collisson, E. A., Mills, G. B., Shaw, K. R., Ozenberger, B. A., Ellrott, K., Shmulevich, I., Sander, C., & Stuart, J. M. (2013). The Cancer Genome Atlas Pan-Cancer analysis project. *Nature genetics*, *45*(10), 1113–1120. https://doi.org/10.1038/ng.2764
- **56.** Cerami, E., Gao, J., Dogrusoz, U., Gross, B. E., Sumer, S. O., Aksoy, B. A., Jacobsen, A., Byrne, C. J., Heuer, M. L., Larsson, E., Antipin, Y., Reva, B., Goldberg, A. P., Sander, C., & Schultz, N. (2012). The cBio cancer genomics portal: an open platform for exploring multidimensional cancer genomics data. *Cancer discovery*, *2*(5), 401–404. https://doi.org/10.1158/2159-8290.CD-12-0095
- 57. Gao, J., Aksoy, B. A., Dogrusoz, U., Dresdner, G., Gross, B., Sumer, S. O., Sun, Y., Jacobsen, A., Sinha, R., Larsson, E., Cerami, E., Sander, C., & Schultz, N. (2013). Integrative analysis of complex cancer genomics and clinical profiles using the cBioPortal. *Science signaling*, 6(269), pl1. https://doi.org/10.1126/scisignal.2004088
- **58.** Sathishkumar, K., Chaturvedi, M., Das, P., Stephen, S., & Mathur, P. (2022). Cancer incidence estimates for 2022 & projection for 2025: Result from National Cancer Registry Programme, India. *The Indian journal of medical research*, *156*(4&5), 598–607. https://doi.org/10.4103/ijmr.ijmr-1821-22
- **59.** Xu, Y., Gong, M., Wang, Y., Yang, Y., Liu, S., & Zeng, Q. (2023). Global trends and forecasts of breast cancer incidence and deaths. *Scientific data*, *10*(1), 334. https://doi.org/10.1038/s41597-023-02253-5
- **60.** Sawhney, R., Nathani, P., Patil, P., Bhandarkar, P., Veetil, D. K., et al., (2023). Recognising sociocultural barriers while seeking early detection services for breast cancer: a study from a Universal Health Coverage setting in India. *BMC cancer*, 23(1), 881. https://doi.org/10.1186/s12885-023-11359-3
- **61.** Srinath, A., van Merode, F., Rao, S. V., & Pavlova, M. (2023). Barriers to cervical cancer and breast cancer screening uptake in low- and middle-income countries: a systematic review. *Health policy and planning*, *38*(4), 509–527. https://doi.org/10.1093/heapol/czac104
- **62.** Sung, H., Ferlay, J., Siegel, R. L., Laversanne, M., Soerjomataram, I., Jemal, A., & Bray, F. (2021). Global Cancer Statistics 2020: GLOBOCAN Estimates of Incidence and Mortality Worldwide for 36 Cancers in 185 Countries. *CA: A Cancer Journal for Clinicians*, 71(3), 209-249. https://doi.org/10.3322/caac.21660

- **63.** Cheng, Y., He, C., Wang, M., Ma, X., Mo, F., Yang, S., Han, J., & Wei, X. (2019). Targeting epigenetic regulators for cancer therapy: Mechanisms and advances in clinical trials. *Signal Transduction and Targeted Therapy*, 4(1), 1-39. https://doi.org/10.1038/s41392-019-0095-0
- **64.** Giorgi, G., & Del Re, B. (2021). Epigenetic dysregulation in various types of cells exposed to extremely low-frequency magnetic fields. *Cell and tissue research*, *386*(1), 1–15. https://doi.org/10.1007/s00441-021-03489-6
- **65.** Simon, J. A., & Lange, C. A. (2008). Roles of the EZH2 histone methyltransferase in cancer epigenetics. *Mutation research*, *647*(1-2), 21–29. https://doi.org/10.1016/j.mrfmmm.2008.07.010
- **66.** Liu, Y., & Yang, Q. (2023). The roles of EZH2 in cancer and its inhibitors. *Medical oncology (Northwood, London, England)*, 40(6), 167. https://doi.org/10.1007/s12032-023-02025-6
- **67.** Tee, W. W., Pardo, M., Theunissen, T. W., Yu, L., Choudhary, J. S., Hajkova, P., & Surani, M. A. (2010). Prmt5 is essential for early mouse development and acts in the cytoplasm to maintain ES cell pluripotency. *Genes & development*, 24(24), 2772–2777. https://doi.org/10.1101/gad.606110
- **68.** Kim, H., & Ronai, Z. A. (2020). PRMT5 function and targeting in cancer. *Cell stress*, *4*(8), 199–215. https://doi.org/10.15698/cst2020.08.228
- **69.** Yamada, Y., Venkadakrishnan, V. B., Mizuno, K., Bakht, M., Ku, S. Y., Garcia, M. M., & Beltran, H. (2023). Targeting DNA methylation and B7-H3 in RB1-deficient and neuroendocrine prostate cancer. *Science translational medicine*, *15*(722), eadf6732. https://doi.org/10.1126/scitranslmed.adf6732
- **70.** Liang, T., Wang, F., Elhassan, R. M., Cheng, Y., Tang, X., Chen, W., Fang, H., & Hou, X. (2023). Targeting histone deacetylases for cancer therapy: Trends and challenges. *Acta Pharmaceutica Sinica B*, 13(6), 2425-2463. https://doi.org/10.1016/j.apsb.2023.02.007
- **71.** Chiba S. (2017). Dysregulation of TET2 in hematologic malignancies. *International journal of hematology*, 105(1), 17–22. https://doi.org/10.1007/s12185-016-2122-z
- **72.** Zhu, L. Y., Yuan, J. B., Zhang, L., He, C. X., Lin, X., Xu, B., & Jin, G. H. (2022). Loss of MLL Induces Epigenetic Dysregulation of Rasgrf1 to Attenuate Kras-Driven Lung Tumorigenesis. *Cancer research*, 82(22), 4153–4163. https://doi.org/10.1158/0008-5472.CAN-22-1475
- 73. Thomas, D., Wu, M., Nakauchi, Y., Zheng, M., Thompson-Peach, C. A. L., Lim, K., Landberg, N., Köhnke, T., Robinson, N., Kaur, S., Kutyna, M., Stafford, M., Hiwase, D., Reinisch, A., Peltz, G., & Majeti, R. (2022). Dysregulated Lipid Synthesis by Oncogenic IDH1 Mutation Is a Targetable Synthetic Lethal Vulnerability. In Cancer Discovery (Vol. 13, Issue 2, pp. 496–515). American Association for Cancer Research (AACR). https://doi.org/10.1158/2159-8290.cd-21-0218
- **74.** Dong, J., Pervaiz, W., Tayyab, B., Li, D., Kang, L., Zhang, H., Gong, H., Ma, X., Li, J., Agboyibor, C., Bi, Y., & Liu, H. (2022). A comprehensive comparative study on LSD1 in different cancers and tumor specific LSD1 inhibitors. *European Journal of Medicinal Chemistry*, 240, 114564. https://doi.org/10.1016/j.ejmech.2022.114564
- 75. Zhao, L., Duan, Y. T., Lu, P., Zhang, Z. J., Zheng, X. K., Wang, J. L., & Feng, W. S. (2018). Epigenetic Targets and their Inhibitors in Cancer Therapy. *Current topics in medicinal chemistry*, 18(28), 2395–2419. https://doi.org/10.2174/1568026619666181224095449
- **76.** Yu, X., Li, M., Guo, C., Wu, Y., Zhao, L., Shi, Q., Song, J., & Song, B. (2021). Therapeutic Targeting of Cancer: Epigenetic Homeostasis. In Frontiers in Oncology (Vol. 11). Frontiers Media SA. https://doi.org/10.3389/fonc.2021.747022
- 77. Rotondo, J. C., Lanzillotti, C., Mazziotta, C., Tognon, M., & Martini, F. (2021). Epigenetics of Male Infertility: The Role of DNA Methylation. *Frontiers in Cell and Developmental Biology*, 9. https://doi.org/10.3389/fcell.2021.689624
- **78.** Falkenberg, K. J., & Johnstone, R. W. (2014). Histone deacetylases and their inhibitors in cancer, neurological diseases and immune disorders. *Nature reviews. Drug discovery*, *13*(9), 673–691. https://doi.org/10.1038/nrd4360
- **79.** Wenke, N. K., & Baumbach, J. CTCF and Its Multi-Partner Network for Chromatin Regulation. *Cells*, 12(10), 1357. https://doi.org/10.3390/cells12101357
- **80.** Zhao, Q., Zhang, X., Cai, H., Zhang, P., Kong, D., Ge, X., ... Dong, W. (**2018**). Anticancer effects of plant derived Anacardic acid on human breast cancer MDA-MB-231 cells. *American Journal of Translational Research*, 10(8), 2424–2434.
- **81.** Cui, L., Miao, J., Furuya, T., Fan, Q., Li, X., Rathod, P. K., ... Cui, L. (**2008**). Histone acetyltransferase inhibitor anacardic acid causes changes in global gene expression during in vitro Plasmodium falciparum development. *Eukaryotic Cell*, 7(7), 1200–1210.

- **82.** Król, S. K., Kiełbus, M., Rivero-Müller, A., & Stepulak, A. (**2015**). Comprehensive Review on Betulin as a Potent Anticancer Agent. *BioMed Research International*, 2015, 1–11.
- **83.** Jiang, W., Li, X., Dong, S., & Zhou, W. (2021). Betulinic acid in the treatment of tumour diseases: Application and research progress. *Biomedicine & Pharmacotherapy*, 142, 111990. https://doi.org/10.1016/j.biopha.2021.111990
- **84.** Bello-Martinez, J., Jiménez-Estrada, M., Rosas-Acevedo, J.et al., (**2017**). Anti-proliferative activity of *Haematoxylum brasiletto* H. Karst. *Pharmacognosy Magazine*, 13(50), 289.
- **85.** Handayani, S., Susidarti, R. A., Jenie, R. I., & Meiyanto, E. (**2017**). Two Active Compounds from Caesalpinia sappan L. in Combination with Cisplatin Synergistically Induce Apoptosis and CellCycle Arrest on WiDr Cells. *Advanced Pharmaceutical Bulletin*, 7(3), 375–380.
- **86.** Kim, B., Kim, S.-H., Jeong, S.-J., Sohn, E. J., Jung, J. H., et al., (**2012**). Brazilin Induces Apoptosis and G2/M Arrest via Inactivation of Histone Deacetylase in Multiple Myeloma U266 Cells. *Journal of Agricultural and Food Chemistry*, 60(39), 9882–9889.
- **87.** Chatterjee, B., Ghosh, K., Swain, A., Nalla, K. K., Ravula, H., Pan, A., & Kanade, S. R. (2021). The phytochemical brazilin suppresses DNMT1 expression by recruiting p53 to its promoter resulting in the epigenetic restoration of p21 in MCF7cells. *Phytomedicine*, 95, 153885. https://doi.org/10.1016/j.phymed.2021.153885
- **88.** Yen, C.-T., Nakagawa-Goto, K., Hwang, T.-L., Wu, P.-C., Morris-Natschke, S. L., Lai, W.-C., Lee, K.-H. (**2010**). Antitumor agents. 271: Total synthesis and evaluation of brazilein and analogs as anti-inflammatory and cytotoxic agents. Bioorganic & Medicinal Chemistry Letters, 20(3), 1037–1039.
- **89.** Brown, K. C., Witte, T. R., Hardman, W. E., Luo, H., Chen, Y. C., Carpenter, A. B., ... Dasgupta, P. (**2010**). Capsaicin Displays Anti-Proliferative Activity against Human Small Cell LungCancer in Cell Culture and Nude Mice Models via the E2F Pathway. *PLoS ONE*, 5(4), e10243.
- **90.** Hassell, K. N. (2019). Histone Deacetylases and Their Inhibitors in Cancer Epigenetics. *Diseases*, 7(4). https://doi.org/10.3390/diseases7040057
- **91.** Sultan, A. S., Mohammed, F. Z., & Abas, A. M. (**2017**). In Vitro Studies on Anticancer Activity of Capsaicin a Component of Hot Chili Pepper against Human Hepatocellular Carcinoma Cells. *Int Jcell Sci & mol biol* 2(4): IJCSMB.MS.ID.555591 (2017).
- **92.** Lavorgna, M., Orlo, E., Nugnes, R., Piscitelli, C., Russo, C., & Isidori, M. (**2019**). Capsaicin inHot Chili Peppers: In Vitro Evaluation of Its Antiradical, Anti-proliferative and Apoptotic Activities. *Plant Foods for Human Nutrition*, 74(2), 164–170.
- **93.** Wang, F., Zhao, J., Liu, D., Zhao, T., Lu, Z., Zhu, L., ... Cai, Y. (**2016**). Capsaicin reactivates hMOF in gastric cancer cells and induces cell growth inhibition. *Cancer Biology & Therapy*, 17(11),1117–1125.
- **94.** Heltweg, B., Gatbonton, T., Schuler, A. D., Posakony, J., Li, H., Goehle, S., ... Bedalov, A. (**2006**). Antitumor Activity of a Small-Molecule Inhibitor of Human Silent Information Regulator 2 Enzymes. *Cancer Research*, 66(8), 4368–4377.
- **95.** Isham, C. R., Tibodeau, J. D., Jin, W., Xu, R., Timm, M. M., & Bible, K. C. (**2007**). Chaetocin:a promising new antimyeloma agent with in vitro and in vivo activity mediated via imposition of oxidative stress. *Blood*, 109(6), 2579–2588.
- **96.** Cherblanc, F. L., Chapman, K. L., Brown, R., & Fuchter, M. J. (**2013**). Chaetocin is a nonspecific inhibitor of histone lysine methyltransferases. *Nature Chemical Biology*, 9(3), 136–137.
- **97.** Carlos-Reyes, Á., López-González, J. S., Meneses-Flores, M., Gallardo-Rincón, D., et al., (**2019**). Dietary Compounds as Epigenetic Modulating Agents in Cancer. *Frontiers in Genetics*, 10, 79.
- **98.** Niero, E. L. de O., & Machado-Santelli, G. M. (**2013**). Cinnamic acid induces apoptotic cell death and cytoskeleton disruption in human melanoma cells. *Journal of Experimental & Clinical Cancer Research*, 32(1), 31.
- **99.** Mehta, K., Pantazis, P., McQueen, T., & Aggarwal, B. B. (**1997**). Anti-proliferative effect of curcumin (diferuloylmethane) against human breast tumor cell lines. *Anti-Cancer Drugs*, 8(5), 470–481.
- **100.**Ono, M., Higuchi, T., Takeshima, M., Chen, C., & Nakano, S. (**2013**). Anti-proliferative and apoptosis-inducing activity of curcumin against human gallbladder adenocarcinoma cells. *AnticancerResearch*, 33(5), 1861–1866.
- **101.**Boyanapalli, S. S. S., & Kong, A.-N. T. (**2015**). "Curcumin, the King of Spices": Epigenetic Regulatory Mechanisms in the Prevention of Cancer, Neurological, and Inflammatory Diseases. *Current Pharmacology Reports*, 1(2), 129–139.

- 102. Hassan, F., Rehman, M. S., Khan, M. S., Ali, M. A., Javed, A., Nawaz, A., & Yang, C. (2019). Curcumin as an Alternative Epigenetic Modulator: Mechanism of Action and Potential Effects. *Frontiers in Genetics*, 10, 514.
- **103.**Hua, W.-F., Fu, Y.-S., Liao, Y.-J., Xia, W.-J., Chen, Y.-C., Zeng, Y.-X., ... Xie, D. (**2010**). Curcumin induces down-regulation of EZH2 expression through the MAPK pathway in MDA-MB-435 human breast cancer cells. *European Journal of Pharmacology*, 637(1–3), 16–21.
- **104.**Ratovitski, E. A. (**2017**). Anticancer Natural Compounds as Epigenetic Modulators of Gene Expression. *Current Genomics*, 18(2), 175–205.
- **105.**Shirakami, Y., Shimizu, M., Adachi, S., Sakai, H., Nakagawa, T., Yasuda, Y., ... Moriwaki, H.(**2009**). (-)-Epigallocatechin gallate suppresses the growth of human hepatocellular carcinoma cells by inhibiting activation of the vascular endothelial growth factor-vascular endothelial growth factor receptor axis. *Cancer Science*, 100(10), 1957–1962.
- **106.**Shankar, S., Marsh, L., & Srivastava, R. K. (**2013**). EGCG inhibits growth of human pancreatictumors orthotopically implanted in Balb C nude mice through modulation of FKHRL1/FOXO3a and neuropilin. *Molecular and Cellular Biochemistry*, 372(1–2), 83–94.
- **107.** Nalla, K., Chatterjee, B., Poyya, J., Swain, A., Ghosh, K., Pan, A., ... & Kanade, S. R. (2024). Epigallocatechin-3-gallate inhibit the protein arginine methyltransferase 5 and Enhancer of Zeste homolog 2 in breast cancer both in vitro and in vivo. *bioRxiv*, 2024-02.
- **108.**Ceci, C., Lacal, P., Tentori, L., De Martino, M., Miano, R., Graziani, G., ... Graziani, G. (**2018**). Experimental Evidence of the Antitumor, Antimetastatic and Antiangiogenic Activity of Ellagic Acid. *Nutrients*, 10(11), 1756.
- **109.**Shin, H.-J. R., Kim, H., Kim, K. Il, & Baek, S. H. (**2016**). Epigenetic and transcriptional regulation of autophagy. *Autophagy*, 12(11), 2248–2249.
- **110.**Kang I, Okla M, Chung S. (2014). Ellagic acid inhibits adipocyte differentiation through coactivator-associated arginine methyltransferase 1-mediated chromatin modification. J Nutr Biochem. 25(9):946-53.
- **111.**Nalla, K., Chatterjee, B., Poyya, J., Swain, A., Ghosh, K., Pan, A., ... & Kanade, S. R. (2024). Ellagic acid: a potential inhibitor of enhancer of zeste homolog-2 and protein arginine methyltransferase-5. *bioRxiv*, 2024-05.
- **112.** Abdullah, M. L., Hafez, M. M., Al-Hoshani, A., & Al-Shabanah, O. (**2018**). Anti-metastatic and anti-proliferative activity of eugenol against triple negative and HER2 positive breast cancer cells. *BMC Complementary and Alternative Medicine*, 18(1), 321.
- **113.** Jaganathan, S. K., & Supriyanto, E. (**2012**). Anti-proliferative and molecular mechanism of eugenolinduced apoptosis in cancer cells. *Molecules (Basel, Switzerland)*, 17(6), 6290–6304.
- **114.**Fouad, M. A., Sayed-Ahmed, M. M., Huwait, E. A., Hafez, H. F., & Osman, A. M. (2021). Epigenetic immunomodulatory effect of eugenol and astaxanthin on doxorubicin cytotoxicity in hormonal positive breast Cancer cells. *BMC pharmacology & toxicology*, 22(1), 8. https://doi.org/10.1186/s40360-021-00473-2
- **115.**Melchini, A., Traka, M. H., Catania, S., Miceli, N., Taviano, M. F., Maimone, P., ... Costa, C.(**2013**). Anti-proliferative Activity of the Dietary Isothiocyanate Erucin, a Bioactive Compound from Cruciferous Vegetables, on Human Prostate Cancer Cells. *Nutrition and Cancer*, 65(1), 132–138.
- **116.** Azarenko, O., Jordan, M. A., & Wilson, L. (**2014**). Erucin, the major isothiocyanate in arugula(Eruca sativa), inhibits proliferation of MCF7 tumor cells by suppressing microtubule dynamics. *PloSOne*, 9(6), e100599.
- **117.** Azarenko, O., Jordan, M. A., & Wilson, L. (2014). Erucin, the Major Isothiocyanate in Arugula (Eruca sativa), Inhibits Proliferation of MCF7 Tumor Cells by Suppressing Microtubule Dynamics. *PLOS ONE*, *9*(6), e100599. https://doi.org/10.1371/journal.pone.0100599
- **118.**Lee, P. N. H., & Ho, W. S. (**2013**). Anti-proliferative activity of gambogic acid isolated from Garcinia hanburyi in Hep3B and Huh7 cancer cells. *Oncology Reports*, 29(5), 1744–1750.
- **119.**Gao, G., Bian, Y., Qian, H., Yang, M., Hu, J., Li, L., ... Qian, X. (**2018**). Gambogic acid regulates the migration and invasion of colorectal cancer via microRNA-21-mediated activation of phosphatase and tensin homolog. *Experimental and Therapeutic Medicine*, 16(3), 1758–1765.
- **120.**Xu, H., Zhang, D., Wei, R., Zhou, Y., Dai, G., Li, J., Sun, Y., Li, F., & Xi, L. (2022). Gambogic Acid Induces Pyroptosis of Colorectal Cancer Cells through the GSDME-Dependent Pathway and Elicits an Antitumor Immune Response. *Cancers*, *14*(22), 5505. https://doi.org/10.3390/cancers14225505

- **121.**Ranjbarnejad, T., Saidijam, M., tafakh, M. sadat, Pourjafar, M., Talebzadeh, F., & Najafi, R. (**2017**). Garcinol exhibits anti-proliferative activities by targeting microsomal prostaglandin E synthase-1 in human colon cancer cells. *Human & Experimental Toxicology*, 36(7), 692–700.
- **122.**Duan, Y.-T., Yang, X.-A., Fang, L.-Y., Wang, J.-H., & Liu, Q. (**2018**). Anti-proliferative and anti-invasive effects of garcinol from Garcinia indica on gallbladder carcinoma cells. *Die Pharmazie*,73(7), 413–417.
- **123.**Collins, H. M., Abdelghany, M. K., Messmer, M., Yue, B., Deeves, S. E., Kindle, K. B., ... Heery, D. M. (**2013**). Differential effects of garcinol and curcumin on histone and p53 modifications in tumour cells. *BMC Cancer*, 13, 37.
- **124.**Sanaei, M., Kavoosi, F., Valiani, A., & Ghobadifar, M. (**2018**). Effect of genistein on apoptosisand proliferation of hepatocellular Carcinoma Hepa1-6 Cell Line. *International Journal of Preventive Medicine*, 9(1), 12.
- 125.de Lima, R. M. T., dos Reis, A. C., de Menezes, A.-A. P. M., Santos, J. V. de O., Filho, J. W.G. de O., Ferreira, J. R. de O., ... Melo-Cavalcante, A. A. de C. (2018). Protective and therapeutic potential of ginger (*Zingiber officinale*) extract and [6]-gingerol in cancer: A comprehensive review. *Phytotherapy Research*, 32(10), 1885–1907.
- **126.**Zhao, M., Yao, Y., Du, J., Kong, L., Zhao, T., Wu, D., Man, L., & Zhou, W. (2021). 6-Gingerol Alleviates Neonatal Hypoxic-Ischemic Cerebral and White Matter Injury and Contributes to Functional Recovery. *Frontiers in pharmacology*, *12*, 707772. https://doi.org/10.3389/fphar.2021.707772
- **127.**Semwal, R. B., Semwal, D. K., Vermaak, I., & Viljoen, A. (**2015**). A comprehensive scientificoverview of Garcinia cambogia. *Fitoterapia*, 102, 134–148.
- **128.** Yu, X., Ma, R., Wu, Y., Zhai, Y., & Li, S. (2018). Reciprocal Regulation of Metabolic Reprogramming and Epigenetic Modifications in Cancer. *Frontiers in Genetics*, 9. https://doi.org/10.3389/fgene.2018.00394
- 129. Alonso-Castro, A. J., Ortiz-Sánchez, E., Domínguez, F., Arana-Argáez, V., Juárez-Vázquez, M.del C., Chávez, M., ... García-Carrancá, A. (2012). Antitumor and immunomodulatory effects of Justicia spicigera Schltdl (Acanthaceae). *Journal of Ethnopharmacology*, 141(3), 888–894.
- 130. Govindarasu, M., Ganeshan, S., Ansari, M. A., Alomary, M. N., AlYahya, S., Alghamdi, S., Almehmadi, M., Rajakumar, G., Thiruvengadam, M., & Vaiyapuri, M. (2021). In silico modeling and molecular docking insights of kaempferitrin for colon cancer-related molecular targets. *Journal of Saudi Chemical Society*, 25(9), 101319. https://doi.org/10.1016/j.jscs.2021.101319
- **131.**Weng, J.-R., Lai, I.-L., Yang, H.-C., Lin, C.-N., & Bai, L.-Y. (**2014**). Identification of KazinolQ, a Natural Product from Formosan Plants, as an Inhibitor of DNA Methyltransferase. *Phytotherapy Research*, 28(1), 49–54.
- **132.** Takeshima, M., Ono, M., Higuchi, T., Chen, C., Hara, T., & Nakano, S. (**2014**). Anti-proliferative and apoptosis-inducing activity of lycopene against three subtypes of human breast cancer cell lines. *Cancer Science*, 105(3), 252–257. King-Batoon, A., Leszczynska, J. M., & Klein, C. B. (**2008**). Modulation of gene methylation by genistein or lycopene in breast cancer cells. *Environmental and Molecular Mutagenesis*, 49(1), 36–45.
- **133.**Satyan, K. S., Swamy, N., Dizon, D. S., Singh, R., Granai, C. O., & Brard, L. (**2006**). Phenethyl isothiocyanate (PEITC) inhibits growth of ovarian cancer cells by inducing apoptosis: Role of caspaseand MAPK activation. *Gynecologic Oncology*, 103(1), 261–270.
- **134.**Dai, M.-Y., Wang, Y., Chen, C., Li, F., Xiao, B.-K., Chen, S.-M., & Tao, Z.-Z. (**2016**). Phenethyl isothiocyanate induces apoptosis and inhibits cell proliferation and invasion in Hep-2 laryngeal cancer cells. *Oncology Reports*, 35(5), 2657–2664.
- **135.**Boyanapalli, S. S. S., Li, W., Fuentes, F., Guo, Y., Ramirez, C. N., Gonzalez, X.-P., ... Kong, A.-N. T. (**2016**). Epigenetic reactivation of RASSF1A by phenethyl isothiocyanate (PEITC) and promotion of apoptosis in LNCaP cells. *Pharmacological Research*, 114, 175–184.
- **136.**Park, H., Hwang, T., Youn, H., Kim, J., & Um, J. (2019). Piperine inhibits adipocyte differentiation via dynamic regulation of histone modifications. *Phytotherapy Research*, *33*(9), 2429-2439. https://doi.org/10.1002/ptr.6434
- **137.**Paarakh, P. M., Sreeram, D. C., D, S. S., & Ganapathy, S. P. S. (**2015**). In vitro cytotoxic and in silico activity of piperine isolated from *Piper nigrum* fruits Linn. *In Silico Pharmacology*, 3(1), 9.
- **138.**Wang, S., Jiang, K., Muthusamy, R., Kalaimani, S., Selvababu, A. P., Balupillai, A., Narenkumar, J., & Jeevakaruniyam, S. J. (2022). Protosappanin-B suppresses human melanoma cancer cell growth through

- impeding cell survival, inflammation and proliferative signaling pathways. *Process Biochemistry*, 122, 78-85. https://doi.org/10.1016/j.procbio.2022.08.023
- **139.** Yang, X., Ren, L., Zhang, S., Zhao, L., & Wang, J. (**2016**). Antitumor Effects of Purified Protosappanin B Extracted From Lignum Sappan. *Integrative Cancer Therapies*, 15(1), 87–95.
- **140.**Ahn, M. Y., Jung, J. H., Na, Y. J., & Kim, H. S. (**2008**). A natural histone deacetylase inhibitor, Psammaplin A, induces cell cycle arrest and apoptosis in human endometrial cancer cells. *Gynecologic Oncology*, 108(1), 27–33.
- **141.**Lee, R. H., Cho, J. H., Jeon, Y.-J., Bang, W., Cho, J.-J., Choi, N.-J., ... Chae, J.-I. (**2015**). Quercetin Induces Anti-proliferative Activity Against Human Hepatocellular Carcinoma (HepG2) Cells by Suppressing Specificity Protein 1 (Sp1). *Drug Development Research*, 76(1), 9–16.
- **142.** Alvarez, M. C., Maso, V., Torello, C. O., Ferro, K. P., & Saad, S. T. O. (**2018**). The polyphenolquercetin induces cell death in leukemia by targeting epigenetic regulators of pro-apoptotic genes. *Clinical Epigenetics*, 10(1), 139.
- **143.**Pozo-Guisado, E., Alvarez-Barrientos, A., Mulero-Navarro, S., Santiago-Josefat, B., & Fernandez-Salguero, P. M. (**2002**). The Anti-proliferative activity of resveratrol results in apoptosis in MCF-7 but not in MDA-MB-231 human breast cancer cells: cell-specific alteration of the cell cycle. *Biochemical Pharmacology*, 64(9), 1375–1386.
- **144.**Colin, D., Lancon, A., Delmas, D., Lizard, G., Abrossinow, J., Kahn, E., ... Latruffe, N. (**2008**). Anti-proliferative activities of resveratrol and related compounds in human hepatocyte derived HepG2cells are associated with biochemical cell disturbance revealed by fluorescence analyses. *Biochimie*, 90(11–12), 1674–1684.
- **145.**Chaudhuri, D., Orsulic, S., & Ashok, B. T. (**2007**). Anti-proliferative activity of sulforaphane in Aktoverexpressing ovarian cancer cells. *Molecular Cancer Therapeutics*, 6(1), 334–345.
- **146.**Kaufman-Szymczyk, A., Majewski, G., Lubecka-Pietruszewska, K., & Fabianowska- Majewska, K. (**2015**). The Role of Sulforaphane in Epigenetic Mechanisms, Including Interdependence between Histone Modification and DNA Methylation. *International Journal of Molecular Sciences*, 16(12), 29732–29743.
- **147.**Su, X., Jiang, X., Meng, L., Dong, X., Shen, Y., & Xin, Y. (**2018**). Anticancer Activity of Sulforaphane: The Epigenetic Mechanisms and the Nrf2 Signaling Pathway. *Oxidative Medicine and Cellular Longevity*, 2018, 1–10.
- **148.**Woo, H. J., Lee, S. J., Choi, B. T., Park, Y.-M., & Choi, Y. H. (**2007**). Induction of apoptosis and inhibition of telomerase activity by trichostatin A, a histone deacetylase inhibitor, in human leukemic U937 cells. *Experimental and Molecular Pathology*, 82(1), 77–84.
- **149.**Yim, E.-K., Lee, M.-J., Lee, K.-H., Um, S.-J., & Park, J.-S. (**2006**). Anti-proliferative and antiviral mechanisms of ursolic acid and dexamethasone in cervical carcinoma cell lines. *International Journal of Gynecologic Cancer*, 16(6), 2023–2031.
- **150.**Kim, H., Ramirez, C. N., Su, Z.-Y., & Kong, A.-N. T. (**2016**). Epigenetic modifications of triterpenoid ursolic acid in activating Nrf2 and blocking cellular transformation of mouse epidermal cells. *The Journal of Nutritional Biochemistry*, 33, 54–62.
- **151.**Shabbeer, S., Kortenhorst, M., Kachhap, S., Galloway, N., & Carducci, M. (**2006**). Multiple mechanisms explain the anti-proliferative effect of valproic acid on prostate cancer cells *in vitro* and *in vivo*. *Cancer Research*, 66(8 Supplement).
- 152.(https://www.cancer.gov/ccg/research/genome-sequencing/tcga)
- 153.(https://www.cbioportal.org/)
- 154.https://gco.iarc.fr/en
- 155. Chiang, K., Zielinska, A. E., Shaaban, A. M., Sanchez-Bailon, M. P., Jarrold, J., Clarke, T. L., Zhang, J., Francis, A., Jones, L. J., Smith, S., Barbash, O., Guccione, E., Farnie, G., Smalley, M. J., & Davies, C. C. (2017). PRMT5 Is a Critical Regulator of Breast Cancer Stem Cell Function via Histone Methylation and FOXP1 Expression. *Cell Reports*, 21(12), 3498-3513. https://doi.org/10.1016/j.celrep.2017.11.096
- **156.**Kumar, Y., Welker, A. M., An, M., Yang, X., Zhou, W., Shi, G., Imitola, J., Li, C., Hsu, S., Wang, J., Phelps, M., Zhang, J., Beattie, C. E., Baiocchi, R., & Kaur, B. (2018). PRMT5 as a druggable target for glioblastoma therapy. *Neuro-Oncology*, *20*(6), 753-763. https://doi.org/10.1093/neuonc/nox206
- **157.**Sloan, S. L., Brown, F., Long, M., Weigel, C., Koirala, S., Chung, J.-H., Pray, B., Villagomez, L., Hinterschied, C., Sircar, A., Helmig-Mason, J., Prouty, A., Brooks, E., Youssef, Y., Hanel, W., Parekh, S., Chan, W. K., Chen, Z., Lapalombella, R., ... Alinari, L. (2023). PRMT5 supports multiple oncogenic

- pathways in mantle cell lymphoma. In Blood (Vol. 142, Issue 10, pp. 887–902). American Society of Hematology. https://doi.org/10.1182/blood.2022019419
- **158.**Hu, R., Zhou, B., Chen, Z., Chen, S., Chen, N., Shen, L., Xiao, H., & Zheng, Y. (2022). PRMT5 Inhibition Promotes PD-L1 Expression and Immuno-Resistance in Lung Cancer. In Frontiers in Immunology (Vol. 12). Frontiers Media SA. https://doi.org/10.3389/fimmu.2021.722188
- **159.**Xiao, W., Chen, X., Liu, L., Shu, Y., Zhang, M., & Zhong, Y. (2019). Role of protein arginine methyltransferase 5 in human cancers. *Biomedicine & Pharmacotherapy*, 114, 108790. https://doi.org/10.1016/j.biopha.2019.108790
- **160.**Ma, Y., Zhong, Y., & Huang, W. (2019). Role of PRMT5 in bladder cancer: A comprehensive study. *Translational Cancer Research*, 8(2), 491-498. https://doi.org/10.21037/tcr.2019.03.05
- **161.**Xie, F., Zhang, H., Zhu, K., Jiang, S., Zhang, X., Chang, H., Qiao, Y., Sun, M., Wang, J., Wang, M., Tan, J., Wang, T., Zhao, L., Zhang, Y., Lin, J., Zhang, C., Liu, S., Zhao, J., Luo, C., . . . Shan, C. (2023). PRMT5 promotes ovarian cancer growth through enhancing Warburg effect by methylating ENO1. *MedComm*, *4*(2), e245. https://doi.org/10.1002/mco2.245
- **162.**Liu, Y., & Yang, Q. (2023). The roles of EZH2 in cancer and its inhibitors. *Medical Oncology (Northwood, London, England)*, 40(6). https://doi.org/10.1007/s12032-023-02025-6
- **163.**Park, S. H., Fong, K., Mong, E., Martin, M. C., Schiltz, G. E., & Yu, J. (2021). Going beyond Polycomb: EZH2 functions in prostate cancer. *Oncogene*, *40*(39), 5788-5798. https://doi.org/10.1038/s41388-021-01982-4
- **164.**Moral-Morales, A. D., González-Orozco, J. C., Hernández-Vega, A. M., Hernández-Ortega, K., Peña-Gutiérrez, K. M., & Camacho-Arroyo, I. (2022). EZH2 Mediates Proliferation, Migration, and Invasion Promoted by Estradiol in Human Glioblastoma Cells. *Frontiers in Endocrinology*, *13*. https://doi.org/10.3389/fendo.2022.703733
- **165.**Lachat, C., Boyer-Guittaut, M., Peixoto, P., & Hervouet, E. (2019). Epigenetic Regulation of EMT (Epithelial to Mesenchymal Transition) and Tumor Aggressiveness: A View on Paradoxical Roles of KDM6B and EZH2. *Epigenomes*, *3*(1). https://doi.org/10.3390/epigenomes3010001
- **166.**Lachat, C., Bruyère, D., Etcheverry, A., Aubry, M., Mosser, J., Warda, W., Herfs, M., Hendrick, E., Ferrand, C., Borg, C., Delage-Mourroux, R., Feugeas, P., Guittaut, M., Hervouet, E., & Peixoto, P. (2020).
- **167.** EZH2 and KDM6B Expressions Are Associated with Specific Epigenetic Signatures during EMT in Non Small Cell Lung Carcinomas. *Cancers*, *12*(12). https://doi.org/10.3390/cancers12123649
- 168. Yang, L., Shi, P., Zhao, G., Xu, J., Peng, W., Zhang, J., Zhang, G., Wang, X., Dong, Z., Chen, F., & Cui, H. (2020). Targeting cancer stem cell pathways for cancer therapy. *Signal Transduction and Targeted Therapy*, 5(1), 1-35. https://doi.org/10.1038/s41392-020-0110-5
- **169.**Flotho, C., Claus, R., Batz, C., Schneider, M., Sandrock, I., Ihde, S., Plass, C., Niemeyer, C. M., & Lübbert, M. (2009). The DNA methyltransferase inhibitors azacitidine, decitabine and zebularine exert differential effects on cancer gene expression in acute myeloid leukemia cells. *Leukemia*, *23*(6), 1019–1028. https://doi.org/10.1038/leu.2008.397
- 170. Buocikova, V., Tyciakova, S., Pilalis, E., Mastrokalou, C., Urbanova, M., Matuskova, M., Demkova, L., Medova, V., Longhin, E. M., Rundén-Pran, E., Dusinska, M., Rios-Mondragon, I., Cimpan, M. R., Gabelova, A., Soltysova, A., Smolkova, B., & Chatziioannou, A. (2022). Decitabine-induced DNA methylation-mediated transcriptomic reprogramming in human breast cancer cell lines; the impact of DCK overexpression. Frontiers in pharmacology, 13, 991751. https://doi.org/10.3389/fphar.2022.991751
- 171.Kagan, A. B., Garrison, D. A., Anders, N. M., Webster, J. A., Baker, S. D., Yegnasubramanian, S., & Rudek, M. A. (2023). DNA methyltransferase inhibitor exposure–response: Challenges and opportunities. *Clinical and Translational Science*, 16(8), 1309-1322. https://doi.org/10.1111/cts.13548
- 172.Ruiz-Magaña, M. J., Martínez-Aguilar, R., Lucendo, E., Campillo-Davo, D., Schulze-Osthoff, K., & Ruiz-Ruiz, C. (2016). The antihypertensive drug hydralazine activates the intrinsic pathway of apoptosis and causes DNA damage in leukemic T cells. *Oncotarget*, 7(16), 21875–21886. https://doi.org/10.18632/oncotarget.7871
- **173.**Duvic, M., & Vu, J. (2007). Vorinostat in cutaneous T-cell lymphoma. *Drugs of today (Barcelona, Spain : 1998)*, *43*(9), 585–599. https://doi.org/10.1358/dot.2007.43.9.1112980
- **174.**Bubna A. K. (2015). Vorinostat-An Overview. *Indian journal of dermatology*, *60*(4), 419. https://doi.org/10.4103/0019-5154.160511

- 175.Blumenschein, G. R., Jr, Kies, M. S., Papadimitrakopoulou, V. A., Lu, C., Kumar, A. J., Ricker, J. L., Chiao, J. H., Chen, C., & Frankel, S. R. (2008). Phase II trial of the histone deacetylase inhibitor vorinostat (Zolinza, suberoylanilide hydroxamic acid, SAHA) in patients with recurrent and/or metastatic head and neck cancer. *Investigational new drugs*, 26(1), 81–87. https://doi.org/10.1007/s10637-007-9075-2
- **176.**Barbarotta, L., & Hurley, K. (2015). Romidepsin for the Treatment of Peripheral T-Cell Lymphoma. *Journal of the advanced practitioner in oncology*, *6*(1), 22–36.
- **177.**Sawas, A., Radeski, D., & O'Connor, O. A. (2015). Belinostat in patients with refractory or relapsed peripheral T-cell lymphoma: a perspective review. *Therapeutic advances in hematology*, *6*(4), 202–208. https://doi.org/10.1177/2040620715592567
- 178. Eleutherakis-Papaiakovou, E., Kanellias, N., Kastritis, E., Gavriatopoulou, M., Terpos, E., & Dimopoulos, M. A. (2020). Efficacy of Panobinostat for the Treatment of Multiple Myeloma. *Journal of Oncology*, 2020. https://doi.org/10.1155/2020/7131802
- **179.** Yuan, X. G., Huang, Y. R., Yu, T., Jiang, H. W., Xu, Y., & Zhao, X. Y. (2019). Chidamide, a histone deacetylase inhibitor, induces growth arrest and apoptosis in multiple myeloma cells in a caspase-dependent manner. *Oncology letters*, 18(1), 411–419. https://doi.org/10.3892/ol.2019.10301
- **180.**Myers, R. A., Wirth, S., Williams, S., & Kiel, P. J. (2018). Enasidenib: An Oral IDH2 Inhibitor for the Treatment of Acute Myeloid Leukemia. *Journal of the advanced practitioner in oncology*, 9(4), 435–440.
- **181.**Woods, A., Norsworthy, K. J., Wang, X., Vallejo, J., Chiu Yuen Chow, E., Li, R. J., Sun, J., Charlab, R., Jiang, X., Pazdur, R., Theoret, M. R., & de Claro, R. A. (2024). FDA Approval Summary: Ivosidenib in Combination with Azacitidine for Treatment of Patients with Newly Diagnosed Acute Myeloid Leukemia with an IDH1 Mutation. *Clinical cancer research : an official journal of the American Association for Cancer Research*, 30(7), 1226–1231. https://doi.org/10.1158/1078-0432.CCR-23-2234
- **182.**Straining, R., & Eighmy, W. (2022). Tazemetostat: EZH2 Inhibitor. *Journal of the advanced practitioner in oncology*, 13(2), 158–163. https://doi.org/10.6004/jadpro.2022.13.2.7
- 183.Marzochi, L. L., Cuzziol, C. I., Nascimento Filho, C. H. V. D., Dos Santos, J. A., Castanhole-Nunes, M. M. U., Pavarino, É. C., Guerra, E. N. S., & Goloni-Bertollo, E. M. (2023). Use of histone methyltransferase inhibitors in cancer treatment: A systematic review. *European Journal of Pharmacology*, 944, 175590. https://doi.org/10.1016/j.ejphar.2023.175590
- **184.**Stein, E. M., Garcia-Manero, G., Rizzieri, D. A., Tibes, R., Berdeja, J. G., Savona, M. R., Jongen-Lavrenic, M., Altman, J. K., Thomson, B., Blakemore, S. J., Daigle, S. R., Waters, N. J., Suttle, A. B., Clawson, A., Pollock, R., Krivtsov, A., Armstrong, S. A., DiMartino, J., Hedrick, E., Löwenberg, B., ... Tallman, M. S. (2018). The DOT1L inhibitor pinometostat reduces H3K79 methylation and has modest clinical activity in adult acute leukemia. *Blood*, *131*(24), 2661–2669. https://doi.org/10.1182/blood-2017-12-818948
- **185.**Feustel, K., & Falchook, G. S. (2022). Protein Arginine Methyltransferase 5 (PRMT5) Inhibitors in Oncology Clinical Trials: A review. *Journal of immunotherapy and precision oncology*, *5*(3), 58–67. https://doi.org/10.36401/JIPO-22-1
- **186.**Chen, Y., Shao, X., Zhao, X., Ji, Y., Liu, X., Li, P., Zhang, M., & Wang, Q. (2021). Targeting protein arginine methyltransferase 5 in cancers: Roles, inhibitors and mechanisms. *Biomedicine & Pharmacotherapy*, 144, 112252. https://doi.org/10.1016/j.biopha.2021.112252
- 187. Ernzen, K., Melvin, C., Yu, L., Phelps, C., Niewiesk, S., Green, P. L., & Panfil, A. R. (2023). The PRMT5 inhibitor EPZ015666 is effective against HTLV-1-transformed T-cell lines *in vitro* and *in vivo*. *Frontiers in microbiology*, 14, 1101544. https://doi.org/10.3389/fmicb.2023.1101544
- **188.**Chen, C., Zhou, M., Ge, Y., & Wang, X. (2020). SIRT1 and aging related signaling pathways. *Mechanisms of Ageing and Development*, 187, 111215. https://doi.org/10.1016/j.mad.2020.111215
- **189.**Wössner, N., Alhalabi, Z., González, J., Swyter, S., Gan, J., Schmidtkunz, K., Zhang, L., Vaquero, A., Ovaa, H., Einsle, O., Sippl, W., & Jung, M. (2020). Sirtuin 1 Inhibiting Thiocyanates (S1th)-A New Class of Isotype Selective Inhibitors of NAD⁺ Dependent Lysine Deacetylases. *Frontiers in oncology*, *10*, 657. https://doi.org/10.3389/fonc.2020.00657
- 190. Vázquez, R., Riveiro, M. E., Astorgues-Xerri, L., Odore, E., Rezai, K., Erba, E., Panini, N., Rinaldi, A., Kwee, I., Beltrame, L., Bekradda, M., Cvitkovic, E., Bertoni, F., Frapolli, R., & D'Incalci, M. (2017). The bromodomain inhibitor OTX015 (MK-8628) exerts anti-tumor activity in triple-negative breast cancer models as single agent and in combination with everolimus. *Oncotarget*, 8(5), 7598–7613. https://doi.org/10.18632/oncotarget.13814

- 191.Blum, K. A., Supko, J. G., Maris, M. B., Flinn, I. W., Goy, A., Younes, A., Bobba, S., Senderowicz, A. M., Efuni, S., Rippley, R., Colak, G., Trojer, P., & Abramson, J. S. (2022). A Phase I Study of Pelabresib (CPI-0610), a Small-Molecule Inhibitor of BET Proteins, in Patients with Relapsed or Refractory Lymphoma. Cancer research communications, 2(8), 795–805. https://doi.org/10.1158/2767-9764.CRC-22-0060
- **192.**Dalpatraj, N., Naik, A., & Thakur, N. (2023). GSK-J4: An H3K27 histone demethylase inhibitor, as a potential anti-cancer agent. *International journal of cancer*, 153(6), 1130–1138. https://doi.org/10.1002/ijc.34559
- 193. Chianese, U., Papulino, C., Passaro, E., Evers, T. M., Babaei, M., Toraldo, A., De Marchi, T., Niméus, E., Carafa, V., Nicoletti, M. M et al. (2022). Histone lysine demethylase inhibition reprograms prostate cancer metabolism and mechanics. *Molecular metabolism*, 64, 101561. https://doi.org/10.1016/j.molmet.2022.101561
- 194. Lewis P.H. New mutants: Report of P. Lewis. Drosoph. Inf. Serv. 1947;21:69
- **195.**Kyba M., Brock H.W. The Drosophila polycomb group protein Psc contacts ph and Pc through specific conserved domains. Mol. Cell Biol. 1998;18:2712–2720. doi: 10.1128/MCB.18.5.2712.
- **196.**Ng J., Hart C.M., Morgan K., Simon J.A. A Drosophila ESC-E(Z) protein complex is distinct from other polycomb group complexes and contains covalently modified ESC. Mol. Cell Biol. 2000;20:3069–3078. doi: 10.1128/MCB.20.9.3069-3078.2000
- **197.**Kuzmichev A., Nishioka K., Erdjument-Bromage H., Tempst P., Reinberg D. Histone methyltransferase activity associated with a human multiprotein complex containing the Enhancer of Zeste protein. Genome Res. 2002;16:2893–2905. doi: 10.1101/gad.1035902.
- **198.**Gutiérrez L., Oktaba K., Scheuermann J.C., Gambetta M.C., Ly-Hartig N., Müller J. The role of the histone H2A ubiquitinase Sce in Polycomb repression. Development. 2012;139:117–127. doi: 10.1242/dev.074450.
- **199.**Kaito, S., & Iwama, A. (2020). Pathogenic Impacts of Dysregulated Polycomb Repressive Complex Function in Hematological Malignancies. *International journal of molecular sciences*, 22(1), 74. https://doi.org/10.3390/ijms22010074
- **200.** Iwama, A. (2017). Polycomb repressive complexes in hematological malignancies. In Blood (Vol. 130, Issue 1, pp. 23–29). American Society of Hematology. https://doi.org/10.1182/blood-2017-02-739490
- 201.Liu, J., Fan, H., Liang, X., & Chen, Y. (2023). Polycomb repressor complex: Its function in human cancer and therapeutic target strategy. Biomedicine & Pharmacotherapy, 169, 115897. https://doi.org/10.1016/j.biopha.2023.115897
- 202. Niewmierzycka, A., & Clarke, S. (1999). S-Adenosylmethionine-dependent Methylation in Saccharomyces cerevisiae: IDENTIFICATION OF A NOVEL PROTEIN ARGININE METHYLTRANSFERASE. Journal of Biological Chemistry, 274(2), 814-824. https://doi.org/10.1074/jbc.274.2.814
- 203.Pal, S., Vishwanath, S. N., Erdjument-Bromage, H., Tempst, P., & Sif, S. (2004). Human SWI/SNF-associated PRMT5 methylates histone H3 arginine 8 and negatively regulates expression of ST7 and NM23 tumor suppressor genes. *Molecular and cellular biology*, 24(21), 9630–9645. https://doi.org/10.1128/MCB.24.21.9630-9645.2004
- **204.**Stopa, N., Krebs, J.E. & Shechter, D. The PRMT5 arginine methyltransferase: many roles in development, cancer and beyond. *Cell. Mol. Life Sci.* **72**, 2041–2059 (2015). https://doi.org/10.1007/s00018-015-1847-9
- **205.**Bao, X., Zhao, S., Liu, T., Liu, Y., Liu, Y., & Yang, X. (2013). Overexpression of PRMT5 promotes tumor cell growth and is associated with poor disease prognosis in epithelial ovarian cancer. *The journal of histochemistry and cytochemistry: official journal of the Histochemistry Society*, 61(3), 206–217. https://doi.org/10.1369/0022155413475452
- **206.** Shailesh, H., Zakaria, Z. Z., Baiocchi, R., & Sif, S. (2018). Protein arginine methyltransferase 5 (PRMT5) dysregulation in cancer. *Oncotarget*, *9*(94), 36705-36718. https://doi.org/10.18632/oncotarget.26404
- **207.** Feustel, K., & Falchook, G. S. (2022). Protein Arginine Methyltransferase 5 (PRMT5) Inhibitors in Oncology Clinical Trials: A review. In Journal of Immunotherapy and Precision Oncology (Vol. 5, Issue 3, pp. 58–67). Innovative Healthcare Institute. https://doi.org/10.36401/jipo-22-1
- 208. Dakroub, R., Huard, S., Hajj-Younes, Y., Suresh, S., Badran, B., Fayyad-Kazan, H., & Dubois, T. (2023). Therapeutic Advantage of Targeting PRMT5 in Combination with Chemotherapies or EGFR/HER2 Inhibitors in Triple-Negative Breast Cancers. *Breast Cancer: Targets and Therapy*, 15, 785-799. https://doi.org/10.2147/BCTT.S430513

- **209.** https://www.onclive.com/view/early-trials-of-prmt5-inhibitors-leave-much-to-be-desired-but-optimism-remains
- **210.** <a href="https://medinfo.gsk.com/5f95dbd7-245e-4e65-9f36-1a99e28e5bba/2aa169c7-2996-466f-a218-56a64a114549/2aa169c7-2996-466f-a218-56a64a114549_viewable_rendition_v.pdf?REF--ALL-004395
- **211.**https://investors.preludetx.com/news-releases/news-release-details/prelude-therapeutics-announces-presentation-encouraging-data
- 212.https://jdc.jefferson.edu/cgi/viewcontent.cgi?article=1262&context=medoncfp
- **213.**Gan, L., Yang, Y., Li, Q. *et al.* Epigenetic regulation of cancer progression by EZH2: from biological insights to therapeutic potential. *Biomark Res* **6**, 10 (2018). https://doi.org/10.1186/s40364-018-0122-2
- **214.**Ohuchi, M., Sakamoto, Y., Tokunaga, R., Kiyozumi, Y., et al., (2018). Increased EZH2 expression during the adenoma-carcinoma sequence in colorectal cancer. In Oncology Letters. Spandidos Publications. https://doi.org/10.3892/ol.2018.9240
- **215.**Nourmohammadi, F., Forghanifard, M. M., Abbaszadegan, M. R., & Zarrinpour, V. (2022). EZH2 regulates oncomiR-200c and EMT markers in esophageal squamous cell carcinomas. *Scientific Reports*, *12*. https://doi.org/10.1038/s41598-022-23253-2
- **216.**Kim, K. H., & M. Roberts, C. W. (2016). Targeting EZH2 in cancer. *Nature Medicine*, 22(2), 128. https://doi.org/10.1038/nm.4036
- **217.**Mahmoud, F., Shields, B., Makhoul, I., Hutchins, L. F., Shalin, S. C., & Tackett, A. J. (2016). Role of EZH2 histone methyltrasferase in melanoma progression and metastasis. *Cancer Biology & Therapy*, 17(6), 579-591. https://doi.org/10.1080/15384047.2016.1167291
- **218.**Zimmerman, S. M., Lin, P. N., & Souroullas, G. P. (2023). Non-canonical functions of EZH2 in cancer. *Frontiers in Oncology*, *13*. https://doi.org/10.3389/fonc.2023.1233953
- **219.**Eich, M.-L., Athar, M., Ferguson, J. E., III, & Varambally, S. (2020). EZH2-Targeted Therapies in Cancer: Hype or a Reality. In Cancer Research (Vol. 80, Issue 24, pp. 5449–5458). American Association for Cancer Research (AACR). https://doi.org/10.1158/0008-5472.can-20-2147
- **220.**Tai, Y., & Shang, J. (2023). Wnt/β-catenin signaling pathway in the tumor progression of adrenocortical carcinoma. *Frontiers in Endocrinology*, *14*. https://doi.org/10.3389/fendo.2023.1260701
- 221.Kurmasheva, R. T., Sammons, M., Favours, E., Wu, J., Kurmashev, D., Cosmopoulos, K., Keilhack, H., Klaus, C. R., Houghton, P. J., & Smith, M. A. (2017). Initial testing (stage 1) of tazemetostat (EPZ-6438), a novel EZH2 inhibitor, by the Pediatric Preclinical Testing Program. *Pediatric blood & cancer*, 64(3), 10.1002/pbc.26218. https://doi.org/10.1002/pbc.26218
- 222.Italiano, A., Soria, J. C., Toulmonde, M., Michot, J. M., Lucchesi, C., Varga, A., Coindre, J. M., Blakemore, S. J., Clawson, A et al., (2018). Tazemetostat, an EZH2 inhibitor, in relapsed or refractory B-cell non-Hodgkin lymphoma and advanced solid tumours: a first-in-human, open-label, phase 1 study. *The Lancet. Oncology*, 19(5), 649–659. https://doi.org/10.1016/S1470-2045(18)30145-1
- **223.**Li, C., Wang, Y., Gong, Y., Zhang, T., Huang, J., Tan, Z., & Xue, L. (2021). Finding an easy way to harmonize: a review of advances in clinical research and combination strategies of EZH2 inhibitors. *Clinical epigenetics*, *13*(1), 62. https://doi.org/10.1186/s13148-021-01045-1
- 224. https://clinicaltrials.gov/study/NCT03480646
- **225.**Hoy S. M. (2020). Tazemetostat: First Approval. *Drugs*, 80(5), 513–521. https://doi.org/10.1007/s40265-020-01288-x
- **226.**Rugo, H. S., Jacobs, I., Sharma, S., Scappaticci, F., Paul, T. A., Jensen-Pergakes, K., & Malouf, G. G. (2020). The Promise for Histone Methyltransferase Inhibitors for Epigenetic Therapy in Clinical Oncology: A Narrative Review. *Advances in therapy*, *37*(7), 3059–3082. https://doi.org/10.1007/s12325-020-01379-x
- 227. Wang, J., Elkrief, A., Guo, W., Shukla, N., Gounder, M., & Ladanyi, M. (2021). Prospects for Epigenetic Targeted Therapies of Bone and Soft-Tissue Sarcomas. *Sarcoma*, 2021, 5575444. https://doi.org/10.1155/2021/5575444
- **228.**Morschhauser, F., Salles, G., Batlevi, C. L., Tilly, H., Chaidos, A., Phillips, T., Burke, J., & Melnick, A. (2022). Taking the EZ way: Targeting enhancer of zeste homolog 2 in B-cell lymphomas. *Blood reviews*, 56, 100988. https://doi.org/10.1016/j.blre.2022.100988

CHAPTER# 2

TO SCREEN AND IDENTIFY THE PHYTOCOMPOUNDS WITH ANTIPROLIFERATIVE PROPERTIES AND ITS EFFECTS ON GENE EXPRESSION OF EPIGENETIC REGULATORS.

2.1 Introduction

Epigenetic mechanisms play a fundamental dynamic role in development and maintenance and controls the gene expression patterns in humans ^[1]. Dysregulations in these mechanisms can trigger altered gene expression, initiating malignant cellular transformations. Global changes in the epigenetic landscape are implicated in various molecular mechanisms underlying the "hallmarks of cancer ^[2]. While cancer was perceived as a genetic disease at initially, but now it was recognized that epigenetic abnormalities also lead a significant role in its initiation and progression alongside genetic alterations. The complexity of cancer lies in its manifestation across more than a hundred types, spanning various tissue types, making it a formidable challenge. However, advancements in medical technology have led to the development of several therapeutic modalities, including chemotherapy, immunotherapy, surgical tumor removal, and radiation therapy, all aimed at diagnosis and treatment ^[3]. Often, a combination of these therapies yields better results. Despite this progress, challenges such as poor prognosis persist, although strides in early detection, accurate diagnosis, and precision targeting are gradually improving outcomes.

Recent advances in epigenetic drugs, also known as epidrugs, have shown promise as they target DNA and chromatin structures, disrupting transcriptional and post-transcriptional modifications by regulating crucial enzymes ^[4]. The FDA has approved various epidrugs for cancer treatment ^[5]. These medications, whether administered alone or as part of combination therapies, have showcased effectiveness and promise in both preclinical and clinical trials. However, many of these authorized drugs, along with those undergoing clinical scrutiny, belong to the category of nucleoside analogs ^[6], carrying potential long-term side effects. Multiple research studies have identified anti-proliferative molecules for assessment, with a focus on their influence on the expression of epigenetic regulators like DNA methylating enzymes, histone methyltransferases and genes linked to the polycomb repressive complex (as outlined in Table 1.8). Phytocompounds offer distinct advantages over synthetic drugs such as epidrugs due to their lower or negligible side effects, rendering them potentially safer for prolonged usage. Moreover, their abundance and natural sourcing render them a sustainable and cost-effective alternative for cancer therapy with certain limitations.

Additionally, the diverse chemical compositions of phytocompounds impart a wider range of epigenetic modulatory effects, augmenting their therapeutic potential in cancer treatment. This

approach holds significant promise for devising novel cancer therapy strategies with potentially reduced side effects, tapping into the extensive reservoir of natural compounds found in plants. As research advances along this trajectory, it holds the potential to unveil safer and more efficacious cancer treatments. To tackle this issue, we advocate for the screening of phytocompounds as natural epigenetic modulators, contrasting them with synthetic compounds due to their lower or negligible side effects and enhanced availability.

2.2 Materials & Methods

2.2.1 Databases and Chemicals

2.2.1.1 Databases

The following databases were used in current study, for chemical library preparation we utilized following datasets: PubMed ^[7], Scopus^[8], Google scholar^{[9],} natural drug databases such as Natural Product Activity and Compound Tracking (NPACT)^[10], Natural Product Activity and Screening System (NPASS)^[11], South African Natural Compound Database (SANCDB)^[12], Screening Unified Natural Product Database: Enhanced Natural Products Database for Structure-Activity Relationships (SUPER NATURAL-II)^[13], Yale University Traditional Chinese Medicine (YaTCM)^[14,15], and ADMET prediction analysis by Swiss ADME^[16].

To investigate the roles of PRMT5 and EZH2 in cancer, we utilized the cBioportal dataset ^[17], an exploratory analysis tool designed for exploring large-scale cancer genomic datasets sourced from curated data which includes The Cancer Genome Atlas (TCGA), Therapeutically Applicable Research to Generate Effective Treatments (TARGET), and individual lab publications. To assess the correlation between PRMT5 and EZH2 expression and patient survival in cancer, we employed the Km plotter ^[18]. Specifically, we analyzed data from breast cancer patients and plotted Kaplan-Meier curves for both oncoproteins (PRMT5 and EZH2).

2.2.1.2 Chemicals

Epigallocatechin-3-gallate (EGCG), Ellagic-acid (EA), Brazilin (Brz), Curcumin (Cur), Resveratrol (Rvr), Piperine (Ppr), Quercetin (Qct), Gambogic acid (Gba), Apicidin (Apdn), Anethol (Atl), Eugenol (Egl), capsaicin (Cpcn), Eucalyptol (Ect), Sulforaphane (Sfp), 3-(4,5-Dimethylthiazol-2-yl)-2,5Diphenyltetrazolium-Bromide (MTT), Dimethyl sulfoxide (DMSO), were acquired from Sigma-Aldrich United states. All other chemicals were of analytical or higher standards unless otherwise specified.

2.2.2 Literature and database search for medicinal plants and Indian spices:

In this study, our primary objective was to find medicinal plants and Indian spices by extensively scouring databases and literature. To accomplish this, we utilized widely accessible literature search engines including PubMed, Scopus, and Google Scholar. Additionally, we delved into natural product databases such as Natural Product Activity and Compound Tracking (NPACT) [10], Natural Product Activity and Screening System (NPASS) [11], South African Natural Compound Database (SANCDB) [12], Screening Unified Natural Product Database: Enhanced Natural Products Database for Structure-Activity Relationships (SUPER NATURAL-II) [13], and Yale University Traditional Chinese Medicine (YaTCM) [14].

2.2.3 Chemical library preparation and ADMET analysis

The structural information for all compounds was obtained in line notation format, known as SMILES (Simplified Molecular-Input Line-Entry System), saved from databases such as PubChem [19], ZINC [20], and ChEBI [21]. This data was crucial for conducting ADME analysis using the SwissADME web tool [22]. Compounds lacking proper two-dimensional (2D) or three-dimensional (3D) structures in these databases were excluded from further consideration. For compound selection, we employed two filters, often referred to as rules of drug likeness, based on ADME analysis. The first filter, known as the Lipinski (Pfizer) filter [23] or 'the rule of 5', imposed limits on the molecular weight (\leq 500 Dalton), MLOGP (Moriguchi Log P) (\leq 4.15), hydrogen-bond acceptors number (N or O) (\leq 10), and hydrogen-bond donors' number (NH or OH) (\leq 5). The second filter, termed the Veber (GSK) filter [24], considered the rotatable bond numbers (\leq 10) and the topological polar surface area dimensions were (TPSA) (\leq 140). While most of the phytocompounds had to adhere to these criteria, exceptions were made for a few compounds with certain violations if other properties deemed suitable during ADME analysis.

2.2.4 Chemical preparation of modulators

The purest form of anti-proliferative molecules mentioned in section 2.2.12 were purchased from Sigma-Aldrich. These anti-proliferative molecules were solubilized in either dimethyl sulfoxide (DMSO) or Phosphate buffer saline (PBS) to make 5μ M main stock solution based on their molecular weight and sterilized through $0.2 \mu m$ syringe filter, and final working stock solutions were prepared in serum free media freshly just before use.

2.2.5 Cell culture and maintenance

In-vitro assays utilized various human malignant cell lines obtained from the National Centre for Cell Science (NCCS) in Pune, Maharashtra, India. These included MCF7 (breast), MDA-MB-231 (breast), Du-145 (prostate), A549 (lung), HeLa (cervix), Hep G2 (liver), PC-3 (prostate), and HEK293 (human embryonic kidney). The maintenance of these cell lines followed standard sterile cell culture protocols to ensure low passage numbers. Cells were cultured in DMEM (Dulbecco's Modified Eagle's Medium) high glucose (from Himedia), supplemented with 10% fetal bovine serum (Himedia) and 1x antibiotic-antimycotic solution (Himedia), and maintained at 37°C in a humidified chamber with 95% air and 5% CO₂.

2.2.6 Cell proliferation assay using MTT

When cells reached approximately 80% confluence, detached by using 0.05% trypsin-EDTA solution and sub-cultured. This involved aspirating the media, washing with PBS, incubating with approximately 1 mL trypsin-EDTA for 3-5 minutes at 37°C, neutralizing with DMEM complete media, and subjected to centrifugation at 1500 rpm for 5 minutes. Cell density was determined using the Neubauer chamber with Trypan blue exclusion. Subsequently, cells were seeded at a density of 5 x 10^3 cells/well in a 96-well plate and incubated overnight at 37°C in CO₂ incubator.

The anti-proliferative effects of screened phytochemicals on selected cell lines were examined by using the MTT assay. This assay measures cell viability by assessing the change in optical density resulting from MTT's interaction with the mitochondrial reductase enzyme in live cells. Working concentrations of 1 mM in serum-free media were prepared from 5 mM stock solutions in DMSO for all compounds. Cells were seeded at a density of 5 x 10^3 cells/well in 96-well plates and incubated overnight at 37° C CO₂ incubator. After removing the media, cells were allowed to treat with different concentrations of compounds (control, 0.2% DMSO, 1, 5, 10, 15, 20, 40, 50 μ M) for 24 and 48 hours in culture media.

Cells cultured without any drug served as the negative control, while 0.2% DMSO acted as the positive control for the MTT assay. After the specified incubation period, cell culture media was removed, and cells were washed with PBS twice. Then, 20 μ L of MTT solution (5 mg/ml in 1x PBS) and fresh serum-free media 80 μ L were added to each well, followed by incubation for 3 hours at 37°C. After the formation of purple formazan crystals, solubilization was achieved by adding 100 μ L of DMSO to each well. The resulting color intensity was measured

at 540 nm using a microplate reader. Two independent experiments were conducted in triplicate, and cell viability was considered relative to the control well (considered 100%). Mean ± standard error (SE) was calculated for all phytocompounds studied, and the cell response (%) versus drug concentration (µM) was reported.

2.2.6.1 Trypan blue dye exclusion assay

Trypan blue dye exclusion test was performed as per previously established protocols ⁽²⁵⁾. Begin by preparing a cell suspension containing the cells of interest, either from a culture or obtained from a tissue sample. Treat the cell suspension with EGCG and EA according to the experimental conditions. After the treatment, add Trypan Blue dye to the cell suspension. Trypan Blue is a vibrant dye that can penetrate non-viable cells with compromised membranes, staining them blue. However, viable cells with intact membranes eliminate the dye and appear transparent. Prepare a slide with a small volume of the stained cell suspension and examine it under a microscope. Observe the cells to determine whether they have absorbed (stained blue) or excluded (transparent) the Trypan Blue dye.

To Count blue-stained cells numbers (non-viable) cells and transparent (viable) cells in the microscopic field. Cell viability percentage can be estimated by employing the following formula:

% of Viable Cells =
$$\frac{Number\ of\ viable\ cells}{Total\ Number\ of\ cells}\ X\ 100$$

plotted a graph based on the percentage of viable cells versus non-viable cells.

2.2.7 Impact of phytocompounds on epigenetic regulators through-qPCR (Real time quantitative polymerase chain reaction assay)

To analyse alterations or changes in transcription levels of multiple epigenetic regulators, their mRNA levels were simultaneously quantified using qPCR. Initially, RNA was converted to cDNA and then amplified in a PCR, with real-time detection facilitated by a DNA-binding dye like SYBR Green. The cycle number at which fluorescent signal surpasses background noise, known as Ct value, indicates amplification. Changes in Ct values between samples (Δ Ct) were utilized to determine relative fold increase via the 2- $\Delta\Delta$ Ct formula, normalized with a reference gene, commonly GAPDH.

Total RNA, devoid of DNA, was extracted from samples by using the RNA isolation kit (High Pure RNA Isolation kit manufactured by Roche Diagnostics GmbH, Risch-Rotkreuz, Switzerland) as per the manufacturer's instructions.

Table 2.1. Details of the primers used for RT-PCR studies

Gene	Forward Primer (5'-3')	Reverse Primer (5´-3´)
GAPDH	GTCTCCTCTGACTTCAACAGCG	ACCACCCTGTTGCTGTAGCCAA
DNMT1	AGGTGGAGAGTTATGACGAGGC	GGTAGAATGCCTGATGGTCTGC
DNMT3A	CCTCTTCGTTGGAGGAATGTGC	GTTTCCGCACATGAGCACCTCA
DNMT3B	TAACAACGCAAAGACCGAGGG	TCCTGCCACAAGACAACAGCC
TET1	CAGGACCAAGTGTTGCTGCTGT	GACACCCATGAGAGCTTTTCCC
TET2	GCTTACCGAGACGCTGAGGAAA	AGAGAAGGAGCACCACAGGTT
TET3	CCACAAGGACCAGCATAACCTC	CTCGCTACCAAACTCATCCGTG
PRMT1	TGCGGTGAAGATCGTCAAAGCC	GGACTCGTAGAAGAGGCAGTAG
PRMT2	GCAGTTGGACATGAGAACCGTG	AGGCTCTGGAAGTGGACGCTAA
PRMT3	CACTGTCTGCTGAAGCCGCATT	GTAGATGACGAGCAGGTTCTGAC
PRMT4	TTCCAGTCACCACTGTTCGCCA	CCAGGAGGTTACTGGACTTGGA
PRMT5	TGAGGCCCAGTTTGAGATGCCTTA	AGTAGCCGGCAAAGCCATGTAGTA
PRMT6	TGGCTTTGCCATCTGGTTCCAG	TAGAGGAGCGCCTGTTTCCAGT
PRMT7	CCACGATGACTACTGCGTATGG	GACGTACCGATCAGTTCTGTCC
PRMT8	AGCAAGTGGTGACCAATGCCTG	TGGACGTAGTCGTTGCGCTGTA
PRMT9	GGACATTGGAGCAGGAACTGGA	GTTTGCTGCCACGACATCACAG
KAT1	GGTAGCCTGTCAACAATGTTCCG	CGTGTTTGTGCAAAATCCAGGTG
KAT2A	GAGGTCATGCTGACCATCACTG	CAGTGAGTTGCCGATGACATGG
KAT2B	GCACCATCTCAACGAAGACTGC	GTGTGGTTTCGTACCGAGGTAG
KAT3B	GATGACCCTTCCCAGCCTCAAA	GCCAGATGATCTCATGGTGAAGG
HDAC1	ACCGGGCAACGTTACGAAT	CTATCAAAGGACACGCCAAGTG
HDAC2	TCATTGGAAAATTGACAGCATAGT	CATGGTGATGGTGTTGAAGAAG
HDAC3	TTGAGTTCTGCTCGCGTTACA	CCCAGTTAATGGCAATATCACAGAT
HDAC4	AATCTGAACCACTGCATTTCCA	GGTGGTTATAGGAGGTCGACACT
HDAC5	TTGGAGACGTGGAGTACCTTACAG	GACTAGGACCACATCAGGTGAGAAC
HDAC7	CTGCATTGGAGGAATGAAGCT	CTGGCACAGCGGATGTTTG
HDAC8	TCCCGAGTATGTCAGTATATATGA	GCTTCAATCAAAGAATGCACCAT
SIRT1	TAGACACGCTGGAACAGGTTGC	CTCCTCGTACAGCTTCACAGTC
SIRT2	CTGCGGAACTTATTCTCCCAGAC	CCACCAAACAGATGACTCTGCG
SIRT3	CCCTGGAAACTACAAGCCCAAC	GCAGAGGCAAAGGTTCCATGAG
SIRT4	GTGGATGCTTTGCACACCAAGG	GGTTCAGGACTTGGAAACGCTC
RNF1	CCTATCTGCCTGGACATGCTGA	GCTTCTTTCGGCAGGTAGGACA
RNF2	CAGTCACAGCATTGAGGAAGGAC	GCTTCCTGATTGCTATGTGTGGA
PCGF2	CACTATCGTGGAGTGCCTGCAT	GGTTTTATGGACCTGCACGTCAC
PCGF4	GGTACTTCATTGATGCCACAACC	CTGGTCTTGTGAACTTGGACATC
EZH1	CACCACATAGTCAGTGCTTCCTG	AGTCTGACAGCGAGAGTTAGCC
EZH2	GACCTCTGTCTTACTTGTGGAGC	CGTCAGATGGTGCCAGCAATAG
EED	GACGAGAACAGCAATCCAGACC	TCCTTCCAGGTGCATTTGGCGT
SUZ12	CCATGCAGGAAATGGAAGAATGTC	CTGTCCAACGAAGAGTGAACTGC

The purified RNA was converted into cDNA using the QuantiTect Reverse Transcription Kit (Qiagen, Hilden, Germany) following the instructions. Triplicates of cDNA from each

treatment group were subsequently analyzed by real-time PCR using LightCycler® 480 SYBR Green I Master reagents (Roche) on a LightCycler® 480 Instrument II from Roche according to the recommended protocol. The amplification protocol included an initial 5-minute incubation at 95°C, with 40 cycles of denaturation (10 sec/95°C), annealing @10 sec/55-60°C with single fluorescence acquisition), and elongation (10 sec/72°C).

Melting curve analysis was performed with temperature settings of 30 sec/95°C, 30 sec/65°C, followed by a gradual increase in temperature at 0.1°C/sec while continuously acquiring fluorescence. Finally, the plate was cooled at 40°C for 30 seconds. Ct values of the target gene and the housekeeping gene (GAPDH) were normalized and compared across treatment groups to calculate relative changes in gene expression fold. Specific details of the human primers used in this experiment can be found in Table 2.1.

2.2.8 CBioPortal dataset search for PRMT5 & EZH2 Pathogenesis in cancer

To investigate the roles of PRMT5 and EZH2 in cancer, we utilized the cBioportal dataset, an analytical tool specifically designed for exploring extensive cancer genomic data from large consortiums such as The Cancer Genome Atlas (TCGA), Therapeutically Applicable Research to Generate Effective Treatments (TARGET), and individual laboratory publications. Within the cBioportal platform, we accessed and analyzed available cancer datasets, focusing on data related to EZH2 and PRMT5 genes. Our analysis included parameters such as amplifications, mutations, deletions, and other alterations.

Our objective was to assess the correlation between PRMT5 and EZH2 gene expression levels and patient survival consequences across a dataset encompassing 30,000 samples from 21 different tumor types. These tumor types included breast cancer, ovarian cancer, gastric cancer, lung cancer, colon cancer, acute myeloid leukemia, and myeloma. Through this comprehensive analysis, we aimed to uncover potential associations between the expression of these genes and survival rates among patients with various types of cancer.

2.2.9 Kaplan Meier survival plot analysis of PRMT5 & EZH2 in breast cancer patient datasets

To examine the potential relationship between the expression levels of PRMT5 and EZH2 and the survival outcomes of cancer patients, we conducted an extensive analysis encompassing 30,000 samples derived from 21 distinct tumor types, including breast, ovarian, gastric, lung, colon, acute myeloid leukemia, and myeloma. Our investigation utilized the cBioportal dataset a powerful tool developed specifically for the discovery and validation of survival biomarkers

in cancer research. Specifically, we focused our analysis on breast cancer patients' data and utilized the Kaplan-Meier estimation method to plot survival curves for both PRMT5 and EZH2. The Kaplan-Meier curve is a widely recognized statistical tool used to assess the fraction of subjects (in this case, patients) who survive for a specified duration after treatment. This analysis is particularly valuable in clinical trials and community interventions, as it provides a quantitative measure of the intervention's impact on patient survival over time. By examining the survival curves for PRMT5 and EZH2, we aimed to elucidate any potential associations between the expression levels of these oncoproteins and patient survival outcomes in breast cancer and potentially other tumor types as well.

2.2.10 Statistical analysis

The experiments were conducted with three technical replicates to ensure robustness and reliability. Mean and standard error of the mean (SEM) were calculated from pooled sample data. Statistical significance among multiple groups was evaluated using one-way analysis of variance (ANOVA) followed by Tukey's posthoc test (p < 0.05), conducted using Origin software. Data visualization was carried out using Origin to present the results graphically.

2.3 Results

2.3.1 The ligand library signifies chemically, diverse natural phytochemicals

In pursuit of identifying potential enzymatic inhibitors for PRMT5 and EZH2, a thorough investigation was conducted on natural molecules.

Compounds without defined 2D or 3D structures in chemical databases were excluded from the study. Canonical SMILES representations of all 1200 molecules were retrieved from PubChem or ZINC databases for ADME analysis using the SwissADME web tool. After filtering to comply with Lipinski and Veber rules for drug-likeness, 355 molecules were deemed compliant without any violations. Additionally, 14 molecules with minor violations were considered suitable for limited use in the molecular docking phase of the virtual screening process (**Figure 2.3.1 -2.3.2**).

Chemical Library Preparation Module

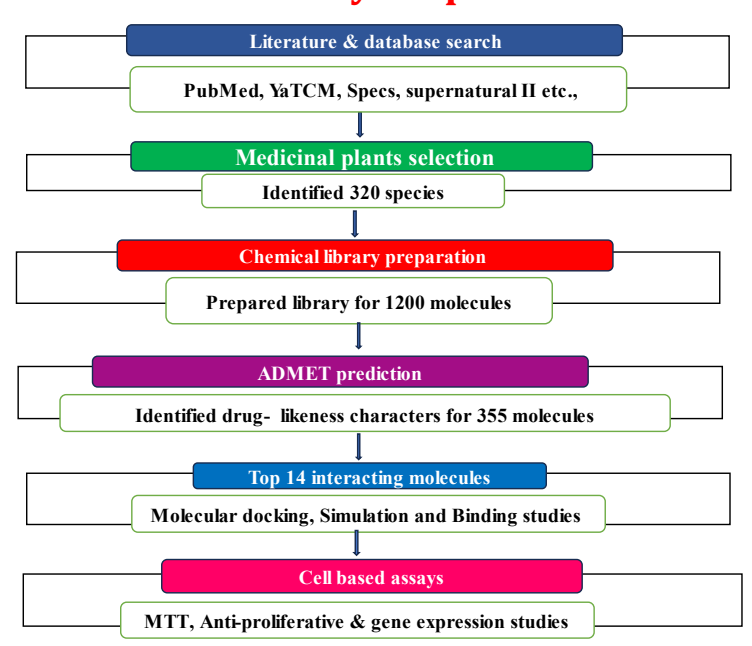


Figure 2.3.1: Chemical Library Preparation Module Workflow. The diagram outlines the step-by-step process for creating a chemical library. The process begins with a literature and database search using sources like PubMed, YaTCM, Specs, and SuperNatural II. This is followed by the selection of medicinal plants, identifying 320 species. Next, a chemical library is prepared, resulting in 1200 molecules. ADMET prediction is then performed to identify drug-likeness characteristics for 355 molecules. The top 14 interacting molecules are selected for molecular docking, simulation, and binding studies. Finally, cell-based assays, including MTT, antiproliferative, and gene expression studies, are conducted to evaluate the biological activity of the compounds.

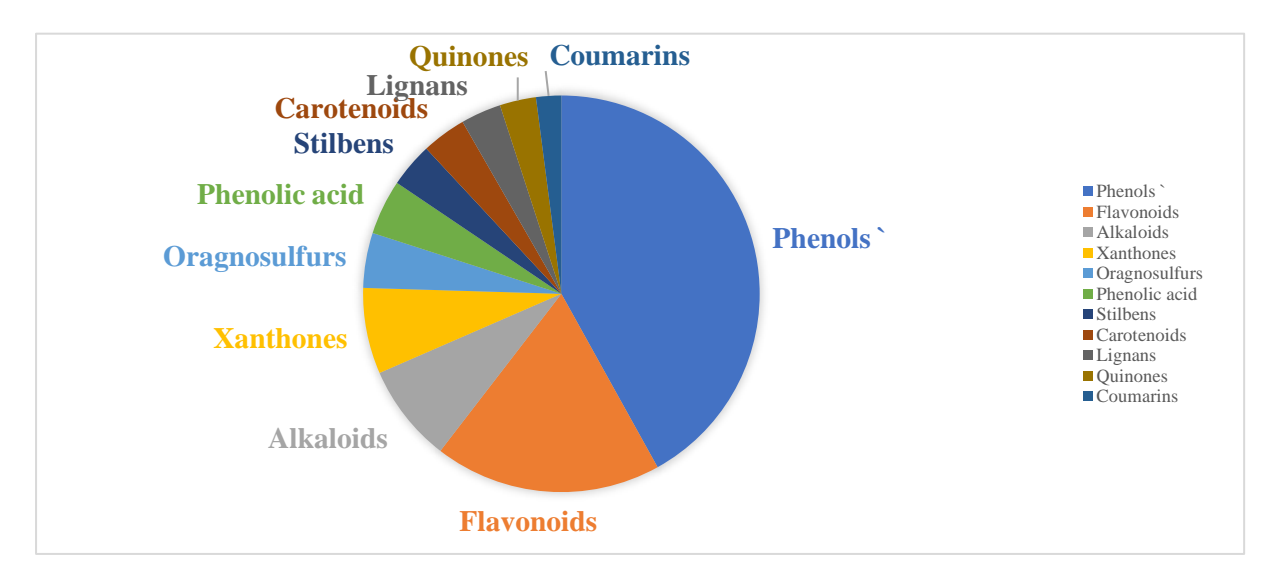


Figure 2.3.2: Diverse Chemical Landscape of natural molecules in ligand library preparation: This figure illustrates the variety of natural molecules used in preparing a ligand library for virtual screening. It highlights the diverse chemical structures and properties of natural compounds selected for inclusion in the library. The purpose of this preparation is to explore and identify potential bioactive molecules through a virtual screening pipeline, which involves computational techniques to predict the interaction of these molecules with biological targets. The diversity of the chemical landscape ensures a broad spectrum of biological activities and potential therapeutic applications.

2.3.2 Impact of anti-proliferative molecules on cancer cell lines at different concentrations 2.3.2.1 MTT assay

Next, we interested to check the impact of these screened anti-proliferative molecules impact on various human malignant cell lines such as MCF7 (breast), MDA-MB-231 (breast), Du-145 (prostate), A549 (lung), HeLa (cervix), Hep G2 (liver), PC-3 (prostate), and HEK293 (human embryonic kidney). These cells were subjected to escalating concentrations of fourteen such anti-proliferative agents- Epigallocatechin-3-gallate (EGCG), Ellagic-acid (EA), Brazilin (Brz), Curcumin (Cur), Resveratrol (Rvr), Piperine (Ppr), Quercetin (Qct), Gambogic acid (Gba), Apicidin (Apdn), Anethol (Atl), Eugenol (Egl), capsaicin (Cpcn), Eucalyptol (Ect), Sulforaphane (Sfp), for both 24 and 48 hours, and calculated the percentage of proliferating cells/viable cells was quantified using the MTT assay. The selection of these compounds was based on their availability in highly pure (≥98%) forms and their potential as "epidrugs," given previous reports of their efficacy as anti-proliferative agents. as described in Section 1.6.

Analysis of live or proliferating cells via the MTT assay revealed that increasing concentrations of the anti-proliferative compounds exerted differential effects on the growth of the screened malignant cells, with most inducing cell death beyond a concentration of 1 µM after 24 hours of exposure, regardless of the cell line (as depicted in **Figures 2.3.3–2.3.9**). Overall, MCF7, MDA-MB231, and DU145 breast carcinoma and prostate cells exhibited a notably higher responsiveness to the selected anti-proliferative compounds, displaying a significantly greater inhibition of proliferation compared to other human malignant cell lines (summarized in **Table 2.2**).

EGCG, a potent catechin found in green tea, and EA, a natural phenol antioxidant found in numerous fruits and nuts, were the focus of this study due to their documented anti-cancer properties. Exposure to these compounds for either 24 or 48 hours exhibited a potent reduction in cell proliferation across all seven malignant cell lines tested as the concentration of the compounds increased. As illustrated in **Figures 2.3.8 and 2.3.9**, concentrations above ten μ M of EGCG and EA significantly decreased the percentage of proliferative cells. MDA-MB231 (triple-negative breast cancer cells) and MCF7 (oestrogen receptor-positive breast cancer cells) exhibited the most pronounced effect under both exposure durations. For instance, after 24 hours of treatment with 10 μ M EGCG, the proliferation of MCF7 cells decreased by 35%, and with 50 μ M EGCG, the reduction was even more substantial at 70%. Similarly, MDA-MB231 cells exhibited a 30% reduction in proliferation at 10 μ M and a 65% reduction at 50 μ M EGCG.

EA demonstrated comparable effects, with significant decreases in cell proliferation at concentrations above 10 μ M, particularly in MCF7 and MDA-MB231 cells.

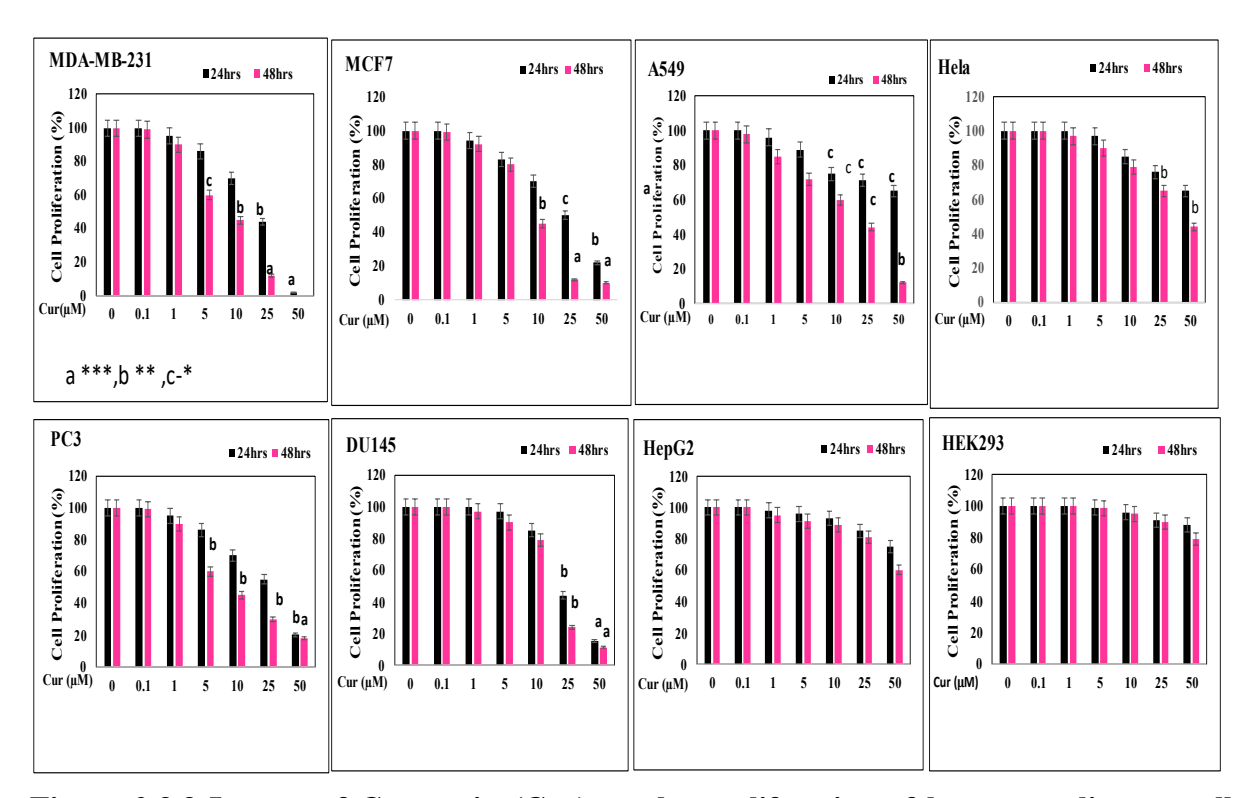


Figure 2.3.3 Impact of Curcumin (Cur) on the proliferation of human malignant cell lines: Cells were treated with increasing concentrations of Curcumin (Cur) for either 24 or 48 hours, and the proliferation rate was assessed using the MTT assay. The data presented are the mean \pm SEM values derived from triplicate samples for each group. Significance levels are denoted as '' for p < 0.01 and '*' for p < 0.001 when compared to the control (DMSO) group.

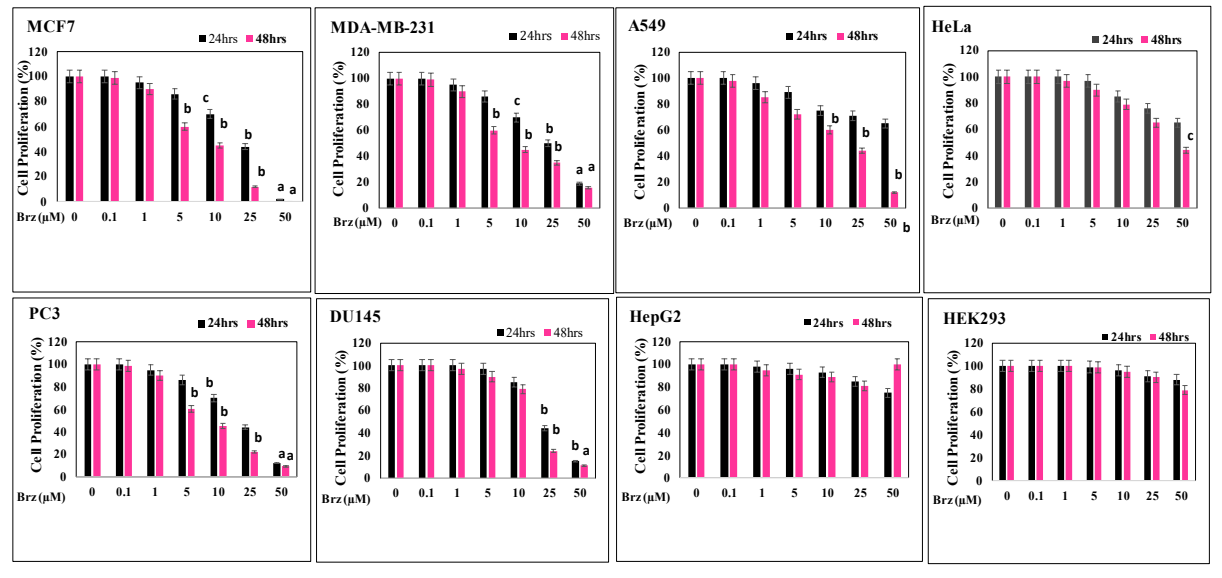


Figure 2.3.4 Impact of Brazilin (Brz) on the proliferation of human malignant cell lines: Cells were treated with increasing concentrations of Brazilin (Brz) for either 24 or 48 hours, and the proliferation rate was assessed using the MTT assay. The data presented are the mean \pm SEM values derived from triplicate samples for each group. Significance levels are denoted as '' for p < 0.01 and '*' for p < 0.001 when compared to the control (DMSO) group.

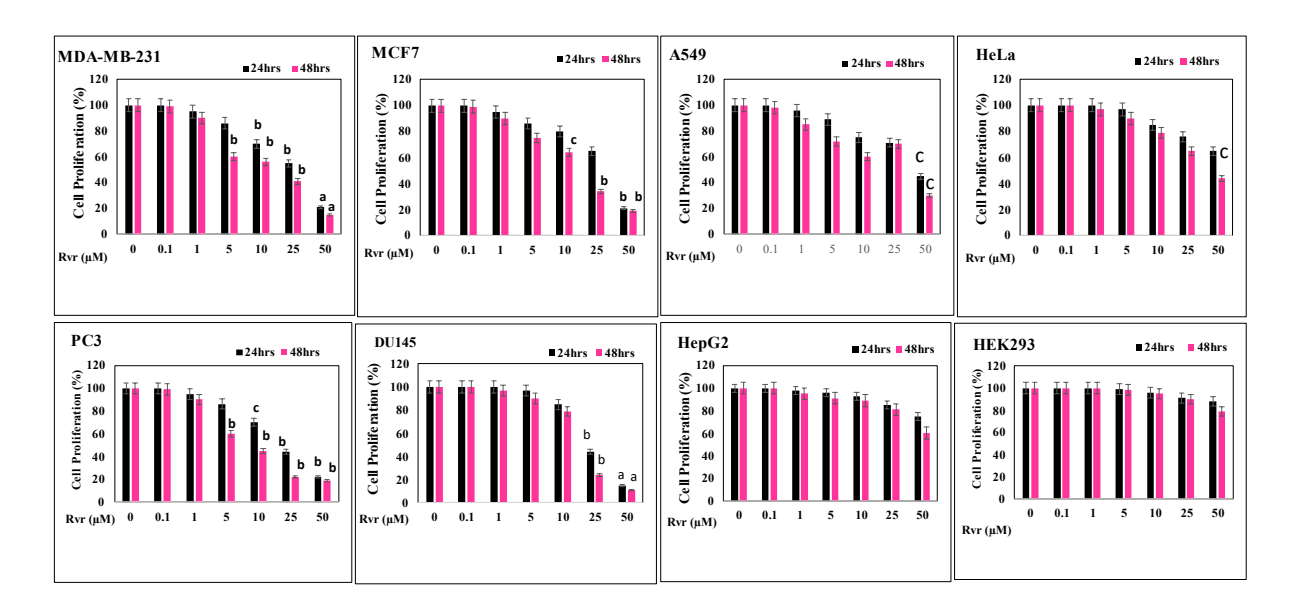


Figure 2.3.5 Impact of Resveratrol (Rvr) on the proliferation of human malignant cell

lines: Cells were treated with increasing concentrations of Resveratrol (Rvr) for either 24 or 48 hours, and the proliferation rate was assessed using the MTT assay. The data presented are the mean \pm SEM values derived from triplicate samples for each group. Significance levels are denoted as '' for p < 0.01 and '*' for p < 0.001 when compared to the control (DMSO) group.

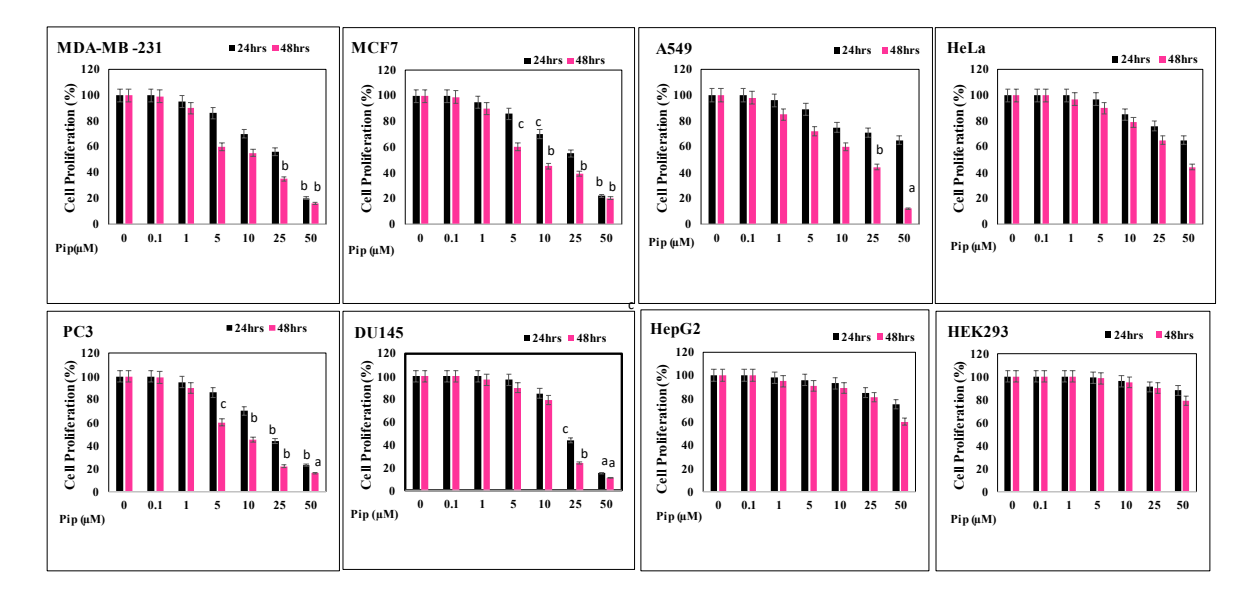


Figure 2.3.6 Impact of Piperine (Ppr) on the proliferation of human malignant cell lines: Cells were treated with increasing concentrations of Piperine (Ppr) for either 24 or 48 hours, and the proliferation rate was assessed using the MTT assay. The data presented are the mean \pm SEM values derived from triplicate samples for each group. Significance levels are denoted as '' for p < 0.01 and '*' for p < 0.001 when compared to the control (DMSO) group.

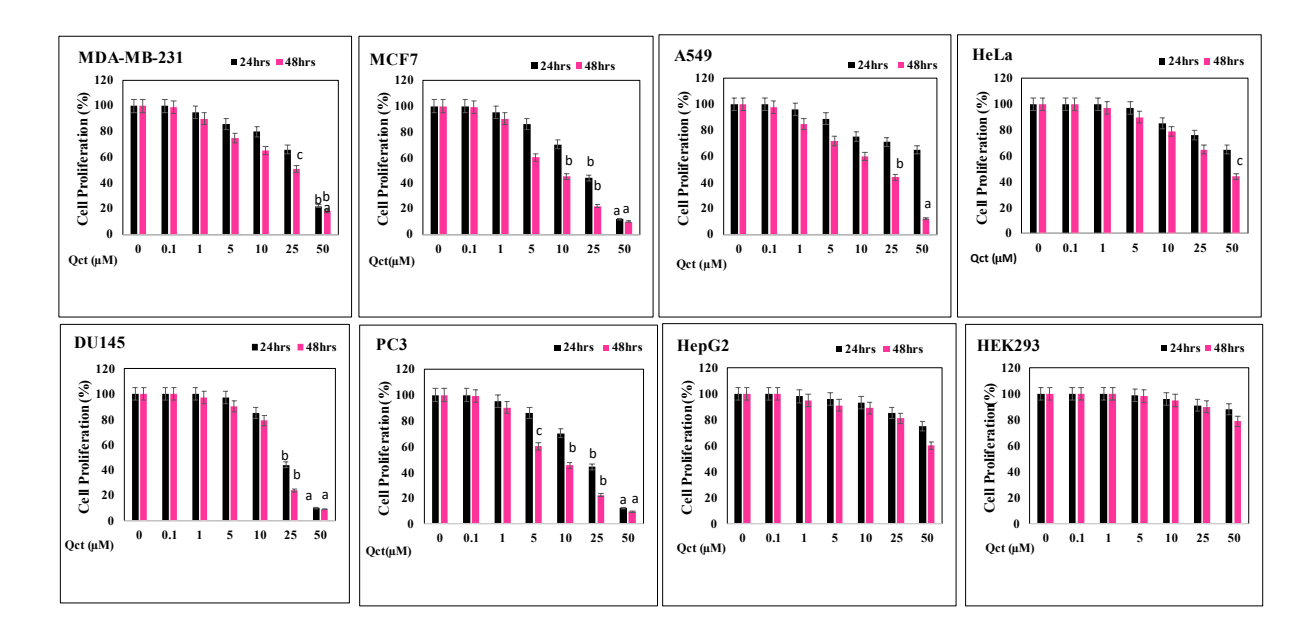


Figure 2.3.7 Impact of Quercetin (Qct), on the proliferation of human malignant cell lines: Cells were treated with increasing concentrations of Quercetin (Qct) for either 24 or 48 hours, and the proliferation rate was assessed using the MTT assay. The data presented are the mean \pm SEM values derived from triplicate samples for each group. Significance levels are denoted as '' for p < 0.01 and '*' for p < 0.001 when compared to the control (DMSO) group.

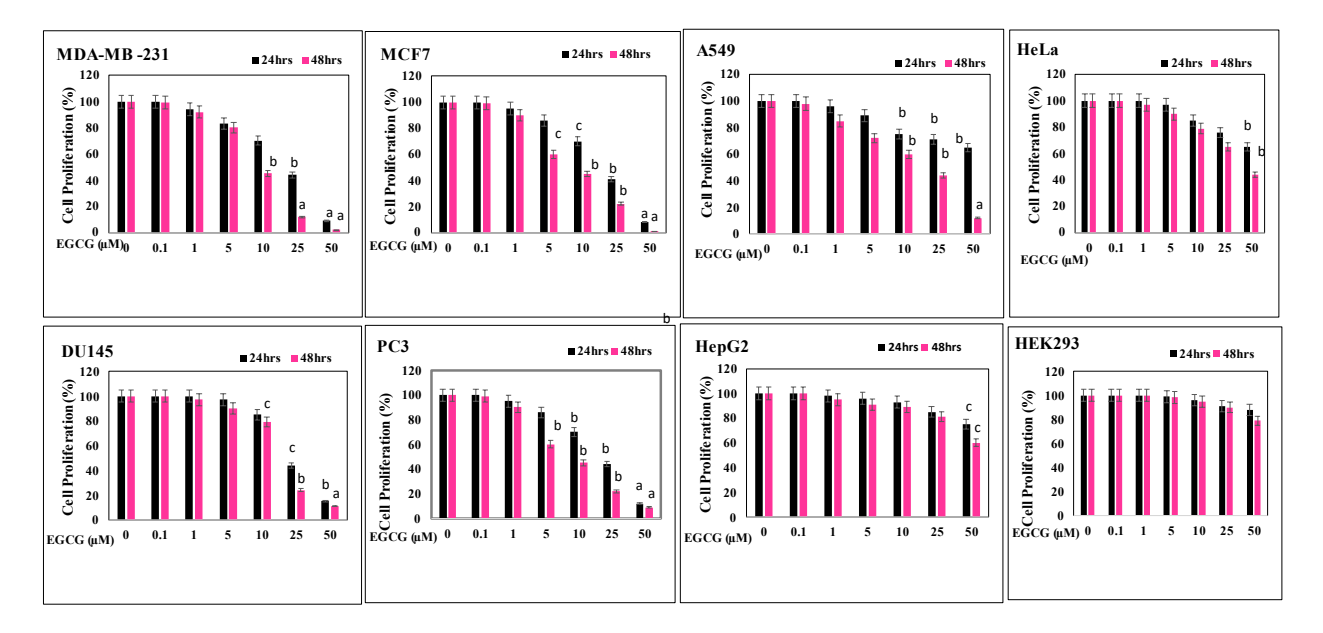


Figure 2.3.8 Impact of Epigallocatechin-3-gallate (EGCG), on the proliferation of human malignant cell lines: Cells were treated with increasing concentrations of Epigallocatechin-3-gallate (EGCG) for either 24 or 48 hours, and the proliferation rate was assessed using the MTT assay. The data presented are the mean \pm SEM values derived from triplicate samples for each group. Significance levels are denoted as "for p < 0.01 and "*" for p < 0.001 when compared to the control (DMSO) group.

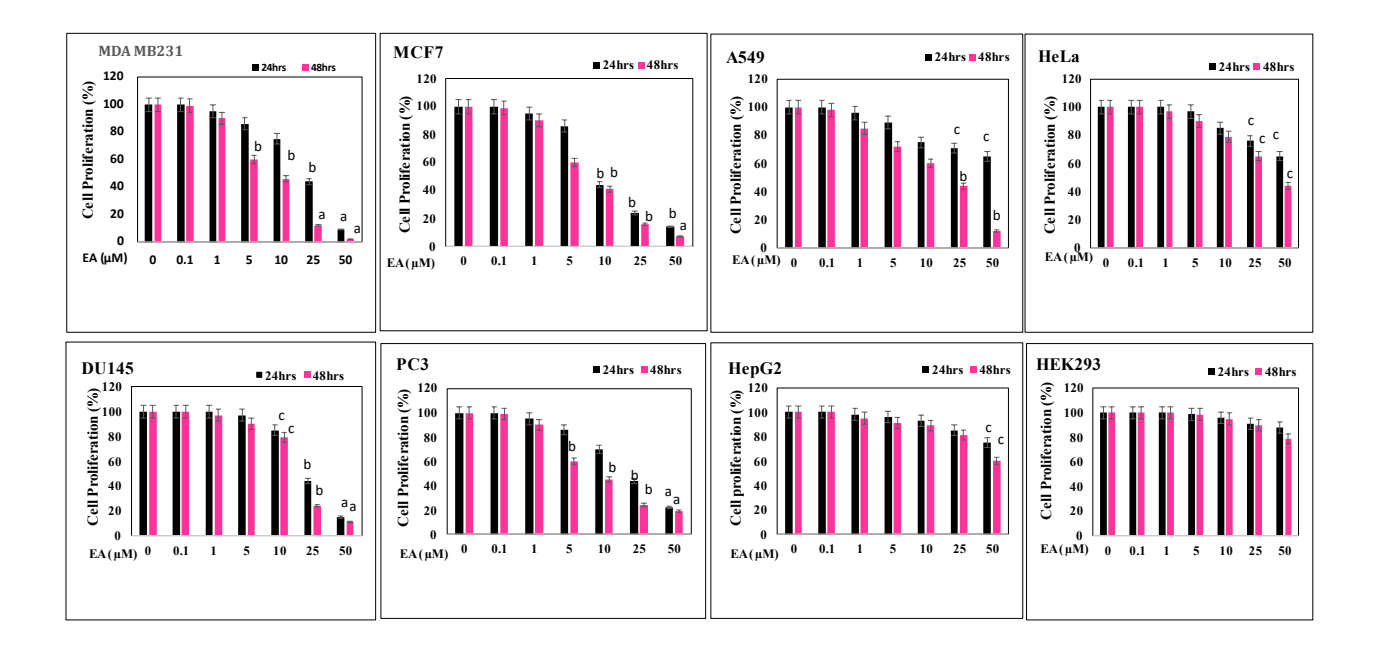


Figure 2.3.9 Impact of Ellagic-acid (EA), on the proliferation of human malignant cell lines: Cells were treated with increasing concentrations of Ellagic-acid (EA) for either 24 or 48 hours, and the proliferation rate was assessed using the MTT assay. The data presented are the mean \pm SEM values derived from triplicate samples for each group. Significance levels are denoted as '' for p < 0.01 and '*' for p < 0.001 when compared to the control (DMSO) group.

However, the impact of EGCG and EA was relatively less pronounced in HepG2 cells (a hepatocellular carcinoma cell line). Even after 48 hours of exposure, only the higher concentration of $50\,\mu\text{M}$ of EGCG and EA markedly decreased the number of proliferative cells compared to the control group treated with DMSO. Specifically, HepG2 cells showed only a 15% reduction in proliferation at 10 μ M EGCG, which increased to 40% at 50 μ M. EA displayed similar results, with minimal impact at lower concentrations and only significant effects at the highest concentration tested.

These findings underscore the differential sensitivity of various cancer cell lines to EGCG and EA, highlighting the potential of these compounds as selective anti-cancer agents. The greater responsiveness observed in MCF7 and MDA-MB231 cells suggests that these compounds might be particularly effective against certain types of breast cancer, while the relatively modest effect on HepG2 cells indicates a need for higher doses or combination treatments to achieve similar efficacy.

Table 2.2. Impact of anti-proliferative molecules on the malignant cell proliferation

Anti- proliferative molecules	Affected cell lines (order of impact)	IC ^{50#} value (μM)			
	(order or impact)	24 hr	48 hr		
Brazilin	MCF7>PC3>DU145>MDA-MB-	19.74±3.1	8.96 ± 2.1		
	231>A549>HeLa> HepG2>HEK293				
EGCG	MDA-MB-	2.5±1.4	0.9 ± 1.2		
	231>MCF7>DU145>PC3>A549>HeLa>				
	HepG2>HEK293				
EA	MDA-MB-	18.8 ± 4.6	15.8 ± 3.3		
	231>MCF7>DU145>PC3>A549>HeLa>				
	HepG2>HEK293				
Curcumin	MDA-MB-231>MCF7>DU145>PC3>A549>	31.3±3.1	16.02 ± 2.8		
	HeLa>HepG2>HEK293				
Resveratrol	DU145>MDA-MB-231>PC3>MCF7>	72.78±3.1	25.4±1.6		
	A549>HeLa>HepG2>HEK293				
Piperine	DU145>PC3>MDA-MB-231> MCF7 >	33.4±3.5	27.9±1.2		
	A549>HeLa> HepG2>HEK293				
Quercetin	MCF7>DU145>PC3> MDA-MB-231>A549>HeLa>	28.8±3.2	20.8±3.7		
	HepG2>HEK293				
# IC50 value for the most effected cell lines I values are calculated from reported					

IC^{50} value for the most affected cell lines, \pm values are calculated from repeated experiments

2.3.2.2 Trypan blue dye exclusion assay

The Trypan Blue exclusion assay was employed to evaluate the viable cell count in a treated cell culture suspension, assessing the potential anti-cancer activity of screened compounds. This method works on the principle that viable cells, with intact membranes, exclude dyes like Trypan Blue and propidium, whereas non-viable cells absorb the dye, appearing blue. After mixing the cell suspension with the dye, examination under a light microscope determined dye uptake or exclusion. Plotting the viable cells percentage (clear white cytoplasm) versus non-viable cells (blue cytoplasm) provided insights into cell viability (Figure 2.3.10). The Trypan Blue assay was crucial for verifying the IC50 values of EGCG and EA, ensuring accuracy in determining their cytotoxic effects.

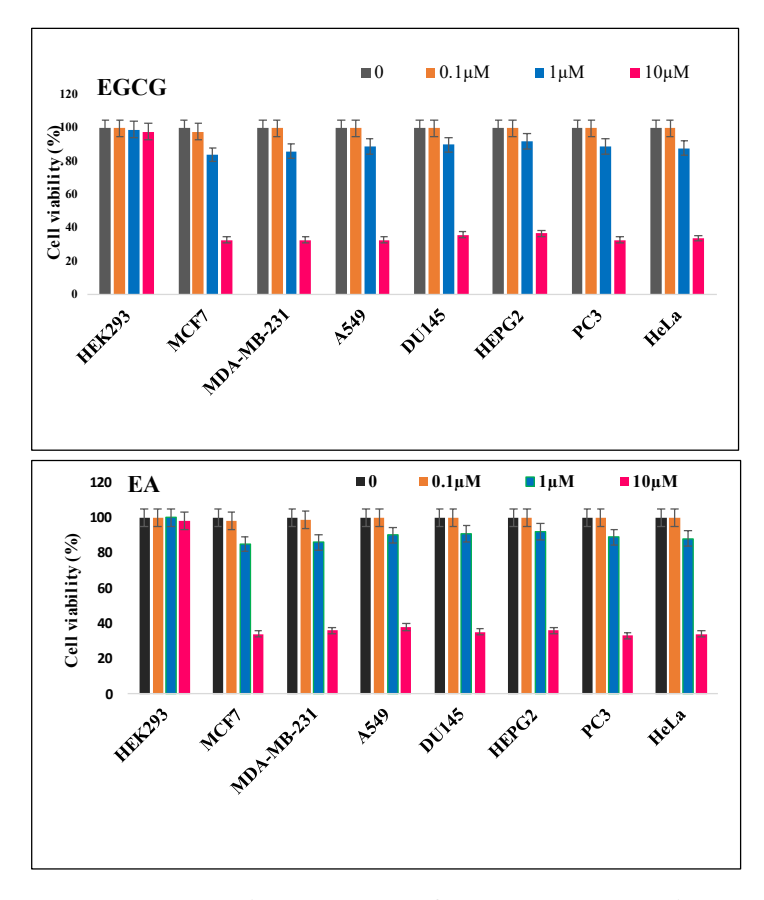


Figure 2.3.10: Trypan blue exclusion assay performed to determine the cell viability of compounds: EGCG and EA, (used their Ic50 concentrations) the data were plotted as a percentage of viable cells in HEK293, MCF7, MDA MB231, A549, DU145, HepG2, PC3 and Hela. Bar represents the mean \pm SD (**P<0.01, ***P<0.001, unpaired Student's t-test, n=3).

2.3.3 Anti-proliferative molecules targeted the expression of epigenetic regulators

Once anti-proliferative properties of these screened phytocompounds were carried out and IC_{50} values were obtained and tabulated in table 2.2. We next focused to study the relative gene expression levels of different epigenetic markers upon treatment with phytochemicals on various human malignant cell lines such as DU145, PC3, A549, MCF-7, MDA-MB231, DU145, PC3, A549, HeLa and were assessed by qPCR analysis.

To accomplish this, we allowed cells attachment and growth until reaching confluency (approximately 70%) in the designated culture medium, followed by total RNA purification and qPCR analysis. For reference and standardization, GAPDH expression was quantified alongside the mRNA levels of selected epigenetic genes responsible for DNA and histone methylation, histone acetylation, and the core catalytic/regulatory members of two polycomb repressive complexes.

As detailed in section 2.3.1, increasing concentrations of five selected anti-proliferative plant-derived molecules (chosen for their commercial availability in purified form) were observed to reduce the proliferation of various malignant cell lines after 24 or 48 hours of exposure. To further evaluate the impact of these molecules, the expression of several epigenetic regulatory genes was analyzed using real-time qPCR after exposing the cells to appropriate concentrations of each molecule for 24 hours. The findings are illustrated in Figures 2.3.11 to 2.3.16, and summarized in (Table 2.3.)

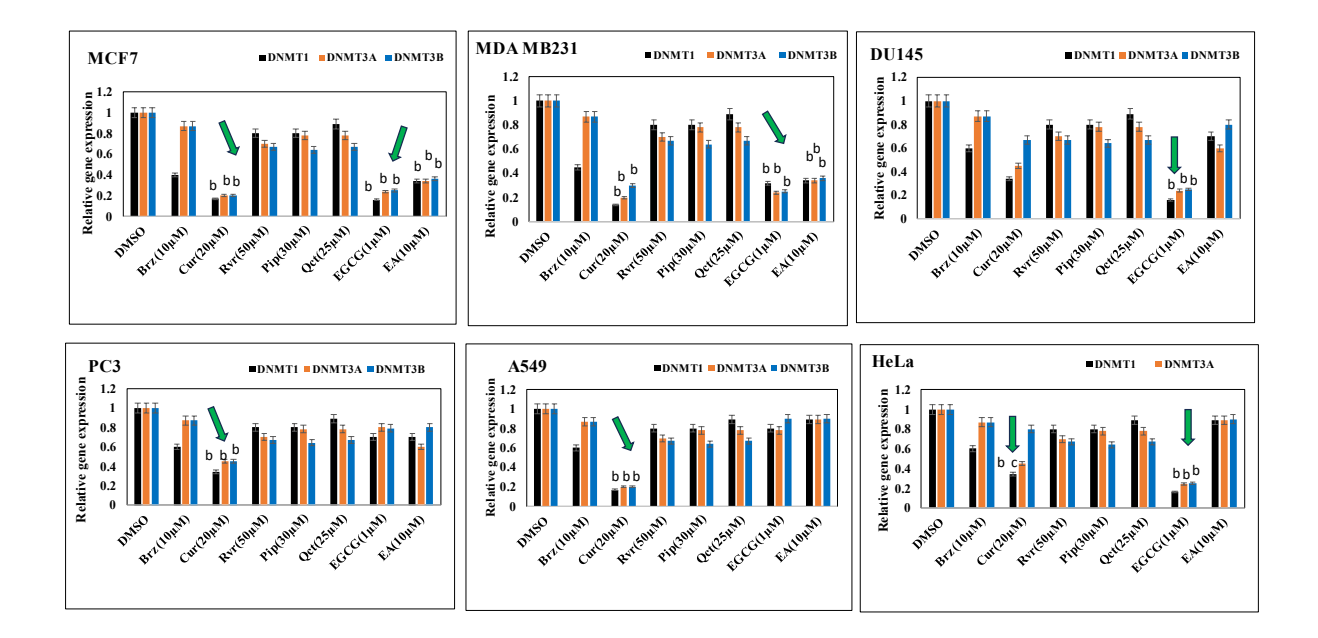


Figure 2.3.11. Impact of anti-proliferative molecules on the expression of DNA methyltransferases. The cells were treated with either DMSO (vehicle control) or one of the five anti-proliferative molecules at specified concentrations for 24 hours. Subsequently, qPCR was conducted to measure the mRNA levels of DNMTs using the 2- $\Delta\Delta$ Ct method. The data (Ct values) were normalized to GAPDH (internal control) and are presented as mean \pm SEM from triplicate samples for each treatment group. Statistical significance is indicated by "for p<0.01 and '*' for p<0.001 when compared to the control (DMSO) group.

Initially, the modulation of three DNA methyltransferases (DNMTs) was assessed via qPCR from total RNA isolated from, A549, MCF7, MD-MB231, and Du145, PC-3 cells. These cells were treated with either DMSO (control), Brz (10 μ M), Cur (20 μ M), EGCG (1 μ M), EA (10 μ M), and Rvr (50 μ M) for 24 hours. The results indicate that these anti-proliferative molecules generally exert a repressive effect on DNMTs, though the response varied depending on the cell line (Figure 2.3.11). Cur significantly affected all three DNMTs across all cell lines, whereas EGCG and EA notably reduced the expression of all three DNMTs in MCF7 and A549 cells, respectively. Rvr significantly decreased the mRNA expression of DNMT3s specifically in A549 and MCF7 cells. Conversely, Brz at a 10 μ M concentration selectively and

significantly reduced the transcript level of DNMT1 in all four cell lines, which expressed this gene at higher levels (Figure 2.3.11).

The PRMTs (PRMT1, PRMT4, and PRMT5), which are abundantly expressed in these malignant cell lines, showed reduced transcript levels in A-431, MCF7, and PC-3 cells treated with curcumin compared to the DMSO control group. As illustrated in Figure 2.3.12, a 24-hour exposure to 20 μ M Cur significantly decreased the transcripts of all three PRMTs. Specifically, PRMT5 expression alone was reduced approximately 8.33-fold in MCF7 cells, 5-fold in PC-3 and A549 cells, and 4.16-fold in A-431 cells. Additionally, a 24-hour exposure to 50 μ M Rvr significantly decreased mRNA levels of PRMT5 in all four malignant cell lines and significantly reduced PRMT1 in A549 cells and PRMT4 in MCF7 cells. Treatment with 1 μ M EGCG and 10 μ M EA also led to a notable reduction in PRMT5 levels across several cancer cell lines. The most pronounced reduction in PRMT5 expression occurred in MDA-MB231 cells, followed by MCF7, PC3, A549, and DU145 cells.

In MDA-MB231 cells, treatments with EGCG and EA resulted in a substantial decrease in PRMT5 levels, indicating high sensitivity of these triple-negative breast cancer cells to both compounds. In MCF7 cells, which are estrogen receptor-positive, the reduction in PRMT5 expression was significant, though slightly less than in MDA-MB231 cells. In PC3 prostate cancer cells, the decrease in PRMT5 levels was moderate but still notable, demonstrating the potential effectiveness of EGCG and EA in inhibiting PRMT5 expression in prostate cancer. A549 lung carcinoma cells exhibited a similar moderate reduction in PRMT5 levels with these treatments. Lastly, DU145 prostate cancer cells showed the least reduction in PRMT5 expression, indicating lower sensitivity to EGCG and EA compared to the other cell lines. Brz significantly reduced PRMT1 expression exclusively in A-549 but did not change PRMT1 than three cell lines and did not significantly affect PRMT4 or PRMT5 expression in these cell lines. Notably, unlike Cur, EGCG and EA did not cause significant changes in the expression of any PRMTs in these cell lines (Figure-2.3.12).

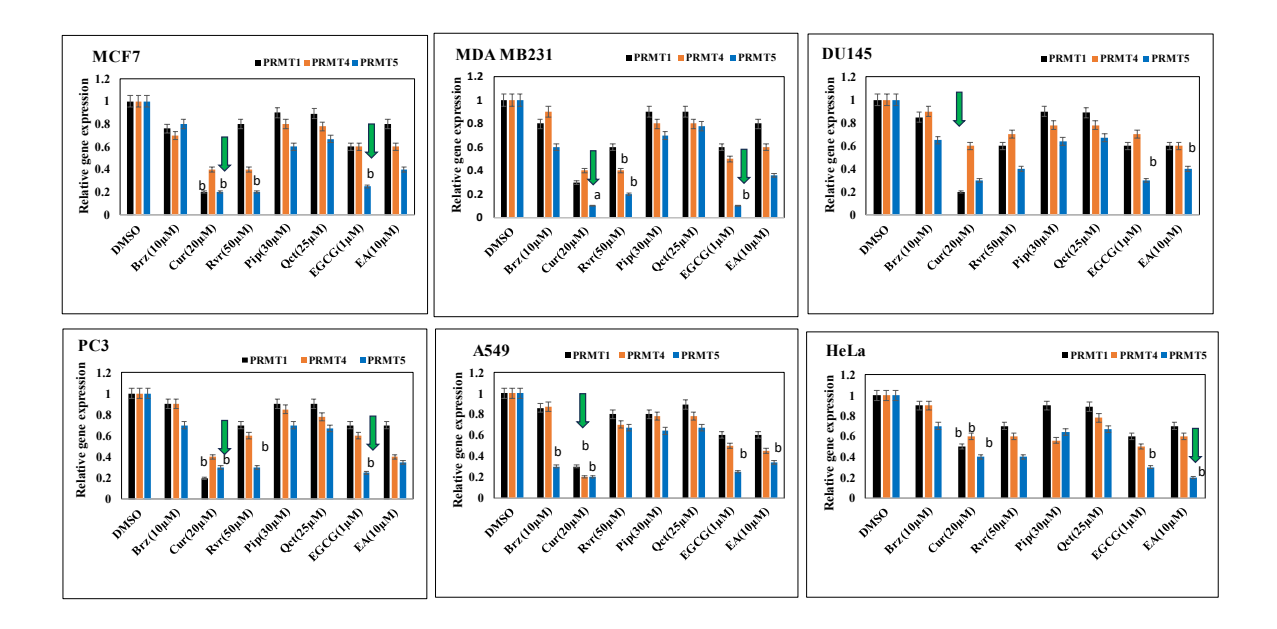


Figure 2.3.12. Impact of anti-proliferative molecules on the expression of protein arginine methyltransferases. The cells were treated with the specified concentrations of five anti-proliferative molecules or DMSO (vehicle control) for 24 hours. To quantify the mRNA levels of the PRMTs, qPCR was conducted using the 2- $\Delta\Delta$ Ct method. The data (Ct values) were normalized to GAPDH (internal control) and presented as mean \pm SEM from triplicate samples for each treatment group. Statistical significance is indicated by "for p<0.01 and '*' for p<0.001 compared to the control (DMSO) group.

The lysine acetyltransferases, except for KAT1, exhibited lower expression levels in malignant cells (Figure 2.3.13). However, exposure to anti-proliferative molecules caused differential changes in the expression of KAT2A/B and KAT3B (p300). As depicted in Figure 2.3.11, Cur and EGCG significantly reduced their expression in A-431, A549, and MCF7 cells, while Brz, EA, and Rvr notably increased the expression of these three KATs across all four cell lines. Notably, treatment with 50 µM Rvr for 24 hours caused in an overall increase in the transcript levels of KAT2A, KAT2B, and KAT3B by approximately 6.6-fold, 4.5-fold, and 5.8-fold, respectively, in A-431 cells. Similarly, exposure of MCF7 cells to Rvr significantly increased KAT2A expression by approximately 6-fold, KAT2B by 4-fold, and KAT3B by 5-fold within 24 hours as compared to control cells.

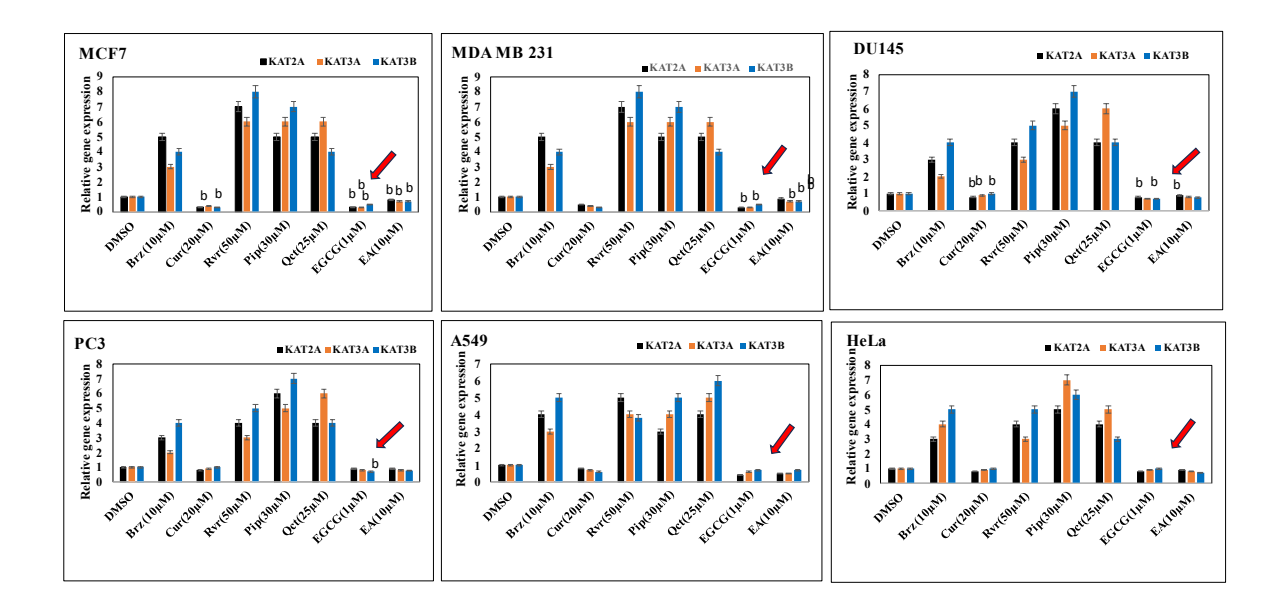


Figure 2.3.13. Impact of anti-proliferative molecules on the expression of the lysine acetyltransferases. The cells were treated with specified concentrations of five anti-proliferative molecules or DMSO (vehicle control) for 24 hours. Subsequently, qPCR was conducted to quantify the mRNA levels of KATs using the 2-ΔΔCt method. The data (Ct values) were normalized to GAPDH (internal control) and are presented as mean \pm SEM from triplicate samples for each treatment group. Statistical significance is denoted by "for p < 0.05, "for p < 0.01, and " for p < 0.001 compared to the control (DMSO) group.

The impact of anti-proliferative molecules on the expression of these HDACs was investigated using qPCR. As illustrated in Figure 2.3.14, these molecules reduced HDAC expression only after 24 hours of exposure. Among them, Cur and EGCG were particularly effective in reducing HDAC mRNA levels across various cell lines. A 24-hour exposure to 20 μ M Cur significantly decreased HDAC1 transcripts by approximately 8-fold in both A549 and MCF7 cells, and reduced SIRT1 levels by about 8.5-fold in A-431 and A549 cells.

EGCG similarly reduced HDAC1, HDAC7, and SIRT1 transcripts by approximately 9.3-fold, 8.5-fold, and 9.7-fold, respectively, specifically in A-431 cells, with comparable effects observed in A549 cells. Conversely, EA exhibited a less significant effect on the transcription of these HDACs. Unlike Brz, Rvr significantly reduced the transcription of all three HDACs in A-431 and MCF7 cells, while selectively decreasing HDAC1 in A549 cells and HDAC1 and HDAC7 in PC-3 cells to a significant extent. Brz exposure notably reduced HDAC1 and SIRT1 transcripts in A-431 cells, and SIRT1 alone in MCF7 cells.

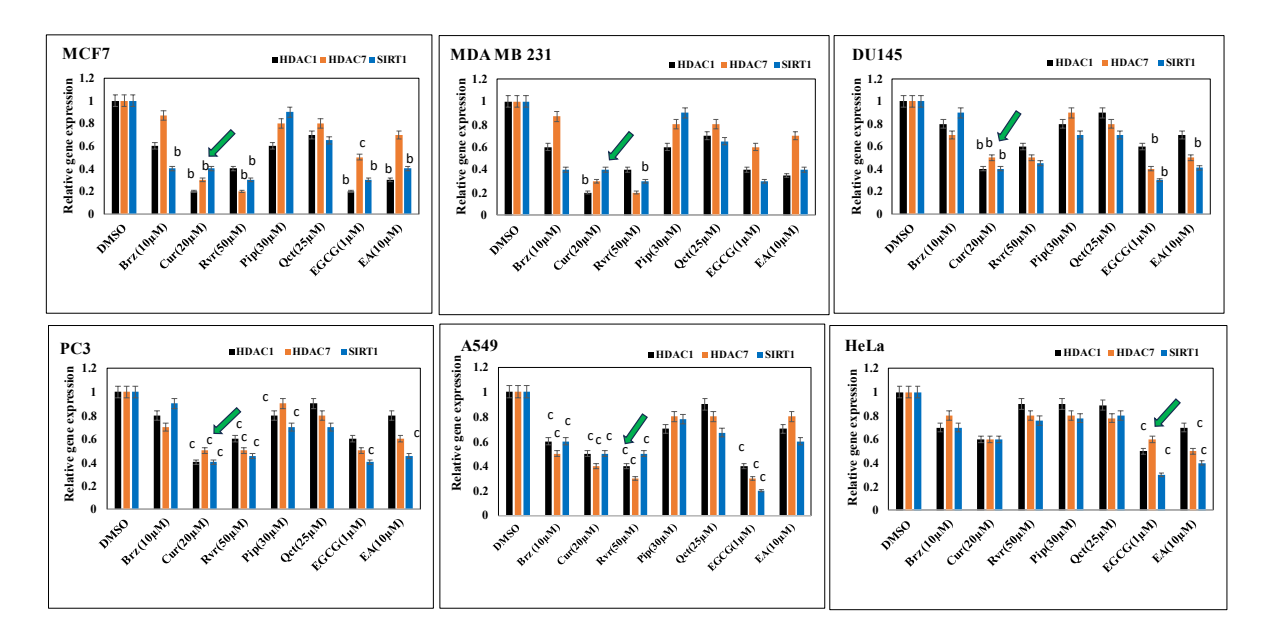


Figure 2.3.14. Impact of anti-proliferative molecules on the expression of the histone deacetylases. The cells were treated with specified concentrations of five anti-proliferative molecules or DMSO (vehicle control) for 24 hours. Subsequently, qPCR was conducted to quantify the mRNA levels of HDACs using the 2- $\Delta\Delta$ Ct method. The data (Ct values) were normalized to GAPDH (internal control) and are presented as mean ± SEM from triplicate samples for each treatment group. Statistical significance is denoted by "**for p<0.01 and '*** for p<0.001 compared to the control (DMSO) group.

To assess the effects of selected anti-proliferative molecules on the expression of core functional subunits of the PRC complexes, the transcript levels of PRC1 components (RNF2, PCGF2, and PCGF4) were evaluated (Figure-2.3.15) Cur exposure at 20 μ M significantly reduced RNF2 and PCGF4 transcripts in A-431, A549, and PC-3 cells, while only RNF2 was affected in MCF7 cells. Brz at 10 μ M notably impacted RNF2 across cell lines except for A-431, and in MCF7 cells alone, it significantly reduced PCGF4 transcript levels.

In contrast, EA at 10 μ M are not induced substantial changes in the expression of PRC1subunits. Interestingly, EGCG at 1 μ M significantly reduced RNF2 expression in A549 cells and PCGF4 expression in both A-431 and MCF7 cells after 24 hours of exposure.

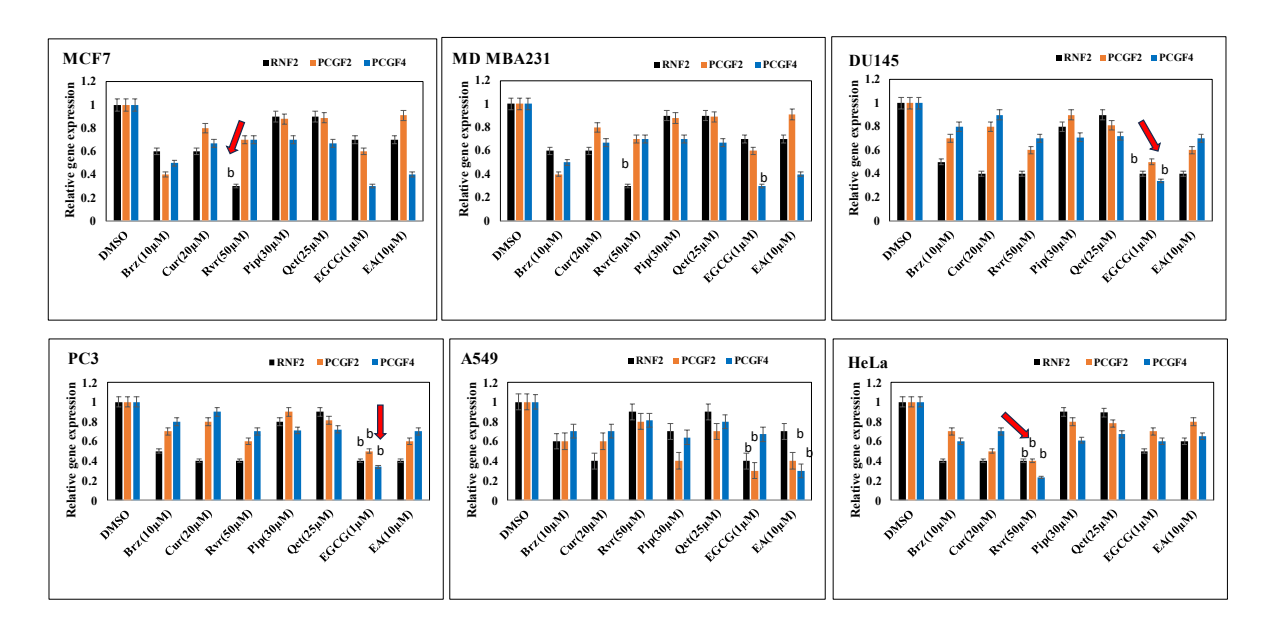


Figure 2.3.15. Impact of anti-proliferative molecules on the expression of the polycomb repressive complex 1 core members: The cells were treated with specified concentrations of five anti-proliferative molecules or DMSO (vehicle control) for 24 hours. Subsequently, qPCR was conducted to quantify the mRNA levels of the core members of PRC1 using the $2-\Delta\Delta$ Ct method. The data (Ct values) were normalized to GAPDH (internal control) and are presented as mean \pm SEM from triplicate samples for each treatment group. Statistical significance is denoted by "for p<0.05, "for p<0.01, and " for p<0.001 compared to the control (DMSO) group.

The transcription of PRC2 core subunit genes was notably influenced by selected anti-proliferative molecules (excluding EA). According to Figure 2.3.16, Rvr was the sole compound significantly reducing EZH2, EED, and SUZ12 transcripts across malignant cell lines. A 24-hour exposure to $50 \,\mu\text{M}$ resveratrol diminished PRC2 transcript levels by over 8.5-fold specifically in MCF7 cells, and approximately 5-fold in A-431 and A549 cells.

EA did not affect the expression of any PRC2 regulators, unlike Brz, Cur and EGCG. As indicated in Figure 2.3.16, treatment with 1 μ M EGCG and 10 μ M EA led to in a notable reduction in EZH2 levels across multiple cancer cell lines, with EA exerting a particularly strong effect. The most significant reduction in EZH2 expression occurred in MDA-MB231 cells, followed by MCF7, PC3 (prostate cancer), and A549 (lung carcinoma) cells. In MDA-MB231 cells, characterized by triple-negative breast cancer, 10 μ M EA significantly reduced EZH2 levels, indicating high sensitivity of these cells to the compound. EGCG at 1 μ M also decreased EZH2 levels, though to a lesser extent compared to EA. Similarly, in MCF7 (oestrogen receptor-positive) breast cancer cells, EA treatment led to a substantial reduction in EZH2 expression, with EGCG also contributing, albeit less significantly. In PC3 prostate cancer cells, EA at 10 μ M showed notable effectiveness in reducing EZH2 levels, while EGCG

at 1 μ M had a less pronounced effect. A549 lung carcinoma cells exhibited a moderate decrease in EZH2 levels upon treatment with both compounds, with EA demonstrating a stronger effect compared to EGCG.

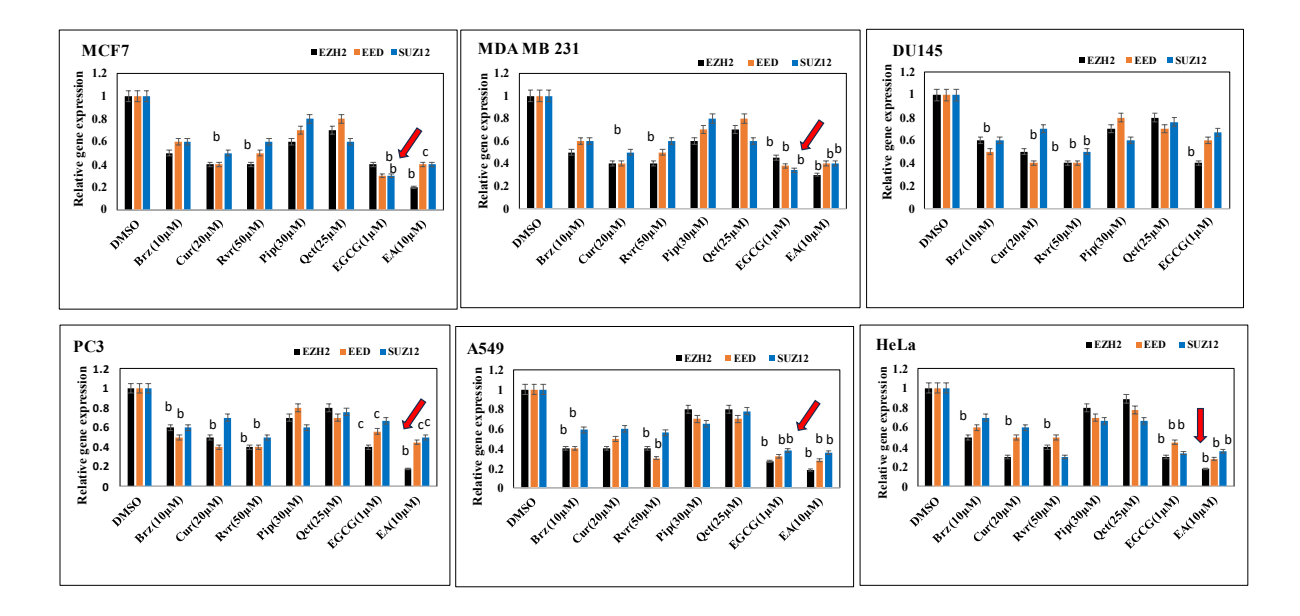


Figure 2.3.16. Impact of anti-proliferative molecules on the expression of the polycomb repressive complex 2 core members. The cells were treated with specified concentrations of five anti-proliferative molecules or DMSO (vehicle control) for 24 hours. Subsequently, qPCR was conducted to quantify the mRNA levels of the core members of PRC2 using the $2-\Delta\Delta$ Ct method. The data (Ct values) were normalized to GAPDH (internal control) and are presented as mean \pm SEM from triplicate samples for each treatment group. Statistical significance levels are denoted by "for p < 0.05, "for p < 0.01, and " for p < 0.001 compared to the control (DMSO) group.

In conclusion, our study reveals that the selected anti-proliferative molecules not only inhibit the proliferation of malignant cells but also exert modulatory effects on multiple epigenetic regulators, as detailed in Table 2.3. Cur, EGCG EA and Rvr, were particularly noteworthy among the seven molecules, affecting a wide array of epigenetic regulator genes at the transcriptional level. Brz demonstrated selective repression of DNMT1 PRMT5, EZH2 and RNF2 while inducing KAT2A and KAT3B expression.

In contrast, EGCG and EA selectively influenced the transcription of lysine acetylation regulator genes. The non-uniform modulation of these genes, dependent on the specific molecule and irrespective of the cell line, underscores EGCG and EA as versatile modulators of epigenetic regulation. The significant reductions in PRMT5 and EZH2 levels across multiple cell lines suggest a dual mechanism conveying fundamental the anti-proliferative effects of these compounds. Their profound impact of both EGCG and EA on PRMT5 and EZH2, particularly in MDA-MB231, MCF7, PC3, and A549 cells, highlights their potential for further

Table 2.3. Impact of the anti-proliferative molecules on epigenetic regulator expression.

Anti- proliferative molecule	Concentration	Epigenetic regulator(s) modulated	Type of modulation [@]	Malignant cell line#
Brazilin (Brz)	10 μΜ	DNMT1	Decreased expression	MCF7
		KAT2A	Increased expression	A-431
		KAT3B	Increased expression	A-431
		RNF2	Decreased expression	MCF7
Curcumin (Cur)	20 μΜ	DNMT1	Decreased expression	MCF7
		DNMT3A	Decreased expression	A549
		DNMT3B	Decreased expression	A549
		PRMT1	Decreased expression	PC-3
		PRMT4	Decreased expression	PC-3
		PRMT5	Decreased expression	MCF7
		KAT2A	Decreased expression	MCF7
		KAT3A	Decreased expression	MCF7
		KAT3B	Decreased expression	A-431
		HDAC1	Decreased expression	A549
		HDAC7	Decreased expression	PC-3
		SIRT1	Decreased expression	A-431
		RNF2	Decreased expression	A549
		PCGF4	Decreased expression	A-431
Epigallocatechin-	1 μΜ	KAT2A	Decreased expression	PC-3
3-gallate (EGCG)		PRMT5	Decreased expression	MCF7, MDA MB231
		EZH2	Decreased expression	MCF7, MDA MB231
		KAT3A	Decreased expression	A-431
		KAT3B	Decreased expression	A-431
		HDAC1	Decreased expression	A-431
		HDAC7	Decreased expression	A-431
		SIRT1	Decreased expression	A-431
Ellagic acid (EA)	10 μΜ	KAT2A	Increased expression	A-431
		PRMT5	Decreased expression	MCF7, MDA MB231
		EZH2	Decreased expression	MCF7, MDA MB231
		KAT3A	Increased expression	A-431
		KAT3B	Increased expression	MCF7
Resveratrol	50 μΜ	PRMT5	Decreased expression	MCF7
(Rvr)		KAT2A	Increased expression	A-431
		KAT3A	Increased expression	PC-3
		KAT3B	Increased expression	A-431
		HDAC1	Decreased expression	MCF7
		HDAC7	Decreased expression	PC-3
		RNF2	Decreased expression	MCF7
		PCGF4	Decreased expression	MCF7
		EZH2	Decreased expression	MCF7
		EED	Decreased expression	MCF7
		SUZ12	Decreased expression	MCF7

Piperine (ppr)	25 μΜ	KAT2A	Decreased expression	MCF7
		KAT3A	Decreased expression	MCF7
		KAT3B	Decreased expression	MCF7
		HDAC1	Decreased expression	MCF7
		HDAC7	Decreased expression	MCF7
		SIRT1	Decreased expression	MCF7
		PRMT5	Decreased expression	MCF7
Quercetin (Qct)	35 μΜ	KAT2A	Decreased expression	MCF7
		KAT3A	Decreased expression	MCF7
		KAT3B	Decreased expression	MCF7
		HDAC1	Decreased expression	MCF7
		HDAC7	Decreased expression	MCF7
		SIRT1	Decreased expression	MCF7
	# T. T.	PRMT5	Decreased expression	MCF7

[®]Recorded in >2 cell lines; [#]Cell line where the maximum level of modulation was recorded.

research and development of targeted cancer therapies. Their ability to inhibit cell proliferation while modifying key epigenetic regulators represents a promising direction in oncological therapeutics.

2.3.4 Comprehensive Analysis of Cancer Types: Insights from CBioPortal Dataset on Amplification, Mutation, Deep Deletion, and Multiple Alterations-

Given that our study identified significant inhibition of PRMT5 and EZH2 by EGCG and EA, and literature indicates that these two oncoproteins are aggressively expressed in several cancers, we decided to further investigate their roles in cancer. To accomplish this, we utilized both cBioPortal database and The Cancer Genome Atlas (TCGA) datasets. This allowed us to elucidate the epigenetic roles of PRMT5 and EZH2 in various cancers, providing a broader context for their impact on tumor progression and potential as therapeutic targets.

In this study, we utilized data from cBioPortal to investigate the alteration frequencies of EZH2 and PRMT5 genes across various cancer types. We focused on four types of mutations, amplifications, genetic alterations, multiple alterations, and deep deletions. By querying the data by gene name, we aimed to comprehend the prevalence and consequence of these alterations in different cancer contexts.

2.3.41 PRMT5 Gene Alterations

The PRMT5 gene analysis included data from 10,851 patients and 11,632 samples, also spanning 25 studies. Like EZH2, PRMT5 amplifications were the most common type of alteration observed. Higher frequencies of PRMT5 amplifications were particularly noted in lymphoid neoplasm diffuse hepatocellular carcinoma and large B-cell lymphoma. The extensive dataset, comprising, mutation data, structural variant data, and CNA data, allowed

for a detailed assessment of PRMT5 alterations (Figure 2.3.17). The recurrent amplifications of PRMT5 in these cancers highlight its potential oncogenic role and importance in cancer biology.

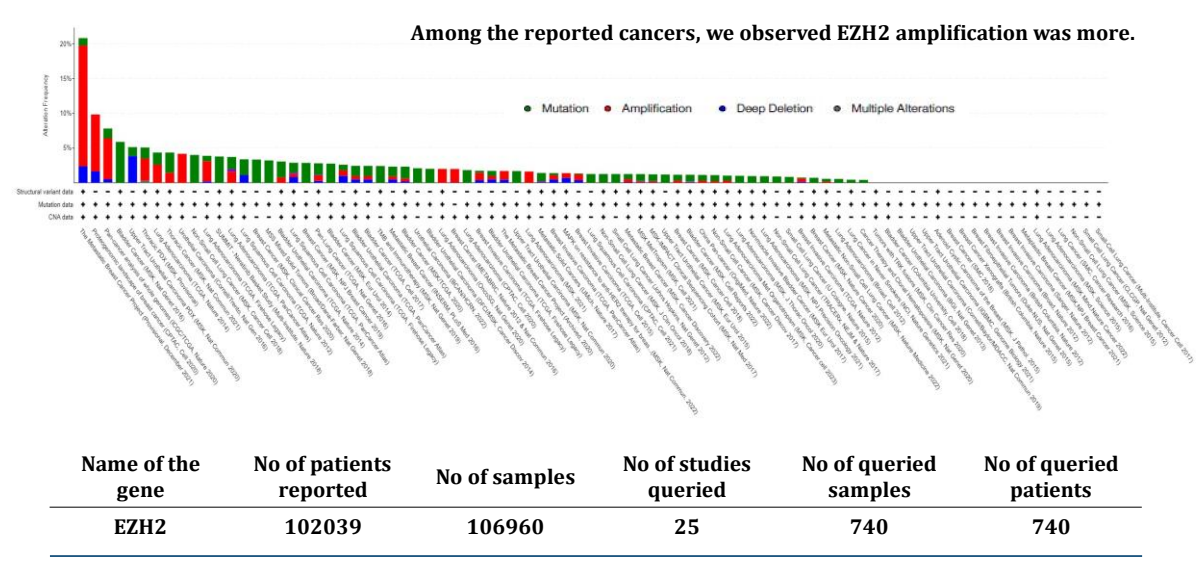
2.3.4.2. EZH2 Gene Alterations

For the EZH2 gene, the data covered 102,039 patients and 106,960 samples from 25 studies. Among the different types of alterations, EZH2 amplification was notably more frequent. The analysis showed that, lung squamous cell carcinoma, bladder urothelial carcinoma and prostate adenocarcinoma exhibited the highest frequencies of EZH2 amplifications. The presence of mutation data, structural variant data, and CNA (Copy Number Alteration) data across these studies provided a comprehensive view of EZH2 alterations (Figure 2.3.18). The significant occurrence of amplifications suggests a versatile role of EZH2 in cancer progression and development

CANCER TYPES SUMMARY (PRMT5) Among the reported cancers, we observed PRMT5 amplification was more. No of queried No of queried No of studies No of patients Name of the gene No of samples samples patients reported queried PRMT5 10851 11632 25 799 791 (https://www.cbioportal.org/)

Figure-2.3.17: Illustration of alteration frequencies of PRMT5 across different cancer types. This figure shows how often PRMT5 is changed in different types of cancer. It uses a bar chart to compare mutations, amplifications, deep deletions, and multiple changes. Across many cancer studies listed on the x-axis, PRMT5 amplification appears most often, shown in red on the chart. The table below summarizes data about PRMT5 from 25 studies, including the 799 and 791 number of patients and samples studied respectively.

CANCER TYPES SUMMARY (EZH2)



(https://www.cbioportal.org/)

Figure-2.3.18: Illustration of alteration frequencies of EZH2 across different cancer types. This figure shows how often EZH2 is changed in different types of cancer. It uses a bar chart to compare mutations, amplifications, deep deletions, and multiple changes. Across many cancer studies listed on the x-axis, EZH2 amplification appears most often, shown in red on the chart. The table below summarizes data about EZH2 from 25 studies, including the 740 number of patients and samples studied.

Given the prominence of amplifications in both EZH2 and PRMT5 genes across multiple cancer types, we decided to further analyze the amplification data for these genes. The detailed examination of amplification events will help in understanding their contribution to tumorigenesis and may guide the progression of targeted therapeutic strategies. The use of cBioPortal's extensive and well-annotated dataset provided a robust foundation for our analysis, enabling us to draw meaningful conclusions about the role of EZH2 and PRMT5 amplifications in cancer.

2.3.5 Amplification Analysis Unveils High-Frequency Presence: PRMT5 and EZH2 Exhibit Over 90% Amplification Frequency in Breast Cancer

From our comprehensive analysis utilizing cBioPortal, we examined the amplification frequencies and Oncoprint data for the PRMT5 and EZH2 genes across various cancer types. The results revealed a significant prevalence of amplifications for both genes. Specifically, breast cancer exhibited over 90% amplification frequencies for both PRMT5 and EZH2. These findings were consistent across multiple datasets, highlighting the robust nature of the observed genetic alterations.

The Oncoprint data analysis further supported these results. The visual representation of the genetic data confirmed that the overexpression of PRMT5 and EZH2 is closely related with the amplification events in the patients. This association was particularly pronounced in breast cancer, where amplification-driven overexpression was evident. The data from Oncoprint provided a clear and detailed view of the amplification patterns, reinforcing the importance of these alterations in cancer biology (Figure 2.3.19).

The high frequency of PRMT5 and EZH2 amplifications observed majorly in breast cancer patients underscores the potential role of these oncogenes in tumorigenesis. The amplification of these genes may contribute to cancer progression through increased gene dosage, leading to enhanced expression of oncogenic proteins. The Oncoprint data, which shows a strong correlation between gene amplification and overexpression, supports this hypothesis. These findings have significant implications for cancer treatment and research.

Analysis of Amplification Counts and Oncoprint Data visualization

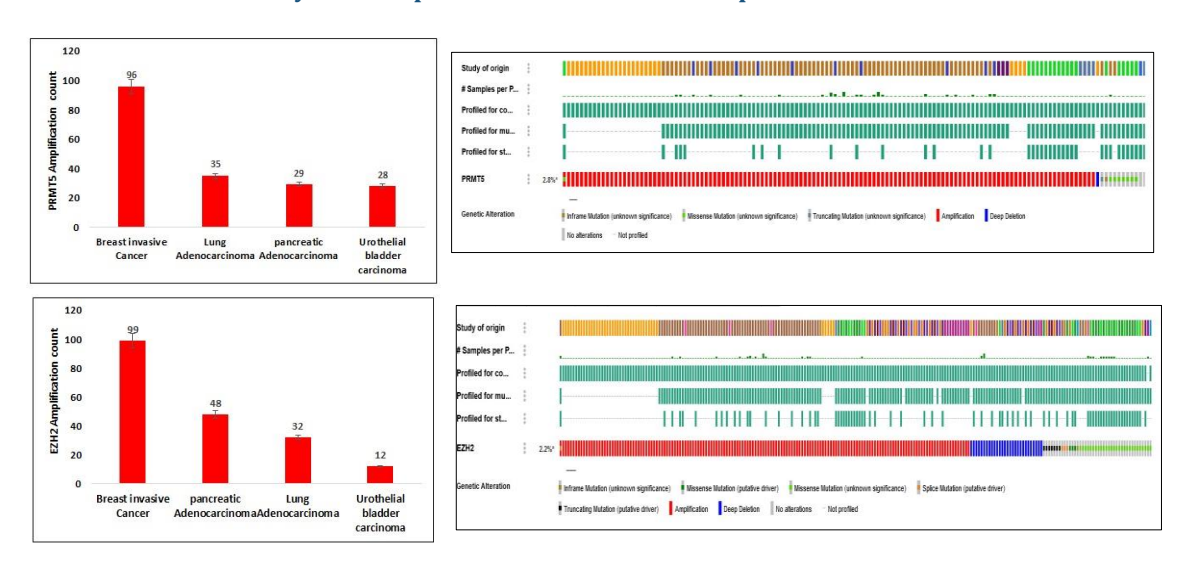


Figure-2.3.19- Amplification Data and Oncoprint Analysis of PRMT5 and EZH2 Genes in Various Cancer Types- From the analysis, it is evident that both PRMT5 and EZH2 amplifications are significantly reported in breast cancer, with more than 90% of the alterations being amplifications. The Oncoprint data analysis corroborates these findings, suggesting that the overexpression of PRMT5 and EZH2 in patients may be attributed to the high frequency of gene amplifications.

Targeting the amplified PRMT5 and EZH2 genes could provide a therapeutic advantage, especially in breast cancer where these alterations are most prevalent. The consistent pattern of amplifications across multiple datasets and studies suggests that PRMT5 and EZH2 could serve as reliable biomarkers for diagnosis and prognosis of cancer. Future research directions must focus on understanding the molecular mechanisms driving the amplification of PRMT5 and

EZH2 and their role in cancer development. Additionally, exploring targeted therapies that specifically inhibit these amplified genes could lead to more effective cancer treatments, improving patient outcomes. The use of cBioPortal and Oncoprint in this study highlights the power of integrative data analysis in uncovering critical genetic alterations and their potential clinical significance.

2.3.6 Survival Analysis Unveils Negative Correlation Between PRMT5 & EZH2 Expression and Patient Survival in Breast Cancer: Oncoprint Data Validation

We constructed a Kaplan-Meier plot to investigate the correlation between the expressions of PRMT5 and EZH2 and patient survival in breast cancer. For this analysis, we utilized data from the cBioPortal dataset, which offers comprehensive and robust cancer genomics data. Our findings indicate that elevated levels of PRMT5 and EZH2 are significantly associated with poorer patient existence or survival outcomes in breast cancer (Figure 2.3.20 & Figure 2.3.21).

Interestingly, the overexpression of PRMT5 exhibits a particularly strong correlation with decreased survival rates compared to EZH2. These outcomes are reliable with previous studies that have highlighted the roles of PRMT5 and EZH2 as critical tumor promoters, both individually and synergistically. The pronounced association of PRMT5 overexpression with poor prognosis underscores its potential as a more prominent biomarker for patient outcomes in breast cancer.

Furthermore, our analysis underscores the therapeutic importance of targeting PRMT5 and EZH2 in cancer treatment strategies. The significant correlation between high expression levels of these proteins and adverse patient survival outcomes reinforces the potential benefits of developing inhibitors for PRMT5 and EZH2. Such therapeutic interventions could improve survival rates for breast cancer patients by mitigating the tumor-promoting activities of these proteins.

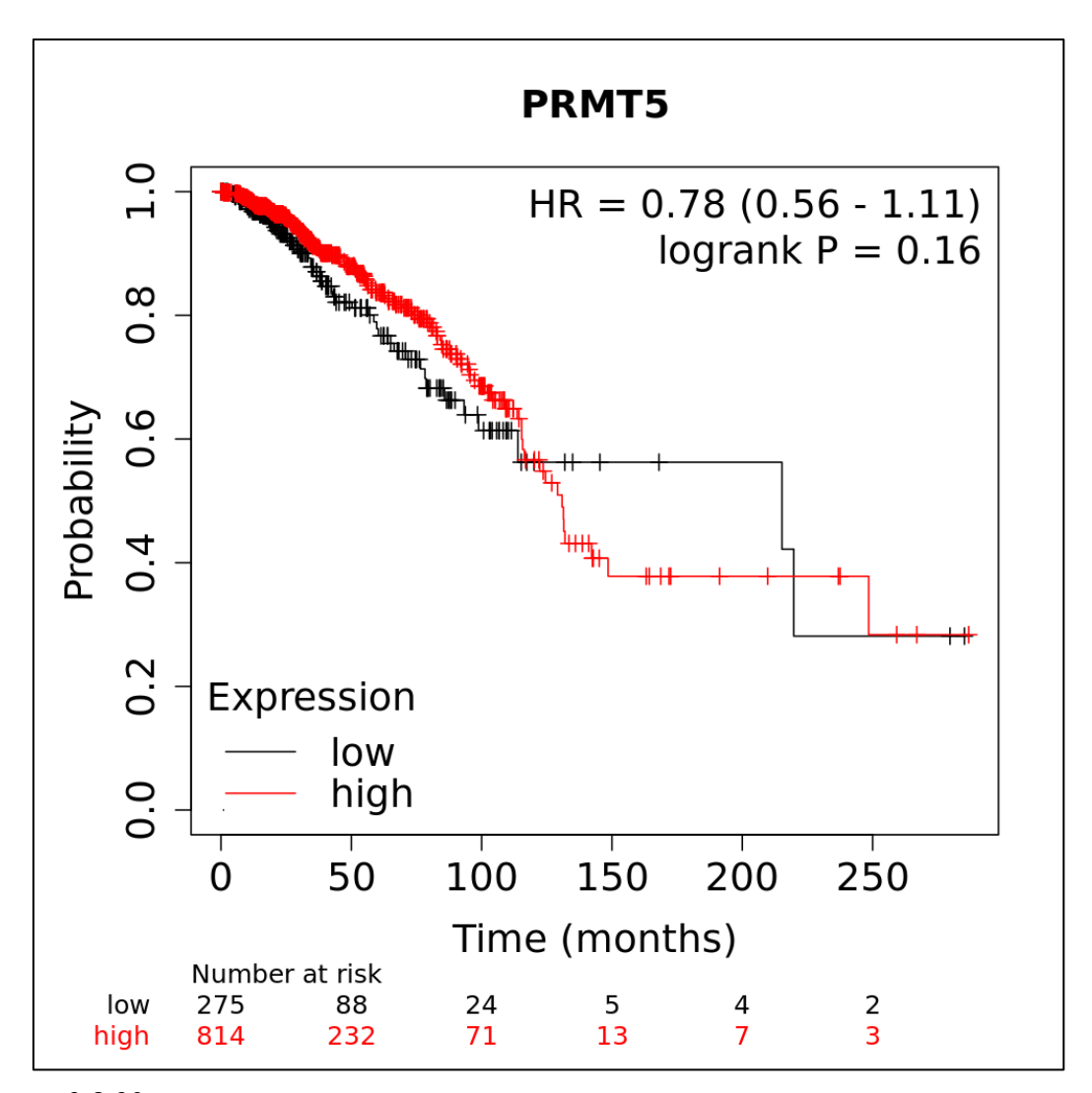


Figure- 2.3.20- Survival Plot (Kaplan-Meier Plot) for PRMT5 in Breast Cancer Patients-This Kaplan-Meier survival plot illustrates the correlation between PRMT5 expression levels and overall patient survival in breast cancer. The plot compares survival rates between patients with high PRMT5 expression (red curve) and those with low PRMT5 expression (blue curve). The data indicates that patients with elevated PRMT5 expression exhibit significantly poorer survival outcomes compared to those with lower expression levels. This finding suggests that high PRMT5 expression is a potential prognostic marker for worse survival in breast cancer patients.

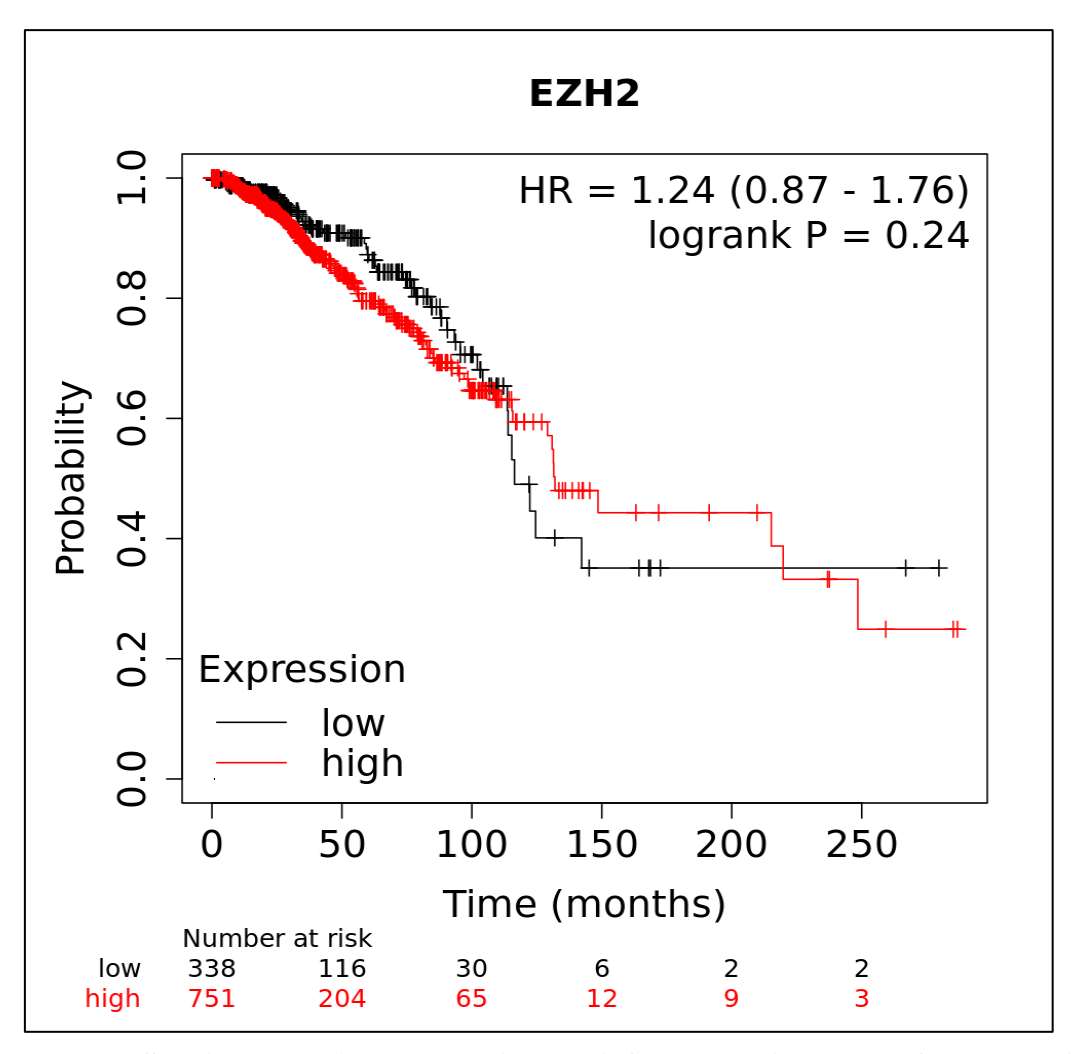


Figure-2.3.21: Survival Plot (Kaplan-Meier Plot) for EZH2 in Breast Cancer Patients—This Kaplan-Meier survival plot demonstrates the association between EZH2 expression levels and overall patient survival in breast cancer. The plot compares survival rates between patients with high EZH2 expression (red curve) and those with low EZH2 expression (blue curve). The results show that patients with higher EZH2 expression tend to have worse survival outcomes than those with lower expression levels. These findings indicate that EZH2, like PRMT5, may serve as a prognostic marker for poor survival in breast cancer patients.

2.3.7 Discussion

In this chapter we aimed to screen the phytocompounds as antiproliferative molecules and checked their action on epigenetic modulators. Research has shown that phytochemicals, such as EGCG, Cur, and Rvr etc., can modulate the activity of key epigenetic enzymes like DNMTs and HDACs ^[64]. And literature search showed that profiling of the basal expression levels of various epigenetic regulators revealed significant overexpression in human malignant cell lines. This elevated expression was observed across several cancer types, including skin, lung, cervical, hepatic, breast, and prostate cancers. Epigenetic regulators such as DNMT1, PRMT1, PRMT5, HDAC1, SIRT1, RNF2, PCGFs, EZH2, EED, and SUZ12 were notably expressed at higher levels. And confirmed that epigenetic dysregulation as a hall mark for cancer ^[24, 25-27].

Overexpression of key epigenetic regulators like DNMT1, PRMT5, HDAC1, and EZH2 significantly contributes to the deregulated proliferation of malignant cells.

For instance, DNMT1 is crucial for maintaining DNA methylation patterns, and its dysregulation can yield into silencing of tumor suppressor genes and oncogenes activation, driving tumorigenesis ^[65]. Similarly, PRMT5, which symmetrically dimethylates arginine residues on histones, is implicated in gene silencing and has been shown to promote malignant cell proliferation in various cancers ^[66]. HDAC1, another crucial regulator, removes acetyl groups from histones, consequential in chromatin condensation and transcriptional repression of tumor suppressor genes. Elevated levels of HDAC1 are correlated with unfavourable prognosis across multiple cancer types ^[67]. EZH2, an integral part of the Polycomb repressive complex 2 (PRC2), catalyzes the methylation of histone H3 at lysine 27 (H3K27), resulting in gene silencing. Overexpression of EZH2 is associated with more aggressive cancer behaviours and worse clinical outcomes ^[68].

These elevated expressions of epigenetic regulators underscore their critical role in cancer biology, particularly in maintaining the malignant phenotype through gene expression modulation. Targeting these regulators with specific inhibitors holds promise for cancer therapy, as evidenced by ongoing clinical trials exploring DNMT, HDAC, and EZH2 inhibitors ^[69]. Thus, understanding the mechanisms through these epigenetic changes contribute to cancer progression is essential for developing effective therapeutic strategies.

DNMT1 is crucial in maintaining DNA methylation patterns during cell replication. It's increased expression is linked to elevated global DNA methylation at CpG islands all around the genome, potentially leading to the silencing of many cell-cycle regulatory genes—a key event in tumorigenesis ^[27,28]. PRMT5 overexpression is associated with the methylation of non-histone proteins, such as p53, and promoter histones (H3R8 and H4R3), resulting in the silencing of tumor suppressor genes and cell cycle regulators like RBL2 and CDKN2A ^[29-31]. This overexpression promotes cell proliferation and neoplastic growth, recurrently observed in various cancers ^[31-33]. HDAC1, a core enzyme in chromatin remodeling complexes, plays a pivotal role in silencing target genes, including cell cycle regulators, through deacetylation of lysine residues on histones. Its aberrant expression is associated with cancer ^[34,35].

Polycomb repressive complexes (PRCs), particularly their catalytic subunits RNF2 and EZH2, modify chromatin histones to maintain gene silencing. Overexpression of these subunits is common in cancer ^[36,37] PRMT5 and EZH2 are overexpressed in several cancers, including endometrial, liver, breast, ovarian, small cell lung cancer, melanoma, prostate, glioblastoma, paediatric glioma, bladder cancer, and lymphomas. This overexpression correlates with disease progression and poor prognosis ^[38-40] PRMT5 and EZH2 functionally subordinate, with PRMT5-mediated histone modifications potentially leading to a synergistic effect ^[41], making a combined therapeutic approach promising.

Phytocompounds have been reported to inhibit or modulate epigenetic regulatory proteins like HDACs, DNMTs, PRC proteins and PRMTs. Compounds such as curcumin, resveratrol, brazilin, catechin, quercetin, and EGCG physically interact with proteins such as DNMT1 and HDAC1 within their catalytic pockets ^[42]. These phytochemicals mediated impact on epigenetic regulators, can cause the changes through directly or indirectly on their activity, exhibiting potential in cancer prevention and treatment, compounds such as genistein, curcumin, and resveratrol have been found to decrease DNMT activity, which results in the activation of tumor suppressor genes. Additionally, sulforaphane inhibits HDAC activity by forming complexes with the active sites of HDACs. ^[43].

In the current study, a panel of anti-proliferative molecules was screened for their optimal concentration and exposure times. The molecules inhibited the growth of multiple malignant cell lines under experimental conditions. Notably, EGCG and EA demonstrated strong IC₅₀ values and regulatory effects on PRMT5 and EZH2 in RT-PCR studies, leading to a focus on these compounds for further research. The IC₅₀ values for Brz, Cur, EGCG, EA, and Rvr in MCF7 cells after 24 hours of exposure were 19.8, 38.3, 2.1, 21.5, and 72.3 μ M, respectively. EGCG reduced the MCF7 cell population by half at about 2 μ M, while resveratrol required a much higher concentration to achieve a similar effect.

These molecules also affected the proliferation of other malignant cells, although the effect varied across cell lines. The anti-growth effect of these natural molecules has been reported in numerous studies both in vitro and in vivo [44-49]. For instance, curcumin has been shown to arrest HAG-1 human gallbladder adenocarcinoma cells in the G2/M phase and induce apoptosis through a MAPK-dependent mechanism [45]. EA exhibits anti-proliferative and

apoptotic effects towards multiple human cancer cells both *in vitro* (cell culture) and *in vivo* (animal models) ^[46]. It inhibits various aspects of tumorigenesis and metastasis, including tumor cell migration, extracellular matrix invasion, and angiogenesis. Resveratrol induces apoptosis in a dose-dependent manner studies in human pancreatic cancer cell lines via the inhibition of multiple proteins in the Hedgehog signaling pathway ^[49]. EGCG exerts an antitumor effect against human pancreatic cancer by activating the forehead transcription factor FOXO3a in vivo ^[46].

The main objective of this study was to investigate and validate whether these anti-proliferative molecules modulate epigenetic mechanisms contributing to their anti-proliferative nature. Exposure to the sappanwood polyphenolic compound brazilin significantly impacted DNMT1 expression, reducing MCF7 cell proliferation to 63.28% after 24 hours. Brazilin has previously been shown to activate HAT and repress HDAC1 and HDAC2 expression, resulting in G2/M-phase arrest and programmed cell death i.e., apoptosis in U266 human myeloma cells ^[50]. The impact of brazilin on DNMT1 expression has not been reported before and warrants further exploration for its therapeutic potential.

Curcumin, a well-studied anti-proliferative molecule, targets multiple epigenetic regulators, including DNMTs, EZH2, HATs, HDACs, and microRNAs ^[51-54]. In this study, curcumin significantly downregulated PRMT1, PRMT4, and PRMT5 expression in human prostate and breast cancer cell lines, whose proliferation was repressed under the same conditions. This suggests that curcumin's modulation of PRMTs, particularly PRMT5, may contribute to the repression of malignant cell proliferation. Given PRMT5's oncogenic potential ^[31-33], its downregulation by curcumin enhances its potential as an anti-cancer therapeutic molecule.

EGCG and EA selectively influenced the transcription of lysine acetylation regulator genes. EGCG at one micromolar concentration non-specifically repressed KAT2A and KAT3A/B, while EA at ten μM increased their expression up to fivefold in human skin cancer A-431 cells. EGCG significantly diminished the expression of HDAC1, HDAC7, and SIRT1, but not EA. EGCG's impact on HDACs and KATs has been previously reported ^{[55,56].} It was hypothesized that EGCG exposure reduced the association of HDAC3 and DNMT3A with E3 ubiquitin ligase UHRF1, resulting in their degradation in methylation-sensitive human colon cancer cells (HCT 116) ^[55]. Another study demonstrated that EGCG inhibited HDAC1 expression and

activity, along with reduced DNMT3B levels, reversing the expression of CDH1, RARβ, and DAPK1 tumor-suppressor genes in HeLa cells ^[56]. Ellagic acid's impact on PRMT4 and HDAC9 is documented ^[57], and its novel KAT-modulatory action is investigated here.

Resveratrol showed a significant inhibitory effect on the expression of crucial polycomb repressive complex genes, including RNF2 and EZH2. Although contradictory impacts of resveratrol on EZH2 expression and H3K27me3 level have been reported ^[58], recent studies show resveratrol downregulates EZH2 via ERK1/2 dephosphorylation-dependent mechanisms, has shown inhibition of growth of ER-positive breast cancer cell lines ^[59]. The underlying mechanisms require further investigation to enhance resveratrol's applicability as an anticancer therapeutic molecule.

Recent reviews by Zhang and Kutateladze ^[60] and Carlos-Reyes and colleagues ^[61] on the epigenetic alterations induced by dietary phytochemicals, including curcumin, EGCG, and resveratrol, highlight the reversible nature of epigenetic mechanisms and the need for novel therapeutic targeting mechanisms. This study explored modulatory molecules with the potential to alter cancer-deregulated epigenetic mechanisms. The initial screening provided evidence that malignant cell lines could serve as ideal *in vitro* models for further investigations. Modulation of DNMT1 by brazilin, PRMT5 by curcumin, and EZH2 and KDAC/KATs by resveratrol are investigated in subsequent chapters.

In contrast, EGCG and EA selectively influenced the transcription of lysine acetylation regulator genes. The non-uniform modulation of these genes, dependent on the specific molecule and irrespective of the cell line, underscores EGCG and EA as versatile modulators of epigenetic regulation. The significant reductions in PRMT5 and EZH2 levels across multiple cell lines suggest a dual mechanism underlying the anti-proliferative effects of these compounds. The profound impact of EGCG and EA on PRMT5 and EZH2, particularly in MDA-MB231, MCF7, PC3, and A549 cells, highlights their potential for further research and development of targeted cancer therapies. Their ability to inhibit cell proliferation while modifying key epigenetic regulators represents a promising direction in oncological therapeutics.

Our comprehensive analysis utilizing cBioPortal examined the amplification frequencies and Oncoprint data for the PRMT5 and EZH2 genes across various cancer types. The results

revealed a significant prevalence of amplifications for both genes, with breast cancer exhibiting over 90% amplification frequencies for PRMT5 and EZH2. These findings were consistent across multiple datasets, highlighting the robust nature of the observed genetic alterations. The Oncoprint data further supported these results, showing that the overexpression of PRMT5 and EZH2 is closely connected with amplification events in patients, particularly pronounced in breast cancer. This data provided a clear and detailed view of the amplification patterns, reinforcing the importance of these alterations in cancer biology. The high frequency of PRMT5 and EZH2 amplifications in breast cancer models underscores the potential role of these oncogenes in tumorigenesis, potentially contributing to cancer progression through increased gene dosage and enhanced expression of oncogenic proteins. The Oncoprint data shows a strong correlation between gene amplification and overexpression, supporting this hypothesis. Interestingly, the overexpression of PRMT5 shows a particularly strong correlation with decreased survival rates compared to EZH2. These results are steady with previous studies highlighting the roles of PRMT5 and EZH2 as critical tumor promoters, both individually and synergistically. The pronounced association of PRMT5 overexpression with poor prognosis underscores its potential as a more prominent biomarker for patient outcomes in breast cancer. Furthermore, our analysis underscores the therapeutic importance of targeting PRMT5 and EZH2 in cancer treatment strategies. The significant correlation between high expression levels of these proteins and adverse patient survival outcomes reinforces the potential benefits of developing inhibitors for PRMT5 and EZH2, which could improve survival rates for breast cancer patients by mitigating the tumor-promoting activities of these proteins. In conclusion, the current chapter concludes that the notion that epigenetic dysregulation plays a crucial role in cancer progression. Particularly, DNMT1, PRMT5, HDAC1, and EZH2 are significantly overexpressed, contributing to the deregulated proliferation of malignant cells. The screening of phytocompounds with antiproliferative properties identified EGCG and ellagic acid (EA) as potent modulators of epigenetic regulation, significantly reducing PRMT5 and EZH2 levels across multiple cell lines. This dual mechanism highlights their potential for further research and development of targeted cancer therapies. The comprehensive analysis using cBioPortal further emphasized the critical roles of PRMT5 and EZH2 in tumorigenesis, particularly in breast cancer, where their overexpression correlates with poor patient survival. These findings suggest that targeting PRMT5 and EZH2 could be a promising therapeutic approach to improve survival rates in cancer patients. Our study underscores the importance of developing inhibitors for these proteins, as their modulation could provide significant benefits in cancer treatment.

2.3.8 References

- 1. Orsolic, I., Carrier, A., & Esteller, M. (2023). Genetic and epigenetic defects of the RNA modification machinery in cancer. *Trends in genetics: TIG*, 39(1), 74–88. https://doi.org/10.1016/j.tig.2022.10.004
- 2. Hanahan, D. (2022). Hallmarks of cancer: new dimensions. Cancer discovery, 12(1), 31-46.
- 3. Debela, D. T., Muzazu, S. G., Heraro, K. D., Ndalama, M. T., Mesele, B. W., Haile, D. C., Kitui, S. K., & Manyazewal, T. (2021). New approaches and procedures for cancer treatment: Current perspectives. *SAGE open medicine*, *9*, 20503121211034366. https://doi.org/10.1177/20503121211034366
- 4. Carlos-Reyes, Á., López-González, J. S., Meneses-Flores, M., Gallardo-Rincón, D., Ruíz-García, E., Marchat, L. A., Astudillo-de la Vega, H., Hernández de la Cruz, O. N., & López-Camarillo, C. (2019). Dietary Compounds as Epigenetic Modulating Agents in Cancer. *Frontiers in genetics*, 10, 79. https://doi.org/10.3389/fgene.2019.00079
- Miranda Furtado, C. L., Dos Santos Luciano, M. C., Silva Santos, R. D., Furtado, G. P., Moraes, M. O., & Pessoa, C. (2019). Epidrugs: Targeting epigenetic marks in cancer treatment. *Epigenetics*, 14(12), 1164-1176. https://doi.org/10.1080/15592294.2019.1640546
- 6. Al Awadh, A. A. (2022). Nucleotide and nucleoside-based drugs: Past, present, and future. *Saudi Journal of Biological Sciences*, 29(12). https://doi.org/10.1016/j.sjbs.2022.103481
- 7. https://pubmed.ncbi.nlm.nih.gov/
- 8. https://www.scopus.com/search/form.uri?display=basic#basic
- 9. https://scholar.google.com/schhp?hl=en
- 10. Mangal, M., Sagar, P., Singh, H., Raghava, G. P. S., & Agarwal, S. M. (2013). NPACT: Naturally occurring plant-based anti-cancer compound-activity-target database. *Nucleic Acids Research*, 41(D1).
- 11. Zeng, X., Zhang, P., He, W., Qin, C., Chen, S., Tao, L., ... Chen, Y. Z. (2018). NPASS: Natural product activity and species source database for natural product research, discovery and tool development. *Nucleic Acids Research*, 46(D1), D1217–D1222.
- 12. Hatherley, R., Brown, D. K., Musyoka, T. M., Penkler, D. L., Faya, N., Lobb, K. A., & Tastan Bishop, Ö. (2015). SANCDB: a South African natural compound database. *Journal of Cheminformatics*, 7(1), 29.
- 13. Banerjee, P., Erehman, J., Gohlke, B. O., Wilhelm, T., Preissner, R., & Dunkel, M. (2015). Super Natural II-a database of natural products. *Nucleic Acids Research*, 43(D1), D935–D939.
- 14. Specs Compound Management services and Research Compounds for the Life Science industry. (n.d.). Retrieved November 8, 2019, from https://www.specs.net/
- 15. Li, B., Ma, C., Zhao, X., Hu, Z., Du, T., Xu, X., ... Lin, J. (2018). YaTCM: Yet another Traditional Chinese Medicine Database for Drug Discovery. *Computational and Structural Biotechnology Journal*, 16, 600–610. http://www.swissadme.ch/
- 16. Cerami, E., Gao, J., (2012). The cBio cancer genomics portal: an open platform for exploring multidimensional cancer genomics data. *Cancer discovery*, 2(5), 401–404. https://doi.org/10.1158/2159-8290.CD-12-0095 (https://www.cbioportal.org/)
- 17. https://kmplot.com/analysis/ (KM Plot).
- 18. Friesner, R. A.; Murphy, R. B.; (2006) "Extra Precision Glide: Docking and Scoring Incorporating a Model of Hydrophobic Enclosure for Protein-Ligand Complexes," *J. Med. Chem.* 49, 6177–6196
- 19. Kim, S., Thiessen, P. A., Bolton, E. E., Chen, J., Fu, G., Gindulyte, A., ... Bryant, S. H. (2016). PubChem substance and compound databases. *Nucleic Acids Research*, 44(D1), D1202–D1213.
- 20. Sterling, T., & Irwin, J. J. (2015). ZINC 15 Ligand Discovery for Everyone. *Journal of Chemical Information and Modeling*, 55(11), 2324–2337.
- 21. de Matos, P., Alcántara, R., Dekker, A., Ennis, M., Hastings, J., Haug, K., ... Steinbeck, C. (2009). Chemical entities of biological interest: An update. *Nucleic Acids Research*, 38(SUPPL.1).
- 22. Daina, A., Michielin, O., & Zoete, V. (2017). SwissADME: A free web tool to evaluate pharmacokinetics, drug-likeness and medicinal chemistry friendliness of small molecules. *Scientific Reports*, 7: 42717.
- 23. Lipinski, C. A., Lombardo, F., Dominy, B. W., & Feeney, P. J. (2012). Experimental and computational approaches to estimate solubility and permeability in drug discovery and development settings. *Advanced Drug Delivery Reviews*, 64, 4–17.
- 24. Veber, D. F., Johnson, S. R., Cheng, H. Y., Smith, B. R., Ward, K. W., & Kopple, K. D. (2002). Molecular properties that influence the oral bioavailability of drug candidates. *Journal of Medicinal Chemistry*, 45(12), 2615–2623.
- 25. Rao, K. S., Nalla, K., Ramachandraiah, C., Chandrasekhar, K. B., Kanade, S. R., & Saha, S. (2023). Design and Synthesis of New Triazole-Benzimidazole Derivatives as Potential PRMT5 Inhibitors. *ChemistrySelect*, 8(11), e202204474. DOI: 10.1002/slct.202204474
- 26. Nebbioso, A., Tambaro, F. P., Dell'Aversana, C., & Altucci, L. (2018). Cancer epigenetics: Moving forward. *PLOS Genetics*, 14(6), e1007362.
- 27. Feinberg, A. P., Koldobskiy, M. A., & Göndör, A. (2016). Epigenetic modulators, modifiers, and mediators in cancer etiology and progression. *Nature Reviews Genetics*, 17(5):284-99.

- 28. Flavahan, W. A., Gaskell, E., & Bernstein, B. E. (2017). Epigenetic plasticity and the hallmarks of cancer. *Science*, 357(6348).
- 29. Chatterjee, A., Rodger, E. J., & Eccles, M. R. (2018). Epigenetic drivers of tumorigenesis and cancer metastasis. *Seminars in Cancer Biology*, 51:149-159.
- 30. Baylin, S. B., & Herman, J. G. (2000). DNA hypermethylation in tumorigenesis: epigenetics joins genetics. *Trends in Genetics*, 16(4), 168–174.
- 31. Scoumanne, A., Zhang, J., & Chen, X. (2009). PRMT5 is required for cell-cycle progression and p53 tumor suppressor function. *Nucleic Acids Research*, 37(15), 4965–4976.
- 32. Wang, L., Pal, S., & Sif, S. (2008). Protein arginine methyltransferase 5 suppresses the transcription of the RB family of tumor suppressors in leukemia and lymphoma cells. *Molecular and Cellular Biology*, 28(20):6262-77.
- 33. Richters, A. (2017). Targeting protein arginine methyltransferase 5 in disease. *Future Medicinal Chemistry*, 9(17), 2081–2098.
- 34. Shailesh, H., Zakaria, Z. Z., Baiocchi, R., & Sif, S. (2018). Protein arginine methyltransferase 5 (PRMT5) dysregulation in cancer. *Oncotarget*, 9(94): 36705–36718.
- 35. Xiao, W., Chen, X., Liu, L., Shu, Y., Zhang, M., & Zhong, Y. (2019). Role of protein arginine methyltransferase 5 in human cancers. *Biomedicine and Pharmacotherapy*, 114:108790.
- 36. Yamaguchi, T., Cubizolles, F., Zhang, Y., Reichert, N., Kohler, H., Seiser, C., & Matthias, P. (2010). Histone deacetylases 1 and 2 act in concert to promote the G1-to-S progression. *Genes and Development*, 24: 455-469.
- 37. Li, Y., & Seto, E. (2016). HDACs and HDAC inhibitors in cancer development and therapy. *Cold Spring Harbor Perspectives in Medicine*, 6(10).
- 38. Pasini, D., & Di Croce, L. (2016). Emerging roles for Polycomb proteins in cancer. *Current Opinion in Genetics and Development*, 36:50-8.
- 39. Chan, H. L., Beckedorff, F., Zhang, Y., Garcia-Huidobro, J., Jiang, H., Colaprico, A., ... Morey,L. (2018). Polycomb complexes associate with enhancers and promote oncogenic transcriptional programs in cancer through multiple mechanisms. *Nature Communications*, 9(1):3377.
- 40. Liu, Y., & Yang, Q. (2023). The roles of EZH2 in cancer and its inhibitors. Medical oncology (Northwood, London, England), 40(6), 167.
- 41. Yang, X., Xu, L., & Yang, L. (2023). Recent advances in EZH2-based dual inhibitors in the treatment of cancers. *European journal of medicinal chemistry*, 256, 115461
- 42. Kim, H., & Ronai, Z. A. (2020). PRMT5 function and targeting in cancer. Cell stress, 4(8), 199-215
- 43. Yang, L., Ma, D. W (2021). PRMT5 functionally associates with EZH2 to promote colorectal cancer progression through epigenetically repressing CDKN2B expression. *Theranostics*, 11(8), 3742–3759.
- 44. Yunfeng Qi, Dadong Wang, HEDD (2016): the human epigenetic drug database Database,: pii: baw159.
- 45. Kedhari Sundaram, M., Haque, (2020). Epigallocatechin gallate inhibits HeLa cells by modulation of epigenetics and signaling pathways. *3 Biotech*, *10*(11), 484.
- 46. Bello-Martinez, J., Jiménez-Estrada, M., Rosas-Acevedo, J., Avila-Caballero, L., Vidal- Gutierrez, M., Patiño-Morales, C., ... Robles-Zepeda, R. (2017). Anti-proliferative activity of *Haematoxylum brasiletto* H. Karst. *Pharmacognosy Magazine*, 13(50), 289.
- 47. Ono, M., Higuchi, T., Takeshima, M., Chen, C., & Nakano, S. (**2013**). Anti-proliferative and apoptosis-inducing activity of curcumin against human gallbladder adenocarcinoma cells. *Anticancer Research*, 33(5), 1861–1866.
- 48. Shankar, S., Marsh, L., & Srivastava, R. K. (2013). EGCG inhibits growth of human pancreatic tumors orthotopically implanted in Balb C nude mice through modulation of FKHRL1/FOXO3a and neuropilin. *Molecular and Cellular Biochemistry*, 372(1–2), 83–94.
- 49. Ceci, C., Lacal, P., Tentori, L., De Martino, M., Miano, R., Graziani, G., ... Graziani, G. (2018). Experimental Evidence of the Antitumor, Antimetastatic and Antiangiogenic Activity of Ellagic Acid. *Nutrients*, 10(11), 1756.
- 50. Colin, D., Lancon, A., Delmas, D., Lizard, G., Abrossinow, J., Kahn, E., ... Latruffe, N. (2008). Anti-proliferative activities of resveratrol and related compounds in human hepatocyte derived HepG2 cells are associated with biochemical cell disturbance revealed by fluorescence analyses. *Biochimie*, 90(11–12), 1674–1684.
- 51. Qin, Y., Ma, Z., Dang, X., Li, W., & Ma, Q. (2014). Effect of resveratrol on proliferation and apoptosis of human pancreatic cancer MIA PaCa-2 cells may involve inhibition of the Hedgehog signaling pathway. *Molecular Medicine Reports*, 10(5), 2563–2567.
- 52. Kim, B., Kim, S.-H., Jeong, S.-J., Sohn, E. J., Jung, J. H., Lee, M. H., & Kim, S.-H. (**2012**).Brazilin Induces Apoptosis and G2/M Arrest via Inactivation of Histone Deacetylase in Multiple Myeloma U266 Cells. *Journal of Agricultural and Food Chemistry*, 60(39), 9882–9889.

- 53. Boyanapalli, S. S. S., & Kong, A.-N. T. (2015). "Curcumin, the King of Spices": Epigenetic Regulatory Mechanisms in the Prevention of Cancer, Neurological, and Inflammatory Diseases. *Current Pharmacology Reports*, 1(2), 129–139.
- 54. Hassan, F., Rehman, M. S., Khan, M. S., Ali, M. A., Javed, A., Nawaz, A., & Yang, C. (2019). Curcumin as an Alternative Epigenetic Modulator: Mechanism of Action and Potential Effects. *Frontiers in Genetics*, 10, 514.
- 55. Hua, W.-F., Fu, Y.-S., Liao, Y.-J., Xia, W.-J., Chen, Y.-C., Zeng, Y.-X., ... Xie, D. (2010).
- 56. Curcumin induces down-regulation of EZH2 expression through the MAPK pathway in MDA-MB- 435 human breast cancer cells. *European Journal of Pharmacology*, 637(1–3), 16–21.
- 57. Wu, C., Ruan, T., Liu, W., Zhu, X., Pan, J., Lu, W., ... Zhang, C. (2018). Effect and Mechanism of Curcumin on EZH2 miR-101 Regulatory Feedback Loop in Multiple Myeloma. *Current Pharmaceutical Design*, 24(5), 564–575.
- 58. Moseley, V. R., Morris, J., Knackstedt, R. W., & Wargovich, M. J. (2013). Green tea polyphenol epigallocatechin 3-gallate, contributes to the degradation of DNMT3A and HDAC3 in HCT 116 human colon cancer cells. *Anticancer Research*, 33(12), 5325–5333.
- 59. Khan, M. A., Hussain, A., Sundaram, M. K., Alalami, U., Gunasekera, D., Ramesh, L., ... Quraishi, U. (2015). (-)-Epigallocatechin-3-gallate reverses the expression of various tumor- suppressor genes by inhibiting DNA methyltransferases and histone deacetylases in human cervical cancer cells. *Oncology Reports*, 33(4), 1976–1984.
- 60. Kang I, Okla M, & Chung S. (2014). Ellagic acid inhibits adipocyte differentiation through coactivator-associated arginine methyltransferase 1-mediated chromatin modification. *J Nutr Biochem*. 25(9):946-53.
- 61. Chang, Y.-C., Lin, C.-W., Yu, C.-C., Wang, B.-Y., Huang, Y.-H., Hsieh, Y.-C., ... Chang, W.-W. (**2016**). Resveratrol suppresses myofibroblast activity of human buccal mucosal fibroblasts through epigenetic inhibition of ZEB1 expression. *Oncotarget*, 7(11), 12137–12149.
- 62. Hu, C., Liu, Y., Teng, M., Jiao, K., Zhen, J., Wu, M., & Li, Z. (2019). Resveratrol inhibits the proliferation of estrogen receptor-positive breast cancer cells by suppressing EZH2 through the modulation of ERK1/2 signaling. *Cell Biology and Toxicology*, pp 1–12.
- 63. Zhang, Y., & Kutateladze, T. G. (2018). Diet and the epigenome. *Nature Communications* volume 9, Article number: 3375.
- 64. Carlos-Reyes, Á., López-González, J. S., Meneses-Flores, M., Gallardo-Rincón, D., Ruíz-García, E., Marchat, L. A., ... López-Camarillo, C. (2019). Dietary Compounds as Epigenetic Modulating Agents in Cancer. *Frontiers in Genetics*, 10, 79.
- 65. Carlos-Reyes, Á., López-González, J. S., Meneses-Flores, M., Gallardo-Rincón, D., Ruíz-García, E., Marchat, L. A., Astudillo-de la Vega, H., Hernández de la Cruz, O. N., & López-Camarillo, C. (2019). Dietary Compounds as Epigenetic Modulating Agents in Cancer. Frontiers in genetics, 10, 79. https://doi.org/10.3389/fgene.2019.00079
- 66. Skowronski, K., Dubey, S., Rodenhiser, D., & Coomber, B. (2010). Ischemia dysregulates DNA methyltransferases and p16INK4a methylation in human colorectal cancer cells. *Epigenetics*, *5*(6), 547–556. https://doi.org/10.4161/epi.5.6.12400
- 67. Yang, Y., & Bedford, M. T. (2013). Protein arginine methyltransferases and cancer. *Nature reviews. Cancer*, 13(1), 37–50. https://doi.org/10.1038/nrc3409
- 68. Lane, A. A., & Chabner, B. A. (2009). Histone deacetylase inhibitors in cancer therapy. *Journal of clinical oncology: official journal of the American Society of Clinical Oncology*, 27(32), 5459–5468. https://doi.org/10.1200/JCO.2009.22.1291
- 69. Simon, J.A. and Lange, C.A. (2008) Roles of the EZH2 Histone Methyltransferase in Cancer Epigenetics. Mutation Research/Fundamental and Molecular Mechanisms of Mutagenesis, 647, 21-29. https://doi.org/10.1016/j.mrfmmm.2008.07.010
- 70. Dawson, M. A., & Kouzarides, T. (2012). Cancer epigenetics: from mechanism to therapy. *Cell*, *150*(1), 12–27. https://doi.org/10.1016/j.cell.2012.06.013

CHAPTER#3

TO VALIDATE THE INHIBITION OF *PRMT5* AND *EZH2* BY PHYTOCHEMICALS USING *IN-VITRO* METHODS

3.1 Introduction:

Cancer remains a frightening challenge in global health, necessitating the exploration of new therapeutic strategies to combat its progression ^[1]. One promising area of research involves the use of phytochemicals-naturally occurring compounds found in plants—for their potential anticancer properties ^[2]. PRMT5 and EZH2 are frequently amplified in various malignancies, including breast cancer, where their overexpression is linked to poor prognosis and aggressive tumor behavior. Alterations in histone modifications, like H3K27me3 by EZH2 and H4R3me2s by PRMT5, are crucial in these epigenetic changes. They disrupt normal gene expression, promote oncogene activation, and inhibit tumor suppressor genes ^[3-5].

In the previous chapter, we demonstrated that phytochemicals, such as EGCG and EA, impact both PRMT5 and EZH2. These compounds were chosen for further investigation in the context of cancer therapeutics, as they can modulate epigenetic markers and inhibit cancer cell proliferation. *In-vitro* models offer a controlled setting to investigate the molecular mechanisms through which these compounds exert their anticancer properties. This approach allows for precise measurement of changes in gene expression, protein activity, and cellular behavior in response to treatment. Phytocompounds, derived from medicinal plants, present a natural and potentially less toxic alternative to synthetic drugs. EGCG and EA are two such phytochemicals that have shown significant promise in preclinical studies. These compounds are not only known for their antioxidant and anti-inflammatory effects but also for their ability to modulate various cellular pathways, including those involved in epigenetic regulation. Given the critical roles of PRMT5 and EZH2 in cancer progression, there is a compelling need to validate the inhibitory effects of phytochemicals like EGCG and EA on these targets using *in-vitro* methods ^[5-9].

The current study aims to validate the inhibition of PRMT5 and EZH2 by EGCG and EA using *in-vitro* methods. By exploring the binding efficacy of these phytochemicals to PRMT5 and EZH2, we can gain valuable insights into their potential as targeted therapies for cancer. The significant reductions in PRMT5 and EZH2 levels across multiple cell lines suggest a dual mechanism underlying the anti-cancer effects of these compounds. Future research should focus on detailed binding studies and further validation of their inhibitory effects *in vivo*. This work represents a crucial step towards harnessing the therapeutic potential of EGCG and EA, paving the way for their development as effective epigenetic modulators in cancer treatment. Exploring natural products in cancer therapy could lead to novel, safer, and more effective epigenetic therapies.

3.2 Materials and methods

S-adenosyl methionine (SAM), 3-(4,5-Dimethylthiazol-2-yl)-2,5Diphenyltetrazolium-Bromide (MTT), Dimethyl sulfoxide (DMSO), Recombinant proteins PRMT5:MEP50 complex (SRP0145-25470 and EZH2 (SRP0379) were purchased from Sigma-Aldrich United states. CM5 Sensor chip for SPR studies (cat no: 50-105-5511) was purchased from GE Healthcare Bio-Sciences (Cytiva life sciences-USA). The antibodies Anti-PRMT5 antibody (#2252) Histone (H4) antibody (#2935), H3 antibody (#4499), EZH2 antibody (#5246), H3K27 (#9733), anti-beta actin antibody (#4967), Ki67 antibody (#D3B5) was purchased from Cell Signaling Technology (CST) USA. H4R3me2s Polyclonal antibody (A3718-050) from Epigentek NY-USA, FITC- Annexin V Dead cell/ Apoptosis kit (V13242) from Invitrogen-US. PRMT5 monoclonal antibody (MA-125470), EZH2 monoclonal antibody (MA5-15101) procured from ThermoFisher Scientific US. The antibodies for signaling studies Bad (A1593), Beclin-1 (A7353), PARP (A8770), Cytochrome-c (A0225), BCL-2 (A0208), Bax (A0207), ATG5 (A0203), ATG12 (A19610), ATG7 (A19604), ATG3 (A19594), LC3 I/II (A19665), Cyclin-A2 (A7632), Cyclin-B1 (A19037), Cyclin-E1 (A14225), Cyclin-D2 (A1773) purchased from Abclonal USA. All other chemicals were of analytical or higher standards unless otherwise specified. for molecular docking studies we used Schrödinger platform glide model (Schrödinger Release 2019-3: Glide, Schrödinger, LLC, New York, NY, 2019, For molecular dynamic simulations we utilised Desmond package of Schrodinger.

3.2.1 Preparation of the protein structure

The crystal structures of the *Homo sapiens* PRMT5: MEP50 complex (with sinefungin, a SAM analog) and EZH2 (Enhancer of Zeste Homolog 2), determined by X-ray diffraction at a resolution of 2.35 Å, were obtained from the RCSB Protein Data Bank (PDB IDs for PRMT5: 4X60, 4X61, 4X63; EZH2 PDB IDs: 5HYN and 4Mi5). The missing residues in both proteins were added using the Prime wizard in Schrödinger. The completed protein structures of the PRMT5: MEP50 complex and EZH2 were then processed with the Protein Preparation Wizard in the Maestro tool to assign bond orders, hydrogen atoms, and disulfide bonds. All selenomethionines were converted to methionine residues, and the protein structures were energy minimized using the OPLS3 force field (**Figure-3.2.1**).

Workflow for Molecular docking PDB (4X60) PDB (4X61) PDB (4X63) Schrodinger Protein Preparation Grid generated around the reference ligands Ligand preparation LigPrep wizard Minimized using OPLS3 force field. Docked with glide module Screening done based on Glide score

Figure:3.2.1 Workflow for Molecular Docking-The workflow diagram outlines the molecular docking process using the Schrodinger software suite. The two main protein targets, PRMT5 and EZH2, are prepared using specific PDB files (PRMT5 - PDB 4X60, 4X61, 4X63; EZH2 - PDB 5HYN, 4MI5). The steps include: Protein Preparation: Initial preparation of protein structures. Grid Generation: Creation of a grid around the reference ligands. Ligand Preparation: Preparation of ligands. LigPrep Wizard: Optimization of ligands using the OPLS3 force field. Docking with Glide Module: Docking of ligands to the prepared protein, followed by screening based on Glide score to identify potential binders.

3.2.2 Virtual screening

3.2.2.1 Molecular docking

For docking simulations, receptor grids were created around the active sites of the proteins, based on the interacting residues from the reference molecules in the crystal structures. Using Schrödinger's Glide program (Release 2019-3), all prepared ligands, along with the reference molecules, were docked. Default parameters were used for extra precision (XP) docking, including a Van der Waals radius of 1.0. The workflow included high-throughput virtual screening (HTVS), standard precision (SP), and finally XP mode to ensure accurate scoring and visualization of the docked ligands. The Glide results were analyzed by evaluating individual ligand poses, focusing on atomic proximity (within 5 Å), hydrogen bonds, and other interactions, as well as Glide XP scoring functions (Figure-3.2.2).

Structures of the compounds used for Molecular Docking

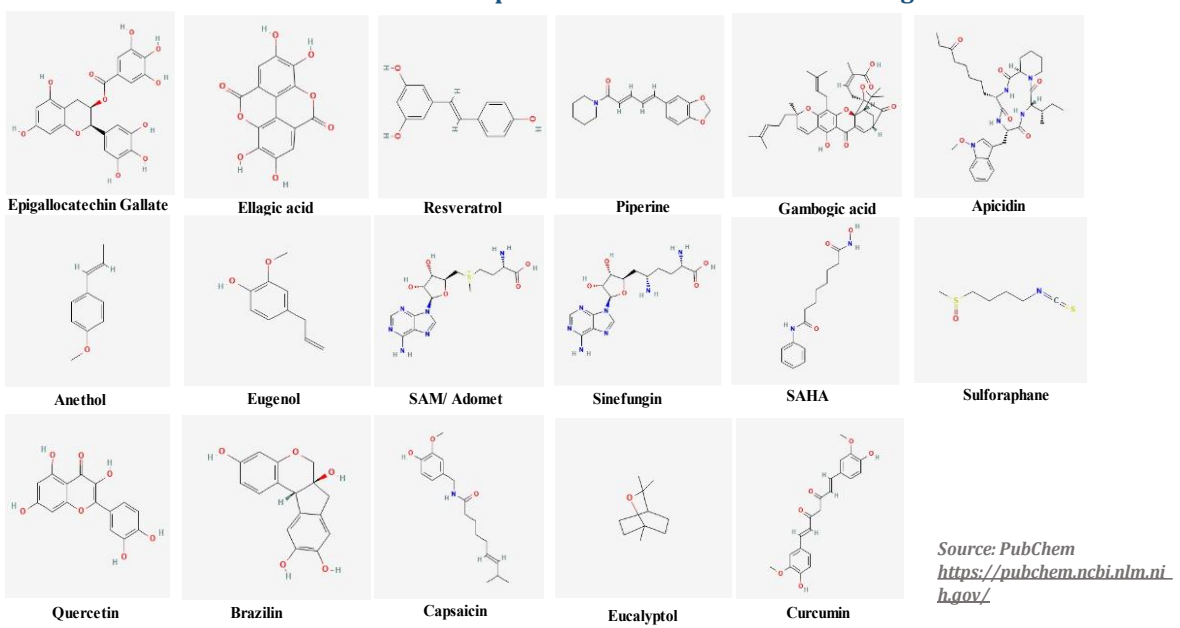


Figure 3.2.2: Structures of Compounds Used for Molecular Docking-This figure presents the chemical structures of various compounds used in the molecular docking studies. The compounds include Epigallocatechin Gallate, Ellagic Acid, Resveratrol, Piperine, Gambogic Acid, Apicidin, Acarbose, Eugenol, SAM (S-Adenosyl Methionine), Adenosyl, Sinefungin, SAHA (Suberoylanilide Hydroxamic Acid), Sulforaphane, Quercetin, Brazilin, Capsaicin, Eucalyptol, and Curcumin. Each structure is sourced from PubChem (https://pubchem.ncbi.nlm.nih.gov/) and is utilized to investigate their potential binding interactions with the target proteins PRMT5 and EZH2.

3.2.2.2 Molecular dynamics (MD) simulations

MD simulations were conducted by employing OPLS 2005 force field in the Desmond package incorporated in the Schrödinger suite ^[10]. MD simulations of the PRMT5 and EZH2 complexes with EGCG and EA were performed for 100 ns each. The Simple Point Charge (SPC) water model was used, and charges were neutralized with NaCl. The simulations began with an NVT ensemble at 10K for 10 ps, followed by an NPT ensemble at 10K. Subsequently, MD simulations were performed for 24 picoseconds (ps) for all non-hydrogen solute atoms in the NPT ensemble at 300K ^[11]. The trajectory of each ligand-protein complex was recorded for further analysis.

3.2.3 Surface plasmon resonance analysis for protein-ligand interaction & pharmacokinetics analysis for phytocompounds

SPR analysis was conducted using the Biacore-T200 system (GE Healthcare). Recombinant PRMT5-MEP50 complex and EZH2 were prepared at a concentration of 1 mg/mL in 1x PBS (pH 7.4). These proteins were immobilized onto a CM5 sensor chip through standard primary

amine coupling, with the immobilized protein amount estimated at 2500 response units (RU) per 2 ng/mm². Reference surfaces (flow cells FC1 and FC3) were deactivated with 1M ethanolamine (pH 8.5). Activation of immobilization surfaces (FC2 for EZH2 and FC4 for PRMT5-MEP50 complex) was achieved using a mixture of 200 mM EDC and 50 mM NHS.

A stable baseline was established by flowing HBS-P buffer (10 mM HEPES pH 7.4, 150 mM NaCl, 0.005% P20 + DMSO) over the immobilized proteins. Measurements were carried out at 25°C using the same buffer. EA, EGCG, and their combination were prepared as 10 mM working stocks in PBS and injected over the PRMT5-MEP50 complex and EZH2 at a flow rate of 30 μ L/min for 60 seconds at 25°C. Three-cycle kinetic analysis was performed with triplicate injections. Sensograms were analyzed using BIA-T200 evaluation software version 2.1 (GE Healthcare). The relationship between protein concentration and RU value was calculated as 1000 RU = 1 ng/mm² for surface concentration and 1000 RU = 10 mg/mL for volume concentration. The dissociation rate constant (kd) was determined using the Langmuir adsorption model, providing insights into the binding kinetics of the interactions.

3.2.4 Cell culture and treatment with EGCG, EA and combination:

For *in vitro* assays, human cancer cell lines MCF7 (breast), MDA-MB-231 (breast), Du-145 (prostate), A549 (lung), HeLa (cervix), Hep G2 (liver), PC-3 (prostate), and HEK293 (human embryonic kidney) were obtained from NCCS (National Centre for Cell Science), Pune-India. These cell lines were maintained and propagated at low passage numbers, by following standard sterile cell culture protocols. The cells were cultured in DMEM (Dulbecco's Modified Eagle's Medium) high glucose (Himedia), supplemented with 10% (v/v) fetal bovine serum (Himedia) and 1x antibiotic-antimycotic solution (Himedia). Cultures were maintained at 37°C CO₂ with 95% air and 5% CO₂.

3.2.5 Cytotoxicity assays:

To assess cytotoxicity, we employed multiple assays, including the trypan blue exclusion assay, Acridine Orange (AO) and Ethidium Bromide (EtBr) dual staining, and Flow Cytometry (FACS) analysis. The Trypan Blue exclusion assays was employed to determine cell viability by counting live versus dead cells under a microscope. AO/EtBr staining allowed for the visualization of live and apoptotic cells based on membrane integrity. Flow Cytometry (FACS) provided a detailed analysis of cell cycle progression and apoptosis by staining cells with specific markers and quantifying fluorescence intensity. These comprehensive methods

ensured accurate evaluation of cell viability and cytotoxic effects. Detailed procedures and results of these assays will be discussed in the following sections.

3.2.5.1 MTT (3-(4,5-Dimethylthiazol-2-yl)-2,5-Diphenyltetrazolium Bromide) assay

The viability test was conducted to assess the anti-proliferative effects of phytocompounds. Cells were seeded at a density of 5000 cells per well in triplicate on 96-well plates and allowed to grow overnight in complete growth medium. Following overnight incubation, the medium was replaced with DMEM and cells were further incubated for 6 hours. Various concentrations of phytocompounds were then added to the wells, and cells were cultured for an additional 24 and 48 hours. Post-incubation, the MTT (3-(4,5-dimethylthiazol-2-yl)-2,5-diphenyltetrazolium bromide) assay was performed. MTT solution was added to each well and incubated for 3 hours, allowing viable cells to convert MTT into formazan crystals. After aspirating the MTT solution, DMSO was added to dissolve the formazan crystals, and the absorbance was measured using a plate reader at 570 nm. The percentage viability of treated cells was calculated relative to untreated control cells based on absorbance readings.

3.2.5.2 Trypan blue dye exclusion assay

The trypan blue dye exclusion test was utilized to evaluate cell viability post-treatment with EA, EGCG, and their combination. This approach hinges on the principle that viable cells possess intact membranes, preventing dye absorption, while non-viable cells with compromised membranes absorb the dye, thereby becoming distinguishable under a light microscope. Post-treatment, cells were incubated with trypan blue dye, and microscopic inspection facilitated differentiation between viable cells (displaying clear white cytoplasm) and non-viable cells (exhibiting blue-stained cytoplasm). A graph depicting cell viability percentages was generated from these observations. Cell viability was quantitatively assessed using the formula:

% Cell Viability = Abs (Test sample) / Abs (Control) \times 100%.

Additionally,

% Cell Inhibition was calculated as 100% minus % Cell Viability providing insights into EA's potential impact on cell survival and proliferation. This assay offers a reliable approach to assess EA's effects on cell viability and its inhibitory potential.

3.2.5.3 Ao-Etbr double staining assay

The EB/AO double staining assay was employed to evaluate cell viability in this study. This method utilizes two fluorescent dyes: AO (acridine orange) and EB (ethidium bromide). AO

penetrates all cells and emits green fluorescence in live cells with intact membranes. In contrast, EB can only enter cells with compromised membranes, such as necrotic or late-stage apoptotic cells, causing them to emit red fluorescence. Cells undergoing necrosis, which absorb both dyes, display orange fluorescence, resembling viable cells under microscopic examination due to minimal changes in chromatin structure. MDA-MB-231 cells treated with EA, EGCG, and their combination were subjected to EB/AO staining after 24 hours of incubation. Fluorescence microscopy was employed to distinguish between live, apoptotic, and necrotic cells based on their fluorescence patterns. This approach provided detailed insights into the impact of EA, EGCG, and their combination on cell viability and the prevalence of apoptosis or necrosis within the cell population.

3.2.6 Western blotting

The cells were treated with varying concentrations of EGCG, EA, and their combination for the specified duration. Following treatment, cells were washed with phosphate-buffered saline and lysed using RIPA buffer supplemented with protease inhibitor cocktail, 1 mM DTT, and 1 mM PMSF (Thermo Scientific) at 4°C. The lysates were then subjected to centrifuged at 10,000 rpm for 10 minutes at 4°C. Protein concentration was determined using Bradford's assay, and equal amounts of proteins were loaded onto 10% SDS-PAGE gels following Laemmli's method. Subsequently, proteins were transferred to nitrocellulose membranes for immunoblotting. The membranes were blocked with skimmed milk in Tris-buffered saline containing Tween-20, follows by overnight incubation with primary antibodies against the target proteins. HRP-conjugated anti-rabbit secondary antibodies at a 1:10,000 dilution was applied. Protein bands were visualized using ClarityTM Western ECL Substrate (Bio-Rad), and band intensities were quantified using a VersaDoc Imaging System with Image LabTM Software version 5.1 (Bio-Rad). β-actin served as a loading control for normalizing protein expression levels.

3.2.7 Histones acid extraction from HEK293 cells

Histones were extracted from HEK293 cells using a modified protocol based on ^{[8],} HEK293 cells were treated with 5 mM sodium butyrate when reaching 50-60% confluency to maintain histone acetylation levels. Following an additional 24 hours incubation, cells were harvested at approximately 80% confluency by trypsinization. The obtained cell pellet was resuspended in TEB (Triton Extraction Buffer-composition is 1X PBS containing 0.5% Triton X-100, 2 mM of PMSF (phenylmethylsulfonyl fluoride), 0.02% NaN3) at a density of 5x103 cells per mL.

The cells were lysed on ice for 10 minutes with gentle stirring, followed by centrifugation at 10,000 rpm/10 minutes in 4°C cooling centrifuge. The supernatant was discarded, and the procedure was repeated to collect the nuclei. The pellet was then resuspended in TEB buffer (half of the original volume), centrifuged again, and resuspended finally in 0.2 N HCl at a density of 4-5x107 nuclei per mL. The acid extraction of histones was achieved by incubating the suspension at 4°C overnight. After centrifugation at 10,000 rpm for 10 minutes at 4°C, the supernatant containing histone proteins was collected, and the acid was neutralized by adding 2M NaOH (1/10 of the supernatant volume). Protein content in each sample was determined using the BCA assay. Aliquots of the extracted histones were stored at -20°C, and two portions were used as substrates for *in vitro* methylation studies.

3.2.7.1 *In-vitro* methylation assay and ELISA

The *in vitro* methylation assay was performed following the method described by Cheng et al., with minor adjustments [8, 9, 12]. PVC microplate wells were initially coated with extracted histones (40-50 µg/mL) in 0.2 M carbonate and bicarbonate buffer (pH 9.6). The microplates were allowed to overnight incubation at 4°C on a rocker. After removing the coating solution, the wells were washed twice with 1X PBS, followed by the addition of 100 µL of appropriately diluted samples containing PRMT5 with SAM or PRMT5 pre-treated with EGCG, EA, and their combination (pre-incubated for 0.5 h at 30°C). The reactions were carried out at 37°C for 1.5 hours. Post-incubation, the reaction mixtures were removed, and the wells were washed twice with 200 µL PBS. Subsequently, the remaining protein binding sites were blocked by adding 200 µL of blocking buffer (5% BSA/PBS per well) and incubating at 37°C for 2 hours. After blocking, the plates were washed thrice with PBS (200 µL each, five minutes per wash). Following washing, 100 µL of diluted detection antibody (H4R3me2s, 1:10000) added to each well, incubated for 2 hours at room temperature. After incubation, the plates were washed with PBS and 100 µL of secondary antibody conjugated (diluted, 1:5000) in blocking buffer was added immediately before use, followed by incubation at room temperature for 1-2 hours. The plates were then washed thrice with 200 µL PBS for five minutes each wash. Substrate reagent TMB (100 µL) was added to each well, and the plates were covered with a lid and foil, followed by incubation for 15-30 minutes. The reaction was stopped by adding 0.2 M H₂SO₄, and the resulting absorbance was measured at 450 nm.

3.2.8 Apoptosis and Cell cycle analysis through flow cytometry

Cells were seeded in a six-well plate at a density of 1.5 million cells per well and treated with varying concentrations (0.1 to 10 µM) of EGCG, EA, and their combination for 24 hours. After

incubation, cells were trypsinized and stained with Annexin V-fluorescein isothiocyanate (FITC) at a 1:100 dilution and propidium iodide (PI) at a concentration of 0.5 μ g/mL for 15 minutes at room temperature. The fluorescence intensities of Annexin V-FITC and PI were measured using a FACScan flow cytometer (Becton Dickinson, San Jose, CA, USA). The cell populations were gated as follows: Annexin V (+)/PI (-) cells were categorized as apoptotic, Annexin V (+)/PI (+) cells indicated cells in secondary necrosis, and Annexin V (-)/PI (+) cells were classified as necrotic. Data analysis was conducted using FlowJo software.

For cell cycle analysis, cells treated with the specified concentrations were trypsinized, fixed in 70% ethanol overnight at -20°C, and then stained with RNase-A ($100 \,\mu\text{g/mL}$) and Propidium Iodide (PI, $50 \,\mu\text{g/mL}$) for 15 minutes. Flow cytometric analysis was performed using a FACScan flow cytometer (Becton Dickinson, San Jose, CA, USA).

3.2.9 Acidic vesicular organelles (AVOs) formation assay

Acridine orange staining was employed to detect AVOs (Acidic Vesicular Organelles), a known hallmark of autophagy, following the method described previously [8,9]. Acridine orange (AO) is recognized for its facility to permeate cell membranes and organelles, and emits fluorescence throughout the cell excluding in acidic compartments like late autophagosomes, where it emits red fluoresces. This dual-color fluorescence indicates the acidification of autophagic vesicles during their maturation, reflecting an active autophagic process. The intensity of red fluorescence connects with the abundance of AVOs present in autophagic cells. After treating the cells with different concentrations of EGCG, EA, and their combination, they were incubated in fresh media with 5 μ g/mL acridine orange for 10 minutes at 37°C. Following incubation, the cells were analyzed using a fluorescent microscope to evaluate the formation of AVOs and the autophagic activity stimulated by the treatments.

3.2.10 Colony formation assay

To assess the effects of EGCG, EA, and their combination on MDA-MB-231 cells, a colony formation assay was conducted. Initially, 500 cells were seeded per 30 mm culture dish and allowed to adhere. Once attached, the cells were treated with different concentrations of EGCG, EA, and their combination $(0, 0.1, 1, \text{ and } 10 \,\mu\text{M})$ and incubated for 24 hours. After treatment, the media was replaced with serum-free media to prevent further cell growth, facilitating colony formation over time.

Visible colonies were subsequently observed. The media was carefully aspirated, and the dishes were washed with PBS to remove non-adherent cells. Each dish was then treated with 2-3 mL of a solution containing 6% glutaraldehyde and 0.5% crystal violet, followed by a 30-minute incubation. After incubation, the excess solution was discarded, and the dishes were gently rinsed with tap water before being air-dried at room temperature for 20 minutes.

The experiment was performed in triplicate, and the number of colonies was counted and recorded. The results, presented as a percentage relative to the control group, provided insights into the potential inhibitory effects of EGCG, EA, and their combination on colony formation, reflecting their impact on cell proliferation and survival.

3.3 Results

3.3.1 Virtual screening revealed top 14 interacting molecules to PRMT5:MEP50 and EZH2

Natural molecules extracted from medicinally significant plants, as reported in scientific literature, were meticulously evaluated during the ADMET (absorption, distribution, metabolism, excretion, and toxicity) analysis. This evaluation adhered to Lipinski's Rule of Five and Veber's rules to ensure the compounds met the necessary criteria. This screening ensured the selection of compounds with drug-like properties, resulting in the creation of a comprehensive ligand library. Each ligand was then prepared using the LigPrep tool, optimizing their structures for docking studies.

Subsequently, the pharmacophores for the PRMT5:MEP50 complex and the EZH2 (a member of PRC2 complex) were developed using the Schrödinger software suite. The pharmacophores represent the spatial arrangement of features necessary for molecular recognition by the target proteins. Once the pharmacophores were established, the ligands were docked to the target proteins using the Glide XP (extra precision) docking program, which predicts the binding affinity and interaction modes of the ligands with the protein targets. In total, from a chemical library of 1,200 natural molecules, 355 molecules were screened out through ADMET prediction and docked with the PRMT5 complex and EZH2 and identified top fourteen interacting molecules The docking results revealed several promising ligands, and the interaction profiles and docking scores of the top interacting molecules. The table 3.1 shows the top fourteen interacting molecules of PRMT5:MEP50 complex along with the known inhibitors SAHA, SAM, and SFG, as well as the known synthetic inhibitor EPZ015666. All

these 18 molecules details were listed in Table 3.1. Similarly, the docking study for the EZH2 (a member of PRC2 complex) identified the top fourteen potential ligands, with their interaction profiles and scores provided in Table 3.2. These results highlight the most promising natural compounds that could serve as potential inhibitors or modulators of these target proteins, which are implicated in various diseases.

Chemically, the molecules displayed a significant diversity among the classes of natural compounds, as illustrated in Figure 2.3.2. This diversity underscores the broad range of structural types within the natural molecules studied. Interestingly, both PRMT5 and EZH2 methyltransferases share a conserved methyltransferase domain, which is evolutionarily conserved. This similarity led to the identification of several molecules that could potentially interact with both methyltransferases. Most of the natural molecules found to interact with PRMT5 and EZH2 methyltransferases obeyed to the Lipinski's Rule of Five and Veber's rules during the ADME prediction analysis. However, there were exceptions, such as EGCG which showed a few violations of these rules. Despite these violations, the natural molecules with the highest docking scores were selected for further investigation due to their promising interactions with the target proteins.

Among the high-scoring molecules, EGCG and EA demonstrated notable interactions with both proteins. EGCG, a polyphenol found in green tea, exhibited strong interactions with the PRMT5 protein pharmacophore (as detailed in Table 3.1). On the other hand, EA, a phenolic compound, showed significant interactions with the EZH2 protein pharmacophore (as detailed in Table 3.2). These interactions were particularly noteworthy as they suggested a predictive and promising outcome from the virtual screening conducted in this study, as depicted in Figure 3.3.1. All docking interaction poses of the top 14 molecules were included in the appendix of the thesis (appendix-1). This dual interaction profile underscores the potential of these natural compounds to target both PRMT5 and EZH2 methyltransferases, offering a foundation for further experimental validation and drug development.

S.	Ligand	Chemical type	Docking score	Residues interacting with	Residues interacting with ligand
No			(kcal/mol)	ligand (Pi-Pi stacking)	(H-bond)
1	SAHA	Natural product (inhibitor)	-12.99	Lys393	Tyr334, Tyr324, Glu392, Cys449, Met420, Asp419, Glu435, Leu437, Glu444
2	SFG	SAM analogue (inhibitor)	-12.77	Lys393	Tyr324, Glu392, Asp419, Met420, Glu435, Glu444
3	SAM	Natural substrate	-12.60	Lys393	Asp419, Met420, Glu392, Tyr324, Glu435, Glu444,
4a	EGCG (4X60)	Flavonoid	-10.26	Lys333	Tyr324, Tyr334, Gly365, Leu437, Glu444, Pro314, Leu319
4b	EGCG (4X61)	Flavonoid	-9.02	Lys333	Leu312, Glu444, Ser310, Ser578, Phe327
4 b	EGCG (4X63)	Flavonoid	-10.62	Lys333	Gln309, Leu312, Tyr304, Phe577, Glu144, Ser578, Phe327
5a	EA (4X60)	Phenolic	-7.78	Lys393	Tyr324, Glu444, Glu-392
5 b	EA (4X61)	Phenolic	-7.37	Phe327	Phe580, Phe577
5c	EA (4X63)	Phenolic	-6.79	Phe327	Phe580, Phe577, Tyr304
6	Vorinostat	Known inhibitor	-11.21	Lys393	Tyr324, Glu444
7	EPZ015666	Known inhibitor	-10.02	Lys393	Met420, Glu435, Glu444
8	Eucalyptol	Terpenoid	-1.91		
9	Resveratrol	Polyphenol	-6.10		Gly365, Arg368, Ser578
10	Apicidin	Fungal metabolite	-4.61	Phe327	Glu444
11	Quercetin	Flavonoid	-3.20	Phe327	Phe580, Phe300
12	Capsaicin	Alkaloid	-4.87	Phe327	Glu444, Lys333, Ser578
13	Brazilin	Flavonoid	-7.43		Glu444, Glu309, Ser578, Glu435
14	Anethole	Flavonoid	-148	Phe327	Phe580
15	Eugenol	Phenylpropanoid	-3.41		Glu444
16	Gambogic acid	Xanthonoid	-3.27	Phe327	Tyr307, Ser310
17	Sulforaphane	Isothiocyanate	-4.61		Phe580, Asn239
18	Piperine	Alkaloid	-3.29		Pro314, Phe580

Table 3.1 Top interacting molecules & known substrates to humanPRMT5:MEP50 complex- This table lists the top interacting molecules and known substrates that have shown significant binding affinity to the human PRMT5:MEP50 complex, identified through molecular docking studies.

S. No	Ligand	Chemical type	Docking score (kcal/mol)	Residues interacting with ligand (Pi-Pi stacking)	Residues interacting with ligand (H-bond)
1a	Vorinostat (5HYN)	Known inhibitor	-6.69	Cys449	Glu392, Lys333, Tyr334, Glu328
1b	Vorinostat (4mi5)	Known inhibitor	-5.16		Leu678, Trp629, Asn693
2a	EA (5HYN)	Phenolic	-10.46		Trp624, Ser664, Ala622, Tyr728, Asp732
2b	EA (4mi5)	Phenolic	-8.29		Leu671, Phe670, Phe72, Ser667
3a	EGCG (5HYN)	Flavonoid	-9.07	Lys735	Ile109, Met110, Typ111, Trp624, Ala733, His689, Asn688, Arg685
3b	EGGC (4mi5)	Flavonoid	-7.05	Leu671	Ser669,Tyr731, Asn693, Trp629
4a	Resveratrol (5HYN)	Polyphenol	-4.06		Gly365, Arg368, Gly328, Ser578
4b	Resveratrol (4mi5)	Polyphenol	-6.02	Trp575	Phe577
5	Piperine	Alkaloid	-3.51		Met420, Lys393
6	Sulforaphane	Isothiocyanate	-3.66		Lys393
7	Anethole	Flavonoid	-2.22		Met420, Lys393
8	Apicidin	Fungal metabolite	-3.66	Phe327	
9	Capsaicin	Alkaloid	-4.66	Phe327	Lys333, Tyr334
10	Quercetin	Flavonoid	-4.71		Glu392, Glu444, Ser578, Lys333
11	Eucalyptol	Terpenoid	-2.86		Gly365
12	Eugenol	Phenylpropanoid	-3.41	Tyr324	Glu328, Arg368
13	Gambogic acid	Xanthonoid			
14a	Brazilin (5HYN)	Flavonoid	-8.08		Tyr324, Glu392, Glu444, Glu435
14b	Brazilin (4mi5)	Flavonoid	-7.92	Phe665	Met662, Ile109, Asn688

Table 3.2 Top interacting molecules & known substrates to human EZH2 complex- This table lists the top interacting molecules and known substrates that have shown significant binding affinity to the human EZH2 complex, identified through molecular docking studies.

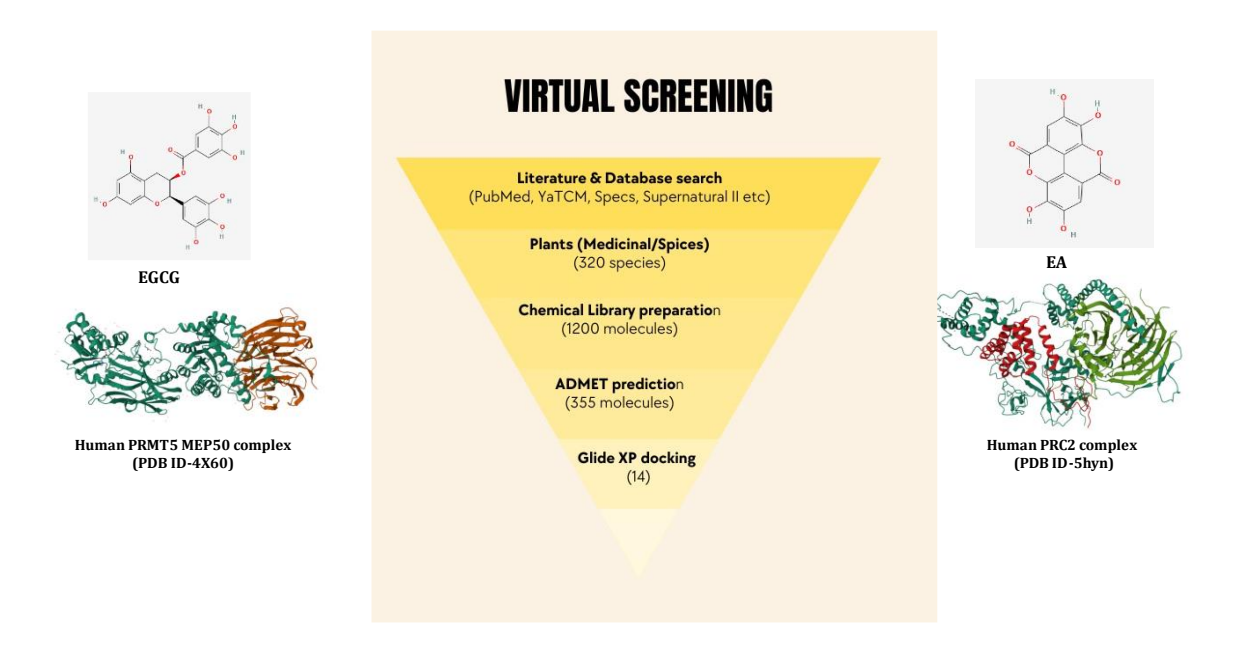


Figure-3.3.1 Schematic Flowchart of *In-Silico* **Screening Results-**This flowchart illustrates the in-silico screening process. Out of 1200 natural molecules analyzed for ADMET properties, 355 molecules were selected for docking studies with the human PRMT5:MEP50 complex and PRC2 (EZH2) complex. The screening identified two molecules that interacted with their respective pharmacophores, achieving the highest docking scores among all natural molecules tested.

3.3.2 Interaction of EGCG with PRMT5:MEP50 & EZH2 (Molecular docking)

The ligand-protein docking revealed that EGCG (Figure 3.3.2.1) was interacting with human PRMT5-MEP50 complex & EZH2. The binding pattern of EGCG was analyzed in all the three forms of structures of PRMT5-MEP50 (4X60, 4X61, 4X63) where ligand is SFG, SAM and SAHA respectively (Figure 3.3.2.2) and with EZH2 (5HYN, 4mi5) where ligand is SAHA and SET domain respectively (Fig2d-2e). As shown in the Figure 2, EGCG has similar interactions as SFG, SAM and SAH, 5HYN, & 4mi5. The SFG interacted with PRMT5 protein at the Tyr324, Glu392, Asp419, Met420, Glu435, Glu444 with H-bonds, and a π -cation interaction at Lys393 position. SAHA interacted with EZH2 protein at the Trp624, Ile109, Ala733, His689, Asn688 and Arg685. Interestingly, EGCG interacted within the same pocket involving a π -cation interaction at Lys 333 and at least five H-bonds with the residues (Tyr324, Tyr334, Gly365, Leu437, and Glu444) in the PRMT5 pharmacophore. Similarly, with 5HYN (EZH2), interacted with five hydrogen bonds (Trp624, Ile109, Ala733, Asn688 and His689), with 4mi5 Leu671, Asn698, Ser669 and Tyr731. The common interactions of EGCG all structural forms of PRMT5 (4X60, 4X61, 4X63) and EZH2 (5HYN, 4mi5) were tabulated in (Table 3.3).

(-)-Epigallocatechin-3-gallate (EGCG)

Figure-3.3.2.1- Chemical structure of Epigallocatechin-3-gallate (Mol wt. 458.372 g/mol, chemical formula: $C_{22}H_{18}O_{11}$

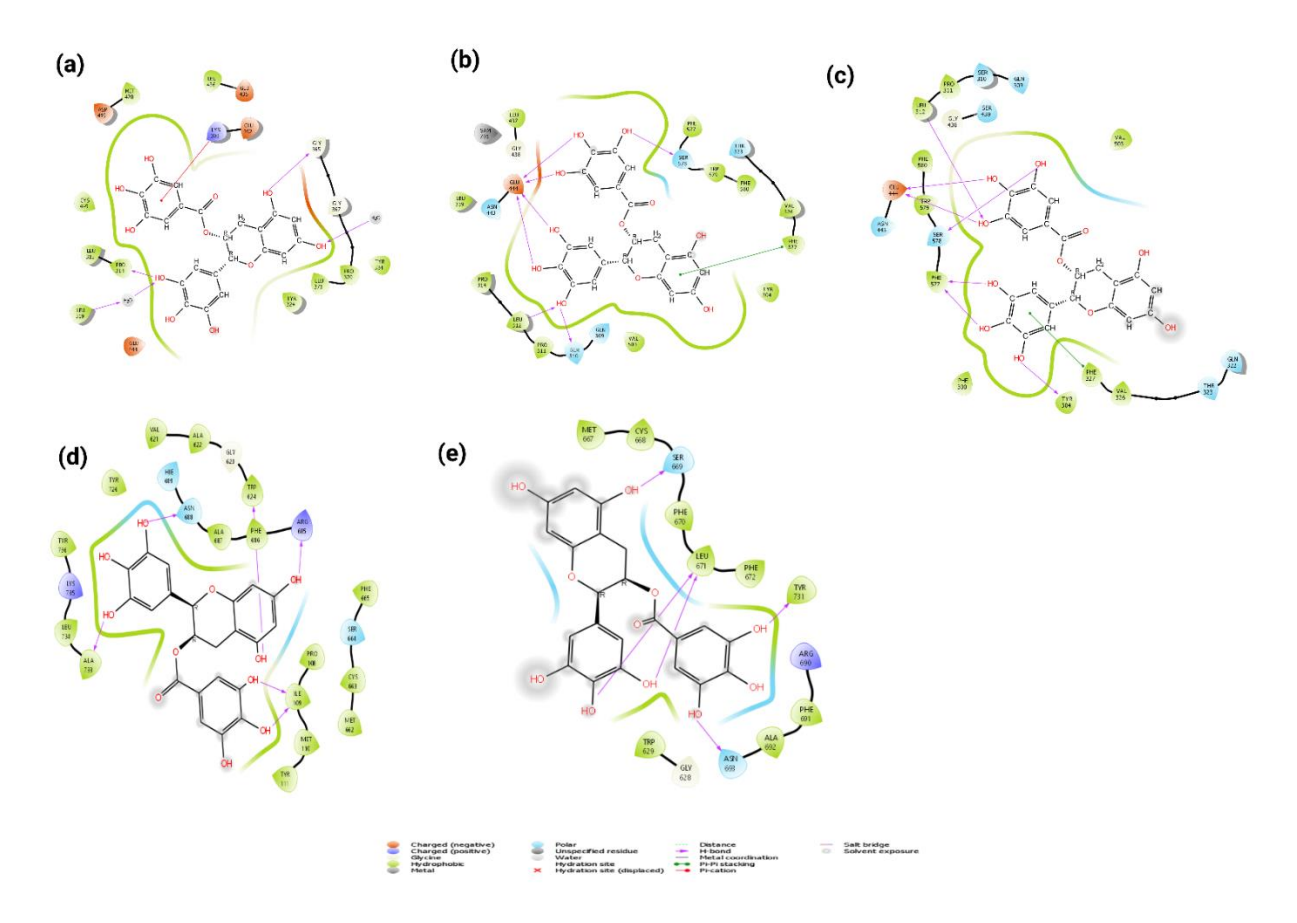


Figure-3.3.2.2- Interaction Profile of EGCG with Human PRMT5 and EZH2 Complexes-

Illustration of the interaction profiles of EGCG with the human PRMT5 complex and EZH2 complex. (a-c) Interaction profiles of EGCG with PRMT5 (PDB IDs: 4X60, 4X61, 4X63). The hydrogen bonds are represented by green dotted lines. The interacting amino acid residues and the ligand SFG are depicted using blue and black ball-and-stick models. Non-bonded interactions are indicated by residues with starbursts. (d-e) Interaction profiles of EGCG with EZH2 (PDB IDs: 5HYN, 4MI5). The ligands are positioned in the centre, with hydrogen bonds shown as purple arrows. The arrowheads indicate the H-bond donor-acceptor relationships. The π -cation interactions between EGCG, SFG, and the lysine side chain are marked with red arrows. Hydrogen bonds are shown in green dotted lines, and interacting amino acid residues, along with the ligand SFG, are displayed in blue and black ball-and-stick models. Non-bonded interactions are represented by residues with starbursts.

Table-3.3 The common interaction profiles of the EGCG with human PRMT5: MEP50 and EZH2

Ligand	XP	π- cation	Residues interacting with the ligand			
	G-score		H-bonding			
PRMT5						
Sfg	-12.776	Lys393	Tyr324, Glu392, Asp419, Met420, Glu435, Glu444,			
Sfg (LigPlot) Leu315, Tyr324, Lys333, Tyr334, Gly365, Ala366, Gly367, Pro370, Glu392, Lys393, Asn394, Ser418, Asp419, Met420, Arg421, Glu435, Leu436, Cys449						
EGCG (4X60)	-10.266	Lys333	Tyr324, Tyr334, Gly365, Leu437, Glu444, Pro314, Leu319			
SAM	-12.617	Lys393	Asp419, Met420, Glu392, Tyr324, Glu435, Glu444,			
SAM (LigPlot) Tyr334, Lys333, Gly365, Met420, Tyr324, Glu392, Arg421, Asp419, Cys449						
EGCG	-9.027	Lys333	Leu312, Glu444, Ser310, Ser578, Phe327			
(4X61)						
SAH	-12.992	Lys333	Tyr334, Tyr324, Glu392, Cys449, Met420, Asp419, Glu435, Leu437, Glu444			
SAH (LigPlot) Tyr334, Tyr324, Cys449, Lys333, Glu392, Asp419, Met420						
EGCG	-10.628	Lys333	Gln309, Leu312, Tyr304, Phe577, Glu144, Ser578,			
(4X63)			Phe327			
EZH2						
EGCG	-9.072	Lys 735	Ile109, Met110, Typ111, Trp624, Ala733, His689,			
(5HYN)			Asn688, Arg685			
EGCG (4mi5)	-7.543	Leu671	Ser669,Tyr731, Asn693, Trp629			

3.3.2.1 Molecular Dynamic Simulation Studies: Interaction of EGCG with PRMT5 and EZH2:

To assess the molecular stability of EGCG with PRMT5 and EZH2, molecular dynamics simulations were conducted, corroborating the docking study results. We examined the root mean square deviation (RMSD) and root mean square fluctuation (RMSF) over a 100 ns time frame. These analyses provided insights into the rigidity of the binding sites and the overall stability of both the ligand and PRMT5, which are crucial for pharmacokinetics. The backbone RMSD ranged between 1-3 Å, and the ligand RMSD correlated with the backbone RMSD. Additionally, the RMSF of the ligand remained within acceptable variations. The hydrogen bonding and hydrophobic π - π interactions were strong. Notably, Glu435 maintained a strong hydrogen bond with EGCG throughout the simulation (Figure 3.32.3), which is involved in peptide binding and is one of the stable bonds observed. More than 75% of the simulation time showed stable hydrophobic interactions involving Phe327, Leu364, and Gly365 (Figure 3.3.2.3). In the case of EZH2 binding, EGCG demonstrated less stability compared to its interaction with PRMT5. The RMSD and RMSF analyses over a 100 ns time course revealed fluctuations indicating lower stability of the EGCG-EZH2 complex. Despite these fluctuations, EGCG still maintained significant interactions with EZH2, though not as strong as with PRMT.

These results indicate that EGCG forms a stable and strong interaction with PRMT5, confirming its potential efficacy as a compound.

RMSD and RMSF of EGCG with PRMT5:MEP50 & EZH2

Protein-Ligand RMSD Protein-Ligand RMSD Residue Index Protein-Ligand RMSD Residue Index Protein-Ligand RMSD Protein-Ligand RMSD Residue Index Res

Figure 3.3.2.3: Root Mean Square Deviation (RMSD) and Root Mean Square Fluctuation (RMSF) Analysis of EGCG with PRMT5:MEP50 Complex and Enhancer of Zeste Homolog 2 (EZH2). This figure illustrates the structural stability and flexibility of the EGCG molecule when

Homolog 2 (EZH2). This figure illustrates the structural stability and flexibility of the EGCG molecule when bound to the PRMT5 complex and EZH2. The RMSD graph shows the time evolution of the deviations in the positions of the protein atoms from a reference structure over the course of the simulation, indicating the overall stability of the protein-ligand complexes. The RMSF graph depicts the average fluctuation of each residue from its mean position, providing insights into the flexibility and dynamic behavior of specific regions within the proteins when interacting with EGCG.

3.3.2.2 Surface Plasmon Resonance studies for EGCG with PRMT5:MEP50 and EZH2

A surface plasmon resonance (SPR) assay was conducted to assess the interaction between EGCG and PRMT5-MEP50, as well as EZH2. Recombinant PRMT5-MEP50 and EZH2 proteins were immobilized on the CM5 chip sensor surface, and sensograms illustrating the immobilization process are provided in (Figure 3.3.2.4). The Real-time bimolecular interaction analysis was employed to investigate the binding kinetics of EGCG with the immobilized PRMT5-MEP50 and EZH2 surfaces (Figure 3.3.2.5).

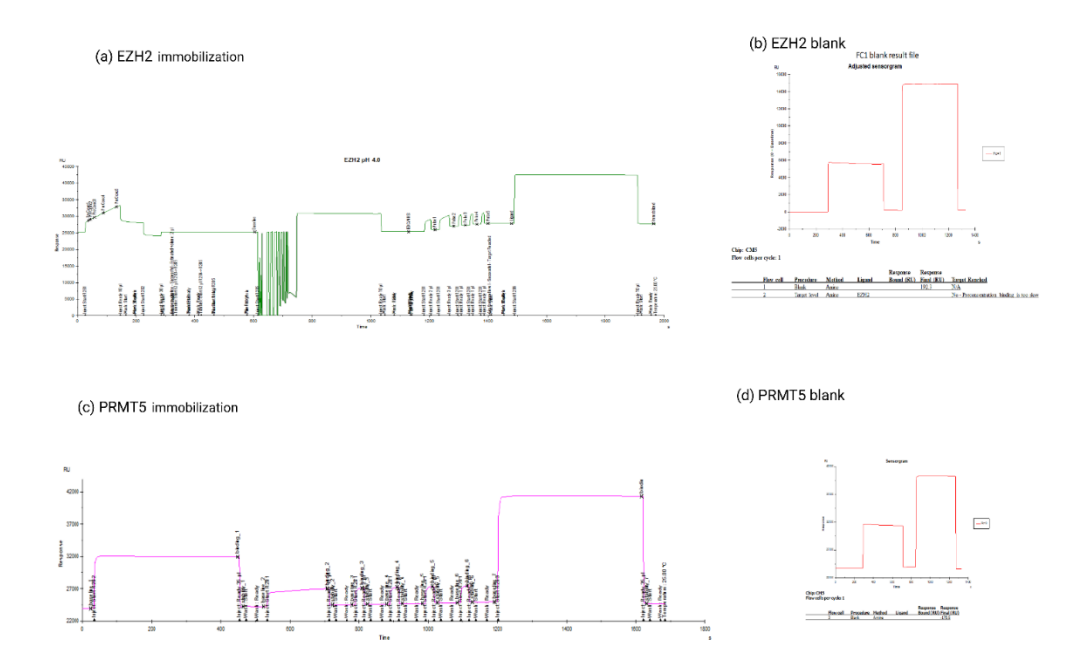


Figure 3.3.2.4: Surface Plasmon Resonance (SPR)- The sensorgram depicting the immobilization of PRMT5 and EZH2 on a CM5 sensor chip are shown in panels (a) and (c), respectively. Panels (b) and (d) illustrate the control experiments where blank injections were performed with EZH2 and PRMT5, respectively.

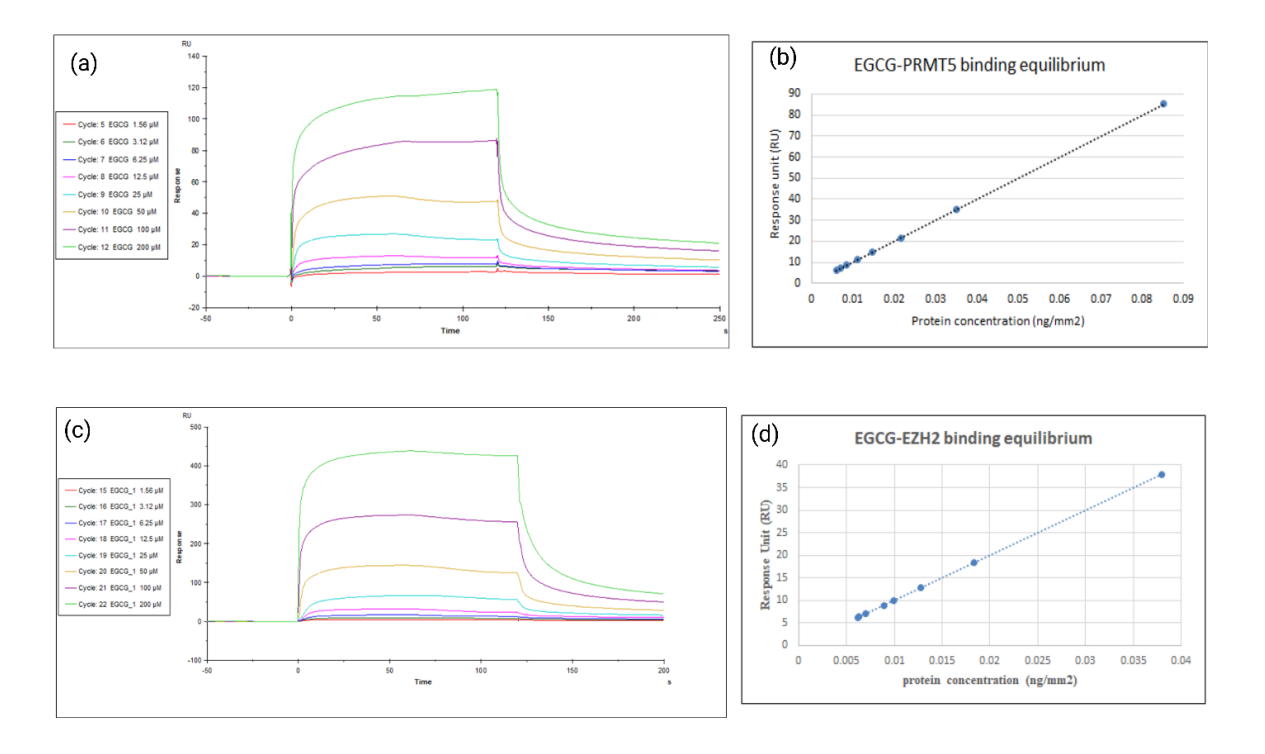


Figure 3.3.2.5: Surface plasmon resonance (SPR): The experiments were conducted to analyze the interaction of EGCG with PRMT5-MEP50 and EZH2 complexes on a CM5 sensor chip. Panel (a) shows the doseresponse sensorgram of EGCG with immobilized PRMT5-MEP50, while panel (b) displays the fitting of response versus concentration using BIAcore T200 Evaluation software version 2.0. Panel (c) presents the dose-response sensorgram of EGCG with immobilized EZH2, with panel (d) depicting the fitting of response versus concentration for EZH2 using the same software. The response units (RU) versus protein concentration plots were linear. The kinetic parameters obtained are as follows: for PRMT5-MEP50, the association constant (Ka) is 2.07E+02 (M^-1 s^-1), the dissociation constant (kd) is 3.61E-03 (s^-1), and the equilibrium dissociation constant (KD) is 1.74E-05 M. For EZH2, the Ka is 82.78 (M^-1 s^-1), kd is 3.63E-03 (s^-1), and KD is 4.39E-05 M.

The results indicated that EGCG exhibited strong binding affinity in the nanomolar concentration range (200-1.56 nM) for both PRMT5-MEP50 and EZH2 proteins. The equilibrium dissociation constants (KD) were determined as 1.74E-05 M and 4.39E-05 M for EGCG with PRMT5-MEP50 and EZH2, respectively. The response versus concentration graph showed a linear relationship (Figure 3.3.2.5), Analysis of the association constant (ka) and dissociation constant (kd) revealed that EGCG has a higher affinity for PRMT5-MEP50 than for EZH2, consistent with the findings from molecular docking studies.

3.3.3. Impact of EGCG on growth of multiple cancer cell lines

The study included human cancer cell lines DU-145 (prostate), A549 (lung), HeLa (cervix), Hep G2 (liver), MCF7 (breast), MDA-MB-231 (breast), PC-3 (prostate), and HEK293 (human embryonic kidney). Cells were treated with varying concentrations of EGCG for 24 and 48 hours, and cell viability was assessed to determine the IC50 values (Figure 3.3.2.6).

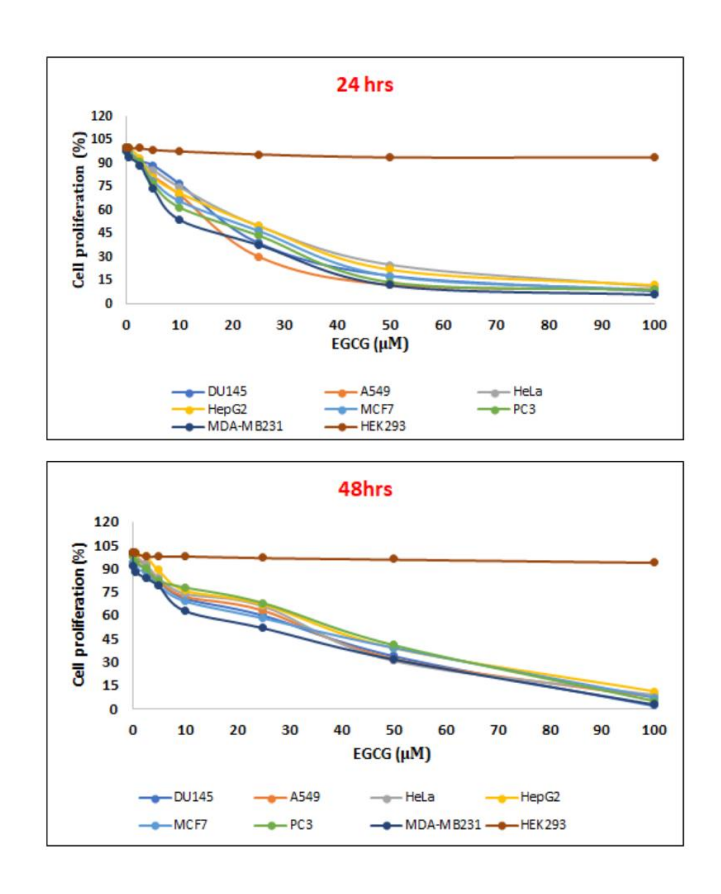


Figure 3.3.2.6: Impact of EGCG on human malignant cell lines: Various human cancer cell lines, including DU-145 (prostate), A549 (lung), HeLa (cervix), Hep G2 (liver), MCF7 (breast), MDA-MB-231 (breast), PC-3 (prostate), and HEK293 (human embryonic kidney), were exposed to different concentrations of EGCG for 24 hours (top panel) and 48 hours (bottom panel) to assess cytotoxicity. IC50 values were calculated and tabulated.

MDA-MB-231 cells were incubated with indicated concentrations of EGCG for 24 hours to assess the levels of catalytic products of PRMT5 and EZH2, specifically H4R3me2s and H3K27me3. Results indicated a significant decrease in H4R3me2s and H3K27me3 levels, particularly at 10 μ M concentration, compared to untreated cells, while the protein levels of PRMT5, EZH2, H4, and H3 remained unchanged. β -actin was used as a loading control (Figure 3.3.2.7 a-b). *In-vitro* methylation assays using PRMT5-MEP50 and EZH2 validated the methylation of H4 and H3 through ELISA. Pre-incubation of PRMT5-MEP50 and EZH2 with EGCG (1 μ M, 10 μ M) resulted in a dose-dependent decrease in symmetrical dimethylation of the third arginine of histone H4 and trimethylation of lysine 27 on histone H3 (Figure 3.3.2.7 c), indicating strong inhibition of PRMT5 and EZH2 activities by EGCG.

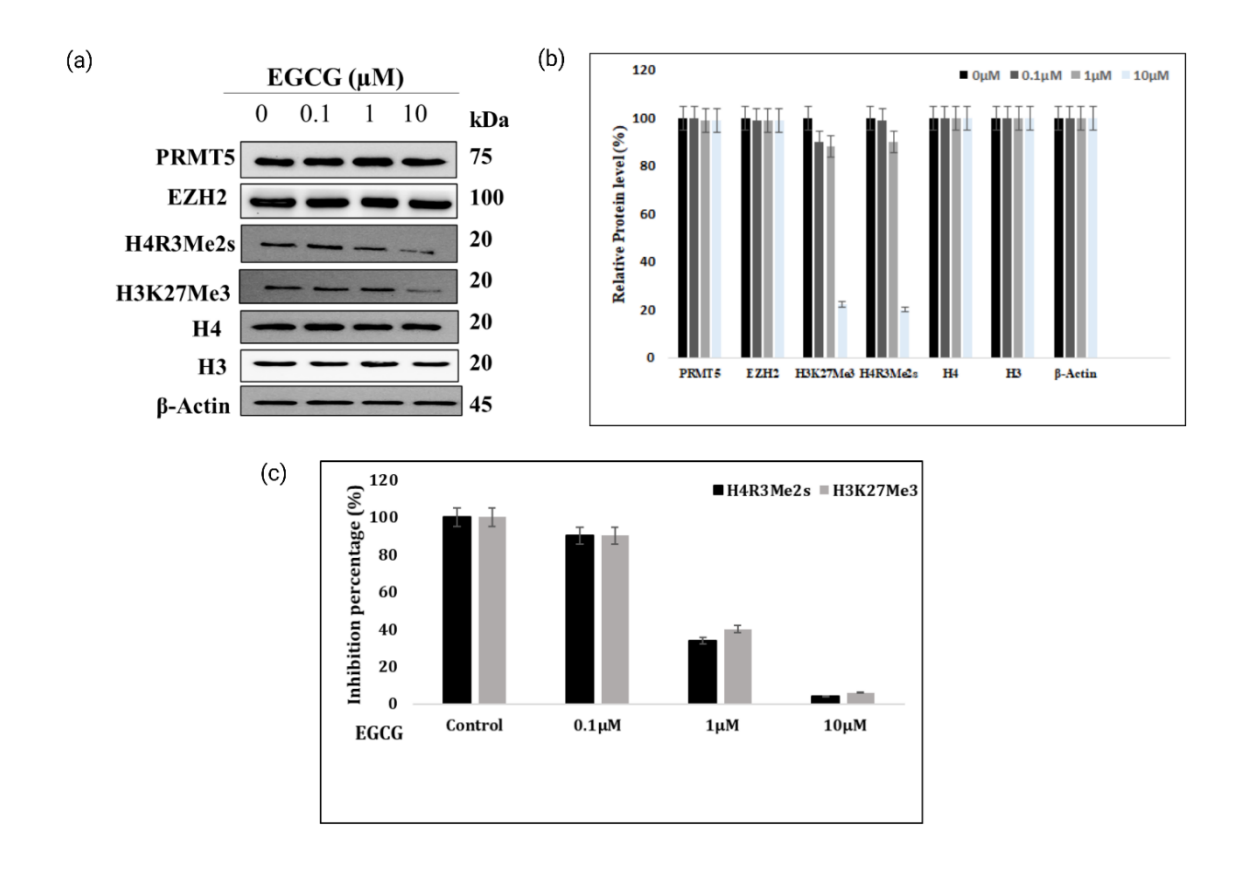


Figure 3.3.2.7: Impact of EGCG on methylation marks: MDA-MB231 cells were treated with increasing concentrations of EGCG (0.1, 1, 10 μ M) for 24 hours. Protein lysates were prepared as described in the methods section and analyzed for levels of H4R3me2s and H3K27me3 using immunoblotting. β-actin served as the loading control. (a) Western blots depict the levels of H4R3me2s and H3K27me3. (b) Protein intensity graphs illustrate the quantification of immunoblotting results. (c) ELISA was performed to assess in-vitro methylation using EZH2 and PRMT5-MEP50 enzyme complexes with histones as substrates.

The trypan blue dye exclusion assay supported the MTT assay, showing a reduction in viable cell numbers with increasing concentrations of EGCG (Figure 3.3.2.8). AO-EtBr double staining revealed crescent-shaped or granular early-stage apoptotic cells in MDA-MB-231 cells

treated with EGCG for 24 hours, whereas no significant apoptosis was observed in the control group (Figure 3.3.2.8a). These findings were corroborated by trypan blue dye exclusion assay and MTT assays (Figure 3.3.2.8b). In colony formation assays, EGCG dose-dependently reduced colony formation compared to the control group (Figure 3.3.2.8c-d), further supporting EGCG's inhibitory effects on PRMT5 and EZH2 activities in vitro.

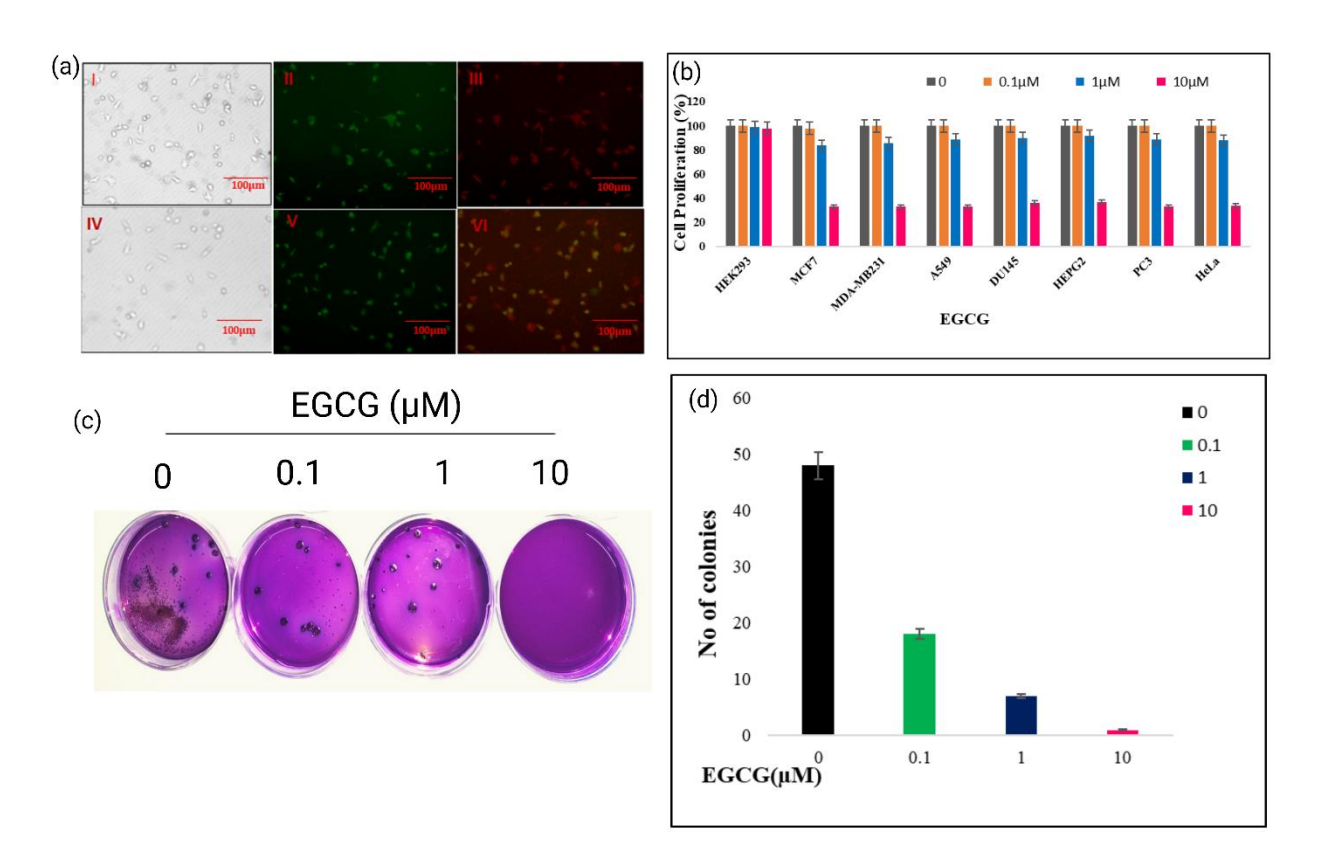


Figure 3.3.2.8: Impact of EGCG on cell proliferation: MDA-MB-231 cells were treated with varying concentrations of EGCG $(0, 0.1, 1, \text{ and } 10 \, \mu\text{M})$, and in-vitro assays were conducted to assess the effects. (a) AO/EtBr assay: MDA-MB-231 cells treated with EGCG for 24 hours were subjected to double staining with ethidium bromide (EB) and acridine orange (AO). Viable cells emitted green fluorescence (AO), while necrotic cells showed predominant red fluorescence (EB) under a fluorescent microscope. (b) Trypan blue dye exclusion assay: After 24 hours of EGCG treatment, DU-145, A549, HeLa, Hep G2, MCF7, MDA-MB-231, PC-3, and HEK293 cells were incubated with Trypan Blue solution. Viable cells excluded the dye, remaining unstained, while non-viable cells absorbed the dye, appearing blue. Cell viability was assessed by counting cells under a microscope, and the results were tabulated and plotted. (c, d) Colony formation assay: 500 cells were seeded and treated according to experimental conditions. After incubation, colonies were fixed, counted, and compared between control and treated groups to evaluate changes in clonogenic potential, providing insights into altered cell survival and proliferation.

3.3.3.1 Effect of EGCG on Apoptosis & Cell cycle

To assess the effect of EGCG on inducing apoptosis in breast cancer cells, we treated MDA-MB-231 cells with increasing concentrations (0, 0.1, 1, and 10 µM) of EGCG for 24 hours. The cells were then stained with Annexin V/PI, and the percentage of apoptotic cells was

determined using flow cytometry. FACS analysis indicated that as the concentration of EGCG increased, the cells progressively entered the late apoptosis stage (Figure 3.3.2.9a-d & i). Additionally, to investigate whether EGCG influences cell cycle progression, we performed flow cytometry to examine cell cycle distribution and analyzed the phases of the cell cycle (Figure 3.3.2.9: e-h & j). The cell cycle analysis revealed that EGCG treatment induced G0/G1 arrest in a dose-dependent manner at concentrations of 1 μ M and 10 μ M compared to the untreated control.

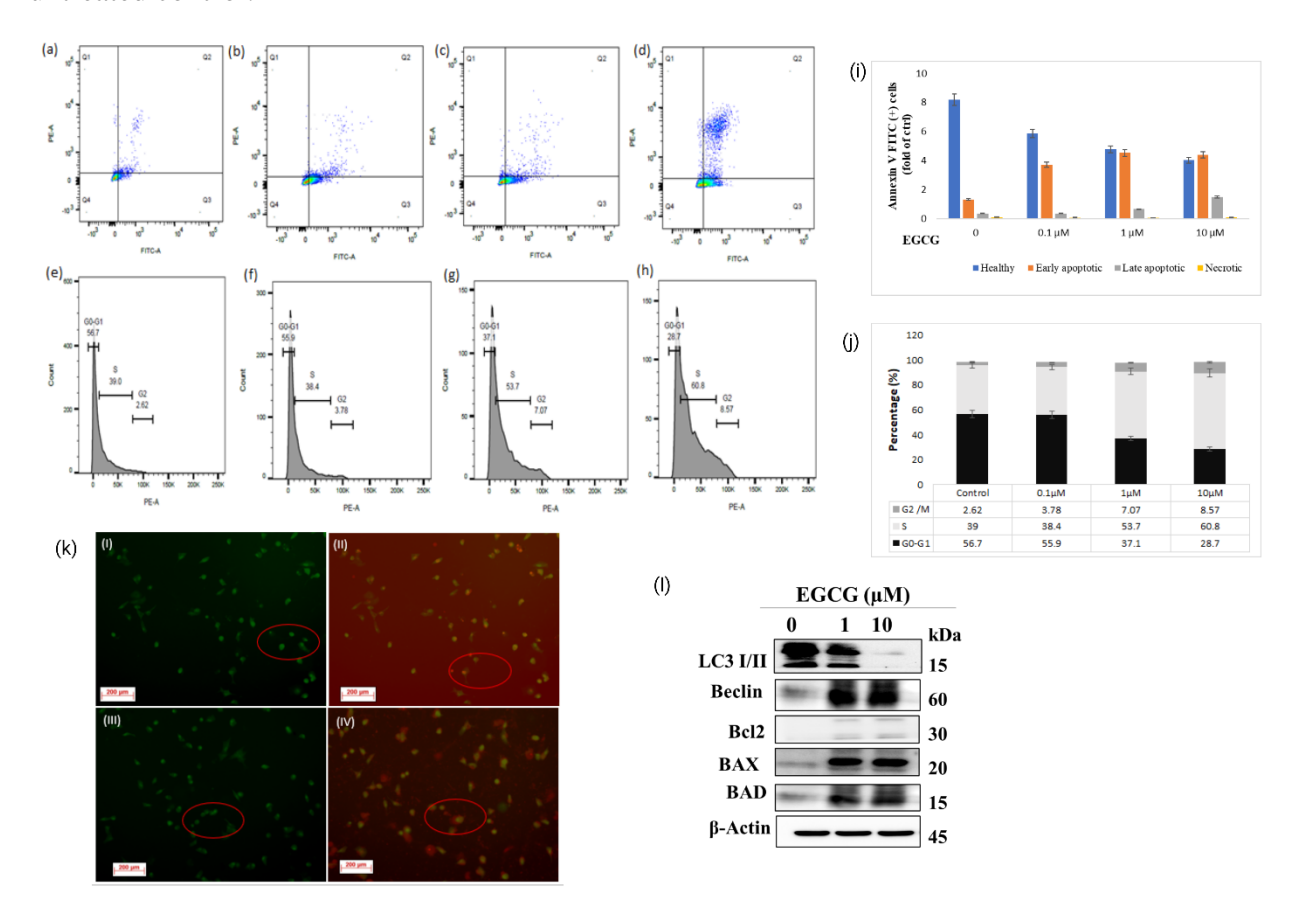


Figure 3.3.2.9: EGCG Induces Apoptosis and Autophagy in Breast Cancer Cells: MDA-MB231 cells treated with EGCG for 24 hours were stained with Annexin V/propidium iodide (PI), and the percentage of apoptotic cells was determined using flow cytometry. The top panel (a-d) shows the flow cytometry analysis of MDA-MB231 cells following EGCG treatment. The bottom panel (e-h) displays cell cycle analysis of MDA-MB231 cells after 24 hours of EGCG treatment. EGCG Induces Autophagy in Breast Cancer Cells: (k) EGCG treatment led to the formation of acidic vesicular organelles in MDA-MB231 cells. (l) Western blot analysis detected LC3 I/II expression in EGCG-treated MDA-MB231 cells. Western blot analysis examined the expression of Beclin-1, BCl2, Bax, and Bad proteins in EGCG-treated MDA-MB231 cells.

3.3.3.2 EGCG induced autophagy in MDA-MB-231 cells

The AO-EtBr assay indicated the presence of apoptotic cells characterized by crescent-shaped or granular morphology. To confirm whether the appearance of granular cells was indicative of apoptosis-mediated autophagy, we assessed the formation of Acidic Vesicular Organelles

(AVOs) following EGCG treatment. AVO formation serves as an indicator of autophagy and was examined using AO (Acridine Orange) staining. EGCG-treated cells exhibited red fluorescent spots, whereas control cells predominantly displayed green cytoplasmic fluorescence (Figure 3.3.2.9k).

Furthermore, we investigated whether EGCG's inhibition affected autophagy-mediated cell death in MDA-MB231 cells by evaluating microtubule-associated protein light chain 3 (LC3), a well-known autophagy marker. Our findings demonstrated that EGCG induced a dose-dependent transition of LC3 (Figure 3.3.2.91). Additionally, to confirm the induction of autophagy, we examined the expression of Beclin-1 and members of the BCL family (BCL2, BAX, and BAD) (Figure 3.3.2.91).

3.4 Interaction of EA with PRMT5 and EZH2

To investigate the interaction between EA (Figure 3.4) and the proteins EZH2 and the PRMT5 complex, we conducted molecular docking studies. These studies assessed the binding patterns of EA across three different structural forms of the PRMT5 complex (4X60, 4X61, 4X63), which were previously reported with the ligands SFG, SAM, and SAHA, respectively. For EZH2, the structures 5HYN and 4MI5 were examined with their reported ligands, the H3K27 peptide, and the SET domain. As shown in Figure 3.4.1, the ligand SFG in the PRMT5 structure formed hydrogen bonds with Tyr324, Glu392, and Glu444, along with a π -cation interaction at Lys393. Similarly, EA's interaction with the PRMT5 complex involved a π -cation interaction at Lys393 and three hydrogen bonds with Tyr324, Glu392, and Glu444 within the PRMT5 binding site. For EZH2, the docking study revealed that EA exhibited strong binding affinity with the 5HYN structure, showing a binding energy of -10.46 kcal/mol and forming at least five hydrogen bonds with residues Trp624, Ser664, Ala622, Tyr728, and Asp732. When docked with the 4MI5 structure, EA interacted with residues Leu671, Phe670, Phe72, and Ser667. The common interactions of EA with all structural forms of PRMT5 (4X60, 4X61, 4X63) and EZH2 (5HYN, 4MI5) are summarized in Table 3.4.

Structure of Ellagic acid

Figure 3.4: Chemical structure of EA (Mol wt. 302.19 g/mol, chemical formula: C14H6O8

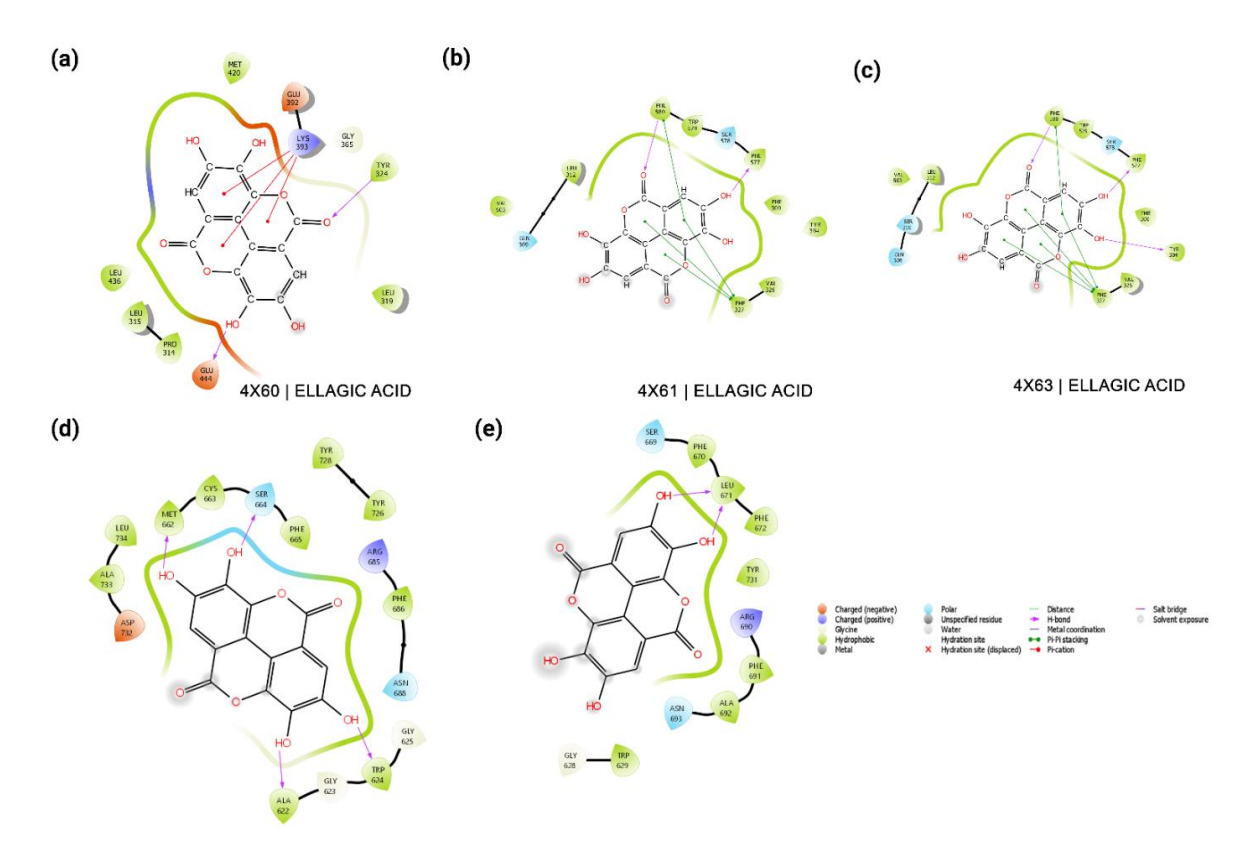


Figure 3.4.1: Interaction profiles of EA with the human EZH2 and PRMT5: MEP50 complex were analyzed. (a-c) Interaction details with the PRMT5: MEP50 complex (PDB IDs: 4X60, 4X61, 4X63) revealed specific hydrogen bonds between EA and amino acid residues, indicated by green dotted lines. The interactions are visualized using a blue/black ball-and-stick model for EA and the ligand SFG. Non-bonded interactions are denoted by starbursts adjacent to the residues. (d-e) In the case of the EZH2 complex (PDB IDs: 5HYN and 4MI5), EA's binding orientation and hydrogen bonding interactions are highlighted. Hydrogen bonds are represented by purple arrows, with arrowheads indicating the direction of donor-acceptor interactions. A significant π -cation interaction involving EA and the lysine side chain is depicted by a red arrow. Like the PRMT5 interactions, EA, and the ligand SFG are shown using a blue/black ball-and-stick model, with non-bonded interactions indicated by starbursts.

Table 3.4: Interaction profiles of EA with human EZH2 and PRMT5 complexes were examined using various protein structures, specifically 5HYN and 4MI5 for EZH2, and 4X60, 4X61, 4X63 for PRMT5. Molecular docking analyses were performed with these complexes. Additionally, the GlideXP docking scores of EA, with SFG, SAM, and SAHA were evaluated and are presented.

Ligand	XP	π - cation	Residues interacting with the ligand			
	G-score		H-bonding			
PRMT5						
Sfg	-12.77	Lys393	Tyr324, Glu392, Asp419, Met420, Glu435, Glu444,			
Sfg (LigPlot)	Sfg (LigPlot) Tyr324, Lys333, Tyr334, Gly365, Glu392, Asp419, Met420, Glu435, Cys449					
EA(4X60)	-7.78	Lys393	Tyr324, Glu444, Glu392,			
SAM	-12.61	Lys393	Asp419, Met420, Glu392, Tyr324, Glu435, Glu444,			
SAM (LigPlot) Tyr334, Lys333, Gly365, Met420, Tyr324, Glu392, Arg421, Asp419, Cys449						
EA (4X61)	-7.37	Phe327	Phe580, Phe577			
SAHA	-12.99	Lys333	Tyr334, Tyr324, Glu392, Cys449, Met420, Asp419, Glu435, Leu437, Glu444			
SAH (LigPlot) Tyr334, Tyr324, Cys449, Lys333, Glu392, Asp419, Met420						
EA (4X63)	-6.79	Phe327	Phe580, Phe577, Tyr304			
EZH2						
EA(5HYN)	-10.46		Trp624, Ser664, Ala622, Tyr728, Asp732			
EA (4mi5)	-8.29		Leu671, Phe670, Phe72, Ser667			

3.4.1 Molecular Dynamics Simulation Results for EA with PRMT5 and EZH2:

To understand the molecular stability of EA with PRMT5:MEP50, molecular dynamics simulations were conducted, supporting the docking study results. We analyzed RMSD and RMSF over a 100 ns time course, this provided insights into the rigidity of the binding sites and the overall stability of both the ligand and the protein complex. The RMSD of the backbone ranged between 1-3Å, with EA showing stability only at certain times. The RMSD of the ligand correlated with the backbone RMSD, with the RMSF of the ligand remaining within acceptable changes, indicating overall stability of the protein. For EA, the ligand-PRMT5 complex was stable. However, the contact of residues with the ligand was relatively weaker compared to EGCG. Hydrophobic π interactions with Phe327 were stable for over 60% of the simulation time. Additionally, Phe300 and Tyr304 frequently contacted the ligand. These findings suggest that while EA forms a stable complex with PRMT5, its interactions are slightly weaker than those of EGCG. In the case of EZH2 binding, EA exhibited greater stability compared to EGCG. This was reflected in the RMSD and RMSF analyses, where EA demonstrated more consistent stability over the 100 ns time course. The interactions with EZH2 were strong,

indicating that EA forms a stable and effective complex with EZH2, surpassing the stability observed with EGCG.

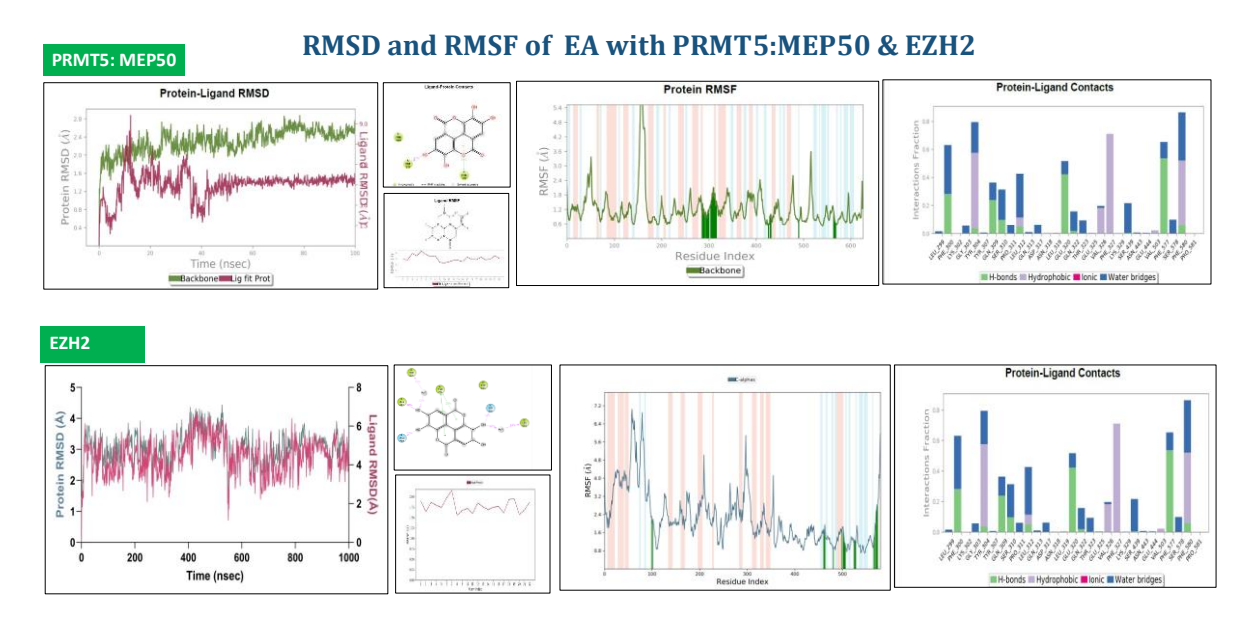


Figure 3.4.2: Molecular dynamics simulations were conducted to assess the stability of EA with PRMT5:MEP50 & EZH2. RMSD and RMSF analyses over a 100 ns simulation period provided insights into the rigidity of the binding sites and overall complex stability. The backbone RMSD ranged from 1 to 3 Å, indicating moderate stability of the protein-ligand complex. EA showed intermittent stability over the simulation time, correlating with the backbone RMSD. The RMSF of EA remained within acceptable limits, suggesting consistent stability of the ligand within the protein environment. Specific interactions, such as hydrophobic π interactions with Phe327 and frequent contacts with Phe300 and Tyr304 residues, were observed throughout the simulation, albeit weaker compared to interactions observed with EGCG. In comparison, EA exhibited greater stability in binding with EZH2 than EGCG, as evidenced by more consistent RMSD and RMSF profiles over the simulation period. These findings highlight EA's potential as a stable and effective inhibitor of EZH2, surpassing the stability observed with EGCG.

3.4.2 Binding study of EA with PRMT5:MEP50 and EZH2 by Surface Plasmon Resonance

SPR Analysis of EA Binding Affinity with EZH2 and PRMT5: SPR was employed to measure the binding affinity of EA with EZH2 and PRMT5. Recombinant EZH2 and PRMT5-MEP50 were immobilized on a CM5 sensor chip (Figure 3.3.2.4). Real-time bimolecular interaction analysis was conducted to evaluate the interaction and affinity of EA with these proteins. Binding kinetics were assessed by introducing varying concentrations of the ligand over the immobilized protein surfaces (Figure 3.3.2.12a & c).

The results indicated that EA exhibited strong binding affinity in the micromolar concentration range (200-1.56 nM) with both PRMT5-MEP50 and EZH2. The equilibrium dissociation constant (KD) values, representing the strength of biomolecular interactions, were found to be 3.28E-06 M for EZH2 and 6.54E-05 M for PRMT5-MEP50. The response versus concentration

plots demonstrated linearity (Figure 3.3.2.12b & d). Further analysis of the association constant (ka) and dissociation constant (kd) revealed that EA had a higher affinity for EZH2 compared to PRMT5, which is consistent with the molecular docking study results.

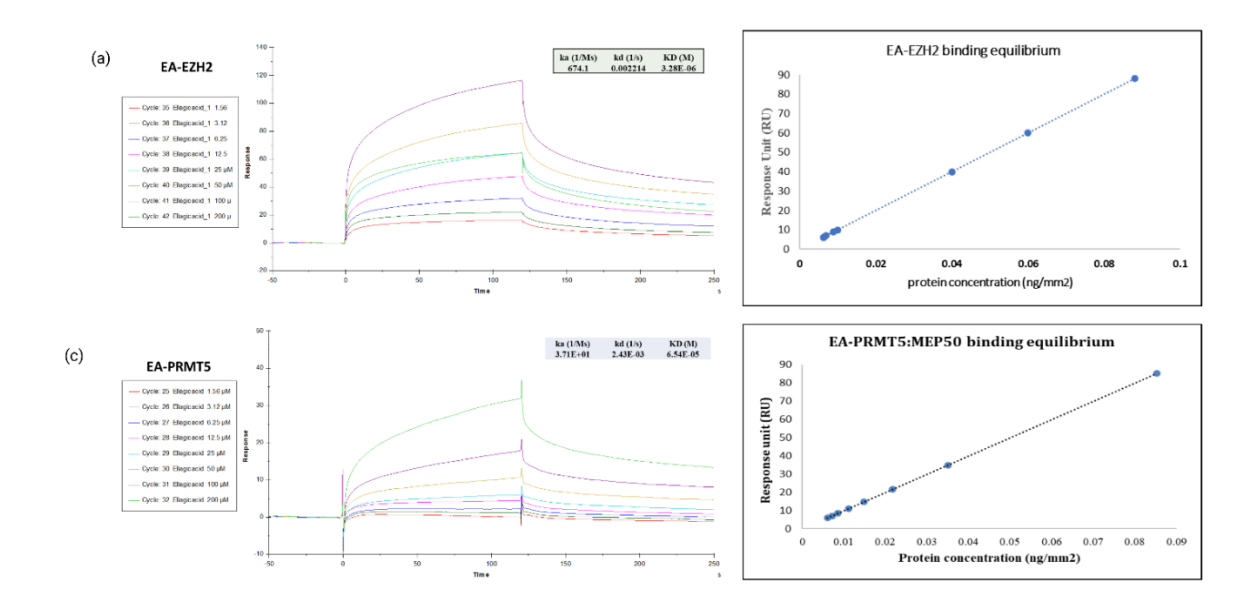


Figure 3.4.3: Surface Plasmon Resonance Analysis was performed to investigate the interaction of EA with EZH2 and the PRMT5 complex using a CM5 sensor chip. (a) Dose-response sensorgram for EA interacting with immobilized EZH2. (b) Fitting of response and concentration data using BIAcore T200 Evaluation software version 2.0. (c) Dose-response sensorgram for EA with immobilized PRMT5. (d) Fitting of response and concentration data for this interaction using the same software. The plot of response units (RU) versus protein concentration demonstrated a linear relationship. The determined kinetic parameters are as follows: For EA with EZH2: association rate constant (ka) = 674.1, dissociation rate constant (kd) = 0.002214, equilibrium dissociation constant (KD) = 3.28E-06. For EA with PRMT5:MEP50: association rate constant (ka) = 37.1, dissociation rate constant (kd) = 0.00243, equilibrium dissociation constant (KD) = 6.54E-05.

3.4.3 Inhibition of EA on growth of multiple cancer cell lines

In this study, a range of human cancer cell lines were utilized, including MCF7 and MDA-MB-231 (breast cancer), DU-145 and PC-3 (prostate cancer), A549 (lung cancer), HeLa (cervical cancer), Hep G2 (liver cancer), and HEK293 (human embryonic kidney). The cells were exposed to varying concentrations of EA for 24 and 48 hours, and cell viability was measured to determine the IC50 value (Figure 3.4.4). The results revealed a significant reduction in the levels of H3K27me3 and H4R3me2s, particularly at a concentration of 10 μ M, compared to untreated cells. However, the protein levels of EZH2, PRMT5, H3, and H4 remained mostly unchanged (Figure 3.4.5a-b), with β -actin serving as the loading control. Furthermore, *in vitro* methylation assays of H3 and H4, followed by ELISA (Figure 3.4.5c), demonstrated a dosedependent decrease in H3K27me3 and H4R3me2s at concentrations of 1 μ M and 10 μ M.

AO-EtBr double staining indicated the presence of early-stage apoptotic cells, identifiable by their crescent-shaped or granular morphology, in MDA-MB-231 cells treated with EA for 24 hours. In contrast, the control group showed no significant apoptosis (Figure 3.4.6a). This finding was corroborated by the results from the trypan blue dye exclusion assay and MTT assays (Figure 3.4.6b). Additionally, the colony formation assay showed a dose-dependent reduction in colony formation in the EA-treated group compared to the control group (Figure 3.4.6c-d). Collectively, these *in vitro* assays demonstrated that EA effectively inhibits the activity of EZH2 and PRMT5.

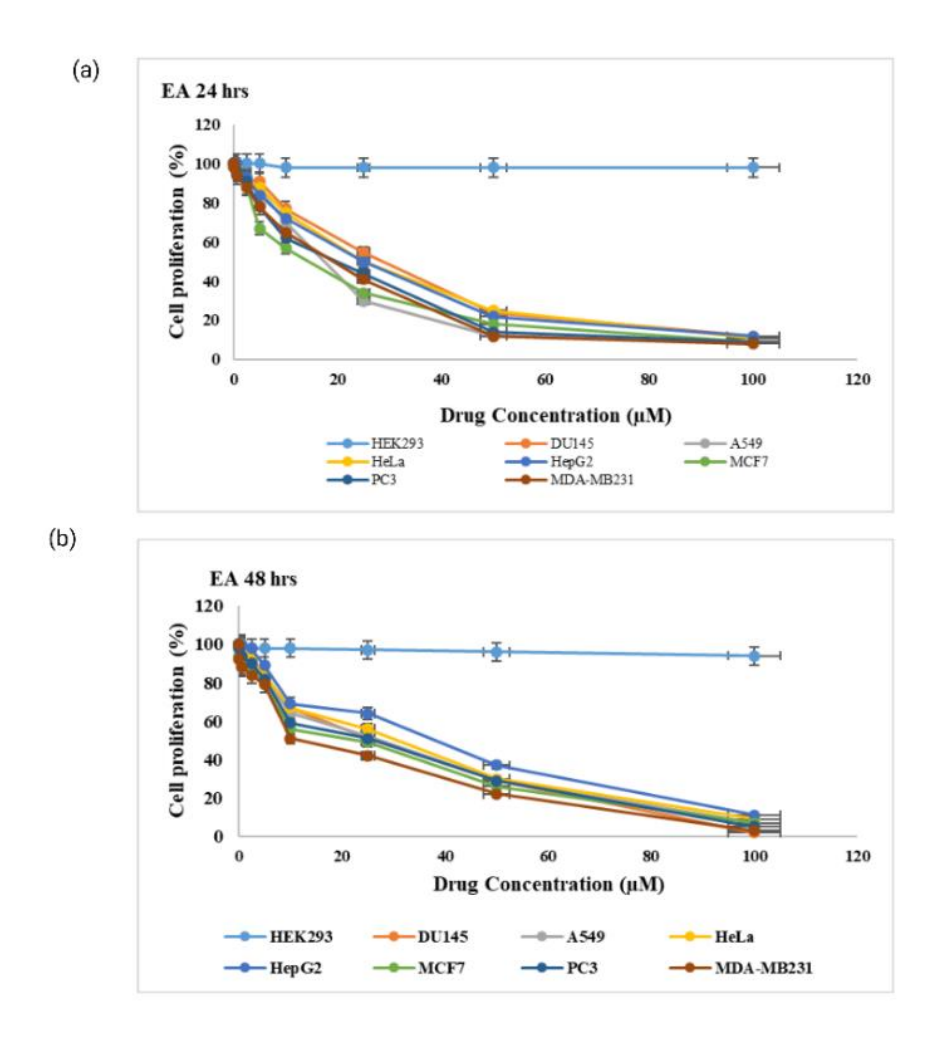


Figure 3.4.4: Impact of EA on Human Cancer Cell Lines: Various human cancer cell lines, including MCF7 (breast), MDA-MB-231 (breast), Du-145 (prostate), A549 (lung), Hep G2 (liver), HeLa (cervix), PC-3 (prostate), and HEK293 (human embryonic kidney), were treated with different concentrations of EA. Cytotoxicity was assessed, and IC50 values were determined and tabulated. The top panel (a) shows results for EA treatment over 24 hours, while the bottom panel (b) shows results for EA treatment over 48 hours.

.

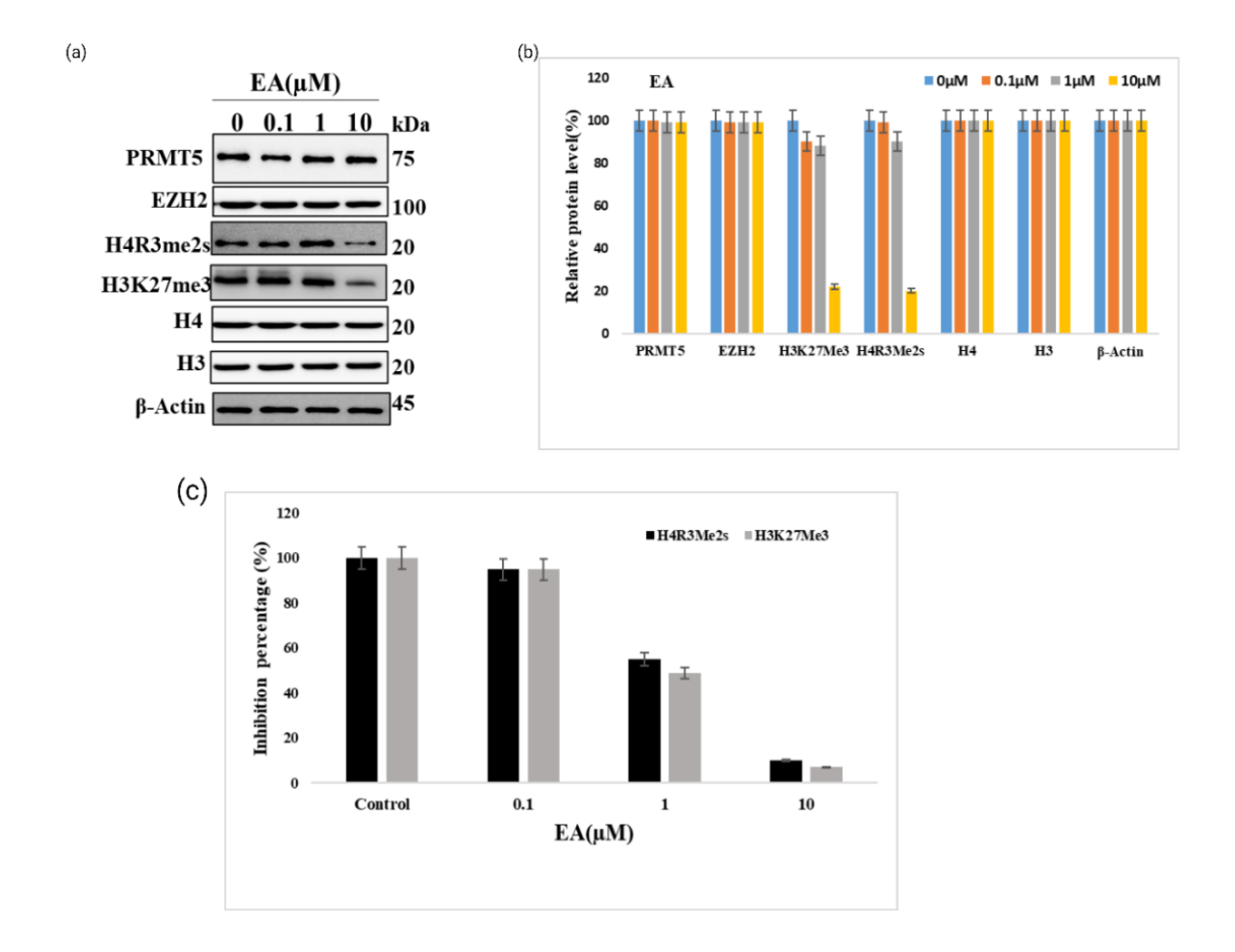


Figure-3.4.5: Effect of EA on H3K27me3 and H4R3me2s Methylation Marks. MDA-MB231 cells were treated with increasing concentrations of EA (0.1, 1, 10 μM) for 24 hours. Protein lysates were then prepared as per the described methods and analyzed for H4R3me2s and H3K27me3 levels via immunoblotting, using β-actin as a loading control. (a) Western blots showing the methylation levels. (b) Graphs depicting the intensity of the proteins from the western blots. (c) *In vitro* methylation assays were performed as described in the methods, and methylation levels were quantified using ELISA. These assays utilized EZH2 and PRMT5-MEP50 enzyme complexes with histones as substrates.

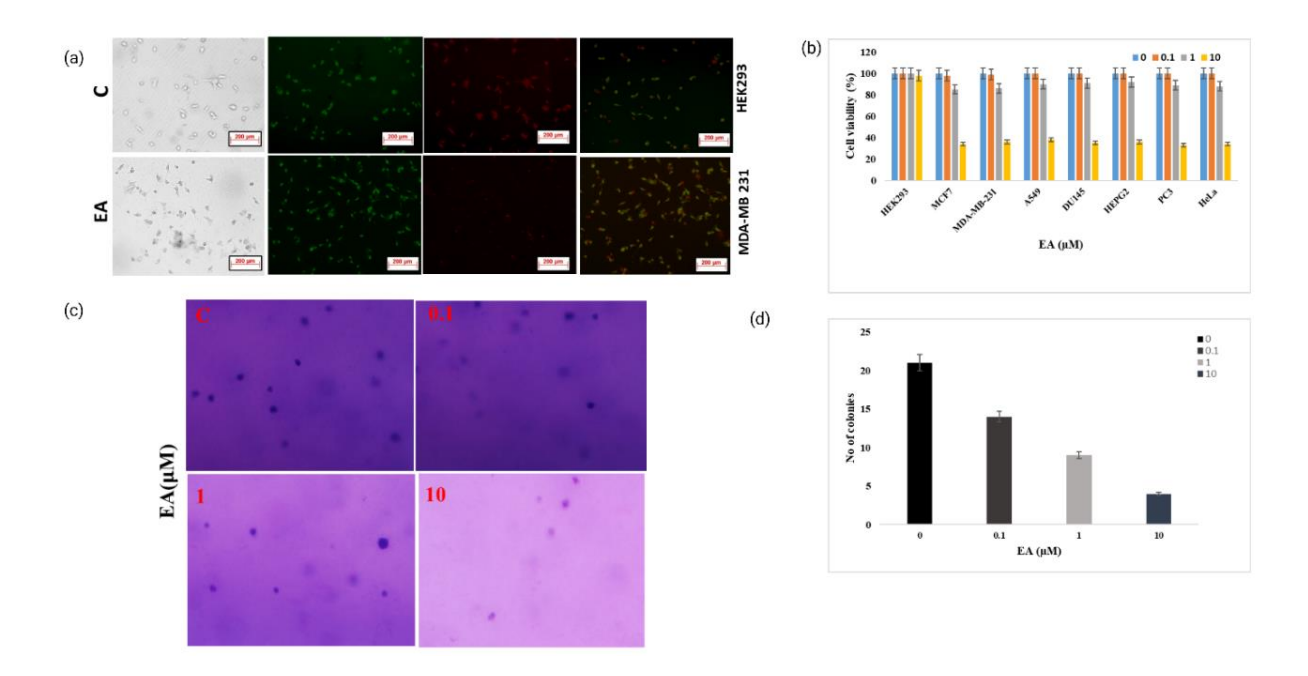


Figure-3.4.6: Effect of EA on Cellular Proliferation Dynamics: Cells were treated with EA at various concentrations and durations, followed by multiple cell-based assays to assess the impact. (a) AO/EtBr assay: Cells were double-stained with ethidium bromide and acridine orange (EB/AO) and observed under a fluorescent microscope. Viable cells emitted green fluorescence (AO), while necrotic cells showed predominant red fluorescence (EB). (b) Trypan blue dye exclusion assay: A549, MCF7, MDA-MB-231, Du-145, PC-3, HeLa, Hep G2, and HEK293 cells were treated with EA for 24 hours. Post-treatment, cells were incubated with Trypan Blue solution. Viable cells excluded the dye, while non-viable cells absorbed it, appearing blue. Cell viability was assessed under a microscope, and the results were tabulated and graphed. (c & d) Colony formation assay: 500 cells were seeded and subjected to EA treatment under experimental conditions. After incubation, colonies were fixed and counted to evaluate clonogenic potential. These studies provide insights into how EA alters cell survival and proliferation.

3.4.4 Impact of EA on Apoptosis and Cell cycle

We explored the impact of EA on apoptosis in MDA-MB-231 cells by exposing them to various concentrations $(0, 0.1, 1, \text{ and } 10 \,\mu\text{M})$ of EA for 24 hours. Post-treatment, the cells were stained with Annexin V/propidium iodide (PI) and analyzed for apoptosis levels using flow cytometry. The results revealed a progressive increase in the number of cells undergoing late apoptosis with higher EA concentrations (Figure 3.4.7a, b). Additionally, we assessed the effect of EA on cell cycle progression to determine cell cycle distribution and phase transition (Figure 3.4.7c, d). The findings indicated that EA induced G0/G1 phase arrest in a dose-dependent manner at concentrations of 1 μ M and 10 μ M, compared to the control group.

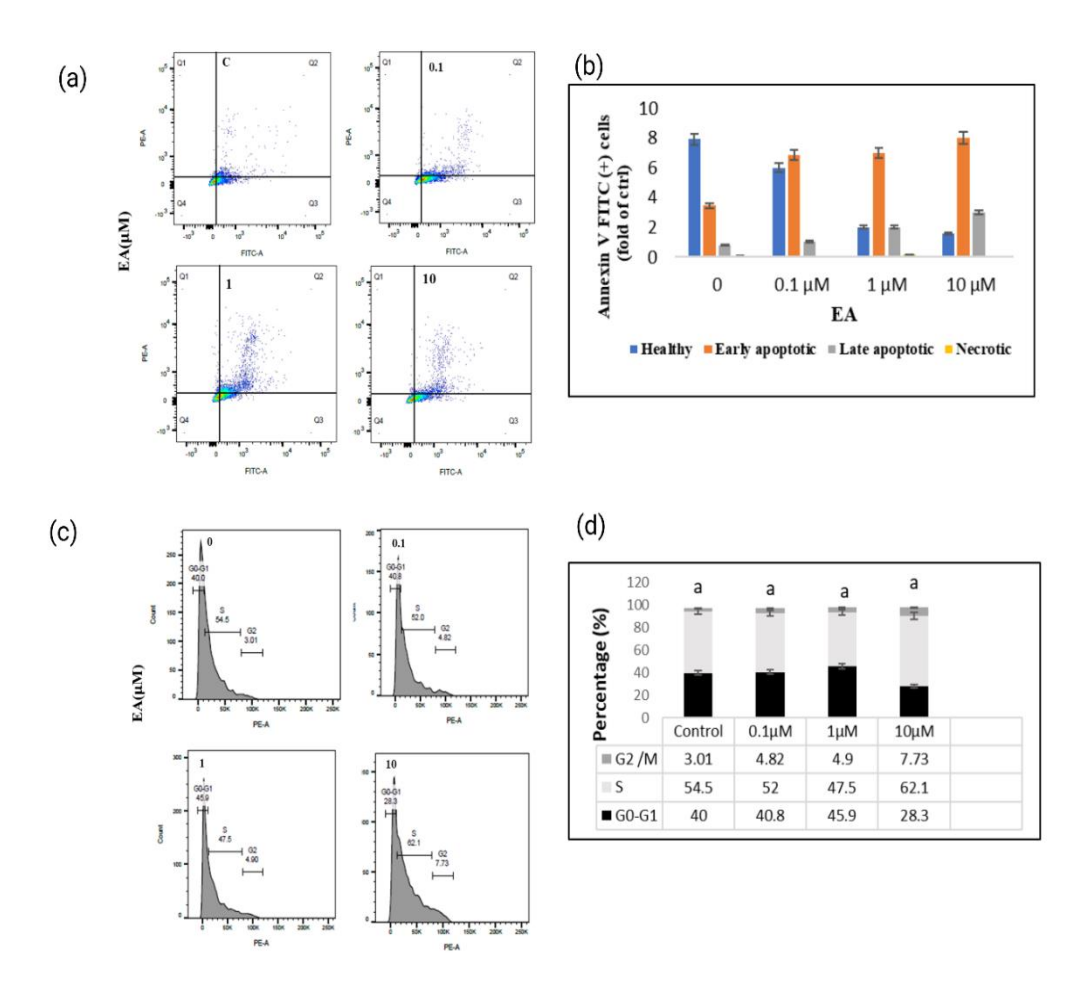


Figure 3.4.7: Induction of Apoptosis by EA in Breast Cancer Cells: MDA-MB231 cells were treated with EA for 24 hours. Subsequently, cells were stained with Annexin V/propidium iodide (PI) to assess the percentage of apoptotic cells using flow cytometry. (a & b) Flow cytometry analysis of MDA-MB231 cells treated with EA. (c & d) Analysis of cell cycle progression in MDA-MB231 cells after 24 hours of EA treatment.

3.4.5 EA mediate the autophagy in cells

The AO-EtBr assay indicated the presence of apoptotic cells, characterized by crescent or granular shapes. To investigate whether these granular cells were indicative of apoptosis-induced autophagy, we examined the formation of Acidic Vesicular Organelles (AVOs) following EA treatment.

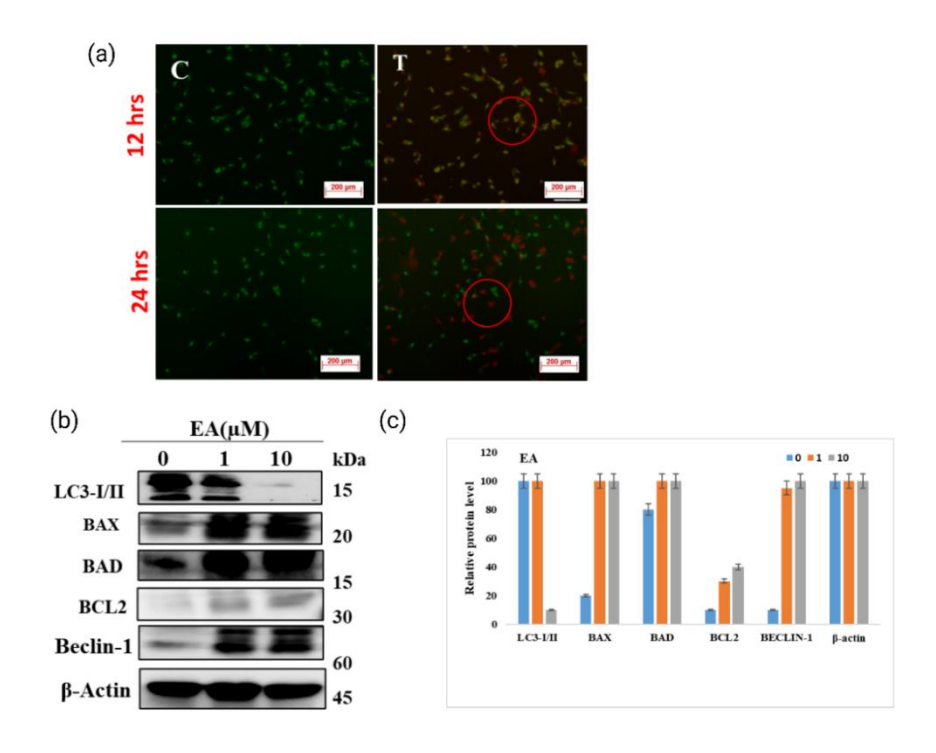


Figure 3.4.8: EA Induces Autophagy in Breast Cancer Cells: MDA-MB231 cells were exposed to EA for 24 hours, revealing induction of autophagy. (a) Treatment with EA led to the formation of acidic vesicular organelles (AVOs) in cells. (b & c) Western blot analysis was conducted to assess LC3 I/II expression and evaluate the levels of Beclin-1, Bax, Bad, and BCl2 proteins in EA-treated MDA-MB231 cells.

AVO formation is a marker of autophagy. In treated cells, we observed red fluorescent spots, whereas control cells primarily exhibited green cytoplasmic fluorescence (Figure 3.4.8a). We also assessed whether EA induced autophagy-mediated cell death in MDA-MB-231 cells by measuring the expression of microtubule-associated protein light chain 3 (LC3), a key marker for autophagy. Our findings showed a dose-dependent increase in LC3 transition induced by EA (Figure 3.4.7b). To further confirm autophagy induction, we evaluated the expression levels of Beclin-1 and members of the BCL protein family (BCL2, BAX, and BAD) (Figure 3.4.7b, c).

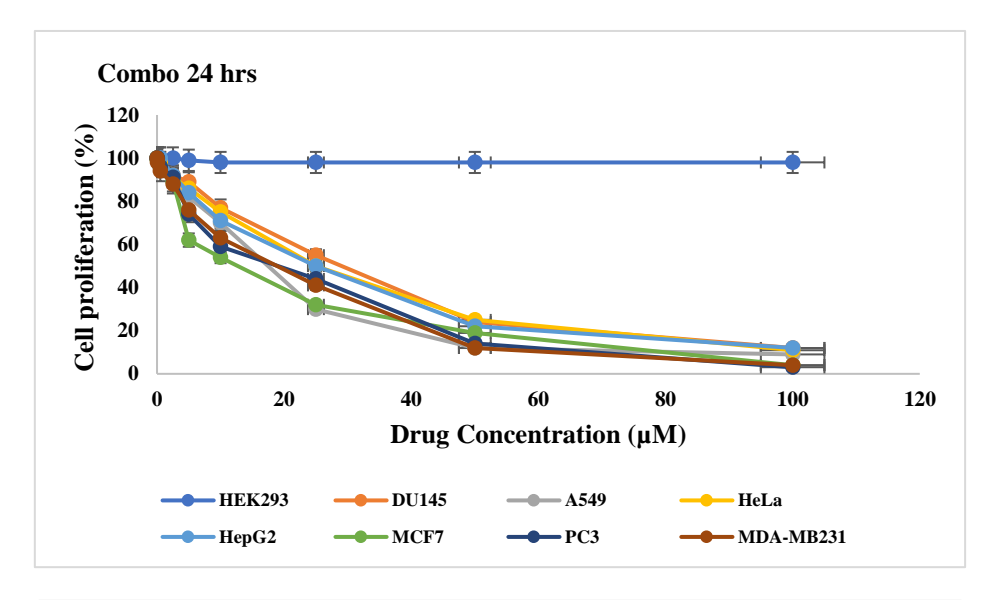
3.5 Impact of Combination (EGCG+EA

After individually evaluating the effect of EGCG and EA on malignant cell lines, we aimed to investigate their combined effects. Our interest lies in understanding how their combination may influence cell behavior and therapeutic potential.

3.5.1 Impact of Combo on human malignant cell lines:

In this study, a variety of human cancer cell lines were used, including MCF7 and MDA-MB-231 (breast cancer), DU-145 and PC-3 (prostate cancer), A549 (lung cancer), HeLa (cervical

cancer), Hep G2 (liver cancer), and HEK293 (human embryonic kidney). The cells were exposed to different concentrations of Combination for 24 and 48 hours, and cell viability was measured to determine the IC50 value (Figure 3.5).



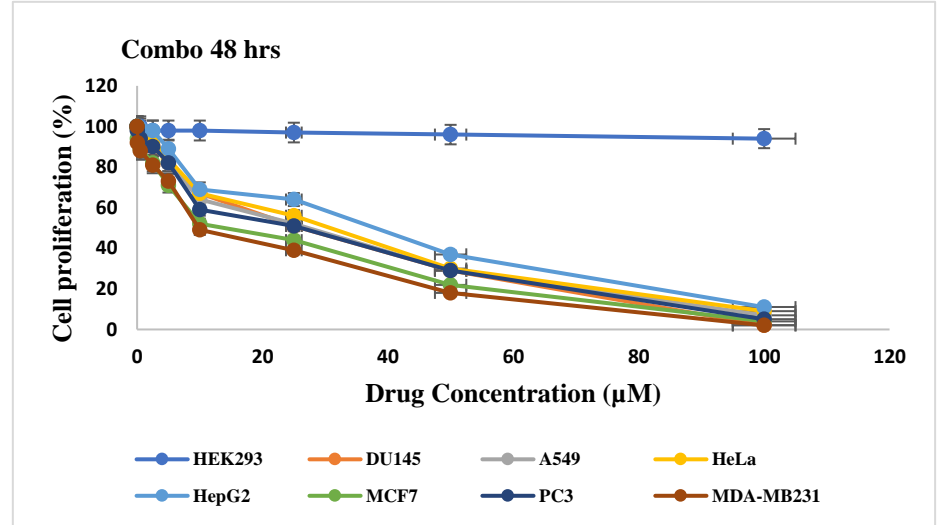


Figure-3.5: Impact of Combo on Human Cancer Cell Lines: Various human cancer cell lines, including MCF7 (breast), MDA-MB-231 (breast), Du-145 (prostate), A549 (lung), Hep G2 (liver), HeLa (cervix), PC-3 (prostate), and HEK293 (human embryonic kidney), were treated with different concentrations of Combo. Cytotoxicity was assessed, and IC50 values were determined and tabulated. The top panel (a) shows results for Combo treatment over 24 hours, while the bottom panel (b) shows results for Combo treatment over 48 hours.

3.5.2: Surface Plasmon Resonance Analysis of combination with EZH2 and PRMT5:MEP50

We conducted a Surface Plasmon Resonance (SPR) assay to investigate the interactions of PRMT5-MEP50 and EZH2 with a combination of EGCG and EA (Combo). Recombinant

PRMT5-MEP50 and EZH2 proteins were immobilized on a CM5 sensor chip, with the immobilization sensograms displayed in Figure 3.3.2.4. Real-time analysis was performed to assess the interaction and binding affinity of Combo with PRMT5-MEP50 and EZH2. Binding kinetics were analyzed by introducing varying concentrations of Combo to the immobilized protein surfaces (Figures 3.5.1).

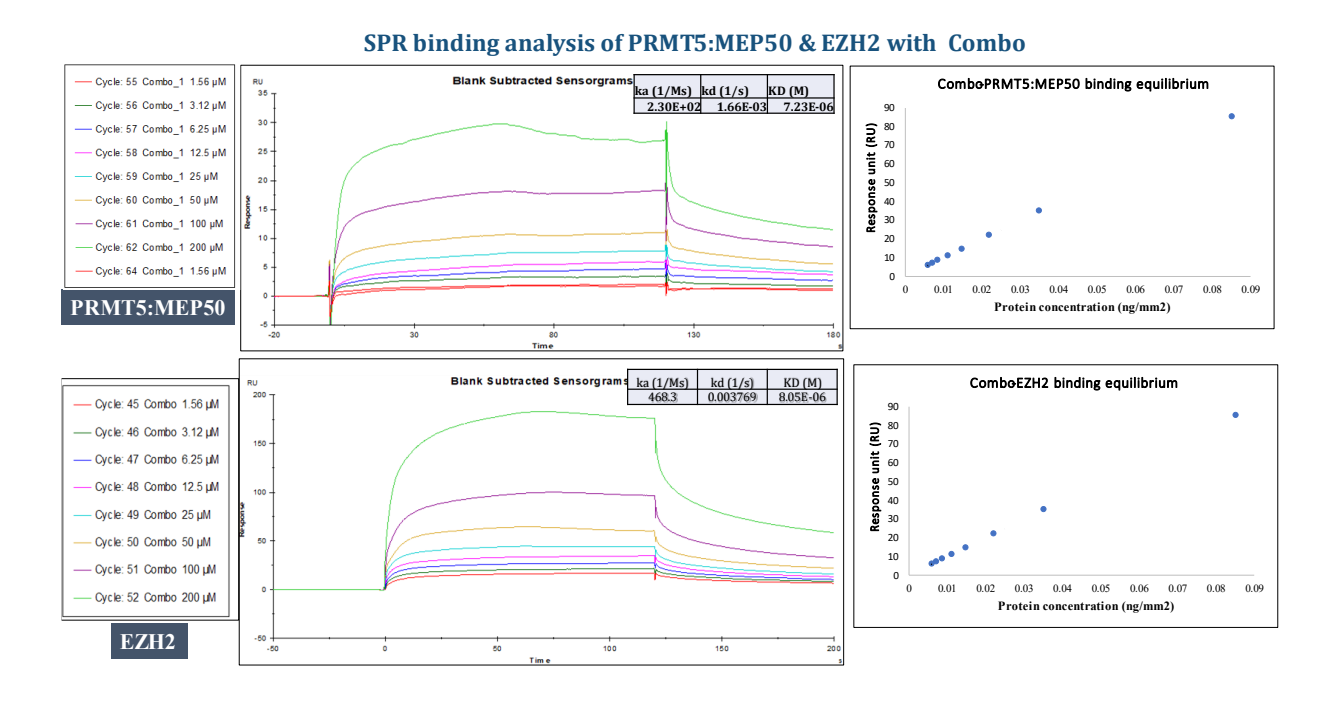


Figure-3.5.1: Surface Plasmon resonance Studies for Combo with PRMT5:MEP50 and

EZH2- The sensorgram analysis of the Combo (EA+EGCG) interaction with PRMT5 and EZH2 complexes was conducted using a CM5 sensor chip. Panel (a) depicts the dose-response sensorgram of the combo interacting with immobilized PRMT5-MEP50. Panel (b) shows the fitting of the response and concentration data using BIAcore T200 Evaluation software version 2.0. Panel (c) illustrates the dose-response sensorgram of the combo with immobilized EZH2. Panel (d) presents the fitting of the response and concentration data using the same software. The plot of response units (RU) versus protein concentration demonstrates a linear relationship. The determined association rate constant (ka), dissociation rate constant (kd), and equilibrium dissociation constant (KD) values are as follows: For Combo (EA+EGCG) with PRMT5 complex: Ka = 2.30E+02, kd = 1.66E-03, KD = 7.23E-06. For Combo (EA+EGCG) with EZH2: Ka = 76.13, kd = 0.003361, KD = 4.42E-05.

The SPR assay results revealed strong interactions of Combo with PRMT5-MEP50 and EZH2 complexes immobilized on the CM5 sensor chip. Specifically, Combo demonstrated a KD of 7.23E-06 for PRMT5-MEP50 and 4.42E-05 for EZH2, indicating a higher binding affinity for EZH2. The association rate constant (ka) was 2.30E+02 for PRMT5-MEP50 and 76.13 for EZH2, while the dissociation rate constant (kd) was 1.66E-03 for PRMT5-MEP50 and

0.003361 for EZH2. These findings highlight the strong binding affinity of Combo towards EZH2, suggesting its potential as a targeted therapeutic agent in cancer treatment.

3.5.3: Effect of combination on H3K27me3 and H4R3me2s Methylation Marks:

The results showed a marked reduction in H3K27me3 and H4R3me2s levels, particularly at a concentration of $10~\mu M$, compared to untreated cells. Despite this, the protein levels of EZH2, PRMT5, H3, and H4 remained largely unchanged (Figure 3.5.2a-b), with β -actin used as a loading control. Furthermore, *in vitro* methylation assays of H3 and H4, followed by ELISA (Figure 3.5.2c), indicated a dose-dependent decrease in H3K27me3 and H4R3me2s at concentrations of $1~\mu M$ and $10~\mu M$.

Combination Influence on PRMT5 & EZH2: reduced Histone Repressive Marks Combo(µM) (a) 0 0.1 1 10 kDa PRMT5 75 EZH2 100 H4R3me2s 20 H3K27me3 20 Н3 β-Actin (c) **2** 100 percentage

Figure-3.5.2: Effect of Combo on H3K27me3 and H4R3me2s Methylation Marks. MDA-MB231 cells were treated with increasing concentrations of Combo (0.1, 1, 10 μ M) for 24 hours. Protein lysates were then prepared as per the described methods and analyzed for H4R3me2s and H3K27me3 levels via immunoblotting, using β-actin as a loading control. (a) Western blots showing the methylation levels. (b) Graphs depicting the intensity of the proteins from the western blots. (c) *In vitro* methylation assays were performed as described in the methods, and methylation levels were quantified using ELISA. These assays utilized EZH2 and PRMT5-MEP50 enzyme complexes with histones as substrates.

3.5.4: Effect of combination on Cellular Proliferation Dynamics:

AO-EtBr double staining revealed the presence of early-stage apoptotic cells, characterized by crescent-shaped or granular nuclei, in MDA-MB-231 cells treated with Combo for 24 hours. This staining method uses Acridine Orange (AO) and Ethidium Bromide (EtBr) to differentiate live, apoptotic, and necrotic cells based on their fluorescence properties. Early-stage apoptotic

cells exhibited distinct morphological features, such as crescent-shaped or granular nuclei, which fluoresced green to yellow/orange under the staining protocol due to partial membrane permeability. This contrasted sharply with the control group, where most cells retained a uniform green fluorescence, indicating live cells with intact membranes and no significant apoptosis. The findings, as illustrated in Figure 3.5.3a, demonstrate that the Combo treatment effectively induces early apoptosis in the MDA-MB231 cell line, whereas the untreated control group shows no notable signs of apoptotic activity.

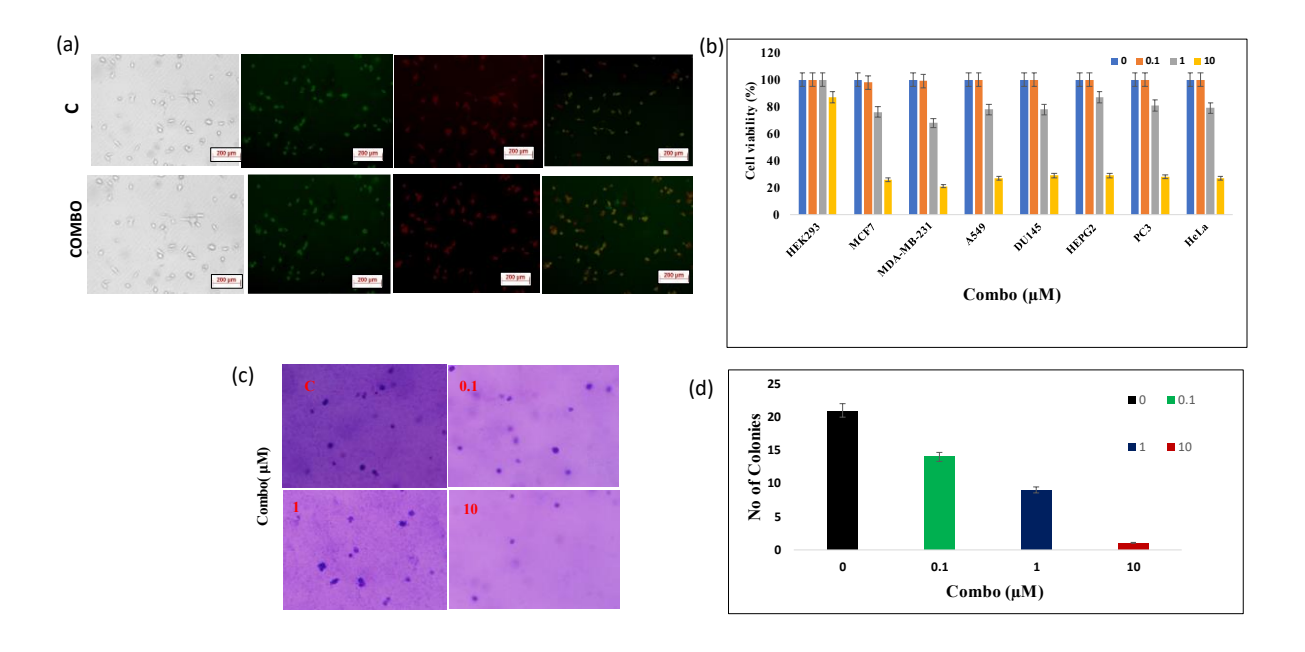


Figure-3.5.3: Effect of Combo on Cellular Proliferation Dynamics: Cells were treated with Combo at various concentrations and durations, followed by multiple cell-based assays to assess the impact. (a) AO/EtBr assay: Cells were double-stained with ethidium bromide and acridine orange (EB/AO) and observed under a fluorescent microscope. Viable cells emitted green fluorescence (AO), while necrotic cells showed predominant red fluorescence (EB). (b) Trypan blue dye exclusion assay: A549, MCF7, MDA-MB-231, Du-145, PC-3, HeLa, Hep G2, and HEK293 cells were treated with Combo for 24 hours. Post-treatment, cells were incubated with Trypan Blue solution. Viable cells excluded the dye, while non-viable cells absorbed it, appearing blue. Cell viability was assessed under a microscope, and the results were tabulated and graphed. (c & d) Colony formation assay: 500 cells were seeded and subjected to Combo treatment under experimental conditions. After incubation, colonies were fixed and counted to evaluate clonogenic potential. These studies provide insights into how Combination of drugs alters cell survival and proliferation.

These observations were corroborated by results from the trypan blue dye exclusion assay and MTT assays (Figure 3.5.3b). Additionally, the colony formation assay indicated a dose-dependent decrease in colony formation in the Combo-treated group compared to the control group (Figure 3.5.3c-d). Together, these *in vitro* assays provided compelling evidence that Combo effectively suppresses the activity of EZH2 and PRMT5.

3.5.5: Induction of Apoptosis by combination in Breast Cancer Cells

We investigated the impact of Combo on apoptosis in MDA-MB-231 cells by treating them with varying concentrations (0 μ M, 0.1 μ M, 1 μ M, and 10 μ M) of Combo for 24 hours. The Combo treatment comprised equal parts of EGCG and EA, meaning that 0.1 μ M Combo included 0.05 μ M each of EGCG and EA, 1 μ M Combo included 0.5 μ M each, and 10 μ M Combo included 5 μ M each. After treatment, cells were stained with Annexin V/propidium iodide (PI) and analyzed for apoptosis levels using flow cytometry. Our findings revealed a gradual increase in cells progressing into late apoptosis with higher concentrations of Combo (Figure 3.5.4-a, b). Furthermore, we examined the effect of Combo on cell cycle progression to assess cell cycle distribution and phase transition (Figure 3.5.4-c, d). The results indicated that Combo induced G0/G1 phase arrest in a dose-dependent manner at concentrations of 1 μ M and 10 μ M, compared to the control group.

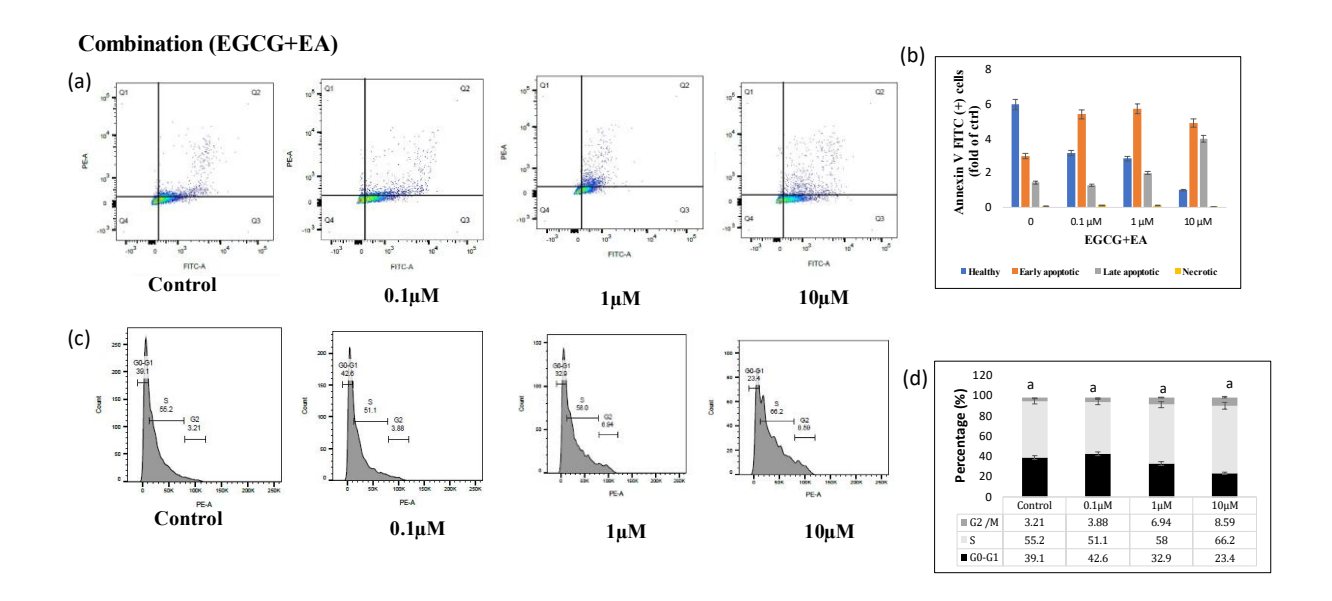


Figure 3.5.4: Induction of Apoptosis by combo in Breast Cancer Cells: MDA-MB-231 cells were treated with Combo for 24 hours. Subsequently, cells were stained with Annexin V/propidium iodide (PI) to assess the percentage of apoptotic cells using flow cytometry. The Combo treatment consisted of equal parts EGCG and EA, with 0.1 μ M Combo containing 0.05 μ M each of EGCG and EA, 1 μ M Combo containing 0.5 μ M each, and 10 μ M Combo containing 5 μ M each. (a & b) Flow cytometry analysis of MDA-MB-231 cells treated with Combo. (c & d) Analysis of cell cycle progression in MDA-MB-231 cells after 24 hours of Combo treatment.

3.5.6: Combination Induces Autophagy in Breast Cancer Cells

The AO-EtBr assay identified apoptotic cells characterized by crescent or granular shapes. To investigate whether these granular cells indicated apoptosis-induced autophagy, we examined the formation of Acidic Vesicular Organelles (AVOs) following Combo treatment. AVO

formation serves as a marker of autophagy. Treated cells displayed red fluorescent spots, whereas control cells predominantly showed green cytoplasmic fluorescence (Figure 3.5.5a).

Moreover, we explored whether Combo induced autophagy-mediated cell death in MDA-MB231 cells by evaluating the expression of microtubule-associated protein light chain 3 (LC3), a well-established autophagy marker. Our results revealed a dose-dependent increase in LC3 levels induced by Combo (Figure 3.5.5b). Additionally, to confirm autophagy induction, we assessed the expression of Beclin-1 and members of the BCL protein family (BCL2, BAX, and BAD) (Figure 3.5.5b, c).

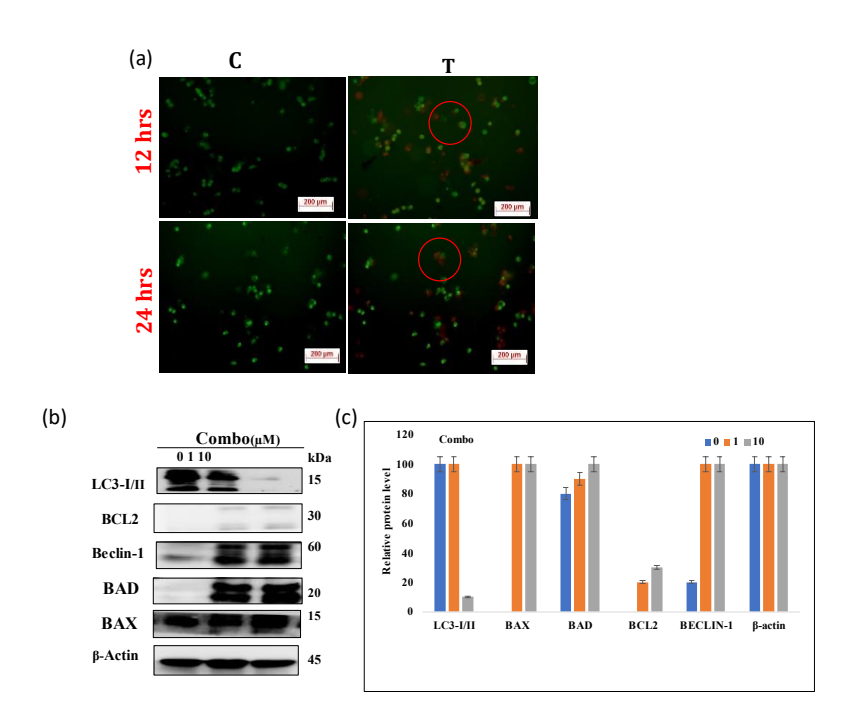


Figure 3.5.5: Combo Induces Autophagy in Breast Cancer Cells: MDA-MB231 cells were exposed to combo for 24 hours, revealing induction of autophagy. (a) Treatment with combo led to the formation of acidic vesicular organelles (AVOs) in cells. (b & c) Western blot analysis was conducted to assess LC3 I/II expression and evaluate the levels of Beclin-1, Bax, Bad, and BCl2 proteins in E combo -treated MDA-MB231 cells.

3.6 Discussion:

Cancer remains a significant global health challenge, causing millions of deaths annually and straining healthcare systems worldwide. According to the World Health Organization (WHO), cancer constitutes approximately one-sixth of all global deaths and profoundly impacts nearly every household. In 2022, an estimated 20 million new cancer cases led to 9.7 million deaths worldwide [13,14]. Projections suggest that by 2050, the burden of cancer will rise by about 77%, posing significant challenges for health systems, individuals, and communities [13,14].

In the United States, around 2.0 million people were diagnosed with cancer in 2023, with breast cancer being the most prevalent among women and prostate cancer among men [15]. Factors such as obesity, age, physical activity, family history, and oral contraceptive use can influence the onset of these cancers, which involve genetic and epigenetic changes such as DNA methylation and histone modifications [16]. These alterations affect chromatin structure and various pathways associated with cancer development.

In recent decades, significant advancements have been made in cancer therapy development, focusing on drugs that target critical epigenetic regulators such as histone deacetylases (HDACs), DNA methyltransferases (DNMTs), histone methyltransferases (HMTs), histone demethylases (HDMs), and bromodomain and extra-terminal proteins (BETs) [17-23]. Notably, inhibitors of DNMTs (DNMTi), HDACs (HDACi), and BET proteins (BETi) have been approved for specific cancers, underscoring their clinical effectiveness [23]. There is also increasing interest in developing inhibitors targeting protein arginine methyltransferase 5 (PRMT5) and enhancer of zeste homolog 2 (EZH2) due to their versatile roles in cancer therapy [24-27].

PRMT5 and EZH2 are frequently overexpressed in various cancers, including breast, endometrial, liver, ovarian, prostate, small cell lung cancer, melanoma, glioblastoma, pediatric glioma, bladder, and lymphomas, often correlating with disease progression and poor prognosis [24, 26-28]. Their interaction, particularly in mediating histone marks like EZH2-mediated H3K27me3 trimethylation and PRMT5-mediated H4R3me2s symmetric dimethylation, suggests synergistic effects, highlighting potential for combined therapeutic strategies [29].

These histone modifications play crucial roles in driving epigenetic alterations within cancer cells [30-31]. Dysregulation of these modifications disrupts the balance between active and repressive chromatin states, leading to abnormal gene expression profiles that promote tumorigenesis [32]. Understanding these epigenetic changes is essential for deciphering the molecular mechanisms underlying cancer development and identifying potential therapeutic targets to restore normal epigenetic regulation and impede tumor progression [33-34].

Despite advances in therapeutic strategies, conventional treatments such as chemotherapy often induce severe side effects in cancer patients. Researchers are exploring the potential of natural compounds with minimal adverse reactions to combat cancer. Phytocompounds derived from plants, including curcumin, resveratrol, brazilin, catechin, quercetin, EGCG, and EA, have

emerged as promising candidates for modulating epigenetic mechanisms associated with different cancer hallmarks. These compounds have shown the ability to interact with key epigenetic regulators like DNMT1 and HDAC1 within their catalytic pockets [35-37], suggesting their potential to influence the activity of crucial epigenetic enzymes involved in cancer progression [38].

EA exerts protective effects through several mechanisms. It activates antioxidant enzymes such as superoxide dismutase (SOD), catalase (CAT), glutathione peroxidase (GPx), and glutathione-S-transferase (GST). Additionally, EA modulates various signaling pathways including nuclear erythroid 2-related factor 2 (Nrf2), phosphoinositide 3-kinase (PI3K), glycogen synthase kinase 3 beta (GSK-3β), and suppresses pro-inflammatory markers such as cyclooxygenase (COX-2) and nuclear factor-kappa B (NF-κB) [39]. Furthermore, EA exhibits potent radical scavenging activity against hydroxyl radicals (OH•), methoxyl radicals (OCH3•), and nitrogen dioxide radicals (NO2•) [31, 32]. Previous studies have underscored EA's beneficial effects against various malignancies including colorectal, breast, and prostate cancers, leukemia, lymphoma, and melanoma [40-45].

Molecular docking-based virtual screening is an essential computational method used to design drugs by predicting the binding affinities between potential ligands and protein targets [59]. Our study revealed that EA preferentially binds to the catalytic pocket of EZH2 over PRMT5. EGCG, rich in π electrons, formed at least five hydrogen bonds with key residues within PRMT5's catalytic pocket, including Tyr324, Tyr334, Gly365, Leu437, and Glu444 in the SAM-dependent methyltransferase domain of the double E loop. EGCG also engaged in π - π stacking interactions with Phe327 and notably interacted with Glu435. These residues are shared with sinefungin and are close to the SAM-binding region, suggesting EGCG's potential to inhibit catalysis, potentially contributing to reduced H4R3me2s methylation in exposed cells. Further investigations indicated that the combination of EA and EGCG exhibited stronger inhibition than either compound alone [38, 46, 47].

Docking studies provided insights into EA's binding modes across various structural forms of PRMT5-MEP50 and EZH2. EA displayed similar interaction patterns to known ligands such as SFG, SAM, SAH, 5HYN, and 4mi5. In PRMT5, EA formed a π -cation interaction with Lys393 and established three hydrogen bonds with residues Tyr324, Glu392, and Glu444. In EZH2, EA exhibited robust binding, forming multiple hydrogen bonds with residues Trp624, Ser664, Ala622, Tyr728, and Asp732.

The molecular dynamics simulations studies revealed that EGCG and EA exhibit strong and stable interactions with PRMT5 and EZH2, confirming their potential as effective inhibitors. Recent studies also support this approach. In a recent study exploring EGCG and theaflavin digallate as potential inhibitors of druggable cancer targets [60], EGCG and EA emerged as effective inhibitors of PRMT5 and EZH2 in our investigation. Docking and simulation analyses provided compelling evidence of their inhibitory effects. EGCG demonstrated notable binding affinity to PRMT5's catalytic pocket, engaging in multiple hydrogen bonds and π - π stacking interactions with residues such as Tyr324, Tyr334, Gly365, Leu437, and Glu444. These interactions were stable over time, as confirmed by molecular dynamics simulations, which showed consistent RMSD and RMSF values and stable hydrophobic interactions. In contrast, EGCG's binding to EZH2 was less stable, displaying more fluctuations. EA, however, showed a preference for binding to EZH2, creating several hydrogen bonds with important residues such as Trp624, Ser664, Ala622, Tyr728, and Asp732. Although the EA-PRMT5 complex was stable, its interactions were somewhat weaker than those of EGCG. Molecular dynamics simulations indicated that EA maintained more stable interactions with EZH2, as evidenced by steady RMSD and RMSF values. Interestingly, the combination of EA and EGCG led to more effective inhibition of both PRMT5 and EZH2 than either compound alone, suggested a synergistic effect. These results highlight the potential of EGCG and EA as promising therapeutic agents for targeting PRMT5 and EZH2 in cancer treatment [61-63].

The SPR binding analysis confirmed strong binding affinity of EA, both individually and in combination with EGCG. Specifically, for EZH2, EA exhibited association rate constant (ka) = 674.1, dissociation rate constant (kd) = 0.002214, and equilibrium dissociation constant (KD) = 3.28E-06, whereas Combo (EA+EGCG) showed ka = 76.13, kd = 0.003361, and KD = 4.42E-05. Regarding PRMT5, EA displayed ka = 3.71E+01, kd = 2.43E-03, and KD = 6.54E-05, while Combo (EA+EGCG) showed ka = 2.30E+02, kd = 1.66E-03, and KD = 7.23E-06 [63, 68]. These findings further substantiated the preferential binding of EGCG and EA to both the PRMT5-MEP50 complex and EZH2.

Interestingly, EA displayed stronger binding interactions with EZH2 compared to well-studied synthetic molecules such as CPI-0209, CPI-1205, Tazemetostat (EPZ-6438), PF-06821497, and DS-3201 [48-50]. *In vitro* methylation assays followed by ELISA confirmed EA's ability to inhibit EZH2 and PRMT5 activity in MCF-7 and MDA-MB231 cells, leading to a reduction in specific histone methylation marks. Polyphenolic compounds like EA exert their anti-cancer

effects through diverse mechanisms, including antioxidant, anti-inflammatory, and anti-proliferative actions, influencing cellular signaling pathways, inducing cell-cycle arrest, and promoting apoptosis [38].

Numerous studies have reported that inhibiting PRMT5 and EZH2 activity can induce apoptosis, autophagy, and cell cycle arrest [51-53]. For instance, inhibition of EZH2 with 3-deazaneplanocin A (DZNep) has been linked to autophagy induction [54]. EGCG has also been shown to reduce H3K27me3 levels in skin cancer cells, affecting cell cycle regulators like cyclins and p21/p27 [54].

Inhibition of PRMT5 with GSK591 or shRNAs in lung cancer cells induces apoptosis and autophagy, accompanied by reduced Akt/GSK3β phosphorylation and decreased cyclin D1 and E1 expression [55]. PRMT5 inhibition has also been associated with increased apoptosis and reduced cell growth in multiple myeloma [56], influencing autophagy stages and tumorigenesis through specific target modulation [57]. PRMT5-mediated methylation of ULK1 at R532 suppresses ULK1 activation in triple-negative breast cancer cells, highlighting its role in autophagy regulation [57]. Additionally, the epigenetic inhibitor Trichostatin A suppresses cervical cancer cell proliferation by inducing apoptosis and autophagy via the PRMT5/STC1/TRPV6/JNK axis [66].

Our study underscores EA's potential as an inhibitor of PRMT5 and EZH2 activities, suggesting implications for inducing apoptosis and autophagy. Downregulation of EZH2 in colorectal cancer cells has been shown to induce both autophagy and apoptosis, while PRMT5 inhibition in lung cancer cells promotes apoptosis and autophagy by affecting cell cycle regulators and signaling pathways [54, 64]. The global reduction in H4R3me2s and H3K27me3 histone methylation marks observed in our study suggests their involvement in apoptosis and autophagy induction, potentially through mechanisms involving cell cycle arrest [66, 67].

Our findings highlight the promising potential of EGCG and EA, already recognized for its anti-cancer effects and currently undergoing clinical trials [58], as a novel modulator of PRMT5 and EZH2 interactions. In silico, in vitro, and SPR binding studies have demonstrated its efficacy in inhibiting enzyme activity and reducing repressive histone methylation marks, suggesting EA as a candidate for future drug development strategies.

3.7 References:

- 1. Xia, Y., Sun, M., Huang, H., & Jin, W. (2024). Drug repurposing for cancer therapy. *Signal Transduction and Targeted Therapy*, 9(1), 1-33. https://doi.org/10.1038/s41392-024-01808-1
- Choudhari, A. S., Mandave, P. C., Deshpande, M., Ranjekar, P., & Prakash, O. (2019). Phytochemicals in Cancer Treatment: From Preclinical Studies to Clinical Practice. Frontiers in Pharmacology, 10. https://doi.org/10.3389/fphar.2019.01614
- Yang, L., Zhou, X., & Bao, J. (2021). PRMT5 functionally associates with EZH2 to promote colorectal cancer progression through epigenetically repressing CDKN2B expression. *Theranostics*, 11(8), 3742-3759. https://doi.org/10.7150/thno.53023
- **4.** Tao, L., Zhou, Y., Luo, Y., Qiu, J., Xiao, Y., Zou, J., Zhang, Y., Liu, X., Yang, X., Gou, K., Xu, J., Guan, X., Cen, X., & Zhao, Y. (2024). Epigenetic regulation in cancer therapy: From mechanisms to clinical advances. *MedComm Oncology*, *3*(1), e59. https://doi.org/10.1002/mog2.59
- Eich, M.-L., Athar, M., Ferguson, J. E., III, & Varambally, S. (2020). EZH2-Targeted Therapies in Cancer: Hype or a Reality. In Cancer Research (Vol. 80, Issue 24, pp. 5449–5458). American Association for Cancer Research (AACR). https://doi.org/10.1158/0008-5472.can-20-2147
- 6. Balakrishnan, R., Azam, S., Cho, Y., Su-Kim, I., & Choi, K. (2021). Natural Phytochemicals as Novel Therapeutic Strategies to Prevent and Treat Parkinson's Disease: Current Knowledge and Future Perspectives. Oxidative Medicine and Cellular Longevity, 2021. https://doi.org/10.1155/2021/6680935
- Ferrari, E., Bettuzzi, S., & Naponelli, V. (2022). The Potential of Epigallocatechin Gallate (EGCG) in Targeting Autophagy for Cancer Treatment: A Narrative Review. *International Journal of Molecular Sciences*, 23(11). https://doi.org/10.3390/ijms23116075
- **8.** Nalla, K., Chatterjee, B., Poyya, J., Swain, A., Ghosh, K., Pan, A., ... & Kanade, S. R. (2024). Ellagic acid: a potential inhibitor of enhancer of zeste homolog-2 and protein arginine methyltransferase-5. *bioRxiv*, 2024-05.
- **9.** Nalla, K., Chatterjee, B., Poyya, J., Swain, A., Ghosh, K., Pan, A., ... & Kanade, S. R. (2024). Epigallocatechin-3-gallate inhibit the protein arginine methyltransferase 5 and Enhancer of Zeste homolog 2 in breast cancer both in vitro and in vivo. *bioRxiv*, 2024-02.
- **10.** Bowers, K. J., Chow, D. E., Xu, H., Dror, R. O., Eastwood, M. P., Gregersen, B. A., ... Salmon, J. K. (2006). Scalable algorithms for molecular dynamics simulations on commodity clusters. In SC'06: Proceedings of the 2006 ACM/IEEE Conference on Supercomputing (pp. 43–43).
- **11.** Muller, K. M. et al Model and simulation of multivalent binding to fixed ligands. *Analytical Biochemistry* 261: 149-158; (1998).
- **12.** D. Cheng, V. Vemulapalli, M. T. Bedford, Methods applied to the study of protein arginine methylation. In Methods in Enzymology 512 (2012), 71-92. https://doi.org/10.1016/B978-0-12-391940-3.00004-4
- **13.** <u>Cancer fact sheet.</u> World Health Organization; 2022. (https://www.who.int/news-room/fact-sheets/detail/cancer)
- 14. Cancer Tomorrow tool. International Agency for Research on Cancer. (https://gco.iarc.fr/tomorrow/en)
- 15. Cancer Stat Facts: Common Cancer Sites(https://seer.cancer.gov/statfacts/html/common.html)
- Hoxha, I., Sadiku, F., Hoxha, L., Nasim, M., Christine Buteau, M. A., Grezda, K., & Chamberlin, M. D. (2024). Breast Cancer and Lifestyle Factors: Umbrella Review. *Hematology/oncology clinics of North America*, 38(1), 137–170. https://doi.org/10.1016/j.hoc.2023.07.005
- **17.** Ramaiah, M. J., Tangutur, A. D., (2021). Epigenetic modulation and understanding of HDAC inhibitors in cancer therapy. *Life sciences*, 277, 119504.
- **18.** McClure, J. J., Li, X., (2018). Advances and Challenges of HDAC Inhibitors in Cancer Therapeutics. *Advances in cancer research*, *138*, 183–211.
- **19.** Jan, Z., Ahmed, W. S (2023). Identification of a potential DNA methyltransferase (DNMT) inhibitor. *Journal of biomolecular structure & dynamics*, 1–15. Advance online publication.
- **20.** Marzochi, L. L., Cuzziol, C. I., (2023). Use of histone methyltransferase inhibitors in cancer treatment: A systematic review. *European journal of pharmacology*, *944*, 175590.
- **21.** Baby, S., Gurukkala Valapil, D., (2021). Unravelling KDM4 histone demethylase inhibitors for cancer therapy. *Drug discovery today*, 26(8), 1841–1856.

- **22.** Gajjela, B. K., & Zhou, M. M. (2023). Bromodomain inhibitors and therapeutic applications. *Current opinion in chemical biology*, 75, 102323.
- 23. Yunfeng Qi, Dadong Wang, HEDD (2016): the human epigenetic drug database Database,: pii: baw159.
- **24.** Kim, H., & Ronai, Z. A. (2020). PRMT5 function and targeting in cancer. *Cell stress*, *4*(8), 199–215. https://doi.org/10.15698/cst2020.08.228
- **25.** Jarrold J, Davies CC. PRMTs and Arginine Methylation: Cancer's Best-Kept Secret? Trends Mol Med. 2019 Nov;25(11):993-1009. doi: 10.1016/j.molmed.2019.05.007. Epub 2019 Jun 20. PMID: 31230909.
- **26.** Shailesh, H., Zakaria, Z. Z., (**2018**). Protein arginine methyltransferase 5 (PRMT5) dysregulation in cancer. *Oncotarget*, 9(94), 36705–36718.
- **27.** Gan, L., Yang, Y.,. (**2018**). Epigenetic regulation of cancer progression by EZH2: From biological insights to therapeutic potential. *Biomarker Research*, 6:10.
- **28.** Liu, Y., & Yang, Q. (2023). The roles of EZH2 in cancer and its inhibitors. Medical oncology (Northwood, London, England), 40(6), 167.
- **29.** Yang, L., Ma, D. W (2021). PRMT5 functionally associates with EZH2 to promote colorectal cancer progression through epigenetically repressing CDKN2B expression. *Theranostics*, *11*(8), 3742–3759.
- **30.** Verma, A., Singh, A., Singh, M. P., Nengroo, M. A., Saini, K. K., Satrusal, S. R., Khan, M. A., Chaturvedi, P., Sinha, A., Meena, S., Singh, A. K., & Datta, D. (2022). EZH2-H3K27me3 mediated KRT14 upregulation promotes TNBC peritoneal metastasis. *Nature communications*, *13*(1), 7344. https://doi.org/10.1038/s41467-022-35059-x
- **31.** Yang, L., Ma, D. W., Cao, Y. P., Li, D. Z., Zhou, X., Feng, J. F., & Bao, J. (2021). PRMT5 functionally associates with EZH2 to promote colorectal cancer progression through epigenetically repressing CDKN2B expression. *Theranostics*, *11*(8), 3742–3759. https://doi.org/10.7150/thno.53023
- **32.** Mandumpala, J. J., Baby, S., Tom, A. A., Godugu, C., & Shankaraiah, N. (2022). Role of histone demethylases and histone methyltransferases in triple-negative breast cancer: Epigenetic mnemonics. *Life sciences*, 292, 120321. https://doi.org/10.1016/j.lfs.2022.120321
- **33.** Wu, K., Niu, C., Liu, H., & Fu, L. (2023). Research progress on PRMTs involved in epigenetic modification and tumour signalling pathway regulation (Review). *International journal of oncology*, 62(5), 62. https://doi.org/10.3892/ijo.2023.5510
- **34.** Song, X., Gao, T., Wang, N., Feng, Q., You, X., Ye, T., Lei, Q., Zhu, Y., Xiong, M., Xia, Y., Yang, F., Shi, Y., Wei, Y., Zhang, L., & Yu, L. (2016). Selective inhibition of EZH2 by ZLD1039 blocks H3K27 methylation and leads to potent anti-tumor activity in breast cancer. *Scientific reports*, 6, 20864. https://doi.org/10.1038/srep20864
- **35.** Yunfeng Qi, Dadong Wang, HEDD (2016): the human epigenetic drug database Database,: pii: baw159.Akone, S. H., Ntie-Kang, F., Stuhldreier, F., Ewonkem, M. B., Noah, A. M., Mouelle, S. E. M., & Müller, R. (2020). Natural Products Impacting DNA Methyltransferases and Histone Deacetylases. *Frontiers in pharmacology*, *11*, 992. https://doi.org/10.3389/fphar.2020.00992
- 36. Lu, Y., Chan, Y. T., Tan, H. Y., Li, S., Wang, N., & Feng, Y. (2020). Epigenetic regulation in human cancer: the potential role of epi-drug in cancer therapy. *Molecular cancer*, 19(1), 79. https://doi.org/10.1186/s12943-020-01197-3
- **37.** Kedhari Sundaram, M., Haque, (2020). Epigallocatechin gallate inhibits HeLa cells by modulation of epigenetics and signaling pathways. *3 Biotech*, *10*(11), 484.
- **38.** Naraki, K., Rameshrad, M., & Hosseinzadeh, H. (2022). Protective effects and therapeutic applications of ellagic acid against natural and synthetic toxicants: A review article. *Iranian journal of basic medical sciences*, 25(12), 1402–1415. https://doi.org/10.22038/IJBMS.2022.64790.14267
- **39.** Shakeri A, Zirak MR, Sahebkar A. Ellagic acid: A logical lead for drug development? Curr Pharm Des. 2018;24:106–122.
- **40.** Zeb A. Ellagic acid in suppressing in vivo and in vitro oxidative stresses. Mol Cell Biochem. 2018;448:27–41.
- **41.** El-Shitany NA, El-Bastawissy EA, El-desoky K. Ellagic acid protects against carrageenan-induced acute inflammation through inhibition of nuclear factor kappa B, inducible cyclooxygenase and proinflammatory cytokines and enhancement of interleukin-10 via an antioxidant mechanism. Int Immunopharmacol. 2014;19:290–29

- **42.** Kohen R, Nyska A. Oxidation of biological systems: oxidative stress phenomena, antioxidants, redox reactions, and methods for their quantification. Toxicol Pathol. 2002;30:620–650.
- **43.** Alfei S, Marengo B, Zuccari G. Oxidative stress, antioxidant capabilities, and bioavailability: Elagic acid or urolithins? Antioxidants (Basel) 2020;9:707–737
- **44.** Bell C, Hawthorne S. Ellagic acid, pomegranate and prostate cancer -a mini review. J Pharm Pharmacol. 2008;60:139–144.
- **45.** Nalla K; Chatterjee B; Poyya J; Swain A; Ghosh K; Pan A; Joshi Ch; et al., (2024) "Epigallocatechin-3-gallate inhibit the protein arginine methyltransferase 5 and Enhancer of Zeste homolog 2 in breast cancer both in vitro and in vivo" bioRxiv 2024.02.18.580855; doi: https://doi.org/10.1101/2024.02.18.580855
- **46.** Deepika, & Maurya, P. K. (2022). Ellagic acid: insight into its protective effects in age-associated disorders. *3 Biotech*, *12*(12), 340. https://doi.org/10.1007/s13205-022-03409-7
- **47.** Yang, X., Xu, L., & Yang, L. (2023). Recent advances in EZH2-based dual inhibitors in the treatment of cancers. *European Journal of Medicinal Chemistry*, 256, 115461. https://doi.org/10.1016/j.ejmech.2023.115461
- **48.** Lakhani, N. J., Gutierrez, M., Duska, L. R., Do, K. T., Sharma, M., Gandhi, L., ... & Rasco, D. W. (2021). Phase 1/2 first-in-human (FIH) study of CPI-0209, a novel small molecule inhibitor of enhancer of zeste homolog 2 (EZH2) in patients with advanced tumors.
- **49.** Harb, W., Abramson, J., Lunning, M., Goy, A., Maddocks, K., Lebedinsky, C., ... & Flinn, I. (2018). A phase 1 study of CPI-1205, a small molecule inhibitor of EZH2, preliminary safety in patients with B-cell lymphomas. *Annals of Oncology*, *29*, iii7.
- **50.** Ferrari, E., Bettuzzi, S., (2022). The Potential of Epigallocatechin Gallate (EGCG) in Targeting Autophagy for Cancer Treatment: A Narrative Review. *International journal of molecular sciences*, 23(11), 6075.
- **51.** Rong, L., Li, Z., Leng, X., Li, H., Ma, Y., Chen, Y., & Song, F. (2020). Salidroside induces apoptosis and protective autophagy in human gastric cancer AGS cells through the PI3K/Akt/mTOR pathway. *Biomedicine & Pharmacotherapy*, 122, 109726. https://doi.org/10.1016/j.biopha.2019.109726
- **52.** Ni, X., Shang, F. S., Wang, T. F., Wu, D. J., Chen, D. G., & Zhuang, B. (2023). Ellagic acid induces apoptosis and autophagy in colon cancer through the AMPK/mTOR pathway. *Tissue & cell*, *81*, 102032. https://doi.org/10.1016/j.tice.2023.102032
- **53.** Kciuk, M., Alam, M., (2023). Epigallocatechin-3-Gallate Therapeutic Potential in Cancer: Mechanism of Action and Clinical Implications. *Molecules (Basel, Switzerland)*, 28(13), 5246.
- **54.** Li, Y., Yang, Y., (2019). PRMT5 Promotes Human Lung Cancer Cell Apoptosis via Akt/Gsk3β Signaling Induced by Resveratrol. *Cell transplantation*, 28(12), 1664–1673.
- **55.** Vlummens, P., Verhulst, S., (2022). Inhibition of the Protein Arginine Methyltransferase PRMT5 in High-Risk Multiple Myeloma as a Novel Treatment Approach. *Frontiers in cell and developmental biology*, *10*, 879057.
- **56.** Kong, J., Wang, Z., (2023). Protein Arginine Methyltransferases 5 (PRMT5) affect Multiple Stages of Autophagy and Modulate Autophagy-related Genes in Controlling Breast Cancer Tumorigenesis. *Current cancer drug targets*, 23(3), 242–250.
- **57.** Ghadimi, M., Foroughi, F., Hashemipour, S., Rashidi Nooshabadi, M., Ahmadi, M. H., Ahadi Nezhad, B., & Khadem Haghighian, H. (2021). Randomized double-blind clinical trial examining the Ellagic acid effects on glycemic status, insulin resistance, antioxidant, and inflammatory factors in patients with type 2 diabetes. *Phytotherapy research: PTR*, *35*(2), 1023–1032. https://doi.org/10.1002/ptr.6867
- **58.** Lu, W., Zhang, R., Jiang, H., Zhang, H., & Luo, C. (2018). Computer-Aided Drug Design in Epigenetics. *Frontiers in Chemistry*, *6*, 348111. https://doi.org/10.3389/fchem.2018.00057
- **59.** Mhatre, S., Naik, S., & Patravale, V. (2021). A molecular docking study of EGCG and theaflavin digallate with the druggable targets of SARS-CoV-2. *Computers in biology and medicine*, *129*, 104137. https://doi.org/10.1016/j.compbiomed.2020.104137
- **60.** Pinzi, L., & Rastelli, G. (2019). Molecular Docking: Shifting Paradigms in Drug Discovery. *International Journal of Molecular Sciences*, 20(18). https://doi.org/10.3390/ijms20184331
- **61.** Saeki, K., Hayakawa, S., Nakano, S., Ito, S., Oishi, (2018). In Vitro and In Silico Studies of the Molecular Interactions of Epigallocatechin-3-O-gallate (EGCG) with Proteins That Explain the Health

- Benefits of Green Tea. *Molecules : A Journal of Synthetic Chemistry and Natural Product Chemistry*, 23(6). https://doi.org/10.3390/molecules23061295
- **62.** Meng, Y., Zhang, X., Mezei, M., & Cui, M. (2011). Molecular Docking: A powerful approach for structure-based drug discovery. *Current Computer-Aided Drug Design*, 7(2), 146. https://doi.org/10.2174/157340911795677602
- **63.** Chen, S. Q., Li, J. Q et al., (2020). EZH2-inhibitor DZNep enhances apoptosis of renal tubular epithelial cells in presence and absence of cisplatin. *Cell division*, *15*, 8. https://doi.org/10.1186/s13008-020-00064-3
- **64.** Xia, T., Liu, M., et al., (2021). PRMT5 regulates cell pyroptosis by silencing CASP1 in multiple myeloma. *Cell death & disease*, *12*(10), 851. https://doi.org/10.1038/s41419-021-04125-
- **65.** Brobbey, C., Yin, S., et al., (2023). Autophagy dictates sensitivity to PRMT5 inhibitor in breast cancer. *Scientific reports*, *13*(1), 10752. https://doi.org/10.1038/s41598-023-37706-9
- **66.** Mollah, S. A., & Subramaniam, S. (2020). Histone Signatures Predict Therapeutic Efficacy in Breast Cancer. *IEEE open journal of engineering in medicine and biology*, 1, 74–82. https://doi.org/10.1109/OJEMB.2020.2967105
- **67.** Du, X., Li, Y., Xia, L., Ai, M., Liang, J., Sang, P., Ji, L., & Liu, Q. (2016). Insights into Protein–Ligand Interactions: Mechanisms, Models, and Methods. *International Journal of Molecular Sciences*, *17*(2). https://doi.org/10.3390/ijms17020144

CHAPTER#4

TO INVESTIGATE THE TUMOR INHIBITORY POTENTIAL OF PHYTOCOMPOUNDS USING MOUSE XENOGRAFTS

4.1 Introduction

Phytocompounds, bioactive substances derived from plants, have garnered significant attention for their potential anti-cancer properties. These natural compounds offer a promising alternative to conventional chemotherapeutic agents due to their diverse mechanisms of action and generally lower toxicity [1-3]. In the previous chapters, we demonstrated that EGCG and EA, both individually and in combination, showed substantial inhibition of cancer cell proliferation in *in silico* and *in vitro* models. However, to fully ascertain their therapeutic potential, their efficacy and safety need rigorous validation *in vivo*. While *in-vitro* studies provide valuable insights into their mechanisms of action, translating these findings to complex biological systems such as animal models are crucial. Animal models, particularly mice xenograft models utilizing cell lines derived from human tumors, closely mimic the human tumor microenvironment, allowing for a comprehensive evaluation of efficacy, pharmacokinetics, and toxicity profiles of phytocompounds [4]. These models enable the study of tumor growth, metastasis, and overall survival in a living organism, providing critical data necessary for progressing towards clinical trials [5-6].

In-vivo studies are essential for several reasons, including the complexity of biological interactions, pharmacokinetics, pharmacodynamics, and toxicity assessment. Mice xenograft models making process involves the transplantation of human tumor cells into immunocompromised mice, are particularly valuable for evaluating tumor inhibition, studying metastasis, and exploring combination therapies ^[1,7,8]. The primary objectives of validating the tumor inhibitory potential of EGCG and EA using these models include determining their ability to inhibit tumor growth, assessing their impact on survival, understanding their pharmacokinetic profiles, and evaluating their safety. Successful *in vivo* validation of these phytocompounds will pave the way for preclinical studies, clinical trials, and the development of new, plant-derived anti-cancer therapies that offer improved outcomes with fewer side effects. This chapter will discuss the detailed methodologies, results, and implications of *in vivo* studies involving the use of EGCG and EA in mice xenograft models, providing critical insights into their potential as effective anti-cancer agents.

4.2 Materials and methods

Swiss nude mice (female, 4 weeks old) were obtained from the Centre for Cellular and Molecular Biology (CCMB) laboratories in Hyderabad and housed in the University of Hyderabad animal house facility. Ethical approval for all animal procedures was obtained from

the institutional ethics committee (UH/IAEC/SRK/2021-1/49), and the experiments were conducted following the university's guidelines for the care and use of laboratory animals. The mice were housed in cages maintained at 22±4°C with humidity ranging from 50% to 60%, under a 12-hour light/dark cycle. They had ad libitum access to standard laboratory diet and drinking water and were allowed to acclimatize for one week. Subsequently, the mice were randomly assigned to three groups, each consisting of seven mice: (1) Control group-1, (2) Control group-2, and (3) Treatment group.

4.2.1 Tumor Xenografts

MDA-MB-231 cell lines obtained from ATCC were used to establish xenografts following established protocols (reference 24). Each mouse was subcutaneously injected with 2x10⁶ MDA-MB-231 cells on both flanks. Tumor volume was measured every three days using digital vernier calipers and calculated using the formula: Tumor volume = width² x length / 2. Once the tumors reached a volume of 100 mm³, treatment with EA and a combination of EGCG+EA (100 mg/kg) was initiated and continued for 21 days. Tumor samples were harvested at the end of the treatment period for subsequent weighing and analysis.

4.2.2 Preparation of Lysate from Tumor Samples

Tumor tissues from both the treatment and control groups were excised and weighed. The tissues were rinsed with cold 1x PBS and diced into small fragments while maintaining them on ice. Subsequently, 300 µL of ice-cold RIPA buffer supplemented with protease inhibitors was added, and the tissue was homogenized using an electric homogenizer with continuous agitation for 1 hour at 4°C. After homogenization, the lysate was centrifuged at 12,000 rpm for 20 minutes at 4°C. The resulting supernatant was carefully transferred to a new tube kept on ice, and the pellet was discarded. Protein concentration was determined using the BCA assay, and the lysates were then subjected to western blot analysis following the protocol described in the corresponding chapter of the thesis.

4.2.3 Immunohistochemical Assays

Tumor tissues collected from both experimental and control mice were fixed overnight in 10% neutral buffered formalin, embedded in paraffin, and sectioned. Hematoxylin and eosin (H&E) staining was carried out according to the procedure outlined by (24) to visualize cellular and tissue structures in detail. For additional histochemical examinations, tissue sections were deparaffinized and subjected to immunohistochemistry (IHC) using anti-Ki67 antibodies to

evaluate proliferative activity. The stained tissue sections were observed under a microscope after being treated with DAB for visualization.

4.2.4 Study Design

The study aimed to assess the potential anti-tumor effects of phytocompounds using an *in vivo* mice xenograft model. Female Swiss nude mice, aged 4 weeks, were obtained from the Centre for Cellular and Molecular Biology (CCMB) laboratories in Hyderabad and housed in the University of Hyderabad animal facility. Ethical approval for all animal procedures (UH/IAEC/SRK/2021-1/49) was obtained, and guidelines for the care and use of laboratory animals issued by the university authorities were strictly followed. The mice were housed in cages maintained at 22±4°C with humidity levels between 50% and 60%, under a 12-hour light/dark cycle. They had access to standard laboratory diet and water ad libitum. After a one-week acclimatization period, the mice were randomly assigned to three groups, each consisting of seven mice: Control group-1, Control group-2, and Treatment groups 3-5 (Table-4.1).

Table 4.1: Grouping of Mice

S.no	Group name	Number of mice per group	Treatment description	
	G . 1.1	inice per group		
1	Control-1	1	No treatment	
2	Control-2	7	Vehicle control (solvent for EA and EGCG)	
3	EA Treatment	7	EA	
4	EGCG Treatment	7	EGCG	
5	Combination Treatment	7	Combination of EGCG and EA	

4.2.5 Body Weight Measurement and Random Grouping Before Tumor Induction

Before the induction of tumors, the weight of each mouse's body was recorded to ensure even distribution of weights across the groups. The mice were subsequently assigned randomly to three groups: Control group-1, Control group-2, and Treatment groups 3-5, ensuring that each group had an equal number of mice with similar body weights. This randomization helped in minimizing any biases and variations that could affect the outcomes of the study.

4.2.6 Cell Lines Derived Xenograft Model Development

To establish the xenograft model, MDA-MB-231 cell lines sourced from ATCC were utilized. The mice received subcutaneous injections of 2x10⁶ MDA-MB-231 cells on both flanks. Tumor volume was measured every three days using digital vernier calipers and calculated

using the formula: Tumor volume = (width 2 x length)/2. Once the tumors reached a volume of 100 mm^3 , treatment with EA and a combination of EGCG + EA (100 mg/kg) was initiated and continued for 21 days.

4.2.7 Tumor Size Measurement by Digital Vernier Caliper

Tumor dimensions were assessed every three days using a digital vernier caliper, recording both width and length measurements. Tumor volume was calculated using the standard formula $= (width^2 x length)/2$. This consistent monitoring allowed for accurate tracking of tumor growth and the assessment of the treatment's efficacy.

4.2.8 Mice Body Mass Measurement

In addition to tumor size, the body mass of the mice was measured regularly throughout the study. This was crucial to monitor the overall health and well-being of the mice and to detect any potential toxicity or adverse effects of the treatments. Body mass measurements were taken at the same intervals as the tumor size measurements to ensure comprehensive monitoring.

4.2.9 Drug Administration Schedule & Drug Preparation for Oral Dosage

The drug administration schedule was carefully planned to ensure consistent dosing. EGCG, EA, and their combination were orally administered at a dose of 100 mg/kg. The phytocompounds were prepared fresh daily, dissolved in an appropriate vehicle to ensure proper absorption, and administered using oral gavage. This method ensured that the mice received the precise dosage required for the study. The detailed information of drug dosage for 21 days was tabulated in table 4.2.

4.2.10 Tumor Growth Inhibition (TGI) Studies

TGI studies were performed by comparing the tumor volumes in treated groups to those in control groups. The effectiveness of the treatments was evaluated based on the reduction in tumor size compared to the control groups. At the end of the 21-day treatment period, tumor samples were collected for further analysis, including weighing to evaluate the reduction in tumor burden.

 Table 4.2: Drug Dosage Schedule for 21 Days

Day	Control Group-1	Control Group-2	EA Treatment Group	EGCG Treatment Group	Combination Treatment Group
1	No treatment	Vehicle control	100 mg/kg EA	100 mg/kg EGCG	EGCG 50 mg/kg + EA 50 mg/kg
2	No treatment	Vehicle control	100 mg/kg EA	100 mg/kg EGCG	EGCG 50 mg/kg + EA 50 mg/kg
3	No treatment	Vehicle control	100 mg/kg EA	100 mg/kg EGCG	EGCG 50 mg/kg + EA 50 mg/kg
4	No treatment	Vehicle control	100 mg/kg EA	100 mg/kg EGCG	EGCG 50 mg/kg + EA 50 mg/kg
5	No treatment	Vehicle control	100 mg/kg EA	100 mg/kg EGCG	EGCG 50 mg/kg + EA 50 mg/kg
6	No treatment	Vehicle control	100 mg/kg EA	100 mg/kg EGCG	EGCG 50 mg/kg + EA 50 mg/kg
7	No treatment	Vehicle control	100 mg/kg EA	100 mg/kg EGCG	EGCG 50 mg/kg + EA 50 mg/kg
8	No treatment	Vehicle control	100 mg/kg EA	100 mg/kg EGCG	EGCG 50 mg/kg + EA 50 mg/kg
9	No treatment	Vehicle control	100 mg/kg EA	100 mg/kg EGCG	EGCG 50 mg/kg + EA 50 mg/kg
10	No treatment	Vehicle control	100 mg/kg EA	100 mg/kg EGCG	EGCG 50 mg/kg + EA 50 mg/kg
11	No treatment	Vehicle control	100 mg/kg EA	100 mg/kg EGCG	EGCG 50 mg/kg + EA 50 mg/kg
12	No treatment	Vehicle control	100 mg/kg EA	100 mg/kg EGCG	EGCG 50 mg/kg + EA 50 mg/kg
13	No treatment	Vehicle control	100 mg/kg EA	100 mg/kg EGCG	EGCG 50 mg/kg + EA 50 mg/kg
14	No treatment	Vehicle control	100 mg/kg EA	100 mg/kg EGCG	EGCG 50 mg/kg + EA 50 mg/kg
15	No treatment	Vehicle control	100 mg/kg EA	100 mg/kg EGCG	EGCG 50 mg/kg + EA 50 mg/kg
16	No treatment	Vehicle control	100 mg/kg EA	100 mg/kg EGCG	EGCG 50 mg/kg + EA 50 mg/kg
17	No treatment	Vehicle control	100 mg/kg EA	100 mg/kg EGCG	EGCG 50 mg/kg + EA 50 mg/kg
18	No treatment	Vehicle control	100 mg/kg EA	100 mg/kg EGCG	EGCG 50 mg/kg + EA 50 mg/kg
19	No treatment	Vehicle control	100 mg/kg EA	100 mg/kg EGCG	EGCG 50 mg/kg + EA 50 mg/kg
20	No treatment	Vehicle control	100 mg/kg EA	100 mg/kg EGCG	EGCG 50 mg/kg + EA 50 mg/kg
21	No treatment	Vehicle control	100 mg/kg EA	100 mg/kg EGCG	EGCG 50 mg/kg + EA 50 mg/kg

4.2.11 Western Blotting

For western blot analysis, tumor tissues from both the treated and control groups were harvested and weighed. The tissues were rinsed with chilled 1x PBS, cut into small pieces, and homogenized in ice-cold RIPA buffer supplemented with a protease inhibitor cocktail. The homogenate was centrifuged at 12,000 rpm for 20 minutes at 4°C, and the resulting supernatant was collected. Protein concentrations were determined using the BCA assay, and equal amounts of proteins were loaded onto 10% SDS-PAGE gels. Subsequently, proteins were transferred onto nitrocellulose membranes, which were blocked and then incubated with primary and secondary antibodies. Band intensities were analyzed using a Versadoc Imaging System and Image Lab 5.1 software (Bio-Rad).

4.2.12 Immunohistochemistry Tests

Tumor tissues from both experimental and control mice were fixed in 10% neutral buffered formalin overnight, followed by embedding in paraffin and sectioning. Immunohistochemical analysis was conducted using anti-Ki67 antibodies to evaluate cell proliferation. The sections underwent deparaffinization, rehydration, and antigen retrieval prior to incubation with primary antibodies. After washing, HRP-conjugated secondary antibodies were applied, followed by staining with DAB and counterstaining with hematoxylin. The stained sections were examined under a microscope for visualization.

4.2.13 H & E Staining

Hematoxylin and eosin (H&E) staining was conducted on paraffin-embedded sections of tumor tissue to visualize cellular and tissue structures. The sections were deparaffinized, rehydrated, and stained with haematoxylin to identify cell nuclei. Eosin was used to stain the cytoplasm and extracellular matrix. The stained sections were then dehydrated, cleared, and mounted for microscopic examination. This staining method provided detailed insights into the morphological changes induced by the treatments. This comprehensive methodology outlines the in vivo validation of the anti-tumor potential of EGCG, EA, and their combination, ensuring a thorough evaluation of their efficacy and safety.

4.3 Results

4.3.1 Impact of EGCG on tumor xenograft mouse model:

To evaluate the *in vivo* anti-tumor effects of EGCG, MDA-MB231 cells were subcutaneously injected into Swiss nude mice to establish tumor xenografts. Tumor weights were subsequently measured. Treatment with EGCG at 100mg/kg resulted in significant reductions in tumor volume compared to control groups (Fig 4.3.1a-C). Throughout the experiment, the body weight of mice in the control group remained relatively stable (Fig 4.3.1d).

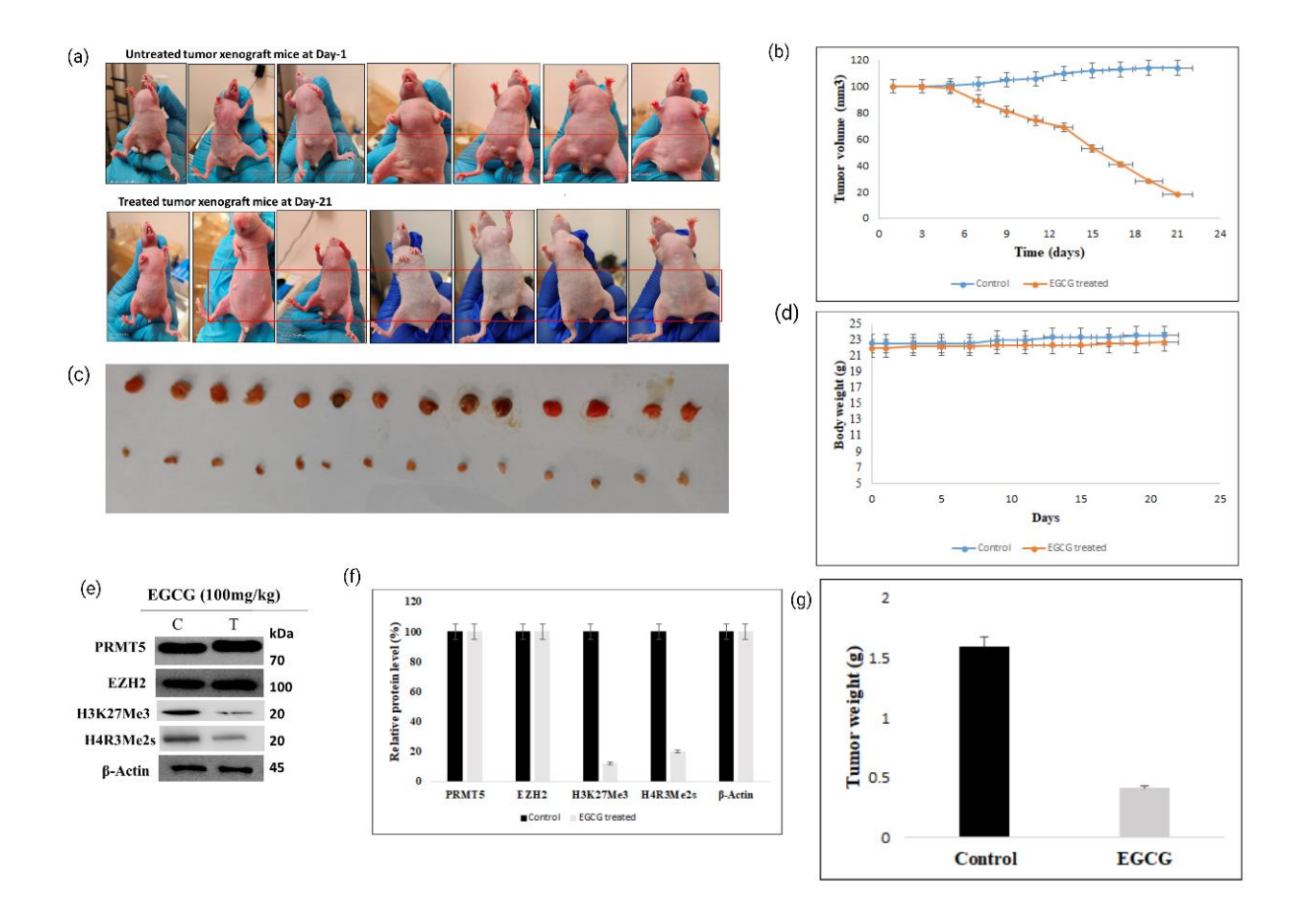


Figure 4.3.1: *In-vivo* Xenograft Studies with oral EGCG Dosage - The mice were randomly divided into three groups, each containing 7 mice: (1) control group-1, (2) control group-2, and (3) treatment group. MDA-MB231 cells were injected subcutaneously into both flanks of the mice. Tumor volume was measured every three days. Once the tumor volume reached 100 mm³, EGCG (100 mg/kg) was administered orally to the treatment group for 21 days. (a) Comparison of EGCG-treated vs. control mice: the first mouse on the left is a control mouse, and the remaining mice (2nd to 7th) bear tumors on the first day of treatment. (b) Tumor growth measurement: the top panel shows control animals, and the bottom panel shows the treatment group. (c) Tumor volume comparison graphs (control vs. treated mice). (d) Body weight measurement graphs (control vs. treated). (e-f) Western blot analysis of tumor lysates from the treatment group, showing levels of PRMT5, EZH2, H4R3me2s, and H3K27me3, with β-actin used as the loading control. (g) Tumor weight comparison graphs (control vs. treated).

H&E staining of tumor tissues revealed that control tumors exhibited highly aggressive sarcomatous neoplastic cells with a vacuolated appearance and a high number of mitotic figures (Fig 4.3.2a-b). In contrast, tumors treated with EGCG showed only subcutaneous and muscular layers without dermal and epidermal tumor regions (Fig 4.3.2c-d). Assessment of cell proliferation using the Ki-67 marker via immunohistochemistry (IHC) demonstrated that EGCG significantly reduced Ki-67 levels in treated tumors compared to controls (Fig 4.3.2e-j). Western blot analysis confirmed that EGCG treatment led to a marked reduction in the catalytic products of PRMT5 (H4R3me2s) and EZH2 (H3K27me3) in tumors (Fig 4.3.1e-f).

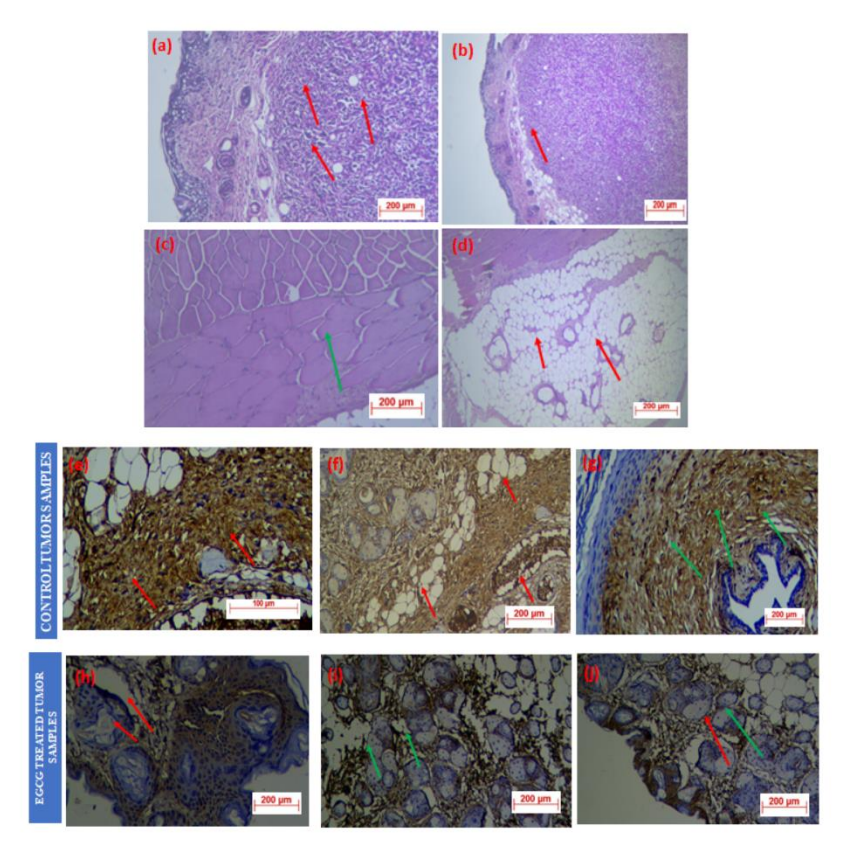


Figure 4.3.2: Immunohistochemistry Studies for EGCG treated mice group - After 21 days of drug administration, mice were euthanized, and tumors were collected from each group (control and treated) for immunohistochemistry (IHC) studies. Tumor samples were analyzed by a histopathology expert to compare control tumors with EGCG-treated tumors. (a-b) H&E staining of control samples revealed highly aggressive neoplastic sarcomatous cells forming nodules in the subcutaneous region and invading the dermal region, with mitotic figures indicated by red arrows. (c-d) EGCG-treated tumor samples showed only subcutaneous and muscular layers, with no tumor regions in the dermal and epidermal layers. The subcutaneous region with adipocytes appeared normal with no metastatic invasion of neoplastic cells (red arrow in d), and the muscular region appeared normal with no metastatic invasion (green arrow in c). (e-g) Ki-67 expression in control tumor samples showed severe expression in the subcutaneous tumor mass (red arrows in e-f) and in neoplastic cells invading the dermal region and hair follicles (green arrow in g). (h-j) EGCG-treated tumor samples showed 10-20 percent Ki-67 expression in pleomorphic anaplastic epithelial cells in the epidermal layer (red arrows). Overexpression of Ki-67 in stromal tissue in the dermal and subcutaneous regions is indicated by green arrows (i-j).

4.3.2 Impact of EA on tumor xenograft mouse model:

To evaluate the *in vivo* anti-tumor effects of EA, MDA-MB231 cells were subcutaneously implanted into Swiss nude mice to establish tumor xenografts, as described previously. Once tumors developed, their weights were measured, and EA was administered at a dosage of 100 mg/kg daily for 21 days. The findings revealed a notable decrease in tumor volume compared to the control groups (Fig 4.4a-c). Conversely, the body weight of mice in the control group exhibited steady increase throughout the experimental period (Fig 4.4g).

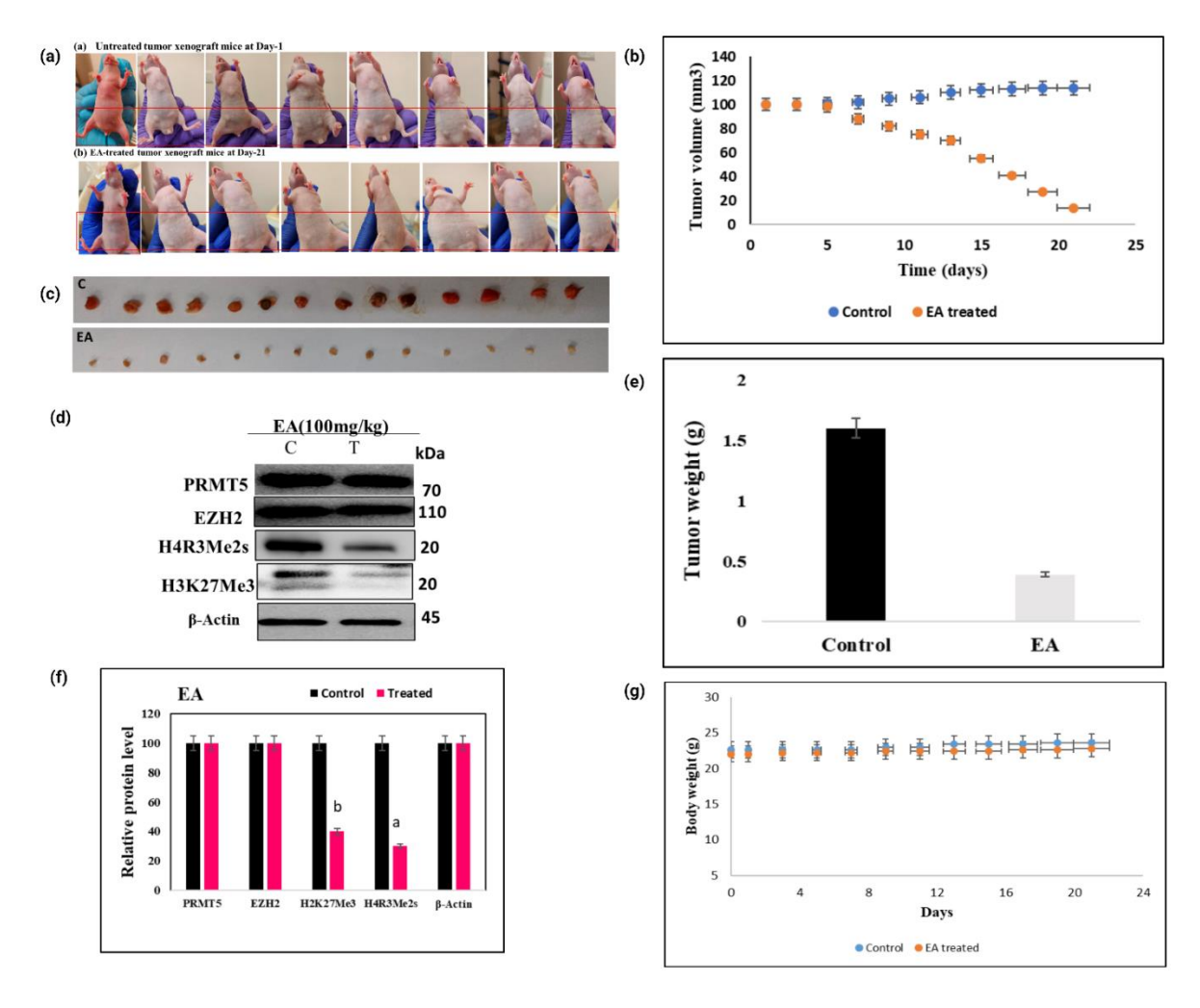


Figure 4.4: *In-vivo* **Xenograft Model Studies with oral EA Dosage** - Mice were randomly assigned to three groups, each containing 7 mice: (1) control group-1, (2) control group-2, and (3) treatment group. MDA-MB231 cells were injected subcutaneously into both flanks of the mice. Tumor volume was monitored every three days, and once it reached 100 mm³, oral administration of EA (100 mg/kg) was initiated for the treatment group and continued for 21 days. (a) Comparative analysis of mice, with the first mouse representing the control group and the remaining mice (2^{nd} to 7^{th}) showing tumor development on the first day of treatment. (b) Graph showing tumor volumes over the 21-day period, comparing control, and treated mice. (c) Evaluation of tumor growth, with the upper panel showing control animals and the lower panel showing treated animals. (d) Western blot analysis of tumor lysates from the treatment group, examining levels of EZH2, PRMT5, H3K27me3, H4R3me2s, with β-actin as the loading control. (e) Graph illustrating tumor weights between control and treated groups. (f) Comparison of protein intensity levels observed in western blot studies between control and treated groups. (g) Graph showing body weight measurements of control and treated mice.

To assess the potential toxicity of EA, we conducted H&E staining on tumor tissues. Comparing control tumors to those treated with EA revealed significant differences. Tumors in the control group displayed highly aggressive sarcomatous neoplastic cells with a vacuolated appearance and elevated mitotic activity (Fig 4.4.1ai, aii).

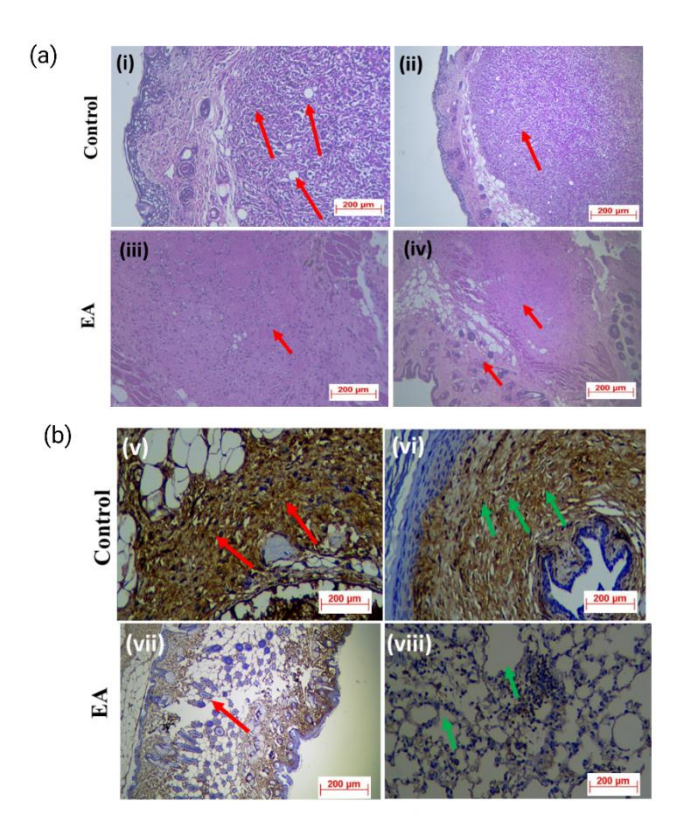


Figure 4.4.1: Immunohistochemistry (IHC) Studies for EA treated mice group - After 21 days of drug administration, the mice were euthanized according to IEC rules, and tumors were collected from the control and treated groups. An expert histopathologist examined the tumor samples for IHC studies to compare control tumors with those treated with EA. In the H&E staining analysis (Fig 4.4.1a (i, ii)), control tumor samples exhibited aggressive neoplastic sarcomatous cells forming nodules in the subcutaneous region and invading the dermal region, as indicated by mitotic figures (red arrows). In contrast, EA-treated tumor samples (Fig 4.4.1a (iii-vi)) displayed only subcutaneous and muscular layers, with no dermal or epidermal tumor regions. The subcutaneous region appeared normal with no metastatic invasion of neoplastic cells (red arrow), and the muscular region showed no metastatic invasion (green arrow). Regarding Ki67 expression (Fig 4.4.1b (v-viii)), control tumor samples demonstrated intense Ki67 expression in the subcutaneous tumor mass (red arrows), with neoplastic cells invading the dermal region and hair follicles (green arrow in viii). Conversely, EA-treated tumor samples showed 10-20% Ki67 expression in pleomorphic anaplastic epithelial cells in the epidermal layer (red arrows). Overexpression of Ki67 was also observed in the stromal tissue of the dermal and subcutaneous regions (green arrows).

Alternatively, treated tumors exhibited sections containing only subcutaneous and muscular layers, without dermal and epidermal tumor regions (Fig 4.4.1a (iii-iv)). Cell proliferation was evaluated using Ki-67, a proliferation marker. Immunohistochemistry (IHC) analysis showed that EA treatment significantly reduced Ki-67 levels in the treated groups compared to the control group (Fig 4.4.1b (v-viii)). To further evaluate the impact of EA on EZH2 and PRMT5

activity, we measured the levels of their catalytic products in tumors from control and EA-treated groups using western blot analysis. The results indicated a significant reduction in H4R3me2s and H3K27me3 levels in EA-treated tumors compared to the control (Fig 4.4d-f).

4.3.3 Impact of Combo on tumor xenografts mouse model:

To evaluate the anti-tumor effects of the combo *in vivo*, MDA-MB231 cells were subcutaneously implanted into Swiss nude mice to create tumor xenografts, as outlined in the methods section. Once the tumors developed, their weights were measured, and the combo treatment was administered at a dosage of 100 mg/kg for up to 21 days. The results indicated a significant reduction in tumor volume compared to the control groups (Fig 4.5a-c). In contrast, the body weight of the control group mice steadily increased throughout the experimental period (Fig 4.5g).

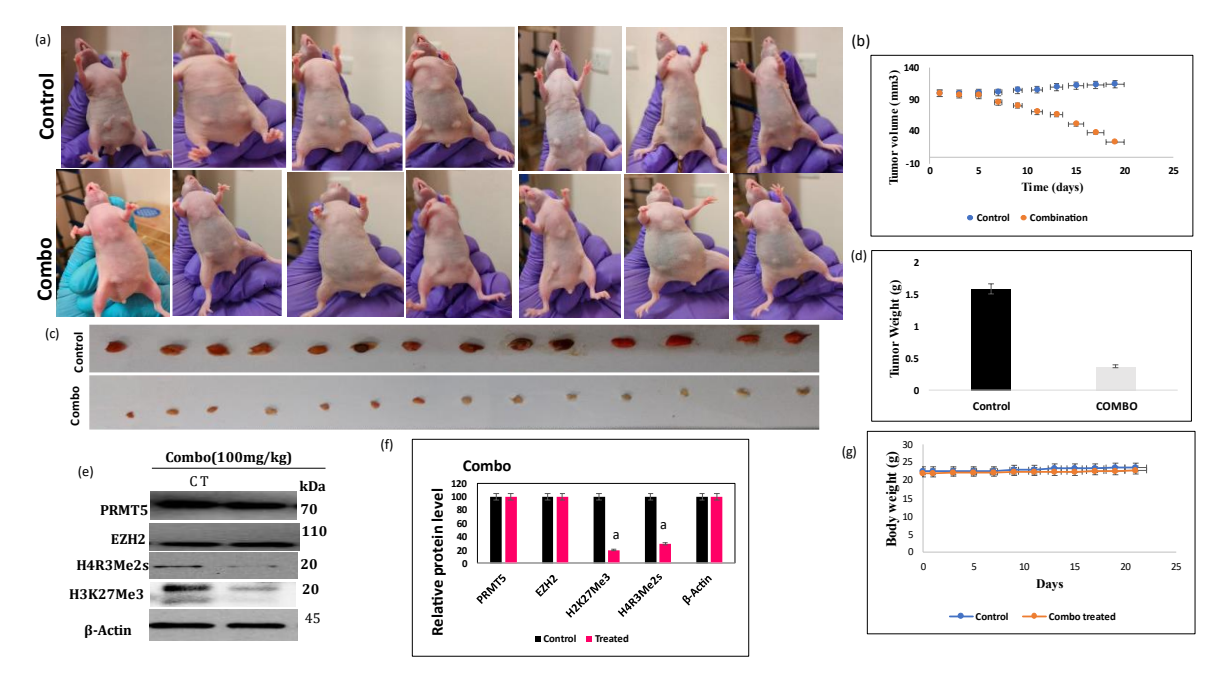


Figure 4.5: *In-vivo* **Xenograft Model Studies with oral Combo Dosage** - Mice were randomly assigned to three groups, each containing 7 mice: (1) control group-1, (2) control group-2, and (3) treatment group. MDA-MB231 cells were injected subcutaneously into both flanks of the mice. Tumor volume was monitored every three days, and once it reached 100 mm³, oral administration of combo (EA (50mg) +EGCG 50 mg/kg) was initiated for the treatment group and continued for 21 days. (a) Comparative analysis of mice, with the first mouse representing the control group and the remaining mice (2nd to 7th) showing tumor development on the first day of treatment. (b) Graph showing tumor volumes over the 21-day period, comparing control, and treated mice. (c) Evaluation of tumor growth, with the upper panel showing control animals and the lower panel showing treated animals. (d) Western blot analysis of tumor lysates from the treatment group, examining levels of EZH2, PRMT5, H3K27me3, H4R3me2s, with β-actin as the loading control. (e) Graph illustrating tumor weights between control and treated groups. (f) Comparison of protein intensity levels observed in western blot studies between control and treated groups. (g) Graph showing body weight measurements of control and treated mice.

Additionally, to assess the potential toxicity of the combo treatment, H&E staining was conducted on tumor tissues. Comparing control tumors to those treated with the combo revealed significant differences. Tumors in the control group displayed highly aggressive sarcomatous neoplastic cells with a vacuolated appearance and heightened mitotic activity (Fig 4.5.1a-d).

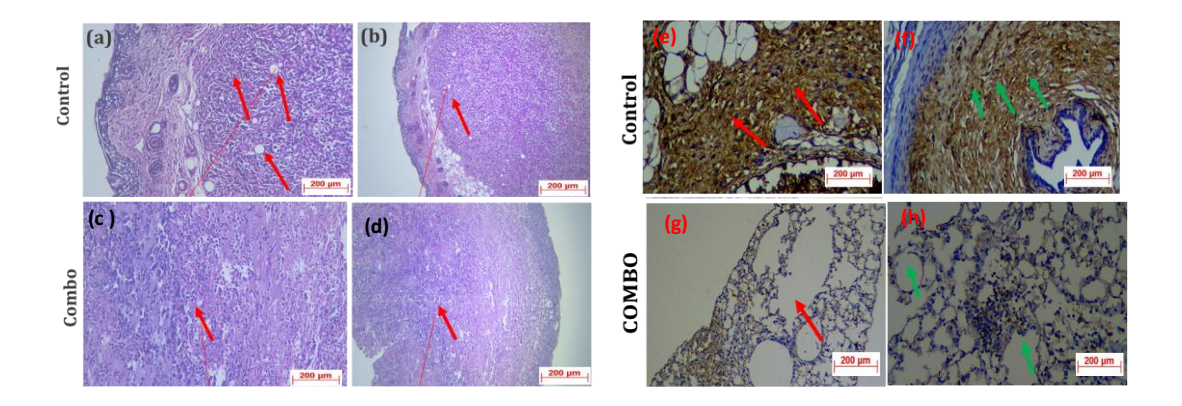


Figure 4.5.1: Immunohistochemistry (IHC) Studies for Combo treated mice group - After 21 days of drug administration, the mice were euthanized according to IEC rules, and tumors were collected from the control and treated groups. An expert histopathologist examined the tumor samples for IHC studies to compare control tumors with those treated with EA. In the H&E staining analysis (Fig 4.5.1a (i, ii)), control tumor samples exhibited aggressive neoplastic sarcomatous cells forming nodules in the subcutaneous region and invading the dermal region, as indicated by mitotic figures (red arrows). In contrast, EA-treated tumor samples (Fig 4.5.1a (iii-vi)) displayed only subcutaneous and muscular layers, with no dermal or epidermal tumor regions. The subcutaneous region appeared normal with no metastatic invasion of neoplastic cells (red arrow), and the muscular region showed no metastatic invasion (green arrow). Regarding Ki67 expression (Fig 4.5.1e-h), control tumor samples demonstrated intense Ki67 expression in the subcutaneous tumor mass (red arrows), with neoplastic cells invading the dermal region and hair follicles (green arrow in viii). Conversely, Combo -treated tumor samples showed 10-20% Ki67 expression in pleomorphic anaplastic epithelial cells in the epidermal layer (red arrows). Overexpression of Ki67 was also observed in the stromal tissue of the dermal and subcutaneous regions (green arrows).

In disparity, treated tumors exhibited sections containing only subcutaneous and muscular layers, devoid of dermal and epidermal tumor regions (Fig 4.5.1a (iii-iv)). The proliferation of cells was evaluated using Ki-67, a marker of proliferation. Immunohistochemistry (IHC) analysis revealed that the Combo treatment significantly reduced Ki-67 levels in the treated groups compared to the control group (Fig 4.5.1b (v-viii)). To further evaluate the impact of Combo on EZH2 and PRMT5 activity, we measured the levels of their catalytic products in tumors from both control and Combo-treated groups using western blot analysis. The results indicated a significant reduction in H4R3me2s and H3K27me3 levels in tumors treated with Combo compared to the control (Fig 4.5d-f).

4.4 Discussion

In vivo validation constitutes a pivotal phase in preclinical research, playing a crucial role in linking *in vitro* findings to clinical trial outcomes [9]. This stage is indispensable for assessing the effectiveness, pharmacokinetics, and safety profiles of prospective therapeutic substances within a live organism. Within the realm of cancer research, *in vivo* models offer invaluable insights into the intricate interactions between compounds and biological systems, encompassing the tumor microenvironment and immune responses [9]. The evolving landscape of epigenetic drugs (epidrugs) underscores their promise in cancer therapy, underscoring the imperative for rigorous preclinical validation prior to advancing to clinical trials [10,11]. These advancements highlight the significance of *in vivo* experimentation in substantiating the therapeutic potential of epidrugs, thereby guiding their translation from bench to bedside.

In this investigation, our focus is on exploring the anti-tumor properties of EGCG, EA, and their combined administration using xenograft mouse models induced with MDA-MB231 cells. Throughout a 21-day experimental period, we noted a notable decrease in tumor dimensions across all treatment cohorts. This finding resonates with prior studies indicating that synthetic compounds targeting EZH2 and PRMT5 exhibit efficacy in tumor size reduction, thereby contributing to cancer remission [12-14]. These results underscore the potential therapeutic benefits of EGCG, EA, and their combined application in combating cancer progression, providing a foundation for further clinical exploration in cancer therapy.

Over the 21-day experimental period, treatment with EGCG and EA led to a substantial decrease in tumor size. [15-21]. This reduction was coincided with by decreased levels of H3K27me3 and H4R3me2s, indicative of their epigenetic modulatory effects. However, western blot analysis of tumor samples did not result in a reduction of EZH2 and PRMT5 protein levels, suggesting that while EGCG and EA inhibits the catalytic products of these enzymes, it does not affect their overall expression. The observed decrease in tumor size was further supported by a substantial reduction in the proliferative marker Ki-67. Despite these findings, direct evidence linking the reduction in tumor size to decreased histone mark levels via specific signaling pathways or promoter occupancy remains elusive [15-21].

Numerous preclinical studies and clinical trials have demonstrated the anticancer potential of EGCG [15-24]. Clinical trials have confirmed the safety and efficacy of EGCG, showing that doses of 200 mg/day were well-tolerated, particularly in the context of prostate cancer. [22].

Additionally, studies on bladder cancer patients disclosed EGCG accumulation in cancer tissue and a decrease in proliferation levels [23]. In colorectal cancer patients, TeavigoTM, a known highly green tea extract consists 94% of purified EGCG, demonstrated chemo preventive effects at 450 mg/day [24]. Our study aligns with these findings, showing a significant reduction in tumor size and histone mark levels in MDA-MB231-induced xenografts treated with EGCG. The observed decrease in Ki-67 further supports its potential as an effective anticancer agent [15-24]. Although the direct relationship between Ki-67 reduction and decreased levels of H4R3me2s and H3K27me3 was not established, the inhibitory/modulatory effects of EGCG on the catalytic activity of PRMT5 and EZH2 highlight its promise for cancer therapy [15-24].

In conclusion, our comprehensive approach, integrating *in silico*, *in vitro*, and *in vivo* models, underscores the therapeutic potential of EA and EGCG as epidrugs. EA's ability to inhibit oncogenic PRMT5 and EZH2 without affecting their expression levels suggests it as a potent anti-cancer agent. Similarly, EGCG shows promise in reducing tumor size and modulating histone marks associated with cancer progression. These natural compounds represent novel avenues for developing effective inhibitors of epigenetic regulators like PRMT5 and EZH2, thereby advancing cancer treatment strategies [15-24].

Additionally, immunohistochemistry (IHC) analysis demonstrated that EGCG, EA and their combination treatment significantly reduced the levels of Ki-67, a marker of cell proliferation, in the treated tumor samples compared to controls. This decrease in Ki-67 levels further supports the anti-proliferative effects of with EGCG, EA and their combination. The consistent reduction in both histone methylation marks and the Ki-67 proliferation marker underscores the potential of with EGCG, EA and their combination as a potent anti-cancer agent. In conclusion, our study shed the light on the potential of EGCG, EA, and their combination as effective anti-cancer or anti-proliferative agents. These findings underscore the significance of in vivo validation in preclinical research and support the continued exploration of natural compounds as epidrugs. The significant reduction in tumor size and proliferation markers observed in our study suggests promising therapeutic potential, warranting further investigation in clinical settings

4.5 References:

Dehelean, C. A., Marcovici, I., Soica, C., Mioc, M., Coricovac, D., Iurciuc, S., Cretu, O. M., & Pinzaru, I. (2021). Plant-Derived Anticancer Compounds as New Perspectives in Drug Discovery and Alternative Therapy. *Molecules (Basel, Switzerland)*, 26(4), 1109. https://doi.org/10.3390/molecules26041109

- Naeem, A., Hu, P., Yang, M., Zhang, J., Liu, Y., Zhu, W., & Zheng, Q. Natural Products as Anticancer Agents: Current Status and Future Perspectives. *Molecules*, 27(23), 8367. https://doi.org/10.3390/molecules27238367
- 3. Asma, S. T., Acaroz, U., Imre, K., Morar, A., Ali Shah, S. R., Hussain, S. Z., Arslan-Acaroz, D., Demirbas, H., Hajrulai-Musliu, Z., Istanbullugil, F. R., Soleimanzadeh, A., Morozov, D., Zhu, K., Herman, V., Ayad, A., Athanassiou, C., & Ince, S. (2022). Natural Products/Bioactive Compounds as a Source of Anticancer Drugs. *Cancers*, 14(24). https://doi.org/10.3390/cancers14246203
- 4. Domínguez-Oliva, A., Hernández-Ávalos, I., Martínez-Burnes, J., Olmos-Hernández, A., Verduzco-Mendoza, A., & Mota-Rojas, D. (2023). The Importance of Animal Models in Biomedical Research: Current Insights and Applications. *Animals : An Open Access Journal From MDPI*, 13(7). https://doi.org/10.3390/ani13071223
- 5. Bouchalova, P., & Bouchal, P. (2022). Current methods for studying metastatic potential of tumor cells. *Cancer Cell International*, 22. https://doi.org/10.1186/s12935-022-02801-w
- **6.** Sajjad, H., Imtiaz, S., Noor, T., Siddiqui, Y. H., Sajjad, A., & Zia, M. (2021). Cancer models in preclinical research: A chronicle review of advancement in effective cancer research. *Animal Models and Experimental Medicine*, 4(2), 87-103. https://doi.org/10.1002/ame2.12165
- 7. Liu, Y., Wu, W., Cai, C., Zhang, H., Shen, H., & Han, Y. (2023). Patient-derived xenograft models in cancer therapy: Technologies and applications. *Signal Transduction and Targeted Therapy*, 8. https://doi.org/10.1038/s41392-023-01419-2
- 8. Workman, P., Aboagye, E. O., Balkwill, F., Balmain, A., Bruder, G., Chaplin, D. J., Double, J. A., Everitt, J., Farningham, D. A., Glennie, M. J., Kelland, L. R., Robinson, V., Stratford, I. J., Tozer, G. M., Watson, S., Wedge, S. R., & Eccles, S. A. (2010). Guidelines for the welfare and use of animals in cancer research. *British Journal of Cancer*, *102*(11), 1555-1577. https://doi.org/10.1038/sj.bjc.6605642
- Wang, X., Chan, Y. S., Wong, K., Yoshitake, R., Sadava, D., Synold, T. W., Frankel, P., Twardowski, P. W., Lau, C., & Chen, S. (2023). Mechanism-Driven and Clinically Focused Development of Botanical Foods as Multitarget Anticancer Medicine: Collective Perspectives and Insights from Preclinical Studies, IND Applications and Early-Phase Clinical Trials. *Cancers*, 15(3). https://doi.org/10.3390/cancers15030701
- **10.** Khalil, A. S., Jaenisch, R., & Mooney, D. J. (2020). Engineered tissues and strategies to overcome challenges in drug development. *Advanced Drug Delivery Reviews*, *158*, 116-139. https://doi.org/10.1016/j.addr.2020.09.012
- **11.** Xia, Y., Sun, M., Huang, H., & Jin, W. (2024). Drug repurposing for cancer therapy. *Signal Transduction and Targeted Therapy*, *9*(1), 1-33. https://doi.org/10.1038/s41392-024-01808-1
- **12.** Xu, M., Xu, C., Wang, R., Tang, Q., Zhou, Q., Wu, W., Wan, X., Mo, H., Pan, J., & Wang, S.(2024). Treating human cancer by targeting EZH2. *Genes & Diseases*, 101313. https://doi.org/10.1016/j.gendis.2024.101313
- **13.** Wu, K., Niu, C., Liu, H., & Fu, L. (2023). Research progress on PRMTs involved in epigenetic modification and tumour signalling pathway regulation (Review). *International journal of oncology*, 62(5), 62. https://doi.org/10.3892/ijo.2023.5510
- **14.** Duan, R., Du, W., & Guo, W. (2020). EZH2: a novel target for cancer treatment. *Journal of hematology & oncology*, *13*(1), 104. https://doi.org/10.1186/s13045-020-00937-8
- **15.** Shankar, S., Marsh, L., & Srivastava, R. K. (2013). EGCG inhibits growth of human pancreatic tumors orthotopically implanted in Balb C nude mice through modulation of FKHRL1/FOXO3a and neuropilin. Molecular and Cellular Biochemistry, 372(1–2), 83–94. https://doi.org/10.1007/s11010-012-1448-y
- **16.** Zhou, D. H., Wang, X., Yang, M., Shi, X., Huang, W., & Feng, Q et al., (2013). Combination of low concentration of (-)-epigallocatechin gallate (EGCG) and curcumin strongly suppresses the growth of non-small cell lung cancer in vitro and in vivo through causing cell cycle arrest. *International journal of molecular sciences*, *14*(6), 12023–12036. https://doi.org/10.3390/ijms140612023
- **17.** Rasheed, Z., Rasheed, N., & Al-Shaya, O. (**2018**). Epigallocatechin-3-O-gallate modulates global microRNA expression in interleukin-1β-stimulated human osteoarthritis chondrocytes: potential role of EGCG on negative co-regulation of microRNA-140-3p and ADAMTS5. *European Journal of Nutrition*, 57(3), 917–928. https://doi.org/10.1007/s00394-016-1375-x

- **18.** Ferrari, E., Bettuzzi, S., & Naponelli, V. (2022). The Potential of Epigallocatechin Gallate (EGCG) in Targeting Autophagy for Cancer Treatment: A Narrative Review. *International journal of molecular sciences*, 23(11), 6075. https://doi.org/10.3390/ijms23116075
- **19.** Alam, M., Ali, S., Ashraf, G. M., Bilgrami, A. L., Yadav, D. K., et al., (2022). Epigallocatechin 3-gallate: From green tea to cancer therapeutics. *Food chemistry*, *379*, 132135. https://doi.org/10.1016/j.foodchem.2022.132135
- **20.** Kciuk, M., Alam, M., Ali, N., Rashid, S., Głowacka, P., Sundaraj, R., et al., (2023). Epigallocatechin-3-Gallate Therapeutic Potential in Cancer: Mechanism of Action and Clinical Implications. *Molecules (Basel, Switzerland)*, 28(13), 5246. https://doi.org/10.3390/molecules28135246
- **21.** Wang, L., Li, P., & Feng, K. (2023). EGCG adjuvant chemotherapy: Current status and future perspectives. *European journal of medicinal chemistry*, 250, 115197. https://doi.org/10.1016/j.ejmech.2023.115197
- **22.** Kumar, N. B., Pow-Sang, J., Spiess, P. E., Park, J., Salup, R., Williams, C. R., et al., (2016). Randomized, placebo-controlled trial evaluating the safety of one-year administration of green tea catechins. *Oncotarget*, 7(43), 70794–70802. https://doi.org/10.18632/oncotarget.12222
- 23. Gee, J. R., Saltzstein, D. R., Kim, K., Kolesar, J., Huang, W., Havighurst, T. C., et al., (2017). A Phase II Randomized, Double-blind, Presurgical Trial of Polyphenon E in Bladder Cancer Patients to Evaluate Pharmacodynamics and Bladder Tissue Biomarkers. *Cancer prevention research (Philadelphia, Pa.)*, 10(5), 298–307. https://doi.org/10.1158/1940-6207.CAPR-16-0167
- **24.** Choudhari, A. S., Mandave, P. C., Deshpande, M., Ranjekar, P., & Prakash, O. (2020). Phytochemicals in Cancer Treatment: From Preclinical Studies to Clinical Practice. *Frontiers in pharmacology*, *10*, 1614. https://doi.org/10.3389/fphar.2019.01614
- **25.** Wajid, S., Samad, F. A., Syed, A. S., & Kazi, F. (2021). Ki-67 and Its Relation With Complete Pathological Response in Patients With Breast Cancer. *Cureus*, 13(7). https://doi.org/10.7759/cureus.16788

CHAPTER#5

SUMMARY AND CONCLUSION

The present study encompasses a comprehensive exploration, starting from initial screening to rigorous *in vitro* and *in vivo* validations, focused at unravelling the potential of selected compounds targeting the epigenetic regulators PRMT5 and EZH2 in breast cancer treatment.

- 1. Screening and Identification of Phytochemicals with Antiproliferative Properties: Phytochemical screening involves the exploration of plant-derived compounds that inhibit cancer cell proliferation. A chemical library comprising 1200 compounds sourced from 320 medicinal plants was screened, revealing 14 molecules with potent antiproliferative effects across multiple human cancer cell lines. Compounds such as EGCG, and EA exhibited remarkable efficacy, modulating the expression of epigenetic regulators, and showing promise as potential therapeutic agents.
- 2. Validation of PRMT5 and EZH2 Inhibition by Phytochemicals: *In vitro* validation focused on confirming the inhibitory effects of selected phytochemicals (e.g., EGCG, EA) on PRMT5 and EZH2. Molecular docking studies and SPR analysis indicated strong binding affinities, with EGCG and EA effectively inhibiting enzymatic activities rather than reducing protein expression. Cell viability assays and apoptotic studies in MDA-MB231 cells highlighted their mechanisms of action through autophagy and apoptosis, demonstrating significant decreases in catalytic products of PRMT5 (H4R3me2s) and EZH2 (H3K27me3) upon treatment with EGCG, EA, and their combination.
- 3. Investigation of Tumor Inhibitory Potential using Mouse Xenograft Models: Mouse xenograft models were employed to validate the efficacy of EGCG, EA, and their combination in inhibiting tumor growth and metastasis *in vivo*. Treatment significantly reduced tumor volumes in MDA-MB231 xenografts, confirming their anti-cancer efficacy. Histological analyses and western blotting further validated reductions in PRMT5 and EZH2 levels, underscoring their potential as effective anticancer agents. Assessment of the anti-tumor potential of EGCG and EA, alone or in combination, using MDA-MB231 tumor xenograft models in Swiss nude mice revealed noteworthy tumor volume reduction and mitotic activity compared to controls. Immunohistochemistry studies demonstrated reduced cell proliferation in drug-treated tumors through Ki-67 staining, while analysis of catalytic products of PRMT5 and EZH2 in treated tumors emphasized their role as inhibitors of tumor growth.

Conclusion: In summary, this study emphasizes the significant impact of epigenetic dysregulation on cancer progression and underscores the potential of phytochemicals to serve as epigenetic modulators and therapeutic agents. Screening efforts identified promising compounds like EGCG and EA, which effectively inhibit PRMT5 and EZH2 activities, demonstrating anticancer effects in both in vitro and in vivo models. Future research direction should emphasis on optimizing these compounds for clinical use, ensuring their efficacy and safety in clinical trials to advance cancer treatment strategies. Each stage of this study builds upon foundational insights into cancer biology and epigenetic mechanisms, progressing from theoretical understanding to practical applications in therapeutic development.

ANNEXURE

Research papers published/communicated

Papers under review:

- 1. Nalla, K., Chatterjee, B., Poyya, J., Swain, A., Ghosh, K., Pan, A., ... & Kanade, S. R. (2024). Ellagic acid: a potential inhibitor of enhancer of zeste homolog-2 and protein arginine methyltransferase-5. *bioRxiv*, 2024-05. doi: https://doi.org/10.1101/2024.05.22.595443 (under review in **FEBS letters**)
- 2. Nalla, K., Chatterjee, B., Poyya, J., Swain, A., Ghosh, K., Pan, A., & Kanade, S. R. (2024). Epigallocatechin-3-gallate inhibit the protein arginine methyltransferase 5 and Enhancer of Zeste homolog 2 in breast cancer both in vitro and in vivo. bioRxiv, 2024-02. (Pre-print) https://doi.org/10.1101/2024.02.18.580855 (under review in Archives of Biochemistry and Biophysics-Elsevier- YABBI-D-24-00583)

Published:

- 1. Baka, D., Kishore, R., Sunkara, S., Varadhi, G., Kashanna, J., Tripuramallu, B. K., Nalla, K., & Kanade, S. R. (2024). Design, Synthesis, and Cytotoxicity of 1H-1,2,3-Triazole Tethered-Benzophenone Based Derivatives as Potent Candidate Anti-Breast Cancer Agents. In ChemistrySelect (Vol. 9, Issue 17). Wiley. https://doi.org/10.1002/slct.202401005
- 2. Rao, K. S., Nalla, K., Ramachandraiah, C., Chandrasekhar, K. B., Kanade, S. R., & Saha, S. (2023). Design and Synthesis of New Triazole-Benzimidazole Derivatives as Potential PRMT5 Inhibitors. *ChemistrySelect*, 8(11), e202204474. https://doi.org/10.1002/slct.202204474
- 3. Ghosh, K., Chatterjee, B., Nalla, K., Behera, B., Mukherjee, A., & Kanade, S. R. (2022). Di(2-ethylhexyl) phthalate triggers DNA methyltransferase 1 expression resulting in elevated
 CpG-methylation and enrichment of MECP2 in the p21 promoter in vitro. *Chemosphere*, 293,
 133569. https://doi.org/10.1016/j.chemosphere
- 4. Chatterjee, B., Ghosh, K., Swain, A., Nalla, K. K., Ravula, H., Pan, A., & Kanade, S. R. (2022). The phytochemical brazilin suppresses DNMT1 expression by recruiting p53 to its promoter resulting in the epigenetic restoration of p21 in MCF7cells. *Phytomedicine*, 95,53885.https://doi.org/10.1016/j.phymed.2021.153885
- Nalla, K.; Manda, N.K.; Dhillon, H.S.; Kanade, S.R.; Rokana, N.; Hess, M.; Puniya, A.K. Impact of Probiotics on Dairy Production Efficiency. *Front. Microbiol.* 2022, 13, 805963. https://doi.org/10.3389/fmicb.2022.805963
- 6. Rao, K. S., Nalla, K., Ramachandraiah, C., Chandrasekhar, K. B., Kanade, S. R., & Saha, S Aridoss G. Design, Synthesis, and Evaluation of Benzimidazole Derivatives: A Comprehensive Study of Antiproliferative Properties (Under review in Medicinal Chemistry Research_MCRE-D-24-00427)

Ellagic acid: a potential inhibitor of enhancer of zeste homolog-2 and protein arginine methyltransferase-5

Short title: Ellagic acid as dual inhibitor of EZH2 & PRMT5

Kirankumar Nalla¹, Biji Chatterjee², Jagadeesha Poyya³, Aishwarya Swain⁴, Krishna Ghosh⁵, Archana Pan⁴ Chandrashekhar G Joshi⁶ Bramanandam Manavathi⁷ and Santosh R Kanade¹*

¹Department of Plant Sciences, School of Life Sciences University of Hyderabad PO Central University Gachibowli, Hyderabad Telangana 500046,

²Department of Genomic Medicine, The University of Texas MD Anderson Cancer Centre, Houston, Texas, USA

³SDM Research Institute for Biomedical Sciences, A constituent unit of Shri Dharmasthala, Manjunatheshwara University, Dharwad -580009, Karnataka, India

Department for Bioinformatics, Pondicherry University, Puducherry-605014, India,

⁵Department of Anaesthesiology and Perioperative Medicine, The University of Texas MD Anderson Cancer Centre, Houston, Texas, USA

⁶Department of Studies in Biochemistry, Mangalore University PG Centre, Jnana Kaveri, Chikka Aluvara, Thorenoor Post Kushalnagar, Somawarpet TQ, Kodagu-571232

Department of Biochemistry, School of Life Sciences, University of Hyderabad PO Central University Gachibowli, Hyderabad Telangana 500046,

* Corresponding author: Prof. Santosh R. Kanade, Department of Plant Sciences, School of Life Sciences, University of Hyderabad, Prof. C. R. Rao Road Gachibowli Hyderabad-500046 Tel; 040-23134545, Cell 91 8277529624,

Epigallocatechin-3-gallate inhibit the protein arginine methyltransferase 5 and Enhancer of Zeste homolog 2 in breast cancer both *in vitro* and *in vivo*

Short title: Inhibition of PRMT5 and EZH2 by Epigallocatechin-3-gallate

Kirankumar Nalla¹, Biji Chatterjee², Jagadeesh Poyya³, Aishwarya Swain⁴, Krishna Ghosh⁵, Archana Pan⁴, Chandrashekhar G Joshi³ Bramanandam Manavathi⁶ and Santosh R Kanade¹*

Department of Plant Sciences, School of Life Sciences University of Hyderabad PO Central University Gachibowli, Hyderabad Telangana 500046,

*Corresponding author:

Prof. Santosh R. Kanade, Department of Plant Sciences, School of Life Sciences, University of Hyderabad, Prof. C. R. Rao Road Gachibowli Hyderabad-500046 Tel; 040-23134545, Cell 91 8277529624, Email: san@uohyd.ac.in

Department of Genomic Medicine, The University of Texas MD Anderson Cancer Center, Houston, Texas, USA

Department of Anesthesiology and Perioperative Medicine, The University of Texas MD Anderson Cancer Center, Houston, Texas, USA

³ Department of Studies in Biochemistry, Mangalore University PG Centre, Jnana Kaveri, Chikka Aluvara, Thorenoor Post Kushalnagar, Somawarpet TQ, Kodagu-571232

Department of Bioinformatics, Pondicherry University, Puducherry-605014, India,

⁶ Department of Biochemistry, School of Life Sciences, University of Hyderabad PO Central University Gachibowli, Hyderabad Telangana 500046,

² Present address

⁵ Present address



www.chemistryselect.org

Design, Synthesis, and Cytotoxicity of 1H-1,2,3-Triazole Tethered-Benzophenone Based Derivatives as Potent Candidate Anti-Breast Cancer Agents

Durgaprasad Baka,^[a] Ravada Kishore,*^[a] Srinivasarao Sunkara,^[a] Govinda Varadhi,^[b] Jajula Kashanna,*^[c] Bharat Kumar Tripuramallu,^[d] Kirankumar Nalla,^[a] and Santosh R. Kanade^[a]

The process of developing potential anticancer molecules comprises the cautious selection of core moiety and tethering pharmacologically active chemical functionalities to biologically active pharmacophores. Here, we report a library of ten 1H-1,2,3-triazole tethered-benzophenone derivatives. Protein-ligand interaction studies through molecular docking of our synthesised compounds were carried out with a novel epigenetic oncogene-enhancer of zeste homolog2 (EZH2). Molecular docking studies disclosed that our synthesized compounds showed potent inhibition against EZH2 and in-vitro validation assays through MTT assay, Trypan blue dye exclusion and in-

vitro methylation assays, these studies revealed the synthesized compounds-9 c, 9 f, 91 showed potent inhibition on EZH2. The anticipated anti-cancer activity of library molecules was assessed in in-vitro against breast and lung cancer (MCF7 and A549) cell lines, supported by in-vitro assays and molecular docking binding studies. Among all ten compounds, 9 c, 9 f, 91 are exerted potential anti-cancer activity against the selected cancer cell line in in-vitro. The results were supported by in-silico docking studies. Further validation studies in in-vivo models will pave a way for developing potent inhibitors against breast cancer and lung cancer.

1. Introduction

Cancer has become one of the most devastating diseases in current eras and among them, lung cancer is one of the major forms of cancer that causes numerous deaths worldwide each year, II-2I However, an important effect those which are such as chemopreventive and chemotherapeutic effects are shown more role in the treatment of human cancer cell lines with S, N-containing heterocyclic compounds, IVI 1,2,3-Triazole derivatives are a class of organic compounds containing a five-membered ring consisting of two carbon atoms and three nitrogen atoms and, they have gained significant attention due to their diverse biological activities. These derivatives can be synthesized by

various methods such as click chemistry, copper-catalyzed azide-alkyne cycloaddition (CuAAC) and Huisgen reaction, ^[5,4] Indeed, 1,2,3-triazole derivatives have been consisting the several potential applications in the development of new drugs and can be used as good activity compounds in biology. So, they can also be used as molecular probes and imaging agents for various biological studies. The presence of specific functional groups and the position of the triazole ring in the molecule can significantly affect the activity of their derivatives. [5-40] For example, some derivatives have been found to exhibit potent antimicrobial activities by inhibiting the growth of bacteria and fungi. [50,11]

Enhancer of Zeste Homolog 2 (EZH2) is a protein that plays a crucial role in epigenetic regulation. Epigenetics refers to changes in gene expression that occur without alterations in the DNA sequence itself. EZH2 is a component of the Polycomb Repressive Complex 2 (PRC2), which is involved in adding a specific chemical mark called a methyl group to histone proteins in chromatin. EZH2 mediated histone methylation and gene silencing are critical for various biological processes, including normal development, cell differentiation, and maintaining cell identity. Nevertheless, dysregulation of EZH2 and PRC2 activity has been implicated in various diseases, like cancer. In some cancer types like breast cancer, EZH2 is overexpressed or mutated, leading to inappropriate gene silencing and contributing to uncontrolled cell growth and tumor formation. EZH2 is the core enzymatic catalytic subunit of polycomb repressive complex2 (PRC2), that alters the downstream target gene expression by trimethylation of H3K27me3 (trimethylation of Lys-27 in histone 3). EZH2 functions such as cell proliferation, senescence and apoptosis have been identi-

- [a] D. Baka, R. Kishore, S. Sunkara
 Department of Chemistry, School of Science, GITAM (Deemed to be University), Visakhapatnam 530045, India

 E-mail: ravadakishore@gmail.com
- [b] G. Varadhi
 Department of Chemistry, Gayatri Vidya Parishad College, Visakhapatnam 530045, India
- [c] J. Kashanna Department of Chemistry, Rajiv Gandhi University of Knowledge Technologies-Basar, Nirmal 504107, India E-mail: jajulakashanna@gmail.com
- [d] B. K. Tripuramallu
 Department of Chemistry, Applied Sciences and Humanities, VFSTR (Deemed to be University), Vadiamudi, Guntur 522213, India
- K. Nalla, S. R. Kanade
 Department of plant sciences, school of life sciences, University of
 Hyderabad, Hyderabad, 500046 India
- Supporting information for this article is available on the WWW under https://doi.org/10.1002/skrt.202401005

ChemistrySelect 2024, 9, e202401005 (1 of 11)

© 2024 Wiley-VCH GmbH

www.chemistryselect.org

Design and Synthesis of New Triazole-Benzimidazole Derivatives as Potential PRMT5 Inhibitors

Katharu Srinivasa Rao,^[a, c] Kirankumar Nalla,^[b] Chennuru Ramachandraiah,*^[a] Kothapalli Bannoth Chandrasekhar,^[a] Santosh Raja Kanade,^[b] and Sanjay Saha^[c]

The art of developing potential anticancer molecules involves a reasonable selection of core moiety and tethering with biologically active pharmacophores. We report a library of rationally designed twelve triazole tethered benzimidazole molecules as novel potential inhibitors for cancer. Their synthesis followed a facile copper-catalysed cycloaddition reaction with good yields. Although in-silico molecular docking studies of the synthesized compounds with epigenetic protein viz., PRMTs showed inhibition, the compounds bearing amino acid and aryl groups exhibited excellent performance. The potential anti-

cancer activity of the library of molecules are further evaluated in vitro against the selected cancer cell lines (MCF-7, DU145, PC3 and HepG2) besides methylation assays. In vitro results revealed that the compounds bearing amino acid and aryl groups exhibited better activity and particularly, 3-CF₁-phenyl derivative (IC₅₀= 4.11 µm against MCF-7) exerted prominent anticancer potency against all the tested cell lines. The observed strong anticancer potency of lead compound is supported by its strong binding nature noted in in-silico molecular docking studies.

Introduction

Cancer is the second-largest non-communicable disease (NCD) affecting global population, as corroborated by World Health Organization (WHO), Cancer continues to be the leading cause of death, accounting for approximately 10 million deaths in the year 2021 alone. The high prevalence is associated with diverse demographical, environmental and lifestyle associated risk factors along with the inherited genetic factors. Cancer is characterized by uncontrolled cell division, forming tumours that invade adjoining tissues and spreading to other organs in the body through metastasis. Breast, lung, colon and rectum, and prostate cancers are the most common cancers in terms of occurrence.[1] Majority of deaths associated with cancer ailments could be prevented with early detection and treatment. Immunotherapy, alongside the classical treatment modalities such as surgical removal of tumours, chemotherapy and radiotherapy aids saving lives. Identification of new drug targets, development of potential drug moieties and robust clinical approaches are crucial for developing new methods for cancer treatment and patient care using anticancer drugs.[2,3]

Chemotherapy is used to treat various cancers either alone or in combination with other treatment modalities.¹⁰ Heterocyclic compounds are rich source of biologically active functional moieties with diverse functionalities ranging from oxygen carriers (haemoglobin) to neurotransmitters to natural antimicrobial agents (diketopiperazines). Inspired from a plethora of applications of natural molecules, synthetic molecules containing heterocyclic entities (N) with potential anticancer properties for various types of cancers are extensively studied across academia and the pharmaceutical industry. Despite the availability of different anticancer drugs, there is ample room for developing potentially active anticancer molecules with improved activity and lower side effects.

Triazole (1,2,3-triazole) moiety is the omnipresent pharmacophores in majority of the marketed drugs aiming for the functions as antimicrobial, anti-inflammatory, analgesic, antiepileptic, antiviral, antineoplastic, antihypertensive, antimalarial, anesthetic, antidepressant, antihistaminic, antioxidant, antitubercular, anti-parkinson's, antidiabetic, anti-obesity, and immunomodulatory agents.^{18–13} Triazole pharmacophore exerts the action mainly by interaction with biological targets such as enzymes through hydrogen bonding and other non-covalent interactions thereby making them promising candidates for developing novel anticancer agents. Triazole embedded or derived molecules were reported to exhibit strong anticancer properties through a range of mechanisms such as vascular endothelial growth factor (VEGF) inhibition.¹¹⁴¹

Similarly, benzimidazole moiety resembling structure of nucleic acid bases is an appraised pharmacophore. The potential biological properties of benzimidazole-containing molecules include but are not limited to anti-HIV, antimicrobial, antihistamine, antioxidant, antiviral, anticoagulant, and anticancer activity. Pland Renowned biological properties associated with simplistic synthetic routes helped the recent development of benzimidazole pharmacophore containing potential anticancer agents. Pland P

Protein arginine methyltransferase-5 (PRMT5) is a type-II arginine methyltransferase that mainly acts by mediating the

 K. S. Roo, Prof. C. Ramachandratah, Prof. K. B. Chandrasekhar Department of Chemistry, Jawaharlal Nehru Technological University, Anantapur-S15002, Andhra Pradesh, India E-mail: cramachandraishi@yahoo.com

[b] K. Nella, Prof. S. R. Kanade Department of Plant Sciences, School of Life Sciences, South Campus, University of Hyderabad, Hyderabad-500046, Telangana, India

[c] K. S. Rao, Dr. S. Saha Department of Chemistry Solutions, Aragen Life Sciences (Formerly known as GVK BIO Science), Hyderabad-500076, Telangana, India

Supporting information for this article is available on the WWW under https://doi.org/10.1002/sict.202204474

ChemistrySelect 2023, & e202204474 (1 of 10)

© 2023 Wiley-VCH GmbH



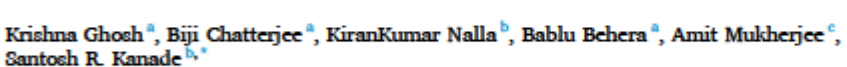
Contents lists available at ScienceDirect

Chemosphere





Di-(2-ethylhexyl) phthalate triggers DNA methyltransferase 1 expression resulting in elevated CpG-methylation and enrichment of MECP2 in the p21 promoter in vitro

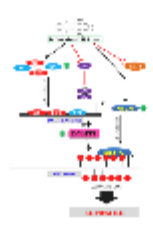


- * Department of Biochemistry and Molecular Biology, School of Biological Sciences, Central University of Kerala, Kusaragod, 671316, Kerala, Ind.
 b Department of Plant Sciences, School of Life Sciences, University of Hyderabad, Central University P.O., Hyderabad, 500046, Telanguna, India
 * Rajiv Gandhi Centre for Diabetes and Endocrinology, JN Medical College, Aligarh Muslim University, Aligarh, 202002, Ultar Pradesh, India

HIGHLIGHTS

- · DEHP induced proliferation of breast cancer cells at very low concentrations.
- DEHP increased global DNA-hypermentylation, and selectively upre- DEHP gulate DNMT1, MECP2.
- DEHP reduced p53 level but elevated occupancy of SP1, E2F1 on DNMT1
- DEHP induced hypermethylation of p21 promoter and enrichment of DNMT1 and MECP2.

GRAPHICAL ABSTRACT



ARTICLE INFO

Handling Editor: Frederik-Jan van Schooten

Keywords: DEHP DNMT1 E2F1 MECP2 p53 SP1

ABSTRACT

Leaching of the plastic constituents leading to their chronic exposure to humans is a major concern for our environmental and occupational health. Our previous and other numerous studies have demonstrated that environmental chemicals like di (2-Ethylhexyl)-phthalate (DEHP) could pose a risk towards the epigenetic mechanisms. Yet, the mechanisms underlying its possible epigenotoxicity are poorly understood. We almed to assess the impact of DEHP exposure to the human breast cancer cells (MCF-7) and resultant changes in DNA methylation regulators ultimately altering the expression of the cell cycle regulator p21 as a model gene. The MCF-7 cells were exposed to environmentally relevant concentrations (50-500 nM) for 24 h. The results showed that DEHP was proliferative towards the MCP-7 cells while it induced global DNA hypermethylation with se-lective upregulation of DNMT1 and MECP2. In addition, DEHP significantly reduced p53 protein and its enrichment to the DNMT1 promoter binding site, while elevating SP1 and E2F1 transcription factor levels, stimulating their binding to the promoter DNA. Coincidently, increased DNMT1 level was highly associated with loss of p21 expression and increased cyclin D1 levels. Importantly, the p21, but not cyclin D1 promoter CpGdinucleotides were hypermethylated after exposure to 500 nM DEHP for 24 h. Furthermore, it was observed that DEHP significantly enriched DNMT1 and MECP2 to the p21 promoter to induce DNA methylation-based

https://doi.org/10.1016/j.chemosphere.2022.133569

Received 3 July 2021; Received in revised form 6 January 2022; Accepted 6 January 2022

Available online 13 January 2022

0045-6535/© 2022 Elsevier Ltd. All rights reserved.

[;] CDKN1A, Cyclin Dependent Kinase Inhibitor 1A; DEHP, Di (2-ethylhexyl) phthalate; DNMT, DNA methyltransferase; MECP2, Methyl-CpG binding protein 2; TET1, Tet methylcytosine dioxygenase 1.

Corresponding author. E-mail address: san@uohyd.ac.in (S.R. Kanade).



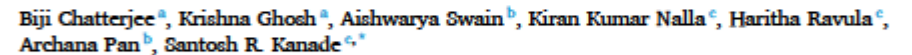
Contents lists available at ScienceDirect

Phytomedicine

journal homepage: www.elsevier.com/locate/phymed



The phytochemical brazilin suppress DNMT1 expression by recruiting p53 to its promoter resulting in the epigenetic restoration of p21 in MCF7cells



- ent of Biochemistry and Molecular Biology, School of Biological Sciences, Central University of Kerala, Kasargod-671316, Kerala, India or Bioinformatics, Pandicherry University, Puducherry-605014, India ent of Plant Sciences, School of Life Sciences, University of Hyderabad, Central University P.O., Hyderabad-500046, Telangana, India

ARTICLE INFO

Brazilin DNMT1 MCP-7 MSP P21

ABSTRACT

Background: Cancer is an outcome of uncontrolled cell division eventually associated with dysregulated epigenetic mechanisms, including DNA methylation. DNA methyltransferase 1 is ubiquitously expressed in the proliferating cells and is essential for the maintenance of DNA methylation. It causes the abnormal silencing of tumor suppressor genes in human cancer which is necessary for proliferation, cell cycle progression, and survival. DNMT1 is involved in tumorigenesis of several cancers, its upregulation potentially upscale the promoter level inactivation of transcription of a tumor inhibitory gene by introducing repressive methylation marks on the CpG islands. This epigenetic perturbation caused by DNMT is targeted for cancer therapeutics.

Purpose: To demonstrate the proliferative inhibitory potential of brazilin in human breast cancer cell line (MCF-7)

with concurrent mitigation of DNMT1 functional expression and to understand its effect on downstream targets

Snaty Design/ Methods: The impact of brazilin on the growth and proliferation of the MCF-7 cells was determined using the XTT assay. The global DNA 5-methyl cytosine methylation pattern was analyzed upon brazilin treatment. The gene and protein expression of DNMTs were determined with quantitative RTPCR and western blots respectively. The potential binding sites of transcription factors in the human DNMT1 promoter were predicted using the Matinspector tool on the Genomatix software. The chromatin immunoprecipitation (ChIP) assay was performed to demonstrate the transcription factors occupancy at the promoter. Methylation of promoter CpG islands was determined by the methylation-specific PCR (MSP) upon brazilin treatment. The molecular docking of the human DNMT1 with brazilin (ligand) was performed using the Schrödinger suite.

Results: The heterotetracyclic compound brazilin, present in the wood of Caesalpinia sap

nia sappan, inhibito liferation of the human breast cancer cell line (MCF-7) and reduced the DNMT1 expression with a decrease in global DNA methylation. Brazilin, by activating p38 MAPK and elevating p53 levels within the exposed cells. The elevated level of p53 enriched the occupancy at binding sites within 200 bp upstream to the tra site in the DNMT1 promoter, resulting in reduced DNMT1 gene expression. Furthermore, the brazilin restored the p21 levels in the exposed cells as the CpGs in the p21 promoter (-128 bp/+17 bp) were significantly dem thylated as observed in the methylation-specific PCR (MSP).

Conclusion: Highly potential anti-proliferative molecule brazilin can modulate the DNMT1 functional expression.

and restore the cell cycle inhibitor p21 expression. We propose that brazilin can be used in therapeutic in-terventions to restore the deregulated epigenetic mechanisms in cancer.

E-mail address: san@uohyd.ac.in (S.R. Kanade).

https://doi.org/10.1016/j.phymed.2021.153885

Received 21 May 2021; Received in revised form 23 November 2021; Accepted 5 December 2021 Available online 8 December 2021 0944-7113/© 2021 Elsevier GmbH. All rights reserved.

Abbreviations: AP-1, activator protein-1; CDKN1A, cyclin-dependent kinase inhibitor 1; ChIP, chromatin immunoprecipitation; DEHP, di(2-ethylhexyl)phthalate; DMEM, Dulbecco's modified Eagle's medium; DMSO, dimethyl sulfoxide; DNMT1, DNA methyltransferase 1; MSP, Methylation specific; PCR XTT, 2,3-Bis-(2-Methoxy-4-Nitro-5-Sulfophenyl)—2H-Tetrazolium-5-Carboxanilide.

Corresponding author at: Department of Plant Sciences, School of Life Sciences, University of Hyderabad, Central University P.O., Hyderabad-500046, Telanga India.



Impact of Probiotics on Dairy Production Efficiency

Kirankumar Nalla^{1‡}, Naresh Kumar Manda^{2‡}, Harmeet Singh Dhillon², Santosh R. Kanade[‡], Namita Rokana^{4*}, Matthias Hess^{5†} and Anil Kumar Puniya^{2*}

¹Department of Plant Science, School of Life Sciences, University of Hyderabad, Hyderabad, India, ²Department of Biosensors and Nanotachnology, CSR-Institute of Microbial Technology, Chandigarh, India, ³Delay Microbiology Division, ICAR-National Dairy Research Institute, Karnel, India, ⁴Department of Dairy Microbiology, College of Dairy Science and Technology, Guru Angad Dev Veterinary and Animal Sciences University, Luchlana, India, ⁵Systems Microbiology and Natural Product Discovery Laboratory, Department of Animal Science, University of California, Davis, Davis, CA, United States

OPEN ACCESS

Edited by:

George Tslamis, University of Patras, Greece

Reviewed by Martha Olivera

University of Antioquia, Colombia

Mohamed Zommiti, Université de Flouen, France

"Correspondence: Namita Rokana

dinamila rokana@gmail.com; namilarokana@gadvasu.h Anil Kumar Puniya aipuniya@gmail.com; anil.puniya@kar.gov.in

*ORCID:

Matthlas Hoss orcid.org/0000-0003-0321-0380

These authors have contributed equally to this work

Specialty section:

This article was submitted to Systems Microbiology, a section of the journal Frontiers in Microbiology

Received: 31 October 2021 Accepted: 07 April 2022 Published: 09 June 2022

Citatio

Nalla K, Manda NK, Dhillon HS, Kanado SR, Rokana N, Hoss M and Puniya AK (2022) Impact of Problotics on Dairy Production Efficiency.

Frant. Microbiol. 13:805963. doi: 10.3389/fmicb.2022.805963 There has been growing interest on probiotics to enhance weight gain and disease resistance in young calves and to improve the milk yield in lactating animals by reducing the negative energy balance during the peak lactation period. While it has been well established that probiotics modulate the microbial community composition in the gastrointestinal tract, and a probiotic-mediated homeostasis in the rumen could improve feed conversation competence, volatile fatty acid production and nitrogen flow that enhances the milk composition as well as milk production, detailed changes on the molecular and metabolic level prompted by probiotic feed additives are still not understood. Moreover, as living biotherapeutic agents, probiotics have the potential to directly change the gene expression profile of animals by activating the signalling cascade in the host cells. Various direct and indirect components of probiotic approaches to improve the productivity of dairy animals are discussed in this review.

Keywords: problotics, feed supplements, biotherapeutics, dairy production, gut microbiome

INTRODUCTION

Livestock production is a dynamic sector, critical to satisfying the growing demand for animal-sourced products and dairy products specifically have become a significant source of income for farmers contributing to the growth of developing economies (Thornton, 2010; Tona, 2021). The increasing pressure of the global population, limited arable land, and climate change has led to the urgent need of advanced approaches to enhance cow health and productivity and to make dairy production sustainable in a rapidly changing environment (Britt et al., 2018). Despite the increasing demand, the dairy sector in low- and middle-income countries is still struggling with the challenge of low animal productivity. The use of natural and inexpensive probiotics-based supplements as alternatives to antibiotics to promote animal growth and health has increased in recent years in the livestock industry, especially since the use of antibiotics as growth promoters has been strictly regulated in many countries to limit the evolution and distribution of antibiotic resistance through the food system (Sharma et al., 2018a).

Probiotics are living non-pathogenic microbes and in many cases are also naturally present to some extent in the gastrointestinal tract. Over the years numerous bacteria and fungi have been identified as probiotics (Table 1) (Choct, 2009; Puniya et al., 2015; Markowiak and

June 2022 | Volume 13 | Article 805963

Frontiers in Microbiology | www.frontiersin.org

Conference/Seminar presentations

Oral Presentations

- Oral presentation on "Epigallocatechin gallate Inhibited protein arginine methyltransferase 5 in breast cancer both invitro and in vivo and reduced the H4R3me2s histone repressive mark" at Current trends and future prospectus of plant biology (CTFPPB) organized by Department of Plant Sciences, School of Life Sciences, university of Hyderabad, held during 23rd -25th February 2023
- 2. Oral presentation on "Novel **phytochemicals targeted for PRMT5 inhibition in breast cancer cell lines**" in 15th International Symposium on Recent Trends in Cancer Prevention and Interception Bench to Bedside organized by School of Life Sciences, Jawaharlal Nehru University, New Delhi, India, February 22-23, **2022.**
- Oral presentation on "PKC mediated phosphorylation of Protein Arginine Methyltransferase-5" -Virtual Conference on Proteomics in Agriculture and Healthcare- School of Life Sciences, University of Hyderabad held during March 13-14, 2021.

Poster Presentations

- 4. Presented a Poster on "Inhibition of protein arginine methyltransferase 5 by natural compounds both in-vitro and in vivo" at EMBL Conference: Chromatin and epigenetics EMBL Advanced Training Centre, Heidelberg-Germany Held during 15 18 May 2023.
- 5. Presented a poster on "Phytocompounds mediated inhibition of Breast cancer: An *in-silico* and *in-vitro* validation studies" "3rd International Conference on Applications of Natural compounds, Nanomaterials, Oncolytic in Cancer Biology and Biotechnology (ICANNOCB-22)" organized by School of Life Sciences and Association of Cancer Education and Research (ACER), B.S. Abdur Rahman Crescent Institute of Science & Technology, Chennai, India in association with Purdue University, USA on 27th-28th October, 2022.
- 6. Presented a poster on "Screening of natural compounds as putative inhibitors for Protein Arginine Methyltransferase-5" in Horizons in Molecular Biology", which took place online September 13th 16th 2021.
- 7. Presented a poster on "Screening of natural plant compounds as putative inhibitors for Protein Arginine Methyltransferase-5". National Conference on Frontiers in Plant Biology, organized by Department of Plant Sciences, School of Life science, University of Hyderabad-February 2020

Awards/Grants received

- National Inspire Fellowship (DST) for Pursuing Ph.D. Awarded to 1st rank holders of universities in India. Date: July 2018
- 2. Junior Member, Cancer Epigenetics Society (CES), Vienna, Austria, Tenure: January 2020 December 2020
- 3. **Prof A R Rao Young Scientist Award,** received for an oral presentation on novel phytochemicals targeted for PRMT5 inhibition in breast cancer cell lines. **Date:** February 2022
- 4. **Best Poster Award,** Won at the 3rd International Conference on Applications of Natural Compounds, Nanomaterials, and Oncolytic in Cancer Biology and Biotechnology (ICANNOCB). **Date:** October 2022, organized by School of Life Sciences and Association of Cancer Education and Research (ACER), B.S. Abdur Rahman Crescent Institute of Science & Technology, Chennai, India in association with Purdue University, USA
- Travel Grant by IoE-University of Hyderabad, provided to attend the EMBL
 "Chromatin and Epigenetics" conference held in Heidelberg, Germany.
 Date: May 2023
- 6. **Academic Member, FABA (Federation of Asian Biotech Associations) Academy**The academy promotes the development and growth of the biotechnology industry in the region, **Tenure:** November 2023 November 2025









Certificate

This is to certify that

Nalla Kirankumar (17LPPH18)

gave an oral presentation on

Epigallocatechin gallate inhibited protein arginine methyltransferase 5 in breast cancer both in vitro and in vivo and reduced the H4R3me2s histone repressive mark in the International Conference on 'Current Trends and Future Prospects of Plant Biology (CTFPPB-2023)' & 14th Plant Sciences Colloquium organized by the Department of Plant Sciences, School of Life Sciences, University of Hyderabad, Telangana, India (February 23-25, 2023)

Prof. S. Rajagopal

Convenor

Dr. M. Muthamilarasan

Organizing Secretary-I

Dr. 5. Siddharthan Organizing Secretary-II



15th International Symposium on Recent Trends in Cancer Prevention and Interception- Bench to Bedside



School of Life Sciences, Jawaharlal Nehru University, New Delhi, India

CERTIFICATE OF PROF. A.R. RAD YOUNG SCIENTIST

IS BEING AWARDED TO

KIRAN KUMAR NALLA

for her/his **ORAL Presentation** on Novel Phytochemicals Targeted for PRMT5 Inhibition in Breast Cancer Cell Lines

Rein

PAULRAJ RAJAMANI

Professor, School of Environmental Sciences, Jawaharlal Nehru University, New Delhi









RANA PRATAP SINGH

Professor of Cancer Biology, Jawaharlal Nehru University, New Delhi









Virtual Conference on Proteomics in Agriculture and Healthcare

School of Life Sciences, University of Hyderabad

Certificate of Merit

This is to certify that Mr. KIRANKUMAR NALLA S/o Nalla Nagendra prasad from University of Hyderabad, Hyderabad has participated in oral presentation in the conference held during March 13-14, 2021.

Prof. MV Jagannadham

MNJary

Prof. S Rajagopal

Dean, School of Life Sciences

Prof. S Dayananda

Convener

Organising Secretary



KIRANKUMAR NALLA

attended the

EMBL Conference: Chromatin and epigenetics

15 - 18 May 2023, EMBL Advanced Training Centre

EMBL
European Molecular Biology Laboratory
Course and Conference Office
Meyerhofstr. 1
D-69117 Heidelberg, Germany

Heidelberg, 30 May, 2023

www.ombl.org









CERTIFICATE

of Participation

This is to Certify that

KIRANKUMAR NALLA

Research Scholar from University of Hyderabad

Has participated in "3rd International Conference on Applications of Natural compounds, Nanomaterials, Oncolytics in Cancer Biology and Biotechnology

(ICANNOCB-22)" organized by School of Life Sciences and Association of Cancer Education and Research (ACER), B.S. Abdur Rahman Crescent Institute of Science & Technology, Chennai, India in association with Purdue University, USA on 27th-28th October, 2022. P. Alma

Dr. P. Ashok Kumar

Coordinator BSACIST

Dr. S. Hemalatha

J. H

Organizing Secretary & Dean **BSACIST**

Horizons in Molecular Biology

International PhD Student Symposium Organizing Committee



Molecular Biology Coordination Office Justus-von-Liebig-Weg 11 37077 Göttingen Germany Phone: +49 551 3912110

Fax: +49 551 393811 Email: participants.horizons@mpibpc.mpg.de Website: https://www.horizons.uni-goettingen.de

Göttingen, 27.09.2021

Mr. Kiran Kumar Nalla School of life sciences, Department of Plant Sciences, Lab no-F43 south campus University of Hyderabad, Gachibolwi Hyderabad Telangana 500046 India

Certificate of Attendance¹

It is hereby certified that Mr. Kiran Kumar Nalla, affiliated with the Department of Plant Sciences, University of Hyderabad, attended the 18th International PhD Student Symposium "Horizons in Molecular Biology", which took place online September 13th - 16th 2021.

Mr. Kiran Kumar Nalla presented his research in the form of a poster titled, 'Screening of natural phytocompounds as putative inhibitors for Protein Arginine Methyltransferase-5'.

The aim of the Symposium is to bring together senior scientists and young researchers from different fields to promote scientific exchange and to provide exciting insights into the frontiers of Molecular Biology. We have put together a group of highly renowned leading scientists to jointly discuss current trends in the fields of biotechnology, cell biology, epigenetics, developmental biology, structural biology, and bioinformatics.

¹This document is generated automatically by our system and it is therefore valid without any stamp or signature





NATIONAL CONFERENCE ON FRONTIERS IN PLANT BIOLOGY

Organized by : Department of Plant Sciences School of Life Sciences, University of Hyderabad

Certificate

This is to certify that Mr./Ms. Kirankumar Nalla has participated and presented a

poster in the National Conference on Frontiers in Plant Biology held on

31st January- 1st February, 2020.

DEPARTMENT OF PLANT SCIENCE:

Prof. G. Padmaja CONVENOR

Dr. Santosh R. Kanade ORGANIZING SECRETARY 1 R. Kumak Dr. Rahul Kumar Organizing secretary 2









CERTIFICATE

of Appreciation

This is to Certify that

KIRANKUMAR NALLA

Research Scholar from University of Hyderabad

Has presented a paper titled Phytocompounds mediated inhibition of Breast cancer: An in-silco and invitro validation studies and won the Best Poster Presentation Award in the

"3rd International Conference on Applications of Natural compounds, Nanomaterials, Oncolytics in Cancer Biology and Biotechnology (ICANNOCB-22)" organized by School of

Life Sciences and Association of Cancer Education and Research (ACER), B.S. Abdur Rahman Crescent Institute of Science & Technology, Chennai, India in association with Purdue University, USA on 27th-28th October, 2022.

Dr. P. Ashok Kumar

P. Allma

Coordinator BSACIST

Dr. S. Hemalatha

Organizing Secretary & Dean BSACIST



IoE-Directorate प्रतिष्ठित संस्थान निर्देशालय University of Hyderabad हैदराबाद विश्वविद्यालय Guehibowli, Hyderabad 500046 गचीबोवली, हैदराबाद - ५०००६६



Date: 05-04-2023

SANCTION ORDER

No. UeH-loE/Travel/22/106

Prof. Suntosh R. Kanade. Dept. of Plant Sciences, School of Life Sciences, University of Hyderabad, Hyderabad 500046. Email: san@uohyd.ac.in

Sub : Sauction of Travel Grant to Mr. Nalla Kiran Kumar, Ph.D. scholar - Reg.

Ref: VC's approval dated: 05-04-2023.

Sir,

The approval and sanction of the Competent Authority is conveyed for the release of financial assistance of Rs. 1,00,000/- (Rupees One Lakh only) towards registration fees, travel expenses and per-diem charges to Mr. Nalla Kiran Kumar (17LPPH18), School of Life Sciences to strend conference entitled "EMBL Conference-Chromatin and Epigenetics" at Heidelberg, Germany from 15-05-2023 to 18-05-2023 under IoE Travel Grant.

l'erms & Conditions:

- 1. The concerned Faculty is permitted to reimburse the expanses incurred for the above on behalf of his student and hills for these expenses should be submitted within 15 days after completion. of the conference.
- PhD scholar is permitted to travel by Air in Economy class, by following all the established. procedures/guidelines for air travel.
- 3. The IoR is obligated to extend the financial support to the extent of sanction conveyed and therefore the onus lies on to the Faculty to confine the expenses within the sanctioned amount.
- 4. PhD scholar should submit a brief report on the outcome and its relevance to the IoE Directorate after completion of the conference.

Copy to:

Dean, School of Life Sciences

University of Pyderabad / सन्तर्यक विश्वविद्धान Deputy Registrar (IoE Cell, F&A) - with a request to create an account in FAMONIS Roo Road / दी. श्री आर शर्व श्रीड Gachibowii / सबीवोदली Travel Grant File Hyderabad - 500046/ हेट स्वाद - ५०००४६

Master File

Expanditure is chargeable under the Head: OH-31.03 - Travel Expenses

M. Thanashyam Director, 108 - 11/27

Director / निवंशक Institution of Eminence / प्रतिस्थित संस्थान No: DST/INSPIRE Fellowship/[JF170921]
GOVERNMENT OF INDIA
MINISTRY OF SCIENCE and TECHNOLOGY
Department of Science and Technology
Technology Bhawan, New Mehrauli Road
New Delhi-110016

Date: 4 July, 2018

Subject: Award of INSPIRE Fellowship to the Research Students [IF170821]

Dear KIRANKUMAR NALLA.

The Government of India has launched a unique Scheme "Innovation in Solence Pursuit for Inspired Research (INSPIRE)" with several components. INSPIRE Fellowship provides fellowship in Basic and Applied Sciences. I am pleased to Inform you that you have been Selected for the award of INSPIRE Fellowship to hostthe same at the University/Institute/College/National Laboratory as Indicated in the application form of your subsequent admission.

The value of the Fellowship will be at Par with the Junior Research Fellowship (JRF) Senior Research Fellowship (SRF) of Government of India along with a Contingency grant. The Fellowship shall be available to you from INSPIRE Fellowship Effective Date (which will be communicated through 1st Sanction Order) for a period of five years or completion of your doctoral (PhD) program, whichever is earlier.

If you are willing to join or switching over from earlier fellowship to INSPIRE Fellowship, you will require to upload the scan copy of Joining-cum-Acceptance Letter (JCA) (available at http://inspire-dst.gov.in/JoiningReport.pdf, and at template in your online dashboard), and also submit Bank details of your Host institute along with the scan copy of cancelled blank cheque of given account details within one month from the date of this letter, in your online portal only, for taking necessary actions at INSPIRE Program Secretariat for releasing of your fellowship amount. Please also note that in the JCA Letter the Host institution, Research Supervisor and Research Topic shall not be change or modification from initially submitted documents/ information for Final Offer. The Terms & Conditions for implementation of INSPIRE Fellowship are enclosed herewith.

Docuents submitted in any other modes like email attachment or by post or in-person shall not be acceptable.

in the event of your having being found ineligible at any state in future for the award/eligibility for INSPIRE Fellowship due to any reason(including unintentional computer error or printer's devil etc.) this offer will be deemed withdrawn.

Dr. 8. Mallikarjuna Babu Scientist 'C'

KIRANKUMAR NALLA

C/O : NALLA NAGENDRA PRASAD Address : 10-252.KOTHAPETA DOWLAISWARAM

City : Rajahmundry

State/UT: ANDHRA PRADESH - 533125

This is a Computer Generated Offer Letter. No Signature is required

Date: 4 July, 2018

GENERAL INSTRUCTIONS Dear KIRANKUMAR NALLA,

Please note that these documents are necessary to upload within one month from the date of this letter at INSPIRE Online Webportal only for financial release after final selection

- 1. Joining-cum-Acceptance (JCA) Letter for INSPIRE Fellowship (template available in your dashboard in online portal))
- Releving Order from previous Fellowship/Job (If availing).
- Copy of Cancelled Blank Cheque of the Host University/ College/ Institute Account for transferring the fund (Account should be registered in Public Financial Management System: https://prims.nic.in).
- PFMS registration certificate, or Unique Agency Code in case of University/College/Institute is newly registered in Public Financial Management System.
- Since the fund would be transferred under Science & Technology Institutional and Human Capacity Building (1817), Hence bank account number of Host University/College/Institute should be registered under this scheme in PFMS.
- Please note that these documents are necessary to upload within one month from the date of this letter at INSPIRE Online
 Webportal only, otherwise it will be treated as the candidate has not intrested in accepting the INSPIRE Fellowship.
 Thanking you,

Dr. 8. Mallikarjuna Babu

Scientist 'C'

APPENDIX-1

CHAPTER-3

1 Molecular docking studies of top interacting molecules and their docking poses (Related to 3.3.2 section of chapter-3 of thesis)

All docking interaction poses of the top molecules with PRMT5:MEP50 complex and EZH2 were mentioned here with their interacting residues and binding energies.

1.1 Interaction with Brazilin

The ligand-protein docking revealed that Brz was interacting with human PRMT5-MEP50 complex & EZH2. The binding pattern of Brz was analyzed in all the three forms of structures of PRMT5-MEP50 (4X60, 4X61, 4X63) where ligand is SFG, SAM and SAHA respectively and with EZH2 (5HYN, 4mi5) where ligand is SAHA and SET domain respectively (Figure 1.1).

(b) (a) LEU 445 4X60 (-7.41kcal/mol) 4X61 (-6.38kcal/mol) 4mi5 (-7.92kcal/mol) 5HYN (-8.086kcal/mol) Interacting residues (H bonding) Pi-Pi stacking 4X60 Tyr686 4X61 Glu444, Gln309, Ser578, Glu435 4X63 5HYN Tyr324,Glu392, Glu444, Glu435 4mi5 Met662, Ile109, Asn688 Phe665

Interaction of PRMT5:MEP50 & EZH2 with Brazilin

Figure-1.1- Interaction Profile of Brazilin with Human PRMT5 and EZH2 Complexes-

Illustration of the interaction profiles of Brz with the human PRMT5 complex and EZH2 complex. (a-b) Interaction profiles of Brz with PRMT5 (PDB IDs: 4X60, 4X61). The hydrogen bonds are represented by green dotted lines. The interacting amino acid residues and the ligand SFG are depicted using blue and black ball-and-stick models. Non-bonded interactions are indicated by residues with starbursts. (c-d) Interaction profiles of Brz with EZH2 (PDB IDs: 5HYN, 4MI5). The ligands are positioned in the centre, with hydrogen bonds shown as purple arrows. The arrowheads indicate the H-bond donor-acceptor relationships. The π -cation interactions between Brz, SFG, and the lysine side chain are marked with red arrows. Hydrogen bonds are shown in green dotted lines, and interacting amino acid residues, along with the ligand SFG, are displayed in blue and black ball-and-stick models. Non-bonded interactions are represented by residues with starbursts. The table shows the interaction residues both H bonding and Pi-Pi stacking with respective to each PDB ID's.

1.2 Interaction with Resveratrol

The ligand-protein docking revealed that Rvr was interacting with human PRMT5-MEP50 complex & EZH2. The binding pattern of Rvr was analyzed in all the three forms of structures of PRMT5-MEP50 (4X60, 4X61, 4X63) where ligand is SFG, SAM and SAHA respectively and with EZH2 (5HYN, 4mi5) where ligand is SAHA and SET domain respectively (Figure 1.2).

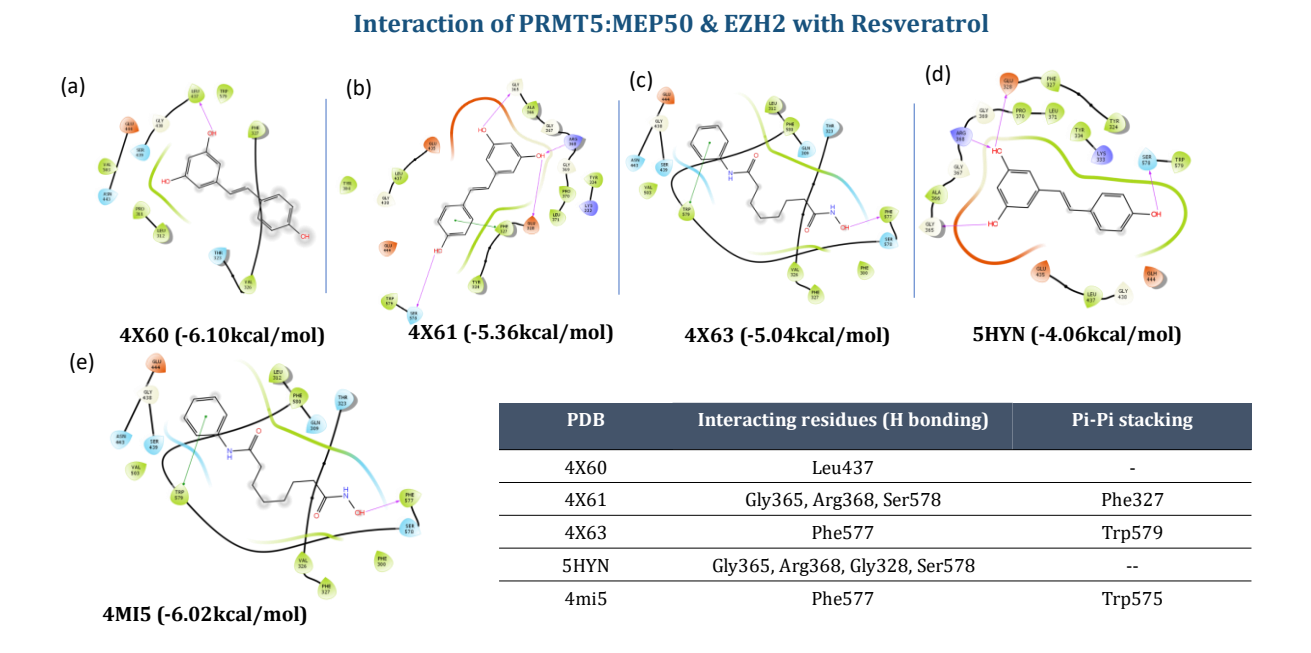


Figure-1.2 - Interaction Profile of Rvr with Human PRMT5 and EZH2 Complexes-Illustration of the interaction profiles of Rvr with the human PRMT5 complex and EZH2 complex. (a-c) Interaction profiles of Rvr with PRMT5 (PDB IDs: 4X60, 4X61). The hydrogen bonds are represented by green dotted lines. The interacting amino acid residues and the ligand SFG are depicted using blue and black ball-and-stick models. Non-bonded interactions are indicated by residues with starbursts. (d-e) Interaction profiles of Rvr with EZH2 (PDB IDs: 5HYN, 4MI5). The ligands are positioned in the centre, with hydrogen bonds shown as purple arrows. The arrowheads indicate the H-bond donor-acceptor relationships. The π -cation interactions between Rvr, SFG, and the lysine side chain are marked with red arrows. Hydrogen bonds are shown in green dotted lines, and interacting amino acid residues, along with the ligand SFG, are displayed in blue and black ball-and-stick models. Non-bonded interactions are represented by residues with starbursts. The table shows the interaction residues both H bonding and Pi-Pi stacking with respective to each PDB ID's.

1.3 Interaction with Sulforaphane

The ligand-protein docking revealed that Sfp was interacting with human PRMT5-MEP50 complex & EZH2. The binding pattern of Sfp was analyzed in all the three forms of structures of PRMT5-MEP50 (4X60, 4X61, 4X63) where ligand is SFG, SAM and SAHA respectively and with EZH2 (5HYN, 4mi5) where ligand is SAHA and SET domain respectively (Figure 1.3).

Interaction of PRMT5:MEP50 & EZH2 with Sulforaphane

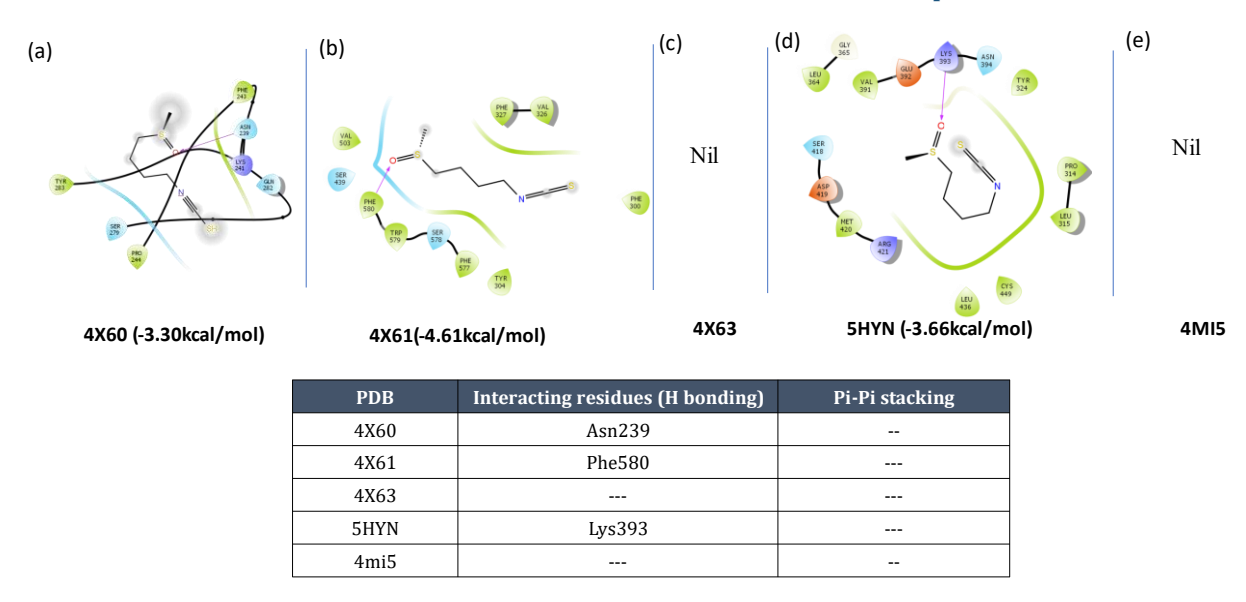


Figure-1.3- Interaction Profile of Sfp with Human PRMT5 and EZH2 Complexes-Illustration of the interaction profiles of Sfp with the human PRMT5 complex and EZH2 complex. (a-c) Interaction profiles of Sfp with PRMT5 (PDB IDs: 4X60, 4X61). The hydrogen bonds are represented by green dotted lines. The interacting amino acid residues and the ligand SFG are depicted using blue and black ball-and-stick models. Non-bonded interactions are indicated by residues with starbursts. (d-e) Interaction profiles of Sfp with EZH2 (PDB IDs: 5HYN, 4MI5). The ligands are positioned in the centre, with hydrogen bonds shown as purple arrows. The arrowheads indicate the H-bond donor-acceptor relationships. The π -cation interactions between Sfp, SFG, and the lysine side chain are marked with red arrows. Hydrogen bonds are shown in green dotted lines, and interacting amino acid residues, along with the ligand SFG, are displayed in blue and black ball-and-stick models. Non-bonded interactions are represented by residues with starbursts. The table shows the interaction residues both H bonding and Pi-Pi stacking with respective to each PDB ID's.

1.4 Interaction with Apicidin

The ligand-protein docking revealed that Apdn was interacting with human PRMT5-MEP50 complex & EZH2. The binding pattern of Apdn was analyzed in all the three forms of structures of PRMT5-MEP50 (4X60, 4X61, 4X63) where ligand is SFG, SAM and SAHA respectively and with EZH2 (5HYN, 4mi5) where ligand is SAHA and SET domain respectively (Figure 1.4).

Interaction of PRMT5:MEP50 & EZH2 with Apicidin

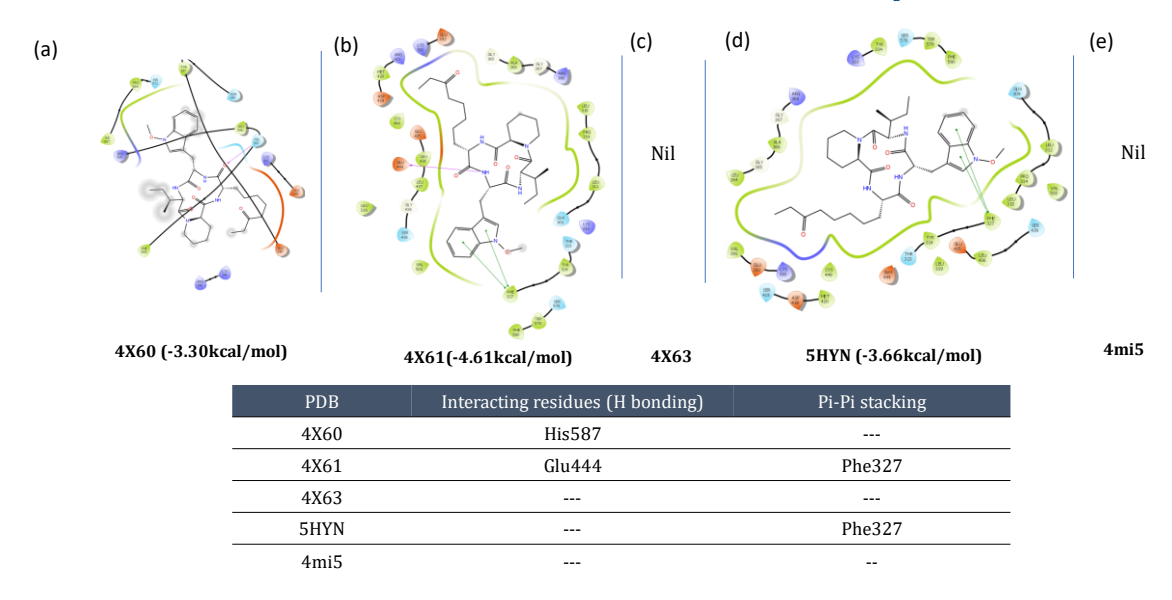


Figure-1.4- Interaction Profile of Apdn with Human PRMT5 and EZH2 Complexes-Illustration of the interaction profiles of Apdn with the human PRMT5 complex and EZH2 complex. (a-c) Interaction profiles of Apdn with PRMT5 (PDB IDs: 4X60, 4X61). The hydrogen bonds are represented by green dotted lines. The interacting amino acid residues and the ligand SFG are depicted using blue and black ball-and-

Interaction profiles of Apdn with PRMT5 (PDB IDs: 4X60, 4X61). The hydrogen bonds are represented by green dotted lines. The interacting amino acid residues and the ligand SFG are depicted using blue and black ball-and-stick models. Non-bonded interactions are indicated by residues with starbursts. (d-e) Interaction profiles of Apdn with EZH2 (PDB IDs: 5HYN, 4MI5). The ligands are positioned in the centre, with hydrogen bonds shown as purple arrows. The arrowheads indicate the H-bond donor-acceptor relationships. The π -cation interactions between Apdn, SFG, and the lysine side chain are marked with red arrows. Hydrogen bonds are shown in green dotted lines, and interacting amino acid residues, along with the ligand SFG, are displayed in blue and black ball-and-stick models. Non-bonded interactions are represented by residues with starbursts. The table shows the interaction residues both H bonding and Pi-Pi stacking with respective to each PDB ID's.

1.5 Interaction with capsaicin

The ligand-protein docking revealed that Cpcn was interacting with human PRMT5-MEP50 complex & EZH2. The binding pattern of Cpcn was analyzed in all the three forms of structures of PRMT5-MEP50 (4X60, 4X61, 4X63) where ligand is SFG, SAM and SAHA respectively and with EZH2 (5HYN, 4mi5) where ligand is SAHA and SET domain respectively (Figure 1.5).

Interaction of PRMT5:MEP50 & EZH2 with Capsaicin

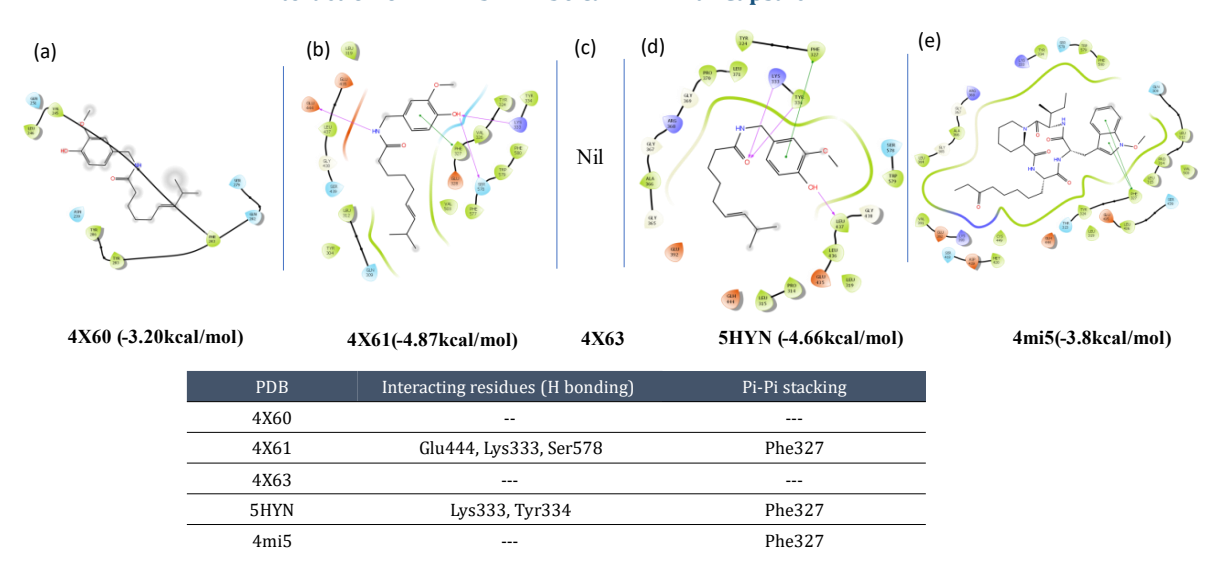


Figure-1.5- Interaction Profile of Cpcn with Human PRMT5 and EZH2 Complexes-Illustration of the interaction profiles of Cpcn with the human PRMT5 complex and EZH2 complex. (a-c) Interaction profiles of Cpcn with PRMT5 (PDB IDs: 4X60, 4X61). The hydrogen bonds are represented by green dotted lines. The interacting amino acid residues and the ligand SFG are depicted using blue and black ball-and-stick models. Non-bonded interactions are indicated by residues with starbursts. (d-e) Interaction profiles of Cpcn with EZH2 (PDB IDs: 5HYN, 4MI5). The ligands are positioned in the centre, with hydrogen bonds shown as purple arrows. The arrowheads indicate the H-bond donor-acceptor relationships. The π -cation interactions between Cpcn, SFG, and the lysine side chain are marked with red arrows. Hydrogen bonds are shown in green dotted lines, and interacting amino acid residues, along with the ligand SFG, are displayed in blue and black ball-and-stick models. Non-bonded interactions are represented by residues with starbursts. The table shows the interaction residues both H bonding and Pi-Pi stacking with respective to each PDB ID's.

1.6 Interaction with Quercetin

The ligand-protein docking revealed that Qct was interacting with human PRMT5-MEP50 complex & EZH2. The binding pattern of Qct was analyzed in all the three forms of structures of PRMT5-MEP50 (4X60, 4X61, 4X63) where ligand is SFG, SAM and SAHA respectively and with EZH2 (5HYN, 4mi5) where ligand is SAHA and SET domain respectively (Figure 1.6).

Interaction of PRMT5:MEP50 & EZH2 with Quercetin

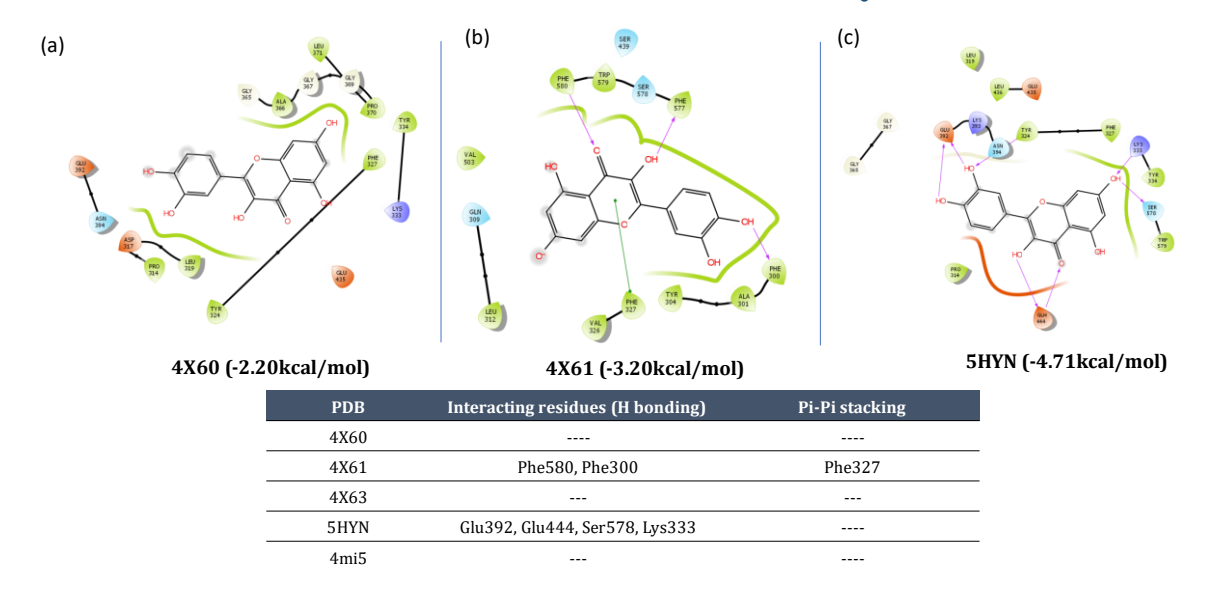


Figure-1.6- Interaction Profile of Qct with Human PRMT5 and EZH2 Complexes. Illustration of the interaction profiles of Qct with the human PRMT5 complex and EZH2 complex. (a-b) Interaction profiles of Qct with PRMT5 (PDB IDs: 4X60, 4X61). The hydrogen bonds are represented by green dotted lines. The interacting amino acid residues and the ligand SFG are depicted using blue and black ball-and-stick models. Non-bonded interactions are indicated by residues with starbursts. (c) Interaction profiles of Qct with EZH2 (PDB IDs: 5HYN). The ligands are positioned in the centre, with hydrogen bonds shown as purple arrows. The arrowheads indicate the H-bond donor-acceptor relationships. The π -cation interactions between Qct, SFG, and the lysine side chain are marked with red arrows. Hydrogen bonds are shown in green dotted lines, and interacting amino acid residues, along with the ligand SFG, are displayed in blue and black ball-and-stick models. Non-bonded interactions are represented by residues with starbursts. The table shows the interaction residues both H bonding and Pi-Pi stacking with respective to each PDB ID's.

1.7 Interaction with Eucalyptol

The ligand-protein docking revealed that Ect was interacting with human PRMT5-MEP50 complex & EZH2. The binding pattern of Apdn was analyzed in all the three forms of structures of PRMT5-MEP50 (4X60, 4X61) where ligand is SFG, SAM and SAHA respectively and with EZH2 (5HYN, 4mi5) where ligand is SAHA and SET domain respectively (Figure 1.7).

Interaction of PRMT5:MEP50 & EZH2 with Eucalyptol

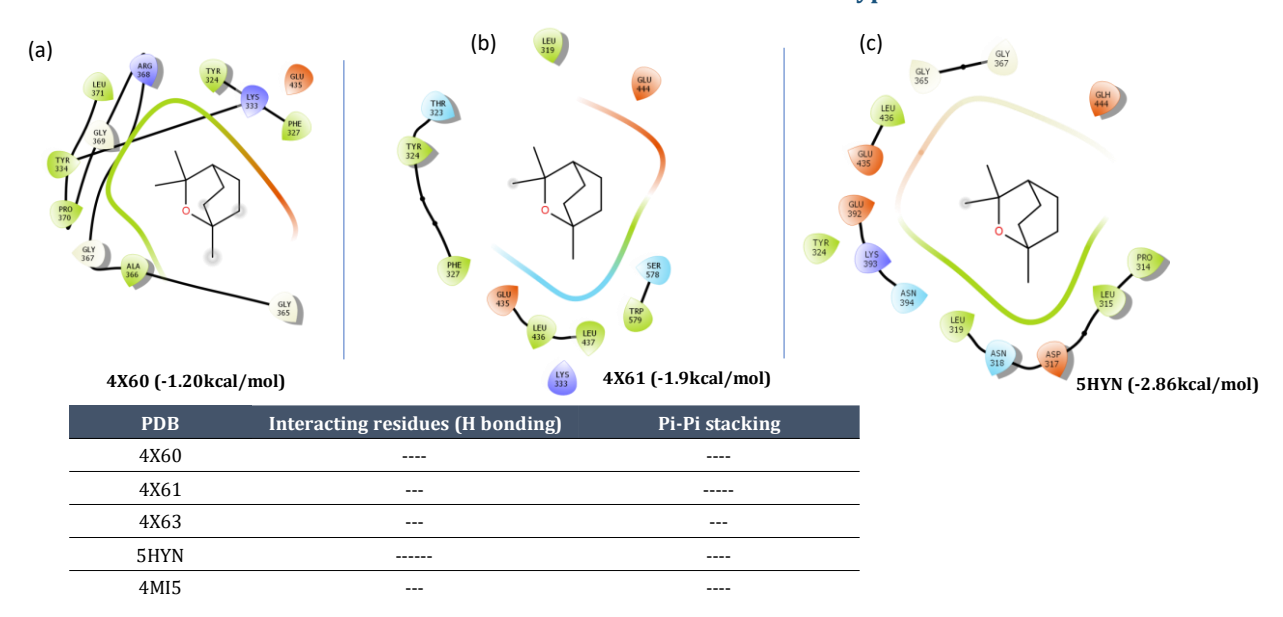


Figure-1.7- Interaction Profile of Ect with Human PRMT5 and EZH2 Complexes-Illustration of the interaction profiles of Ect with the human PRMT5 complex and EZH2 complex. (a-b) Interaction profiles of Ect with PRMT5 (PDB IDs: 4X60, 4X61). The hydrogen bonds are represented by green dotted lines. The interacting amino acid residues and the ligand SFG are depicted using blue and black ball-and-stick models. Non-bonded interactions are indicated by residues with starbursts. (c) Interaction profiles of Ect with EZH2 (PDB IDs: 5HYN). The ligands are positioned in the centre, with hydrogen bonds shown as purple arrows. The arrowheads indicate the H-bond donor-acceptor relationships. The π-cation interactions between Ect, SFG, and the lysine side chain are marked with red arrows. Hydrogen bonds are shown in green dotted lines, and interacting amino acid residues, along with the ligand SFG, are displayed in blue and black ball-and-stick models. Non-bonded interactions are represented by residues with starbursts. The table shows the interaction residues both H bonding and Pi-Pi stacking with respective to each PDB ID's.

1.8 Interaction with Eugenol

The ligand-protein docking revealed that Egl was interacting with human PRMT5-MEP50 complex & EZH2. The binding pattern of Egl was analyzed in all the three forms of structures of PRMT5-MEP50 (4X60, 4X61, 4X63) where ligand is SFG, SAM and SAHA respectively and with EZH2 (5HYN, 4mi5) where ligand is SAHA and SET domain respectively (Figure 1.8).

Interaction of PRMT5:MEP50 & EZH2 with Eugenol

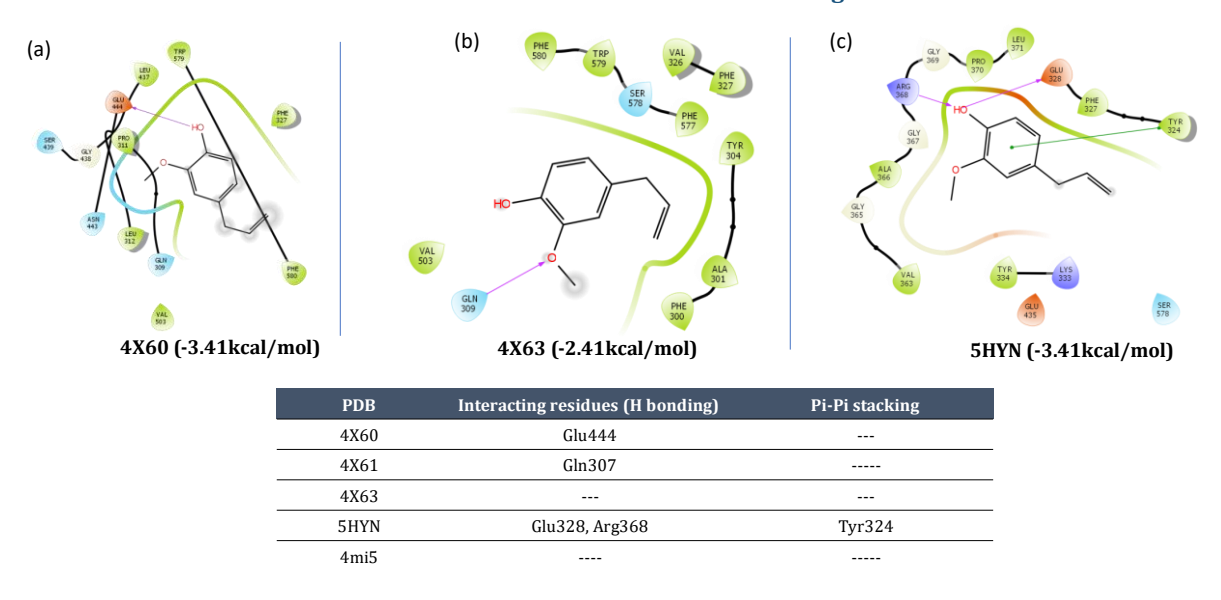


Figure-1.8- Interaction Profile of Egl with Human PRMT5 and EZH2 Complexes-Illustration of the interaction profiles of Egl with the human PRMT5 complex and EZH2 complex. (a-c) Interaction profiles of Egl with PRMT5 (PDB IDs: 4X60, 4X61). The hydrogen bonds are represented by green dotted lines. The interacting amino acid residues and the ligand SFG are depicted using blue and black ball-and-stick models. Non-bonded interactions are indicated by residues with starbursts. (d-e) Interaction profiles of Egl with EZH2 (PDB IDs: 5HYN, 4MI5). The ligands are positioned in the centre, with hydrogen bonds shown as purple arrows. The arrowheads indicate the H-bond donor-acceptor relationships. The π -cation interactions between Egl, SFG, and the lysine side chain are marked with red arrows. Hydrogen bonds are shown in green dotted lines, and interacting amino acid residues, along with the ligand SFG, are displayed in blue and black ball-and-stick models. Non-bonded interactions are represented by residues with starbursts. The table shows the interaction residues both H bonding and Pi-Pi stacking with respective to each PDB ID's.

1.9 Interaction with Gambogic acid

The ligand-protein docking revealed that Gba was interacting with human PRMT5-MEP50 complex & EZH2. The binding pattern of Gba was analyzed in all the three forms of structures of PRMT5-MEP50 (4X60, 4X61, 4X63) where ligand is SFG, SAM and SAHA respectively and with EZH2 (5HYN, 4mi5) where ligand is SAHA and SET domain respectively (Figure 1.9).

Interaction of PRMT5:MEP50 & EZH2 with Gambogic acid

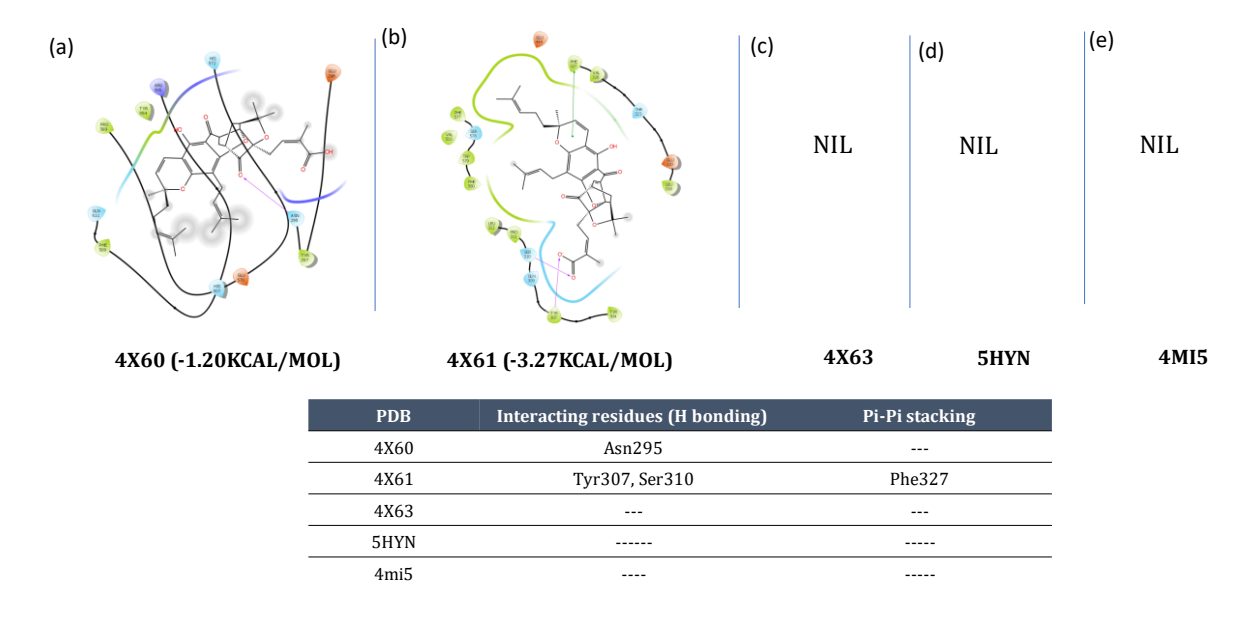


Figure-1.9- Interaction Profile of Gba with Human PRMT5 and EZH2 Complexes-Illustration of the interaction profiles of Gba with the human PRMT5 complex and EZH2 complex. (a-c) Interaction profiles of Gba with PRMT5 (PDB IDs: 4X60, 4X61). The hydrogen bonds are represented by green dotted lines. The interacting amino acid residues and the ligand SFG are depicted using blue and black ball-and-stick models. Non-bonded interactions are indicated by residues with starbursts. (d-e) Interaction profiles of Gba with EZH2 (PDB IDs: 5HYN, 4MI5). The ligands are positioned in the centre, with hydrogen bonds shown as purple arrows. The arrowheads indicate the H-bond donor-acceptor relationships. The π -cation interactions between Gba, SFG, and the lysine side chain are marked with red arrows. Hydrogen bonds are shown in green dotted lines, and interacting amino acid residues, along with the ligand SFG, are displayed in blue and black ball-and-stick models. Non-bonded interactions are represented by residues with starbursts. The table shows the interaction residues both H bonding and Pi-Pi stacking with respective to each PDB ID's.

1.10 Interaction with Vorinostat

The ligand-protein docking revealed that Vorinostat was interacting with human PRMT5-MEP50 complex & EZH2. The binding pattern of Vorinostat was analyzed in all the three forms of structures of PRMT5-MEP50 (4X60, 4X61, 4X63) where ligand is SFG, SAM and SAHA respectively and with EZH2 (5HYN, 4mi5) where ligand is SAHA and SET domain respectively (Figure 1.10).

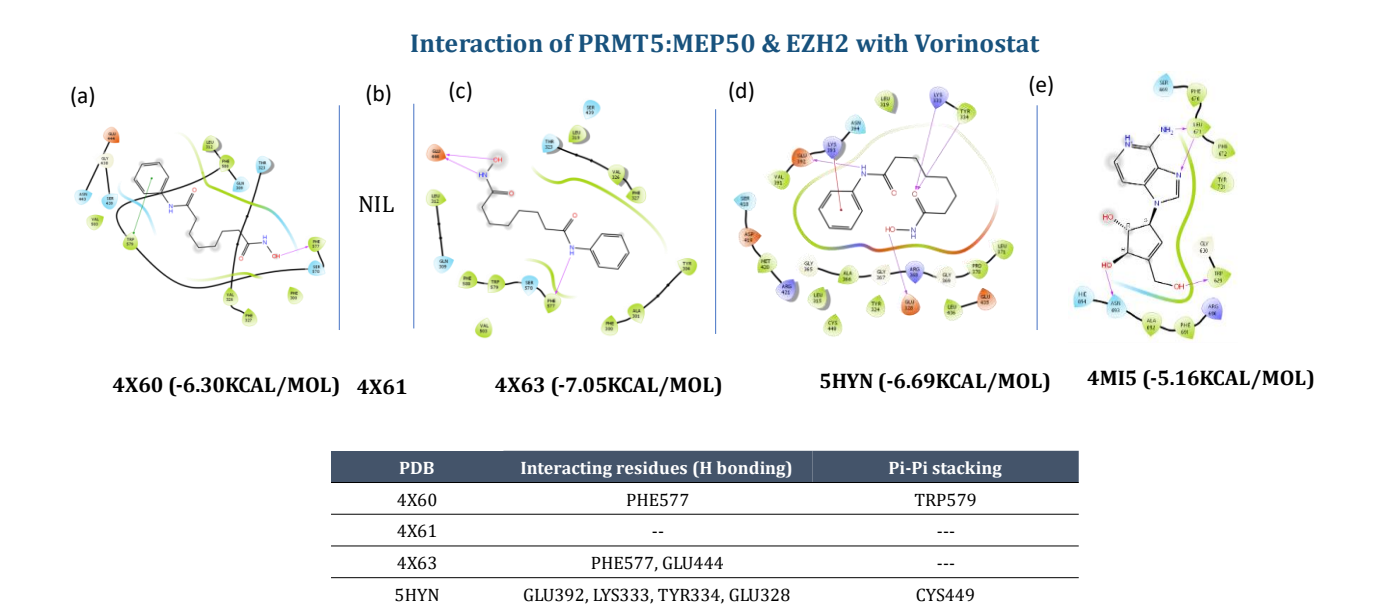


Figure-1.10- Interaction Profile of Vorinostat with Human PRMT5 and EZH2 Complexes- Illustration of the interaction profiles of Vorinostat with the human PRMT5 complex and EZH2 complex. (a-c) Interaction profiles of Vorinostat with PRMT5 (PDB IDs: 4X60, 4X61). The hydrogen bonds are represented by green dotted lines. The interacting amino acid residues and the ligand SFG are depicted using blue and black ball-and-stick models. Non-bonded interactions are indicated by residues with starbursts. (d-e) Interaction profiles of vorinostat with EZH2 (PDB IDs: 5HYN, 4MI5). The ligands are positioned in the centre, with hydrogen bonds shown as purple arrows. The arrowheads indicate the H-bond donor-acceptor relationships. The π -cation interactions between Vorinostat, SFG, and the lysine side chain are marked with red arrows. Hydrogen bonds are shown in green dotted lines, and interacting amino acid residues, along with the ligand SFG, are displayed in blue and black ball-and-stick models. Non-bonded interactions are represented by residues with starbursts. The table shows the interaction residues both H bonding and Pi-Pi stacking with respective to each

LEU678, TRP629, ASN693

TRP575

1.11 Interaction with Piperine

PDB ID's.

4MI5

The ligand-protein docking revealed that Ppr was interacting with human PRMT5-MEP50 complex & EZH2. The binding pattern of Apdn was analyzed in all the three forms of structures of PRMT5-MEP50 (4X60, 4X61, 4X63) where ligand is SFG, SAM and SAHA respectively and with EZH2 (5HYN, 4mi5) where ligand is SAHA and SET domain respectively (Figure 1.11).

Interaction of PRMT5:MEP50 & EZH2 with Piperine

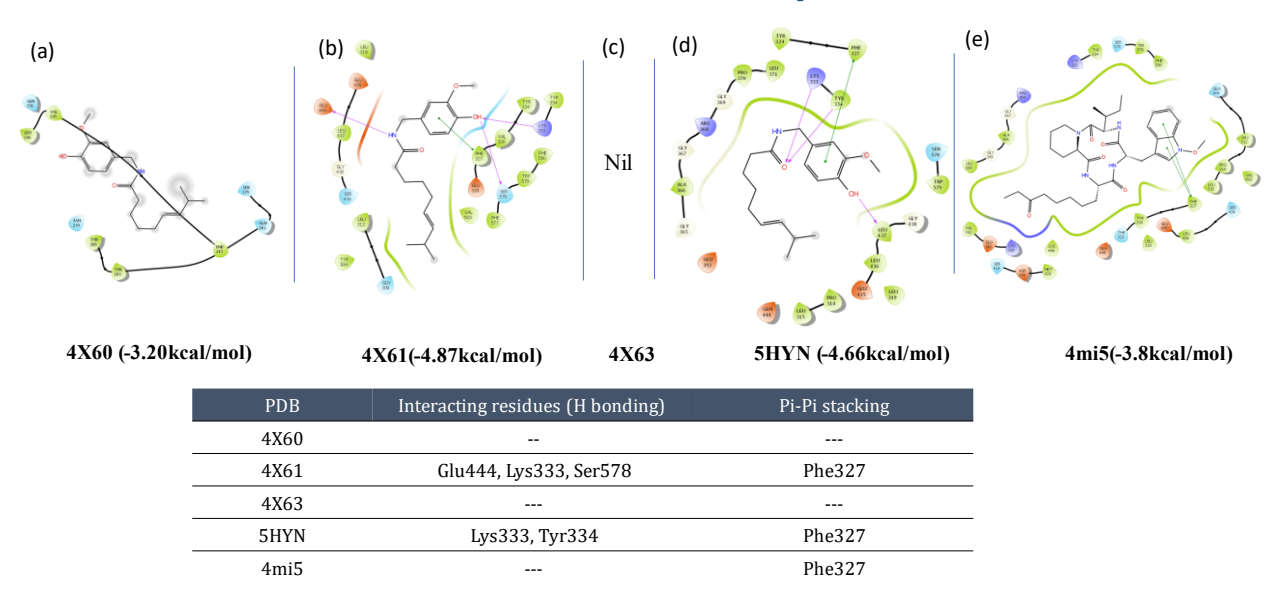


Figure-1.11- Interaction Profile of Ppr with Human PRMT5 and EZH2 Complexes-

Illustration of the interaction profiles of Ppr with the human PRMT5 complex and EZH2 complex. (a-c) Interaction profiles of Ppr with PRMT5 (PDB IDs: 4X60, 4X61). The hydrogen bonds are represented by green dotted lines. The interacting amino acid residues and the ligand SFG are depicted using blue and black ball-and-stick models. Non-bonded interactions are indicated by residues with starbursts. (d-e) Interaction profiles of Ppr with EZH2 (PDB IDs: 5HYN, 4MI5). The ligands are positioned in the centre, with hydrogen bonds shown as purple arrows. The arrowheads indicate the H-bond donor-acceptor relationships. The π -cation interactions between Ppr, SFG, and the lysine side chain are marked with red arrows. Hydrogen bonds are shown in green dotted lines, and interacting amino acid residues, along with the ligand SFG, are displayed in blue and black ball-and-stick models. Non-bonded interactions are represented by residues with starbursts. The table shows the interaction residues both H bonding and Pi-Pi stacking with respective to each PDB ID's.

1.12 Interaction with Anethol

The ligand-protein docking revealed that Atl was interacting with human PRMT5-MEP50 complex & EZH2. The binding pattern of Atl was analyzed in all the three forms of structures of PRMT5-MEP50 (4X60, 4X61, 4X63) where ligand is SFG, SAM and SAHA respectively and with EZH2 (5HYN, 4mi5) where ligand is SAHA and SET domain respectively (Figure 1.12).

Interaction of PRMT5:MEP50 & EZH2 with Anethol

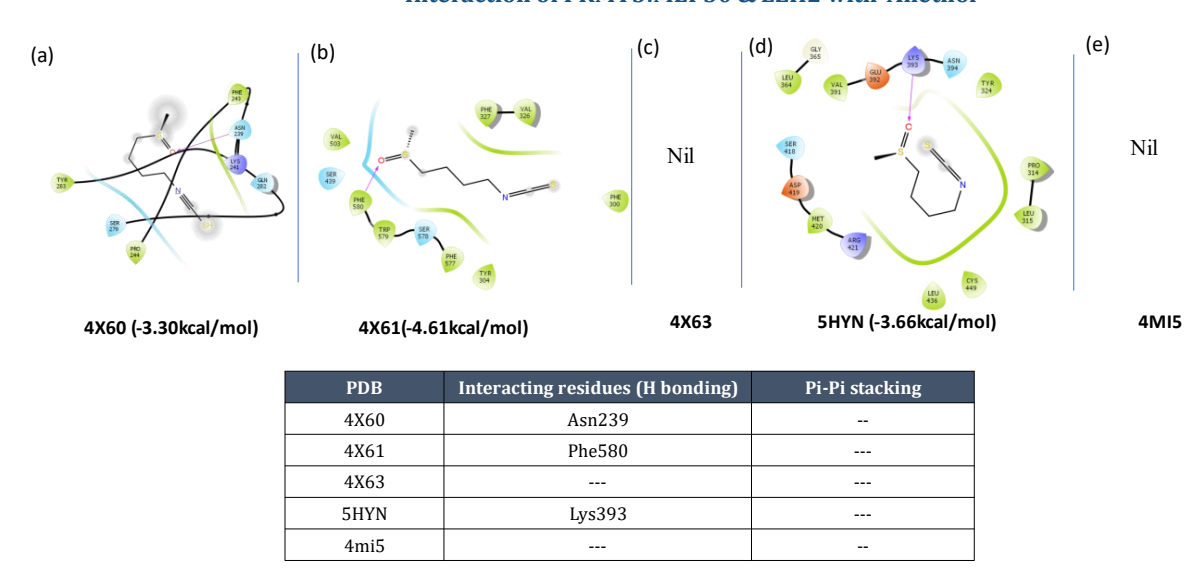
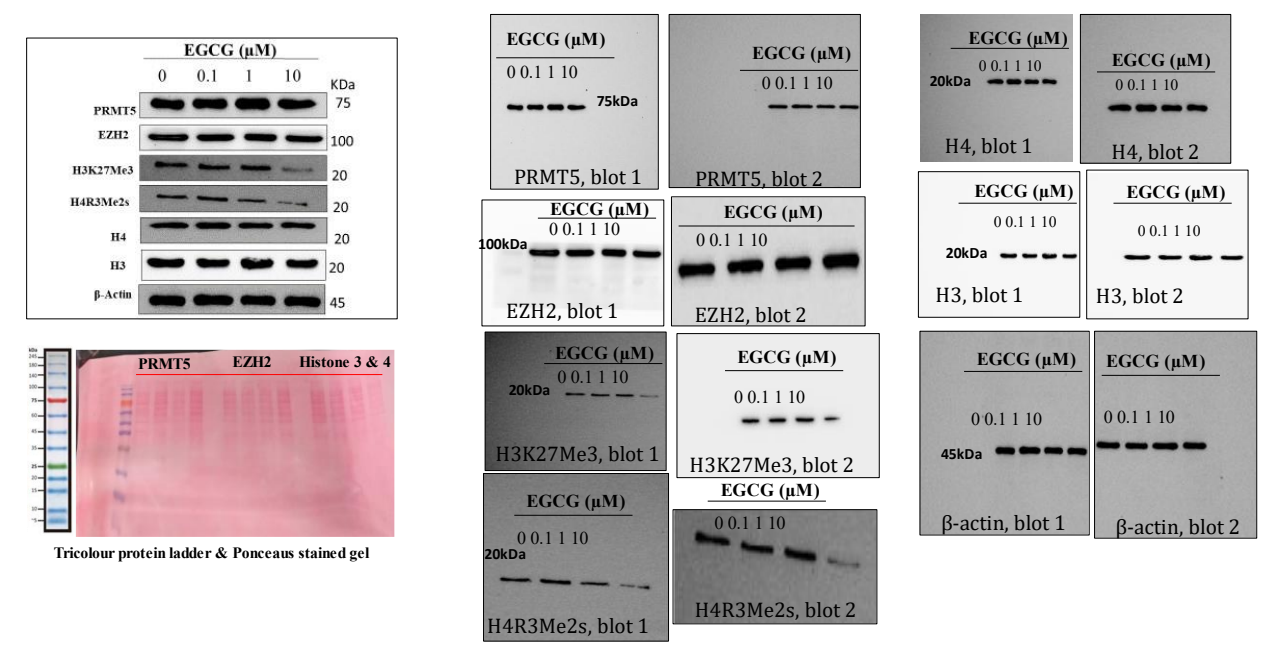


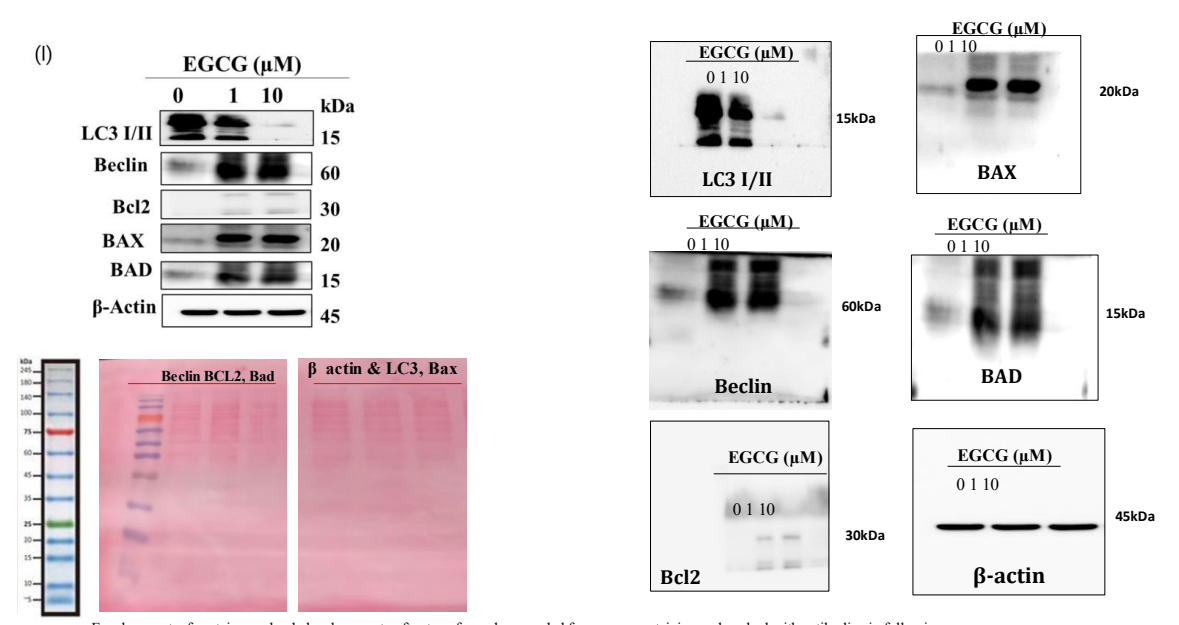
Figure-1.12- Interaction Profile of Atl with Human PRMT5 and EZH2 Complexes-Illustration of the interaction profiles of Atl with the human PRMT5 complex and EZH2 complex. (a-c) Interaction profiles of Atl with PRMT5 (PDB IDs: 4X60, 4X61). The hydrogen bonds are represented by green dotted lines. The interacting amino acid residues and the ligand SFG are depicted using blue and black ball-and-stick models. Non-bonded interactions are indicated by residues with starbursts. (d-e) Interaction profiles of Atl with EZH2 (PDB IDs: 5HYN, 4MI5). The ligands are positioned in the centre, with hydrogen bonds shown as purple arrows. The arrowheads indicate the H-bond donor-acceptor relationships. The π-cation interactions between Atl, SFG, and the lysine side chain are marked with red arrows. Hydrogen bonds are shown in green dotted lines, and interacting amino acid residues, along with the ligand SFG, are displayed in blue and black ball-and-stick models. Non-bonded interactions are represented by residues with starbursts. The table shows the interaction residues both H bonding and Pi-Pi stacking with respective to each PDB ID's.

3.1 Full blot images for EGCG interaction with PRMT5:MEP50 & EZH2 (related to section 3.3.2.7 of thesis 3rd chapter)



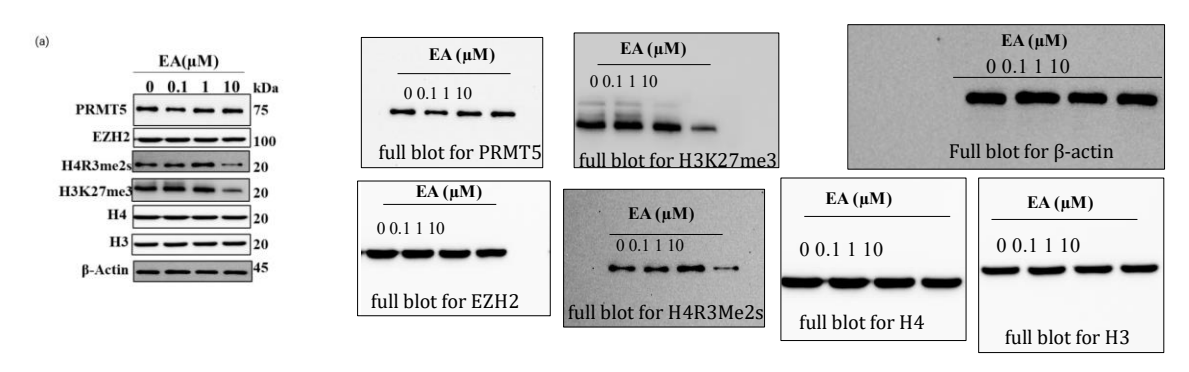
Equal amount of protein was loaded, gel was cute and probed with antibodies in following manner: 1^{st} 4 wells loaded samples were used for PRMT5, & H4R3me2S, 2^{nd} 4 wells used for EZH2, β -Actin , H3K27Me3, 3^{rd} 4 wells used for Histone 3 and restriped for H4.

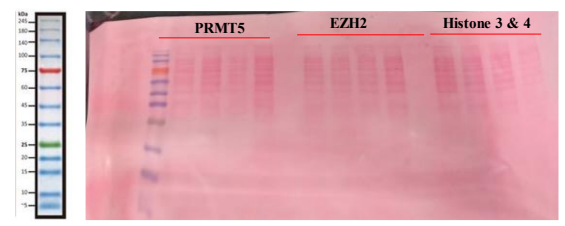
Related to section 3.3.2.9 of thesis 3rd chapter



Equal amount of protein was loaded, gel was cute after transfer and proceeded for ponceaus staining and probed with antibodies in following manner 1^{st} Gel 3 wells loaded samples were used for Beclin, BCl2, & Bad 2^{nd} Gel 3 wells used for β -Actin, LC3 & Bax(restriped)

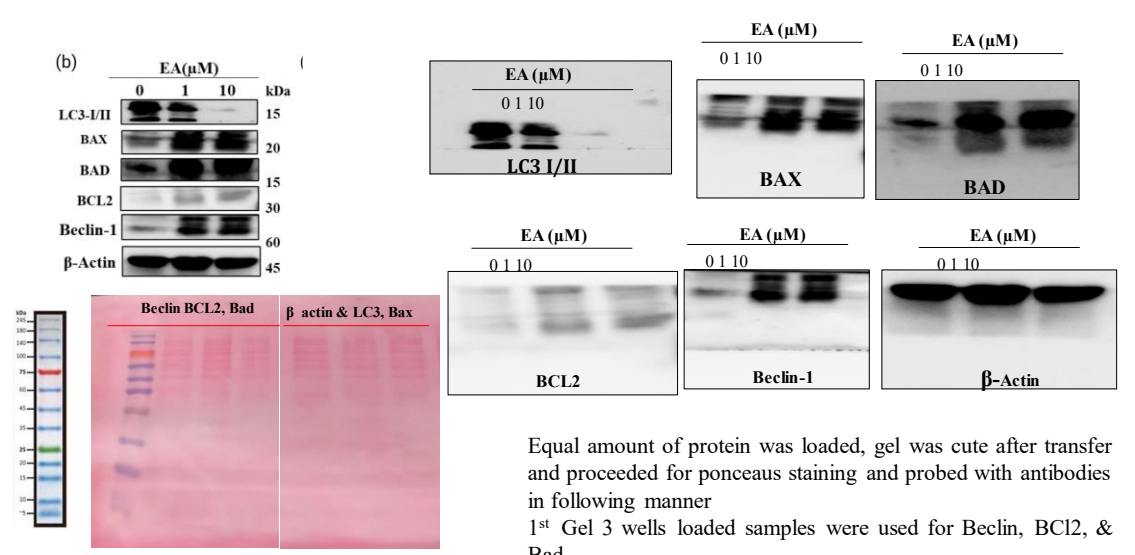
3.2 Full blot images for EA interaction with PRMT5:MEP50 & EZH2 Related to section 3.4.5 of thesis 3rd chapter





Equal amount of protein was loaded, gel was cute and probed with antibodies in following manner: 1^{st} 4 wells loaded samples were used for PRMT5, & H4R3me2S, 2^{nd} 4 wells used for EZH2, $\beta\text{-Actin}$, H3K27Me3, 3^{rd} 4 wells used for Histone 3 and restriped for H4.

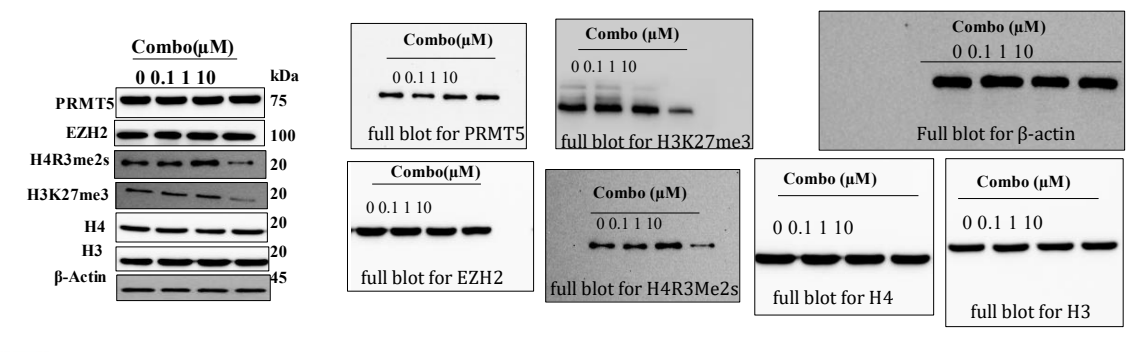
Related to section 3.4.8 of thesis 3rd chapter

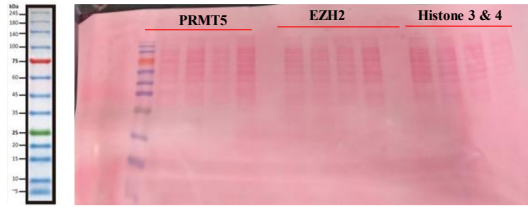


Tricolour protein ladder & Ponceaus stained gel

 2^{nd} Gel 3 wells used for β-Actin, LC3 & Bax(restriped)

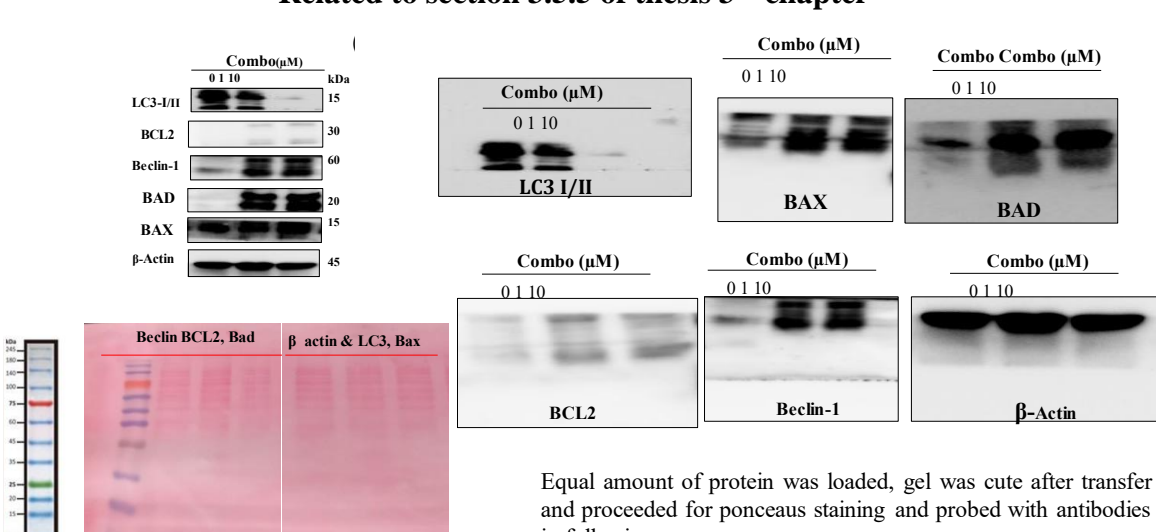
3.3 Full blot images for combo interaction with PRMT5:MEP50 & EZH2 Related to section 3.5.2 of thesis 3rd chapter





Equal amount of protein was loaded, gel was cute and probed with antibodies in following manner: 1st 4 wells loaded samples were used for PRMT5, & H4R3me2S, 2nd 4 wells used for EZH2, β -Actin , H3K27Me3, 3^{rd} 4 wells used for Histone 3 and restriped for H4.

Related to section 3.5.5 of thesis 3rd chapter



Tricolour protein ladder & Ponceaus stained gel

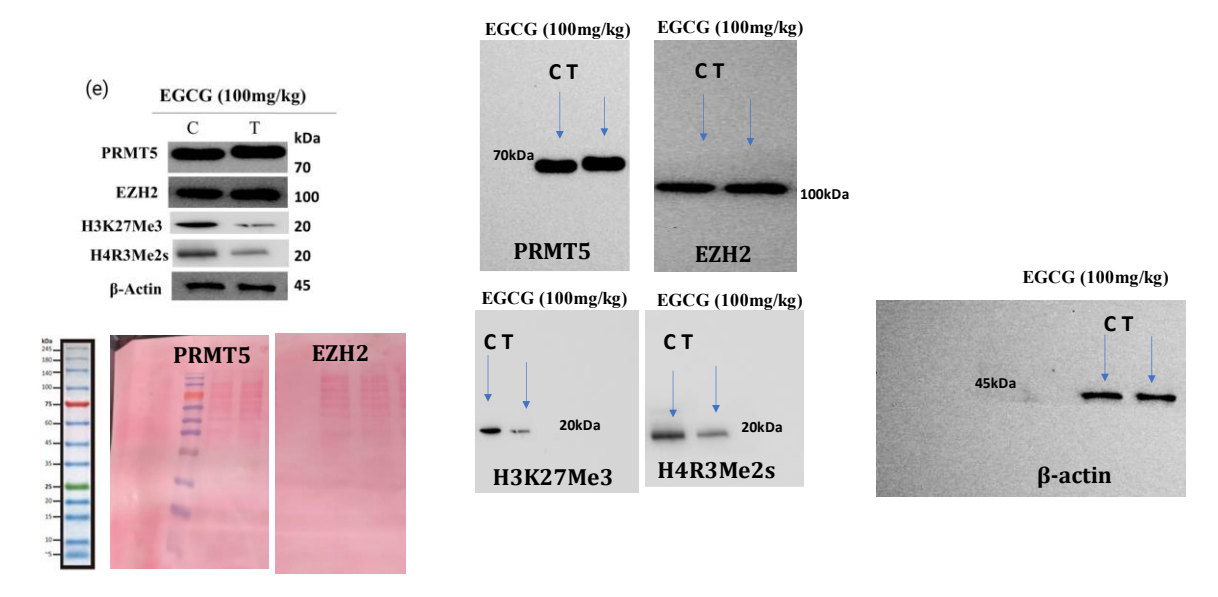
and proceeded for ponceaus staining and probed with antibodies in following manner

1st Gel 3 wells loaded samples were used for Beclin, BCl2, &

2nd Gel 3 wells used for β-Actin, LC3 & Bax(restriped)

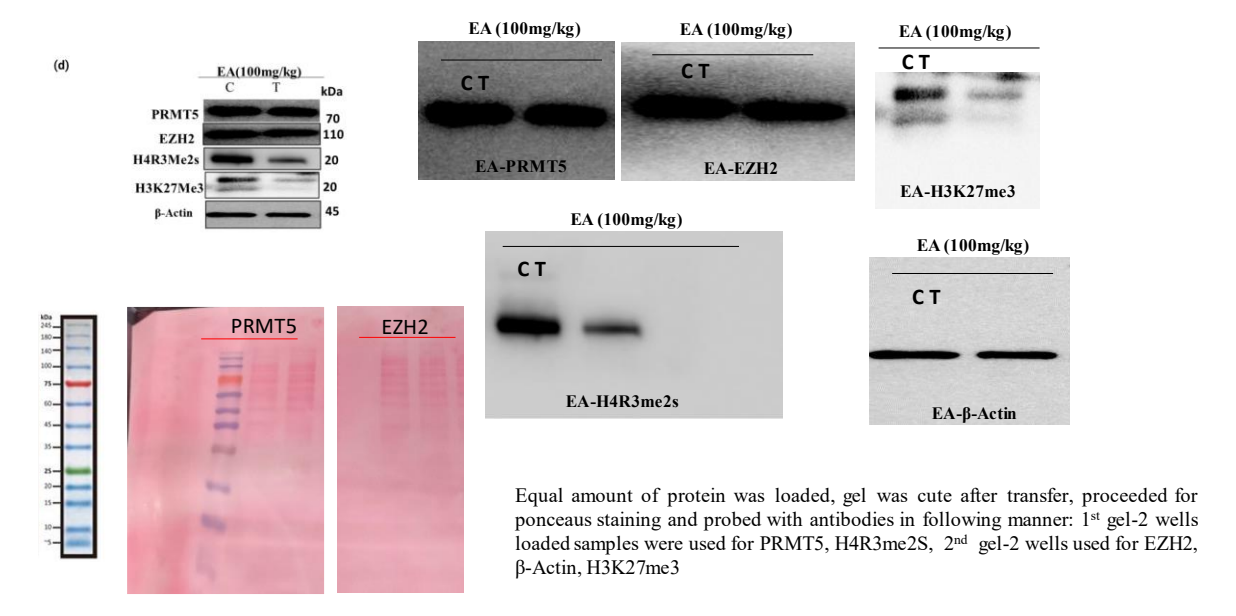
Chapter -4

4.1 EGCG animal studies western blot (related to 4.3.1section of thesis 4th chapter)

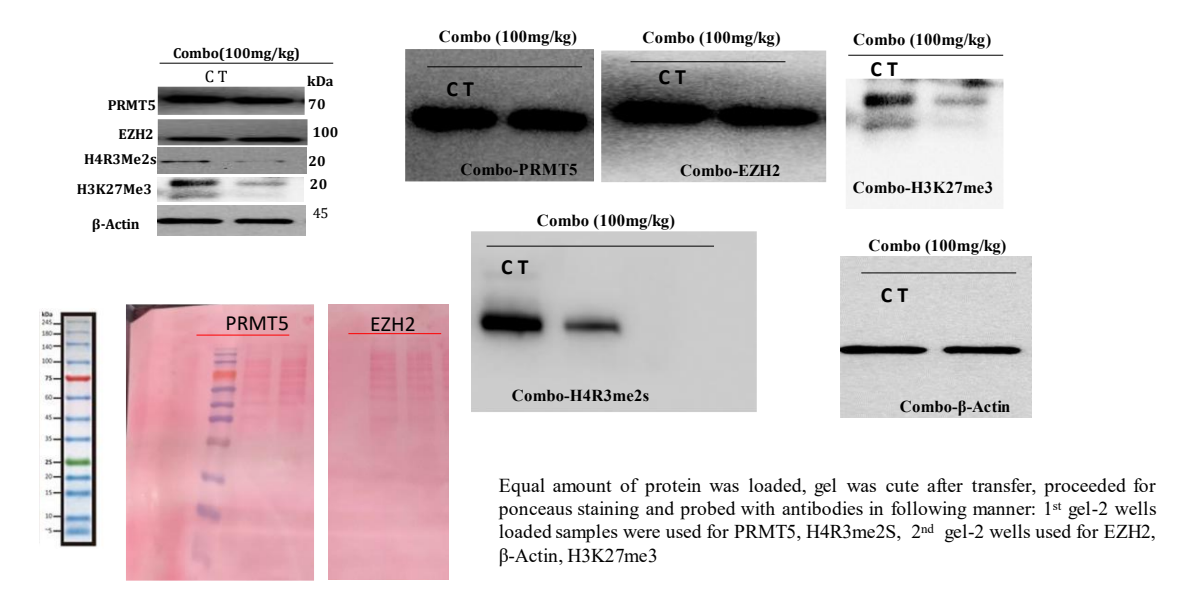


Equal amount of protein was loaded, gel was cute after transfer, proceeded for ponceaus staining and probed with antibodies in following manner: 1^{st} gel-2 wells loaded samples were used for PRMT5, H4R3me2S, 2^{nd} gel-2 wells used for EZH2, β -Actin, H3K27me3

4.2 EA animal studies western blots (related to 4.4 section of thesis 4th chapter)



4.3 Combo animal studies western blots-(related to 4.5 section of thesis 4th chapter)





University of Hyderabad

(A central University established in 1974 by Act of Parliament)
(P.O.) Central University, Gachibowli



Hyderabad-500046

PLAGIARISM FREE CERTIFICATE

192010000 000040

This is to certify that the thesis entitled "Inhibition of Protein Arginine Methyltransferase5 and Enhancer of Zeste Homolog-2 by Phytocompounds" submitted by Mr. Nalla
Kirankumar bearing Reg No: 17LPPH18, in partial fulfillment of the requirements for the
award of Doctor of Philosophy in the Department of Plant Sciences, School of Life Sciences,
is free from Plagiarism and has not been submitted previously in part or in full to this or any
other University or Institution for the award of any degree or diploma.

The similarity index of this thesis as checked by the library of the University of Hyderabad is 25%. Out of this 17% similarity has been found to be identified from the candidate's own publication(s) which forms the major part of the thesis. The details of the student's publication are as follows:

Published in the following publications: List out the Publications here-

- Nalla, K., Chatterjee, B., Poyya, J., Swain, A., Ghosh, K., Pan, A., & Kanade, S. R. (2024). Epigallocatechin-3-gallate inhibit the protein arginine methyltransferase 5 and Enhancer of Zeste homolog 2 in breast cancer both in vitro and in vivo. *bioRxiv*, 2024-02. https://doi.org/10.1101/2024.02.18.580855 (pre-print).
- Nalla, K., Chatterjee, B., Poyya, J., Swain, A., Ghosh, K., Pan, A., ... & Kanade, S. R. (2024). Ellagic acid: a potential inhibitor of enhancer of zeste homolog-2 and protein arginine methyltransferase-5. bioRxiv, 2024-05. doi: https://doi.org/10.1101/2024.05.22.595443 (Pre-print)

About 8% similarity was identified from the external sources in the present thesis which is according to the prescribed regulations of the university. All the publications related to the thesis have been appended at the end of the thesis. Hence the present thesis is considered to be plagiarism-free.

Prof Santosh R Kanade

[Supervisor]

Dr. SANTOSH R. KANADE
Professor
Dept. of Plant Sciences
School of Life Sciences
University of Hyderabad
Hyderabad-500 046. T.S. India.

inhibition of protein arginine methytransferase5 and enhancer of zeste homolog by phytocompounds

by Kiran Kumar Nalla

Submission date: 15-Jul-2024 11:17AM (UTC+0530)

Submission ID: 2417080550

File name: Kiran_theis_drfat_for_plagiarsim_09-07-24.docx (113.93K)

Word count: 25593

Character count: 156823

inhibition of protein arginine methytransferase5 and enhancer of zeste homolog by phytocompounds

ORIGINALITY REPORT

25% SIMILARITY INDEX

12%

I **~**%

INTERNET SOURCES

22%

PUBLICATIONS

18%

STUDENT PAPERS

PRIMARY SOURCES



Submitted to University of Hyderabad, Hyderabad

Student Paper

14%

Kirankumar Nalla, Biji Chatterjee, Jagadeesha Poyya, Aishwarya Swain et al. "Ellagic acid: a potential inhibitor of enhancer of zeste homolog-2 and protein arginine methyltransferase-5", Cold Spring Harbor Laboratory, 2024

2%

Publication

3

Kirankumar Nalla, Biji Chatterjee, Jagadeesh Poyya, Aishwarya Swain et al. "
Epigallocatechin-3-gallate inhibit the protein arginine methyltransferase 5 and Enhancer of Zeste homolog 2 in breast cancer both and ", Cold Spring Harbor Laboratory, 2024

1 %



www.frontiersin.org

Internet Source

1 %

5

www.science.gov



A Tanuma. "Caffeine Enhances the Expression of the Angiotensin II Type 2 Receptor mRNA in BeWo Cell Culture and in the Rat Placenta", Placenta, 2003

<1%

Publication

Publication



Ying Huang, Martin Sendzik, Jeff Zhang, Zhenting Gao et al. "Discovery of the Clinical Candidate MAK683: An EED-Directed, Allosteric, and Selective PRC2 Inhibitor for the Treatment of Advanced Malignancies", Journal of Medicinal Chemistry, 2022

<1%

109

hdl.handle.net
Internet Source

<1%

Exclude quotes Off
Exclude bibliography Off

Exclude matches

Off